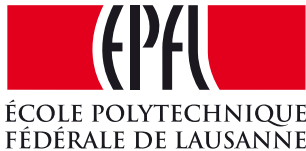


Towards Agility: Definition, Benchmark and Design Considerations for Small, Quadrupedal Robots

THIS IS A TEMPORARY TITLE PAGE

It will be replaced for the final print by a version
provided by the service academique.

Thèse n. 8592
à présenter le 17 Avril 2018
à la Faculté des Sciences et techniques de l'ingénieur
laboratoire Biorobotique
programme doctoral en Robotique, contrôle et
systèmes intelligents
École Polytechnique Fédérale de Lausanne



pour l'obtention du grade de Docteur ès Sciences
par

Peter Eckert

en revue par le jury:

Prof Paik, Jamie, présidente du jury
Prof Ijspeert, Auke J., directeur de thèse
Prof Hutter, Marco, rapporteur
Prof Daley, Monica, rapporteur
Prof Hurst, Jonathan W., rapporteur

Lausanne, EPFL, 2018

To my wonderful wife Maria and our beautiful daughter Alexandra

...

Acknowledgements

Over the past years and with great joy, I have ventured into the realm of building bio-inspired robots. This, on the first glance simple statement, made me realize many things. Robotics is where disciplines meet: science and engineering, mechanics and biology, control theory and hands-on programming or production work. One cannot thrive without the other, and if there is no symbiosis¹ between them, a robot will never function to extend our knowledge of the nature of things. Me, as a bio-mechatronics engineer by trade, I was fortunate to find this symbiosis with the help of my family, many friends, colleagues, and students.

First and foremost, I want to sincerely thank my "Doktorvater," Professor Auke Jan Ijspeert. "Doktorvater" in German means father of one's Ph.D., and it is definitively the right word to use in Auke's case. He welcomed me with the same open, positive and energetic attitude in his lab that he granted me over the following years in which I had the great pleasure working *with and for* him. Thank you Auke for your kindness, your support in good and challenging times, and honestly for being one of the few exceptional people in this world making science generate not only amazing new knowledge but also very fun. I thank my thesis committee, Jamie Paik, Monica Daley, Jonathan Hurst and Marco Hutter for their constructive and positively critic views on my dissertation. I enjoyed having my "final" presentation in front of you and hope we can keep working and discussing together in the future.

Professor Hartmut Witte, who guided me along the path of BioMechatronics from Ilmenau to Lausanne, I want to thank for the never-ending enthusiasm, despite all obstacles, promoting knowledge by practically applying it and thereby granting bored students their highlight of the day. I also want to acknowledge the wonderful collaborations through Master-thesis-projects between FG Biomechatronic and BIOROB. I hope they will continue to exist in the future.

The next in line is Dr. Alexander Spröwitz, who was my first direct supervisor in BIOROB and who introduced me to quadruped locomotion robotics. Alex, it was a great pleasure working with and learning from you, coming at (literally) any time day to the workshop and finding you there developing robots while listening to "Gangnam Style" in an infinity-loop.

Behzad, I want to thank you for the last year, in which our collaboration and friendship deepened. Your positive way of thinking, hard work and ability to find things in life that inspire you and the people around you are inspiring to me to "keep calm and keep going." I hope our

¹Yes, Behzad, I like this word

Acknowledgements

future endeavors will be fruitful, and we can stay friends for a long time to come.

Mostafa (and Lego), Alexandre, and Massimo: It was a great ride, being with you on the same team, sharing ideas, traveling together, doing fun stuff and real science. You are exceptional people, and I enjoyed your cheerful and open personalities. I appreciate your help so very much. Mos: Maria and me, we wish you and your growing family all the best, may you be happy and healthy. Stay the welcoming personalities you are. I hope we cross paths again in the future.

From now on, I will try to keep it short, or this dissertation will gain another 100 pages. I cannot bring to words how thankful I am, having met all the past and current members of BIOROB, so I will make a list only scratching the surface:

Simon (for being as punctual at bbq's as a German and bridging the Rösti-Graben with your confident personality), Mehmet (for your helpful and always cheerful and fun attitude), Robin (for BIOROB-soccer and your kindness), Tomislav (Serval would not have moved without you, I am grateful), Nicolas (for your hidden humor, always showing up at the right moment), Alessandro (Treasure-hunt...do I need to say more?), Hamed (for bringing symmetry to the lab and asking hard questions with a smile), Amy (SENSORIZATION is definitively a word! thank you for being so cheerful and energetic), Jonathan (good luck with your Ph.D., stay positive), Florin (for making me realize that not everything must be strict, all the best to your family and especially your little one, may he be happy and healthy), Salman (for making me realize that robots should be constructed very sturdy and your genius math skills), Jessica (for bringing a bit of Italian liveliness to the lab), Shravan (for your cheerfulness and help with Serval), Kamilo (for your helpful view on science and the resulting discussions), Laura (good luck with your Ph.D., stay positive), Jérémie (for in-depth discussions), Andrej (for coffee breaks and crazy discussions), Rico (for your help with Oncilla and the work on Locomorph), Andrej G. (for studies involving beer and grilled meat), Kostas (Ma..., thank you for Beachvolley, Training in the basement of INN and all the good times singing at bbq's), Sébastien (for introducing "real" French cheese), Soha (for your positively critical mind and helpful spirit), Jesse (for being able to find and resolve literally any coding problem we encountered), Luca (for your happy attitude and hard work at the same time) and Stéphane (for correcting my (in the beginning) horrible French). Thank you all for this great and exciting time we shared. Besides all these wonderful people, there are two lab members I want to thank especially, Sylvie and Francois: You were key-people for me in the lab. I had great pleasure talking to you, asking and receiving advice, complaining about many things and always being able to count on you. Thank you so very much! Another acknowledgment goes to the staff of EPFL, the ateliers (with their tremendous help in producing our prototyped parts), cleaners, administration and so many more, that enable us to have one of the top work environments in the world.

Now it is time to thank the people in my private life and I would like to start with my parents: Mama und Papa, seit (zu diesem Zeitpunkt) mehr als 30 Jahren habt ihr mich unterstützt, gefördert, gelehrt, mir die Welt gezeigt, mir geholfen die wichtigen Entscheidungen zu treffen

und auf eigenen Beinen zu stehen. Dabei habt ihr mir immer meinen eigenen Freiraum gegeben. Dies war bestimmt nicht immer leicht. Umso mehr bin ich euch dankbar, dass ihr so seid, wie ihr seid: Die besten Eltern, die ich mir für mich vorstellen kann. Ich danke euch von ganzem Herzen und ganzer Seele, einfach für ALLES! Ich habe euch sehr lieb, mehr als Worte niederschreiben könnten! Katrin, mein Schwesterherz. Große Schwester sein ist manchmal anstengend, besonders mit einem kleinen Bruder wie mir. Ich kann dir versichern, du machst es klasse. Ich möchte dir für deine Zuversicht und Hilfe über all die Jahre danken. Daniel, Paula und Moritz komplettieren deine Familie und ich kann euch nur eines sagen, euch habe ich auch sehr lieb und ihr werdet mir immer am Herzen liegen!

Владимир и Надежда, я очень благодарен вам за тёплый приём в вашу семью. Мне всегда радостно вас видеть и чувствовать вашу любовь к Марии. Александре и ко мне.

Ich möchte auch meinen Großeltern, Verwandten und alten Freunden danken. Ihr habt mich in meinem Leben geprägt und ich werde euch nie vergessen.

Finally, but for me at first place, my family:

Alexandra, wenn du dies liest, sind wahrscheinlich ein paar Jahre ins Land gegangen. Ich bin bereits jetzt so stolz auf dich und liebe dich so sehr! Ich werde immer für dich da sein!

Maria, mon amour, un mot qui peut decire comment je t'aime n'est pas encore inventé. Comme je suis chercheur et ingénieur, je vais l'essayer de le creer:

Tu me réjouis avec ton souris **ambivalent**. Tu me renforces en toute situation avec **légerté**. Ton **nergie** positiv me fait sentir la joie. Ta **voix** me rappel des ouiseaux du printemps. Te donner un **câlin** est comme la capabilité de sentir le soleil après l'hiver froid. Parler avec toi est comme lire une excellente **nouvelle**. Je vois mon **destin** avec toi près de moi. **Ravi** et content je vais passer ma vie avec toi. J'espère que notre **amour** va être éternelle.

Maria, le mot significant pour mon amour vers toi s'est manifesté dans le miracle qu'on a crée ensemble, ALEXANDRA. Je t'aime avec tout mon coeur et te remerci pour ton incroyable soutien!

Morges, 15 Mai 2018

Peter Eckert

Abstract

Agile quadrupedal locomotion in animals and robots is yet to be fully understood, quantified or achieved. An intuitive notion of agility exists, but neither a concise definition nor a common benchmark can be found. Further, it is unclear, what minimal level of mechatronic complexity is needed for this particular aspect of locomotion.

In this thesis we address and partially answer two primary questions: (Q1) What is agile legged locomotion (agility) and how can we measure it? (Q2) How can we make agile legged locomotion with a robot a reality?

To answer our first question, we define agility for robot and animal alike, building a common ground for this particular component of locomotion and introduce quantitative measures to enhance robot evaluation and comparison. The definition is based on and inspired by features of agility observed in nature, sports, and suggested in robotics related publications. Using the results of this observational and literature review, we build a novel and extendable benchmark of thirteen different tasks that implement our vision of quantitatively classifying agility. All scores are calculated from simple measures, such as time, distance, angles and characteristic geometric values for robot scaling. We normalize all unit-less scores to reach comparability between different systems. An initial implementation with available robots and real agility-dogs as baseline finalize our effort of answering the first question.

Bio-inspired designs introducing and benefiting from morphological aspects present in nature allowed the generation of fast, robust and energy efficient locomotion. We use engineering tools and interdisciplinary knowledge transferred from biology to build low-cost robots able to achieve a certain level of agility and as a result of this addressing our second question. This iterative process led to a series of robots from Lynx over Cheetah-Cub-S, Cheetah-Cub-AL, and Oncilla to Serval, a compliant robot with actuated spine, high range of motion in all joints. Serval presents a high level of mobility at medium speeds. With many successfully implemented skills, using a basic kinematics-duplication from dogs (copying the foot-trajectories of real animals and replaying the motion on the robot using a mathematical interpretation), we found strengths to emphasize, weaknesses to correct and made Serval ready for future attempts to achieve even more agile locomotion. We calculated Serval's agility scores with the result of it performing better than any of its predecessors. Our small, safe and low-cost robot is able to execute up to 6 agility tasks out of 13 with the potential to reach more after extended development. Concluding, we like to mention that Serval is able to cope with step-downs,

Abstract

smooth, bumpy terrain and falling orthogonally to the ground.

Key words: Agility, Benchmark, Quadruped, Bio-Inspiration, Bio-Mechatronics, Design Methodology, Biorobotics

Zusammenfassung

Agile vierbeinige Fortbewegung muss noch vollständig erklärt, quantifiziert und technisch umgesetzt werden. Eine intuitive Vorstellung von Agilität existiert, aber weder eine präzise Definition noch ein allgemein anerkannter Benchmark sind vorhanden. Darüber hinaus ist unklar, welche minimale mechatronische Komplexität benötigt wird, um agile Fortbewegung zu erreichen.

Aus genannten Gründen fokussiert diese Dissertation auf zwei Fragen: (F1) Was bedeutet agile Fortbewegung auf 4 Beinen (Agilität) und wie kann sie gemessen werden? (F2) Wie kann die agile Fortbewegung mit einem Roboter in der Realität umgesetzt werden?

Um die erste Frage zu beantworten, wird „Agilität“ für Roboter und Tier einheitlich definiert, eine gemeinsame Basis zum Verständnis dieser speziellen Fortbewegungskomponente aufgebaut und quantitative Messungen zum verbesserten Vergleich von Roboterbewegungen eingeführt. Die Definition basiert auf und ist inspiriert von Bewegungsmerkmalen, die in der Natur und im Sport beobachtet werden als auch Aspekte, welche in mit Robotik verbundenen Veröffentlichungen Beachtung finden. Diesen Erkenntnissen folgend wird ein neuer und erweiterbarer Benchmark aus dreizehn verschiedenen Aufgaben erstellt, der die Vision der quantitativen Klassifizierung von Agilität umsetzt. Alle Werte werden aus einfachen Messungen wie Zeit, Abständen, Winkeln und charakteristischen geometrischen Werten für die Roboterskalierung berechnet. Alle einheitslosen Werte werden normalisiert, um verschiedene Systeme vergleichen zu können. Eine Überprüfung mit zur Verfügung stehenden Robotern und Vergleich mit echten Agilityhunden finalisiert die Beantwortung der ersten Frage.

Bio-inspirierte Designs, welche morphologische Aspekte der Natur einführen und nutzen, erlauben die Erzeugung schneller, robuster und energieeffizienter Fortbewegungen. Mit dem interdisziplinärem Wissen der Biologie und ingenieurstechnischen Mitteln werden kostengünstige Roboter konstruiert, welche in der Lage sind, eine gewisse Agilität zu erreichen und damit unsere zweite Frage zu beantworten. Dieser iterative Prozess führt von Lynx über Cheetah-Cub-S, Cheetah-Cub-AL und Oncilla zu Serval, einem nachgiebigen Roboter mit aktiver Wirbelsäule und hohem Bewegungsspielraum in allen Gelenken, was eine hohe Mobilität bei mittleren Geschwindigkeiten ermöglicht. Mit vielen erfolgreich implementierten Fähigkeiten, erreicht über eine Kinematikduplizierung von Hunden, wurden Stärken herausgearbeitet, die zu betonen und Schwächen, die zu korrigieren waren und teilweise in der Zukunft noch zu adressieren sind. Serval bereit für zukünftige Versuche, um eine noch agilere Fortbewegung zu erreichen.

Abstract

Die Berechnung der Agilitätswerte für Serval hat eine generelle Verbesserung in Bezug auf seine Vorgänger ergeben. Dieser kleine, sichere und kostengünstige Roboter ist in der Lage, bis zu 6 von insgesamt 13 Agilitätsaufgaben auszuführen. Darüber hinaus ist Serval fähig, Steigungen zu bewältigen, hügeliges Gelände zu überqueren und orthogonal zum Boden zu fallen. Er hat das Potenzial, nach weiterer Entwicklung noch mehr zu erreichen.

Stichwörter: Agilität, Benchmark, Vierbeiner, Bioinspiration, Biomechatronik, Entwicklungsmethodik, Biorobotik

Résumé

La locomotion quadrupède agile exige encore d'être entièrement comprise, déterminée ou atteinte. Il existe une notion intuitive de l'agilité, mais ni une définition concise ni un repère commun ne peuvent être trouvés. En plus, il n'est pas clair, quel niveau minimal de la complexité mécatronique est nécessaire pour réaliser la locomotion agile.

Dans cette thèse, nous abordons et répondons partiellement à deux questions centrales : (Q1) Qu'est-ce que c'est, la locomotion agile (agilité) à pattes et comment pouvons-nous la mesurer? (Q2) Comment pouvons-nous rendre réelle une locomotion agile à pattes avec un robot?

Pour répondre à notre première question, nous définissons l'agilité pour le robot et l'animal, en construisant un espace commun pour cette composante particulière de la locomotion et introduisons des mesures quantitatives pour améliorer l'évaluation et la comparaison des robots. La définition est basée sur et inspirée par des caractéristiques de l'agilité observées dans la nature, le sport, et suggérées dans les publications liées à la robotique. En utilisant les résultats d'observations et de la revue de la littérature, nous construisons une référence (un repère) novatrice et extensible de treize tâches différentes qui met en œuvre notre vision de classer quantitativement l'agilité. Tous les scores sont calculés à partir de mesures simples, telles que le temps, la distance, les angles et les valeurs géométriques typiques pour la mise à l'échelle du robot. Nous standardisons tous les scores sans unité pour atteindre la comparabilité entre différents systèmes. Une mise à l'œuvre initiale avec des robots disponibles et de vrais chiens agiles finalise notre tentative de répondre à la première question.

Des designs bio-inspirés introduisant et jouissant d'aspects morphologiques présents dans la nature ont servi à la conception et réalisation d'une locomotion rapide, robuste et énergétiquement efficace. Nous utilisons des outils d'ingénierie et des connaissances interdisciplinaires empruntées de la biologie pour construire des robots à faible coût, capables d'atteindre un certain niveau d'agilité et, en le faisant, nous répondons à notre deuxième question. Ce processus itératif mené de Lynx à Cheetah-Cub-S, Cheetah-Cub-AL, et à Oncilla vers Serval – un robot docile avec la colonne vertébrale actionnée et de mouvements variés dans tous les joints. Serval est un robot avec un haut niveau de mobilité à des vitesses moyennes. Avec de nombreuses capacités mises en œuvre avec succès, en utilisant une cinématique répétée de chiens, nous avons trouvé des points forts à mettre en valeur, des faiblesses à corriger et ont rendu Serval prêt de parvenir à une locomotion encore plus agile. D'après le calcul

Abstract

des scores d'agilité de Serval nous avons constaté sa meilleure performance parmi tous ses prédécesseurs. Notre petit, secure et stable robot à faible coût est capable d'accomplir jusqu'à 6 tâches d'agilité sur 13 et a le potentiel d'aquerir encore plus après futurs développements. Pour conclure, Serval est capable de faire face à des descentes, aux terrains lisses et bosselés et de tomber au sol d'une manière orthogonale.

Mots clefs : Agilité, Benchmark, Quadrupède, Bio-Inspiration, Bio-Mécatronique, Méthodologie de design, Biorobotique

Contents

Acknowledgements	iii
Abstract (English/Français/Deutsch)	vii
List of figures	xix
List of tables	xxiii
List of Abbrevations	xxv
List of Symbols	xxix
List of QR-codes and links	xxxi
Author Contributions and Thesis Time-Line	xxxiii
Organization of the Thesis	xxxvii
General Notice	xxxix
1 Introduction	1
1.1 Problem Statement	2
1.2 Approach I: Defining and Measuring Agility	3
1.3 Approach II: Achieving Agility by Prototyping Legged Robots	3
1.3.1 Engineering Approach using the V-Model (VDI2206)	3
1.3.2 Bio-mimicry versus Bio-inspiration	6
1.3.3 Hardware versus Simulation	7
1.3.4 Small, Low-cost Robots versus Large High-end Robots	8
1.3.5 Conclusion	8
I Defining and Benchmarking Agility	11
2 Defining Agility	13
	xiii

Contents

2.1	Agility in Wildlife	14
2.2	Agility in Sport	15
2.2.1	Agility in Animal-Sports	15
2.2.2	Agility in Human-Sports	16
2.3	Agility in Legged, Terrestrial Robotics	17
2.4	Conclusion for Agility Definition	17
2.4.1	Conclusion from Wildlife, Human- and Animal-Sports	17
2.4.2	Conclusion from Agility Definitions or Evaluations in Robotics	18
2.4.3	Definition of Agility for Legged, Terrestrial Robots	18
3	Agility Benchmark	19
3.1	Introduction and Review on Characterization and Benchmarking Methods . . .	19
3.1.1	Gaits	20
3.1.2	Dimensionless Numbers	23
3.1.3	Benchmarking Environments and other Robot Benchmarks	24
3.1.4	Conclusion for Benchmarking Methods	25
3.2	Agility Benchmark	26
3.2.1	Proposed Method for Benchmarking Agility	26
3.2.2	First Experimental Implementation	37
3.3	Conclusion	39
II	Achieving Agility with Small, Low-cost Quadrupedal Robots	43
4	Introduction	45
4.1	State-of-the-Art: A General and non-exhaustive Overview	45
4.1.1	Agile Legged, Terrestrial Robots	45
4.1.2	Previously existing Quadruped Robots of BIOROB	50
4.1.3	Overview of built Robots during the Thesis	52
5	Domain Specific Design I: Mechanics	55
5.1	Materials and Methods for Lightweight Structures	55
5.1.1	General Definition	56
5.1.2	Design Principles	57
5.1.3	Materials	59
5.1.4	Strength and Stiffness Considerations: Classical and Computer-assisted Methods	64
5.1.5	Conclusion	68
5.2	Manufacturing Methods for Prototyping	68
5.2.1	Abrasive/Subtractive Prototyping	68
5.2.2	Additive Prototyping	69

5.2.3	Comparison and Conclusion	70
5.3	Application in existing Robots in BIOROB	72
5.3.1	Cheetah-Cub	72
5.3.2	Bobcat	75
5.3.3	Oncilla	78
5.4	Mechanical Development towards Serval	82
5.4.1	Mechanics needed for Agile, Legged Robots	82
5.4.2	Lynx	83
5.4.3	Cheetah-Cub-S	87
5.4.4	Cheetah-Cub-AL	90
5.4.5	Serval	92
6	Domain Specific Design II: Electronics	101
6.1	General Introduction of Electronics used in Quadruped Robots	101
6.1.1	Common Actuators used in Legged Locomotion	101
6.1.2	Common Control Boards used in Legged Locomotion	102
6.1.3	Common Sensors used in Legged Locomotion	104
6.1.4	Conclusion	105
6.2	Application in Existing Robots in BIOROB	105
6.2.1	Cheetah-Cub-Family: (Almost) Sensor-less Robots	105
6.2.2	Oncilla: High Sensor Integration	107
6.3	Electronics Development for Serval	108
6.3.1	Electronics needed for Agile, Legged Robots	108
6.3.2	Implementation	109
7	Domain Specific Design II: Control	111
7.1	General Introduction of High-Level Concepts used for Locomotion Control	111
7.1.1	Central Pattern Generators	112
7.1.2	Reflexes and Posture Adaptation	114
7.1.3	Forward and Inverse Kinematics	115
7.1.4	Conclusion	115
7.2	Application in Existing Robots in BIOROB	115
7.2.1	Open-loop Robots: Cheetah-Cub-Family	116
7.2.2	Closed-loop Robot: Oncilla	117
7.3	Control Development for Serval	119
7.3.1	Control needed for Agility	119
7.3.2	First Implementations	119
8	Conclusion and Cost-Evaluation	123

Contents

9 Experiments and Validation	125
9.1 Experimental Environments and Tools	125
9.1.1 Motion Capture	125
9.1.2 Power Consumption	126
9.1.3 High-speed Video	126
9.1.4 Ground Reaction Forces	127
9.2 Experiments with the Cheetah-Cub-Family and Oncilla	127
9.2.1 Lynx	127
9.2.2 Cheetah-Cub-S	133
9.2.3 Cheetah-Cub-AL	139
9.2.4 Oncilla	140
9.3 Experiments with Serval	149
9.3.1 Flat Terrain	151
9.3.2 Inclined Surfaces	158
9.3.3 Perturbed Surfaces and Stability	159
9.3.4 Artificial Behaviors	162
9.3.5 Conclusion for Agility	164
 III Conclusion and Outlook	 167
10 Conclusion	169
11 For Those Who Follow - Outlook	173
11.1 How to build on this work	173
11.2 Outlook	175
 Appendix	 177
A Side Projects	179
A.1 Friction and Damping of a Compliant Foot based on Granular Jamming for Legged Robots	179
A.2 The Swimming Cheetah - a Comparative Study between Robot and Animal . .	180
A.3 MAR - An Energy Efficient Anguilliform Swimming Robot; a Design, Control and Experimental Study	182
A.4 On Designing an Active Tail for Legged Robots: Simplifying Control via Decoupling of Control Objectives	183
A.5 Force Sensor Setup for Human Machine Interaction using a Stretcher	184
A.6 A Preliminary Head for the COMAN Robot	184
 B Thesis-timeplan and misc. documents	 187

C Leg kinematics	195
C.1 Oncilla kinematic	195
C.2 Inverse Kinematic	199
D Unfoldables	203
Bibliography	211
Curriculum Vitae	227

List of Figures

1	QR-codes and links	xxxi
2	Contribution: Time-Partition	xxxiii
3	Contribution: Thesis time-line	xxxiv
1.1	Introduction: V-Model	4
2.1	Defining Agility: Animals in Wildlife	14
2.2	Defining Agility: Animals in Sport	15
3.1	Agility-Benchmark: Symmetrical gaits	21
3.2	Agility-Benchmark: Rotary gallop of a cheetah	21
3.3	Agility-Benchmark: Asymmetrical gaits	22
3.4	Agility-Benchmark: Lead-sequence by Hildebrand	23
3.5	Agility-Benchmark: Turning with a radius - schematic	28
3.6	Agility-Benchmark: Turning on the spot - schematic	29
3.7	Agility-Benchmark: Jumping and leaping - schematic	30
3.8	Agility-Benchmark: Slope - schematic	31
3.9	Agility-Benchmark: Standing up - schematic	32
3.10	Agility-Benchmark: Side-stepping - schematic	33
3.11	Agility-Benchmark: Foward and backward locomotion - schematic	33
3.12	Agility-Benchmark: Robots for initial test	38
3.13	Agility-Benchmark: Strength-plots for agility of different robots	40
4.1	Introduction Part 2: State-of-the-art in quadruped robotics	49
4.2	Intoduction Part 2: Previously Existing Quadruped Robots of BIOROB	51
5.1	Mechanics: Lightweigt construction	58
5.2	Mechanics: Stress-Strain-behavior of Nitinol	61
5.3	Mechanics: Illustration of subtractive prototyping	69
5.4	Mechanics: Illustration of additive prototyping	69
5.5	QR-code: 3D-PDF for Cheetah-Cub	72
5.6	Mechanics: Cheetah-Cub - CAD	73

List of Figures

5.7	Mechanics: Cheetah-Cub - Detail-figures and schematic	74
5.8	Mechanics: Bobcat - CAD	76
5.9	Mechanics: Bobcat - Detail-figures and schematic	77
5.10	QR-code: 3D-PDF for Oncilla	78
5.11	Mechanics: Oncilla - CAD	79
5.12	Mechanics: Oncilla - Detail-figures and schematic	80
5.13	QR-code: 3D-PDF for Lynx	83
5.14	Mechanics: Lynx - CAD	84
5.15	Mechanics: Lynx - Detail-figures and schematic	85
5.16	QR-code: 3D-PDF for Cheetah-Cub-S	87
5.17	Mechanics: Cheetah-Cub-S - CAD	87
5.18	Mechanics: Cheetah-Cub-S - Detail-figures and schematic	88
5.19	Mechanics: Cheetah-Cub-S - Torsion-effect	89
5.20	QR-code: 3D-PDF for Cheetah-Cub-AL	90
5.21	Mechanics: Cheetah-Cub-AL - CAD	90
5.22	Mechanics: Cheetah-Cub-AL - Detail-figures and schematic	91
5.23	QR-code: 3D-PDF for Serval	92
5.24	Mechanics: Serval - CAD	93
5.25	Mechanics: Serval - Detail-figures and schematic	94
5.26	Mechanics: Serval - AA-elastics FEM	95
5.27	Mechanics: Serval - leg-unit	96
5.28	Mechanics: Serval - trunk-unit	97
5.29	Mechanics: Serval - spine-unit	98
7.1	Control: CPG in animals	112
7.2	Control: CPG parameters in feed-foward control	116
7.3	Control: Expemlary foot-trajectories	120
7.4	Control: Parametrization method for Serval	120
9.1	Experiments: Experimental area	126
9.2	QR-code: Experiments with Lynx	127
9.3	Experiments: Lynx - COT	129
9.4	Experiments: Lynx - Pitch variations	130
9.5	Experiments: Lynx - Distribution of "non-natural" and "natural" looking gaits	131
9.6	Experiments: Lynx - Gaits and footfall-pattern	131
9.7	QR-code: Experiments with Cheetah-Cub-S	133
9.8	Experiments: Cheetah-Cub-S - Radius calculation	134
9.9	Experiments: Cheetah-Cub-S - Turning circle illustation	135
9.10	Experiments: Cheetah-Cub-S - Turning data example	135
9.11	Experiments: Cheetah-Cub-S - Experimental radii calculated	136

9.12	Experiments: Cheetah-Cub - Turning by ASL	137
9.13	Experiments: Cheetah-Cub-S - Slalom run	138
9.14	QR-code: Experiments with Cheetah-Cub-AL	139
9.15	Experiments: Cheetah-Cub-AL - Snapshots and Footfall-pattern	140
9.16	QR-code: Experiments with Oncilla	140
9.17	Experiments: Oncilla - Forward locomotion	142
9.18	Experiments: Oncilla - Trunk roll variations	142
9.19	Experiments: Oncilla - Trunk pitch variations	143
9.20	Experiments: Oncilla - Asymmetric load carriage	144
9.21	Experiments: Oncilla - Activation of LSR after perturbation	145
9.22	Experiments: Oncilla - Descending a slope	145
9.23	Experiments: Oncilla - Climbing an upwards 15 degrees slope	146
9.24	Experiments: Oncilla - SCR activation	147
9.25	Experiments: Oncilla - Rough terrain setup	148
9.26	Experiments: Oncilla - Control signals for rough terrain locomotion	148
9.27	QR-code: Experiments with Serval	149
9.28	Experiments: Serval - Foot-trajectories for walk	151
9.29	Experiments: Serval - Sanpshots of walk	151
9.30	Experiments: Serval - Foot-trajectories for trot	152
9.31	Experiments: Serval - Snapshots of trot	153
9.32	Experiments: Serval - GRF of trot	153
9.33	Experiments: Serval - GRF of bound	154
9.34	Experiments: Serval - Snapshots of bound	155
9.35	Experiments: Serval - Foot-trajectories for gallop	155
9.36	Experiments: Serval - Snapshots of gallop	156
9.37	Experiments: Serval - GRF of gallop	156
9.38	Experiments: Serval - Snapshots of side-step	157
9.39	Experiments: Serval - Snapshot of turning	158
9.40	Experiments: Serval - Snapshots of upslope bound	159
9.41	Experiments: Serval - Snapshots of single step-down	160
9.42	Experiments: Serval - Snapshots of double step-down	160
9.43	Experiments: Serval - Snapshots of falling	161
9.44	Experiments: Serval - Snapshots of rough terrain locomotion	162
9.45	Experiments: Serval - Snapshots of lying	163
9.46	Experiments: Serval - Snapshots of sitting	163
9.47	Experiments: Serval - Strength-plot for Agility	165
A.1	QR-code: Experiments with Oncilla-Granular	179
A.2	Membrane Foot for Oncilla	180
A.3	QR-code: Experiments with Cheetah-Cub-W	181

List of Figures

A.4	Appendix: Cheetah-Cub-W	181
A.5	QR-code: Experiments with MAR	182
A.6	Appendix: MAR	182
A.7	QR-code: Experiments with Cheetah-Cub-T	183
A.8	Appendix: Cheetah-Cub-T	183
A.9	Appendix: Sensor stretcher	184
A.10	Appendix: Coman head	185
C.1	Appendix: Kinematics nomenclature	195
C.2	Appendix: Leg length nomenclature	196
C.3	Appendix: Leg angles	197
C.4	Appendix: Oncilla knee	198
C.5	Appendix: Reference positions	200

List of Tables

1	Contribution: Specific hardware and publication contributions by the author - 1xxxv	
2	Contribution: Specific hardware and publication contributions by the author - 2xxxvi	
1.1	Introduction: List of requirements for legged, bio-inspired, and agile robots . .	5
1.2	Introduction: Advantages and Disadvantages of BI vs. BM	6
1.3	Introduction: Advantages and Disadvantages of a hardware vs. simulation centered approach	7
1.4	Introduction: Advantages and Disadvantages of SLC vs. LHE	8
3.1	Agility-Benchmark: Summary of benchmarking calculations	27
3.2	Agility-Benchmark: Baseline scores - dog	35
3.3	Agility-Benchmark: Baseline scores - aggregated dog	35
3.4	Agility-Benchmark: Experimental equipment (suggestion)	37
3.5	Agility-Benchmark: Agility scores for robots	39
4.1	Introduction Part 2: Quadruped robot comparison	48
4.2	Introduction Part 2: Hypothetic agility capability	50
4.3	Introduction Part 2: Robot characteristics in BIOROB	54
5.1	Mechanics: Characteristic of different materials	67
5.2	Mechanics: Abrasive technologies	69
5.3	Mechanics: Additive technologies	70
5.4	Mechanics: Comparison prototyping technologies	71
6.1	Electronics: Actuator technologies	102
6.2	Electronics: Control boards	103
6.3	Electronics: Sensor technologies	104
8.1	Conclusion: Cost evaluation	124
9.1	Experiments: Lynx - CPG search parameters	128
9.2	Experiments: Lynx - Fastest CPG parameters	129
9.3	Experiments: Lynx - COT-comparison of the fastest gaits	132

List of Tables

9.4	Experiments: Lynx - Speed-comparison	133
9.5	Experiments: Cheetah-Cub-S - Comparison to Cheetah-Cub	138
9.6	Experiments: Serval - Agility scores	164
C.1	Appendix: Kinematic variables	199
C.2	Appendix: Reference angles and ranges	199

List of Abbreviations

Please find this list of abbreviations also as unfoldable page in the very end of the document. The page is designed to be readable at all times and would allow quick checks of unknown abbreviations, without returning to this first list.

AA	Abduction/Adduction	CHF	Swiss franc
ABS	Acrylnitril-Butadien-Styrol	CNC	Computer numerical control
AFRP	Aramid fiber reinforced plastic	COA	Cost of agility
AHP	Analytical Hierarchical Process	COM	Center of mass
AL	Aluminium	COR	Center of rotation
ALSP	Adv. Spring Loaded Panthograph	COT	Cost of transport
ASL	Asymmetric stride length	CPG	Central pattern generator
BI	Bio-inspiration	Cus	Custom
BIROB	Biorobotics laboratory	DC	Direct current
BL	Body length	DF	Duty factor
BM	Bio-mimicry	DLP	Direct Light Processing)
C	Control	DMLS	DirectMetal Laser Sintering
CAD	Computer assisted design	DOF	Degree of freedom
CC	Cheetah-Cub	DS	Diagonal Spring
CCAL	Cheetah-Cub-AL	E	Electronics
CCS	Cheetah-Cub-S	EC	Electronically commutated
CFRP	Carbon fiber reinforced plastic	FB	Fiber breakage

List of Tables

FDM	(Fused Deposition Modeling)	NiTi	Nitinol
FE	Flexion/Extension	O	Optional
FEM	Finite element method	P	Price
FR	Froude number	PA2200	Polyamide 12
FT	Foot trajectory	PAD	Posture adaptation
G	Gear	PCB	Printed Circuit Board
GFRP	Glass fiber reinforced plastic	POM	Polyoxymethylen
GRF	Ground reaction forces	PR	Protraction/Retraction
HM	High modulus	PS	Parallel Spring
HT	High Tenacity	PW	Person weeks
HW	Hardware	PWM	Pulse width modulation
IM	Intermediate Modulus	ROM	Range of motion
IMU	Inertial measurement unit	RPV	Roll pitch variation
LER	Leg extension reflex	RQ	Raibert's Quadruped
LHE	Large, high-end	S	Safety
LIDAR	Light detection and ranging	SBC	Single board computer
LSR	Lateral stepping reflex	SCR	Stumbling correction reflex
LiPo	Lithium Polymere	SLA	Stereo-lithography
M	Mechanics	SLC	Small, low-cost
MA	Master	SLIP	Spring loaded inv. pendulum
MAR	Marine anguilliform robot	SLM	Selective Laser Melting
MB	Matrix breakage	SLS	Selective Laser Sintering
MOCAP	Motion capturing	SMA	Shape memory alloy
Mg	Magnesium	SV	Spine version
N	Necessary	Sim	Simulation
		Ti	Titanium
		UD	Unidirectional

List of Tables

UM Ultra modulus

UT Ultra Tenacity

UV Ultra violet

VDI Verein Deutscher Ingenieure

W Wished

List of Symbols

Please find this list of symbols also as unfoldable page in the very end of the document. The page is designed to be readable at all times and would allow quick checks of unknown symbols, without returning to this first list.

A_{xy}	Agility score	I_{xy}	Moment of inertia
a_{xy}	Amplification	p	Number of full rotations
ϑ	Angle	Π	Pi
Φ	Angle	ν	Poisson's ratio
A	Area	P_{xy}	Power
U	Circumfrence	r_{xy}	Radius
s_{xy}	Deflection	R_{xy}	Radius
d_{xy}	Diameter	G	Shearmodulus
f_{xy}	Frequency	k_{xy}	Spring constant
g	Gravity	t_{xy}	Time
c	Half shoulder to shoulder distance	M_t	Torsionmoment
h_{xy}	Height	q_{xy}	Variance score
i_{xy}	Inclination	v_{xy}	Velocity
l_{xy}	Length	w_{xy}	Width
m_{xy}	Mass	E	Young's modulus

List of QR-codes and Links

QR-codes for 3D-PDF and experimental documentation for the core topics can be found in the following figure. Links to experiments for side-projects can be found in Appendix A



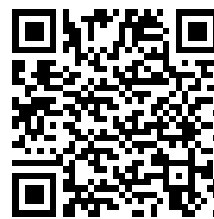
(a) 3D-PDF:
<https://go.epfl.ch/3DPDFCheetahCub>



(b) 3D-PDF:
<https://go.epfl.ch/3DPDFCheetahCubS>



(c) 3D-PDF:
<https://go.epfl.ch/3DPDFCheetahCubAL>



(d) 3D-PDF:
<https://go.epfl.ch/3DPDFLynx>



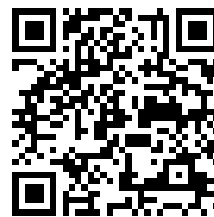
(e) 3D-PDF:
<https://go.epfl.ch/3DPDFOncilla>



(f) 3D-PDF:
<https://go.epfl.ch/3DPDFServal>



(g) Experiments:
<https://go.epfl.ch/ExperimentsCheetahCubS>



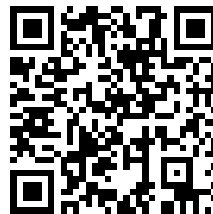
(h) Experiments:
<https://go.epfl.ch/ExperimentsCheetahCubAL>



(i) Experiments:
<https://go.epfl.ch/ExperimentsLynx>



(j) Experiments:
<https://go.epfl.ch/ExperimentsOncilla>



(k) Experiments:
<https://go.epfl.ch/ExperimentsServal>

Figure 1 – QR-codes and links

Author Contributions and Time-line

This thesis consists of the work realized through many collaborative projects, resulting in various publications. To allow a steady reading flow, I list my specific contributions to hardware developments, the respective publications and related work mainly in Table 1 and Table 2. Figure 2 displays the estimated work invested in different parts during my time at BIOROB. In Figure 3 a time-line depicts when the different projects were active. In addition to the hardware projects, I developed an agility benchmark from concept to final form and lead-authored the related publication [1]. I want to thank all my colleagues and co-authors at this point again for their help in my endeavors. The overall original contribution of my thesis is summarized below.

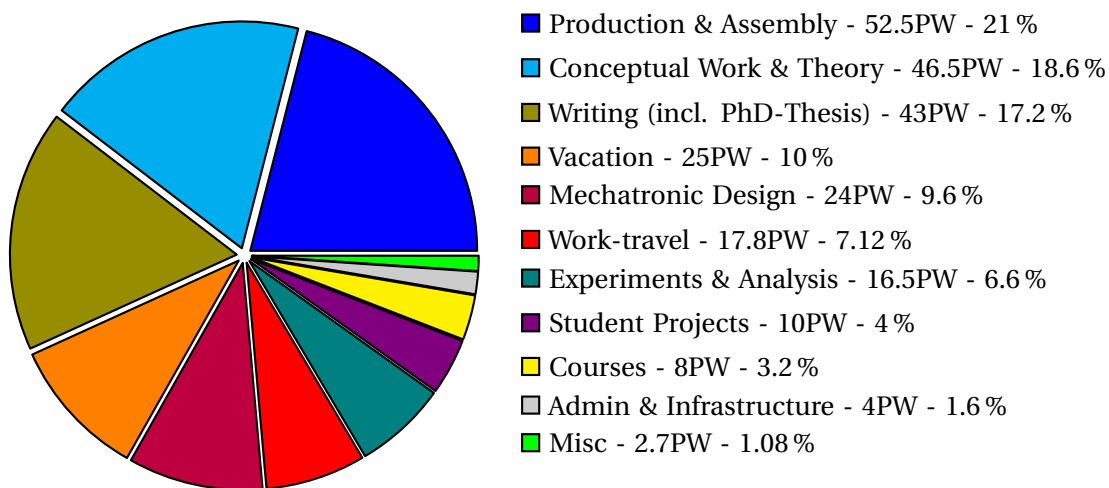


Figure 2 – Approximate time-partition in % and Person Weeks (PW); sum of available weeks: 250; detailed partition is available in Appendix B

List of Tables

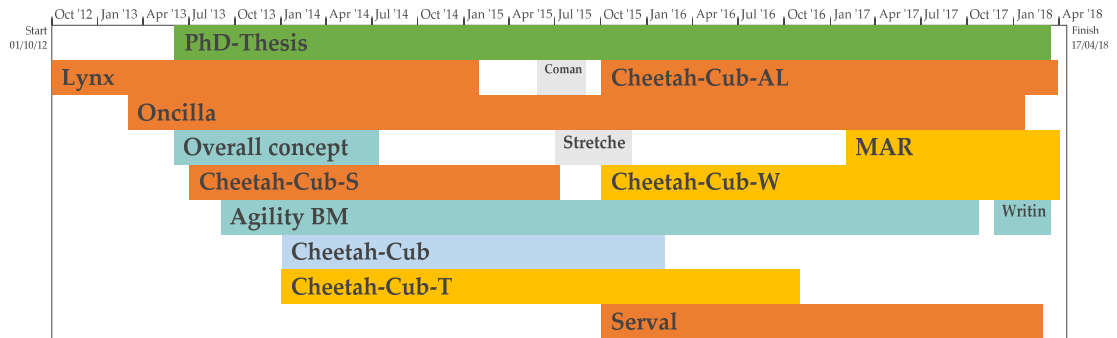


Figure 3 – High-level time-line of the thesis and related project, projects overlap due to parallel work on different parts; not equal to invested person weeks (see Figure 2)

Original Contribution of this Thesis

The overall original contribution of this thesis is summarized in the following list:

1. Definition of agility for locomotion
2. Development of a novel agility benchmark for multi-legged, terrestrial robots
3. Development of different small, cost-efficient and safe quadrupedal robots for agile locomotion

Table 1 – Author’s contribution to hardware development projects and related activities such as publications; Most work was done in collaboration with colleagues, project partners, students and our technician Francois Longchamp (who assisted strongly in addition to my implementation efforts); I include Lynx, although it was the robot initiated in my Masters thesis, as it presents an integral stepping stone the following development and was used for research purposes in the first months of my PhD

Robot	Year	Ref.	Contribution
Lynx	2012-13	[2]	Development of first robot prototype Development of second robot prototype, including 3 spine versions Partial production and assembly Experiments and Analysis lead author in publication
Cheetah-Cub	2013-15	[3]	Project student supervisions in different side projects with design, production, assembly and experimental support Maintenance (reproduction of 2 new copies with different material choices) Lead and co-author in different publications
Cheetah-Cub-S	2013-14	[4]	Conceptual idea Development support for first robot iteration Development of second spine iteration Partial production and assembly Student supervision Maintenance Co-Lead-author in publication
Cheetah-Cub-AL	2015-18		Structural improvement concept for Cheetah-Cub Development of two design iterations Production and assembly Experiments (together with Alexandre Tuleu) Maintenance
Oncilla	2013-18	[5]	Co-Development of a third design iteration (together with Francois Longchamp) Co-Development of a compliant foot design Partial production and assembly of 4 robot copies Experiments Co-supervision of students Maintenance (of all copies, also in partner laboratories) Participation in EU-project review meetings Co-author in publication
Serval	2016-18	[6]	Conceptual idea Development of a two design iterations Production and assembly Partial Experiments and Analysis Lead-author in publication(under review)

List of Tables

Table 2 – Continuation of Table 1

Robot	Year	Ref.	Contribution
Cheetah-Cub-T	2013	[7]	Conceptual support Co-supervision of a student Maintenance Co-author in publication
Cheetah-Cub-W	2016-18	[8]	Conceptual idea (together with Behzad Bayat) Student supervision and design support for first shell iteration Development of second and third design iterations Production and assembly Experiments and partial supervision of and with second student Maintenance Co-lead-author in publication (under review)
MAR	2017-18	[9]	Conceptual idea (together with Behzad Bayat) Student supervision and design support for first iteration Partial Production and assembly Partial Experiments Maintenance Co-supervision of students Co-lead-author in publication (under review)
Coman-Head	2016		Conceptual idea after receiving design requirements Development, production and assembly
Sensor-Stretcher	2016	[10]	Conceptual idea after receiving design requirements Development, production and assembly

Organization of the Thesis

Introduction

As the title suggests, this first part will give an introduction to and motivation for this thesis. The selected approaches towards defining and achieving agility are clarified, including the reasoning behind the employed development method (iterative hardware approach) as well as a motivation why to use bio-inspiration for robotics. We will include our state-of-the-art analysis in Parts 1 and 2, as we have two distinct areas of interest to cover (definition/benchmarking and robot development) and believe this distribution to be beneficial for the reading flow.

Part 1: Defining and Benchmarking Agility

Part 1 is centered around the definition for our keyword agility and its benchmarking for legged systems, based on a state-of-the-art analysis. The generation and first experimental implementation (as a preview of related experiments in Part 2) of a novel benchmarking system, allowing for robot evaluation and a comparison is presented. The Part includes as well a review of existing benchmarking methods and the main elements on how to characterize animal and robot gaits, setting the framework for the evaluation of our constructed robots.

Part 2: Achieving Agility with Small, Low-cost Quadrupedal Robots

A general state-of-the-art in agile, legged terrestrial robots is presented and builds the basis to compare our developed systems. The domain-specific chapters guide through our development process as follows. **Mechanics:** Insights into lightweight construction methods, materials, and manufacturing for prototyping start the first domain-specific design chapter. This is followed by an evaluation of the mechanical implementations in existing quadrupedal robots of BIOROB. The development process towards the latest quadruped, Serval, and its main features close this chapter.

Electronics: Structurally similar to our first domain-specific chapter, Mechanics, a general overview of employable sensors, control boards and actuator technologies is presented and related to the old and new robots of BIOROB.

Control: The 3rd and last of the domain-specific design chapters introduces relevant control strategies, also rating advantages and defaults, as well as their application in our quadrupedal robots.

After the more engineering-oriented chapters, a scientific validation of robots built and their performance evaluation during real-life experiments forms the core of chapter chapter 9.

Part 3: Conclusion

Drawing a summary of our work and taking a look at the future of our benchmark and quadrupedal robots for agility will be performed in the concluding chapter.

Appendix

The appendix consists of tables, technical drawings and other documents, important for this thesis. The respective parts will be referenced in the main body of the text.

One part of the appendix is dedicated to side projects additional to the core topic: During the time in BIOROB, I had the opportunity to work with many collaborators on projects, which were less related to the core topic of this thesis. None the less, we build amazing machines and explored exciting questions. The side-projects chapter consists of said projects, mainly in the form of short publications' presentations resulting from our work. They were included with my colleagues' permissions.

I urge the readers to take a look at the "Important Notice" on the next page to support the reading flow.

Important Notice

Please find a list of abbreviations, symbols, QR-codes and an overview table with characteristic measures of our robots as unfoldable pages in Appendix D. These pages are meant to be readable at all times and would allow quick checks of unknowns, without returning to respective lists and table within the document.

The videos related to our experimental validation in chapter 9 are linked to this document with a QR-Code (readable with any QR-code application on a smartphone) and hyper-link, for direct access, either from the digital or analog version of this thesis.

A 3D-PDF (readable with Adobe Acrobat reader or a respective smartphone application) for each of our robots is available for download. The respective link and QR-code can be found in section 5.3, section 5.4 and the beginning of this dissertation.

All citations and cross-references inside the text are hyper-linked to the respective figure or table, allowing for quick access.

1 Introduction

If you take a look around you, bio-inspiration is everywhere. May it be in the velcro fastener on your jacket (from a plant), the aerodynamics of a plane (from birds) or the way bridges are built (from trees). Without much notice, bio-inspiration made an enormous impact on daily life. Knowledge steadily gathered over decades, if not centuries, by observation and understanding of nature, transforming and advancing it within our technology made this possible. And still, there is so much more to learn and understand from nature, to bring into words, mathematical formula and reproduce with our or current and future technologies.

To investigate and understand nature a little better, I had the privilege to focus my curiosity on the field of locomotion. Easy, is it not? Everybody walks, runs, and balances, animal and human alike. It seems as simple as breathing, but is it? Do we understand locomotion? Can we describe it and even further, (re)produce locomotion? If one looks a bit closer, locomotion might not seem as uniform as we often think. Humans and some other species walk upright, dogs and cats on four feet, spiders easily climb on walls, there are even snakes that can glide through the air, and these are only some animals that live on land. The variety of what can be summarized with the one word, locomotion, is unbelievably high. For me, being welcomed to a fantastic interdisciplinary team in the Biorobotics Laboratory about five years ago, the realm of quadrupedal, mammal-like, terrestrial locomotion. Especially the intelligent mechanics involved became my focus interest and are ever since. In this regard, the agility used by animals to form nimble and elegant movement in symbiosis with their environment is especially fascinating and has been driving my curiosity from the start.

This thesis presents my thoughts and achievements, may they be from an engineering or scientific point of view, on the development of small robots and their use as tools, investigating agile mammal-like quadrupedal and terrestrial locomotion. I hope you will find the impressions, information, and engineering insights gathered throughout many collaborations and hard work useful.

1.1 Problem Statement

This thesis addresses two main questions:

Question 1: What is agile legged locomotion and how can we measure it?

On a principle level, locomotion means displacing one's body from one point in 3D-space to another. In animals, locomotion is achieved by coordination of the musculoskeletal system through high-level brain signals as well as sensory and reflex feedback adapting rhythmic patterns to form stable motion [11]. Not all movement can be called agile. Nimbleness, an often used word in context with agility, is strengthening our impression that slow, steady-state motion is not enough to describe a system as agile. Nevertheless, there is only a general notion of what agility is, but neither a concise definition nor a common benchmarking method exists, leading to the following steps for addressing our first question:

1. Generation of a concise definition of agility in legged systems.
2. Development of a benchmarking method to measure and assess agility in legged locomotion.
3. Testing of the method with existing and new legged robots.

Question 2: How can we make agile legged locomotion with a robot a reality?

On the one hand, machines with relatively simple underlying principles (e.g., car or bike) can move very well in our environment and navigate even through difficult terrains. In legged robotics, on the other hand, whose motivation is often the high possible adaptability to uneven or discrete rough terrains [12], such fast and reliable locomotion is yet to be achieved. It is still unclear, although researched in many laboratories all over the world (see section 4.1), what minimal, i.e., necessary and sufficient, level of mechatronic complexity is needed to realize agile locomotion. Our approach to answering this second question is summarized in the following steps:

1. Development of different low-cost legged robots, to iteratively test added value for locomotion following the implementation of different morphological and mechatronic principles.
2. Combining advantages of previous systems into a final legged robot to form a valuable research platform for agile locomotion.

Our approach to investigate and answer the questions mentioned above is two-fold and executed in parallel as is described in the following sections:

1.2 Approach I: Defining and Measuring Agility

To answer our first question, we aim to define and benchmark agility for robot and animal alike, building a common ground for this particular component of locomotion and introduce quantitative measures to enhance robot evaluation and comparison. This definition is based on and inspired by features of agility observed in nature, sports, and suggested in robotics related publications. Using the results from this observational and literature review, we build a novel and extendable benchmark that implements our vision of quantitatively classify agility. An initial implementation of such a benchmark on available robots as proof-of-concept will finalize our effort of answering the first question.

1.3 Approach II: Achieving Agility by Prototyping Legged Robots

Bio-inspired designs introducing and benefiting from morphological aspects present in nature allowed the generation of fast, robust and energy efficient locomotion, see section 4.1. This trend is visible and pursued already over many years, with focus on the development of (compliant) legs and in special cases the use of compliant trunks. We use engineering tools and interdisciplinary knowledge transferred from biology to build low-cost robots able to achieve a certain level of agility. This iterative process should lead to new insights, on what level of mechatronic and morphological complexity is needed to move effectively and agile in a physical environment.

The following subsections will discuss and evaluate significant choices made and general methods employed, that influenced the robot development decisively and thus represent the basis to our second approach.

1.3.1 Engineering Approach using the V-Model (VDI2206)

Robots in their broadest sense are mechatronic systems, in which mainly three domains interface to form a functioning apparatus. These domains are (1) mechanical, (2) electronics and (3) control engineering. The Association of German Engineers (VDI) presented a norm in 2004 that organizes the development of such a mechatronic system, giving guidelines to developers and specifying the minimal content of the different domains. A major part of this norm is called the V-Model [13].

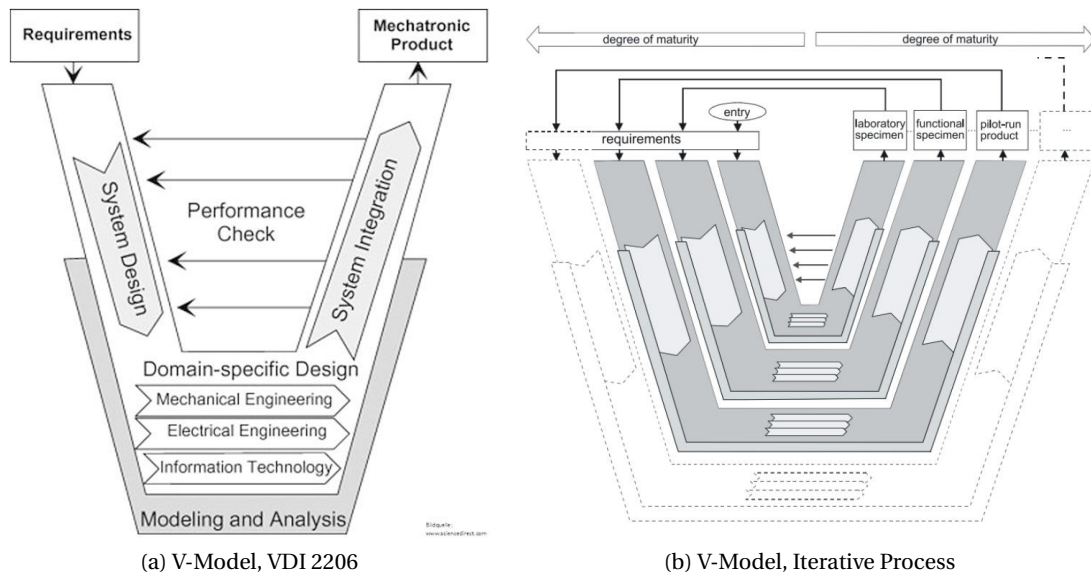


Figure 1.1 – VDI2206, V-model: Development methodology for a mechatronic system; (a) Single development cycle with major features to be considered for a mechatronic design, usually achieved by integrating and managing domain-specific specialists in a development team; (b) Illustration of the iterative process, when adding features to a product/system until final version is obtained, requirements are updated after every iteration, laboratory/research facilities usually produce a functional specimen, including benefits and minimizing disadvantages from previous laboratory specimens

The V-model presents a macro-cycle of product development starting from the formation of a requirement list, over theoretical system design and domain-specific design to system integration and the resulting in a product. Throughout the whole process, validation of expected system performance and future modifications should be performed. In parallel to this cycle, one can, and in many cases should implement modeling and theoretical analysis in the process. Once one cycle is completed (for example when one design iteration has been performed and tested), another cycle can start on its predecessors' results and advance towards the final system, see Figure 1.1 on the right. Our development process, presented in Part II, follows this approach and adds another component, bio-inspiration, and bio-validation in the form of comparison to animal characteristics. A high-level list of the hypothesized requirements for a legged, bio-inspired, and agile robot is found below:

1.3. Approach II: Achieving Agility by Prototyping Legged Robots

Table 1.1 – Subjective list of hypothesized requirements for legged, bio-inspired, and agile robots; N-necessary, W-wished, O-optional; M-mechanics, C-control, E-electronics, P-price, S-safety

Requirement	Category	Classification	Value
Lightweight	M	N	$m < 5000g$
Leg-length	M	N	$h > 150mm$
Modularity	M	N	
Robustness to impacts	M	N	
AA-ROM	M	W	$\phi > \pm 25^\circ$
Hip-ROM	M	W	$\phi > \pm 60^\circ$
Knee-ROM	M	W	$l > 20\% \text{ leg-length}$
Spine-DOF	M	O	$DOF \geq 3$
Single SBC	E	N	
Battery	E	N	
IMU	E	N	
Motor torque	E	N	
Motor oscillation frequency	E	N	$F \geq 1.5Hz \text{ at } \pm 60^\circ$
GRF-sensors	E	W	
Real-time hardware	E	W	
Joint-angle sensors	E	O	
CPG + reflexes	C	W	
Modular architecture	C	W	
Inverse kinematics	C	W	
Real time	C	W	
Torque control	C	O	
Number of handlers needed	S	N	< 2
Torque restriction or control redundancy	S	N	
Harmful materials used	S	N	None
Mechanical compliance	S	W	
Max price per unit	P	N	$P < 10k \text{ CHF}$
Max price per unit	P	W	$P < 5k \text{ CHF}$

1.3.2 Bio-mimicry versus Bio-inspiration

To incorporate information that we gain from observing and analyzing animals, there are generally two possible ways. One is bio-mimicry or trying to copy the role model as exactly as possible, not deviating from anatomy, physiology, control, or other aspects if realizable with technical means. The other is bio-inspiration, where the role-model is analyzed, simplified and broken down to the principle level, where findings can rather easily be extracted and copied. These approaches are often described and used in control templates and anchors [14]. As a result of this, a template, following the strictly bio-inspired direction, is simplifying the animal and its motion to the highest degree, enabling comparison on the principle-level between species. Template models can be tested against empirical data (for example SLIP-model). Anchors build upon templates and embed them in a more complex and realistic morphological and physiological model (towards bio-mimicry). Here details ranging from muscle-placement, specific joint torques up to the underlying neural control networks can and should be integrated. Both templates and anchors for control can then be used in combination with detailed mechanical models to explore specific neuro-mechanical questions. Our work should use such approaches, but find a middle way, to find an acceptable level between biological detail and complexity of implementation. Hence, we evaluated both bio-mimicry and bio-inspiration subjectively in Table 1.2 to decide on our basic approach towards agility in biorobotics.

Table 1.2 – Advantages and Disadvantages of a bio-inspirational (BI) vs. bio-mimicry (BM) approach towards agile robotics; scoring 1 (hard/bad) to 5 (easy/good); the weight and rank distribution, resulting from a subjective Analytical Hierarchical Process [15] analysis by the author, can be found in appendix Appendix B

	Rank	Weight	BI	Weighted	BM	Weighted
Value of results for biology	1	0.23	3	0.689	5	1.148
Value of results for engineering	1	0.23	5	1.148	3	0.689
Available Data	2	0.176	4	0.706	5	0.882
Implementation with current technology	3	0.166	5	0.830	2	0.332
Complexity of implementation	4	0.13	4	0.520	2	0.260
Time needed for concept	5	0.04	3	0.120	5	0.201
Time needed for implementation	6	0.028	4	0.112	3	0.084
Sum/ weighted Sum		1	28	4.126	25	3.597

Based on the results of Table 1.2 we chose to follow the path of bio-inspiration with slight bio-mimicry influences (e.g., in geometry and kinematics), as we think this suited for robot development with current technical means and will achieve higher results for technology while giving advancing knowledge in biology as well.

1.3.3 Hardware versus Simulation

Another basic decision is, whether simulation in combination with hardware is needed for a complete and concise analysis of agility or if one without the other is sufficient. Our questions concerning agility can be partially addressed by either method with simulation being efficient for template-research and hardware more for resulting anchors. Wanting to enhance full body movement towards agile locomotion, a parallel usage of simulation and hardware seems ideal, as advantages and disadvantages complement each other, see Table 1.3. Especially for model validation, real-world experiments are essential, and in contrast, large and versatile parameter explorations are hard to do with hardware. Consequently, pursuing both approaches gives the most complete and accurate results.

Table 1.3 – Advantages and disadvantages of a hardware vs. simulation centered approach towards agile quadrupedal robotics (information on simulation was granted by a colleague and extended by the author; the original version can be found in Appendix B); scoring 1 (hard/bad) to 5 (easy/good), the weight and rank distribution, resulting from a subjective Analytical Hierarchical Process [15] analysis by the author, can be found in appendix Appendix B

	Rank	Weight	HW	Weighted	Sim	Weighted
Real world validation	1	0.143	5	0.715	2	0.286
Translation to hardware	2	0.143	5	0.715	2	0.286
Translation to simulation	3	0.135	3	0.405	5	0.675
Wrong conclusions from results	4	0.133	3	0.399	3	0.399
Validation on the system understanding	5	0.082	4	0.328	4	0.328
Accessibility of states	6	0.065	3	0.195	5	0.325
Freedom of exploration / versatility	7	0.06	3	0.18	5	0.3
Complexity of development	8	0.052	3	0.156	2	0.104
Validation time needed	9	0.047	4	0.188	2	0.094
Total development time needed	10	0.045	3	0.135	3	0.135
Effective implementation of ideas	11	0.043	4	0.172	4	0.172
Rapid implementation of new ideas	12	0.034	2	0.068	5	0.17
Cost	13	0.019	2	0.038	4	0.076
Sum/ weighted Sum		1	44	3.694	46	3.35

Unfortunately, if not part of a large team working together on the same topic, realizing both approaches in a sufficiently satisfying manner, and in the amount of time in one's Ph.D. is rather hard, if not impossible. For my work, coming from a rather hands-on mechanics and hardware mindset, the path of relying on a physical implementation, with very little simulation (kinematics simulation for robot control) seemed the right choice.

1.3.4 Small, Low-cost Robots versus Large High-end Robots

Depending on the goal of one's development, both extreme directions, small and low-cost (SLC) or large and high-end (LHE) have respective strong and weak points. We used the results, depicted in Table 1.4, that we used for our decision process. The state-of-the-art in section 4.1 illustrates the various choices for SLC, LHE or in between, made by different research groups all over the globe and underlines the diversity in today's legged robot development.

Table 1.4 – Advantages and disadvantages of a small, low-cost (SLC) vs. large high-end (LHE) agile robot; adapted form [11] and extended; scoring 1 (hard/bad) to 5 (easy/good), the weight and rank distribution, resulting from a subjective Analytical Hierarchical Process [15] analysis by the author, can be found in appendix Appendix B

	Rank	Weight	SLC	Weighted	LHE	Weighted
Safety in direct handling	1	0.278	4	1.113	2	0.557
Complexity of development	2	0.114	2	0.228	3	0.342
Absolute performance	3	0.095	3	0.284	5	0.474
Available space	4	0.081	2	0.163	5	0.406
Available payload	4	0.081	2	0.163	5	0.406
Cost	4	0.081	4	0.227	2	0.114
Ease of modification	5	0.077	4	0.306	3	0.230
Production time needed	6	0.048	4	0.193	3	0.145
High power requirements	7	0.044	4	0.174	2	0.087
Development time needed	7	0.044	3	0.133	3	0.133
Validation time needed	8	0.041	3	0.123	3	0.123
Operators needed	9	0.022	5	0.111	3	0.067
Test-site size	10	0.018	4	0.071	3	0.053
Sum / weighted Sum		1	44	3.289	42	3.136

For our relatively small team, medium budget and time, as well as the intention of building robots that can easily and safely be handled by untrained personnel (students), the choice of creating small, and low-cost robots became favorable. Deviation from this approach is considered feasible if the handling safety is not diminished (e.g., implementation of high-end sensors for sophisticated control).

1.3.5 Conclusion

As was shown from our (subjective) review on employed base-choices, all approaches are almost equally graded and completely depended on circumstance and research questions to address. We will follow a mainly bio-inspired path (with slight bio-mimicry influences), building multiple quadrupedal robots in hardware, iteratively approaching our goal of achieving

1.3. Approach II: Achieving Agility by Prototyping Legged Robots

agility in legged robotics.

The following parts will highlight our efforts to define and benchmark agility (Part I) as well as our development process and validation towards an agile quadrupedal robot (Part II). The respective states of the art are included in the parts mentioned above. The specific organization can be found in chapter . For the content of this written thesis, I adopted and extended several figures, tables, and text from previously authored content. Authorization from lead- or co-lead-authors was granted, where necessary.

Defining and Benchmarking Agility **Part I**

2 Defining Agility

Agility is one of the terms making people realize that an animal, a robot, or some other system is extraordinary in some manner. It is often associated with the speed of executing a specific task, like moving forward or turning. It is additionally used in a manifold of areas, such as business, production [16], or animal sports, but sometimes with completely different meanings. The same word contains, depending on the field of usage, different key aspects and is thus not homogeneous in its definition. But what exactly is agility then? How can it be described, quantified and what does it imply for the field of mobile robotics? One possible, mainly locomotion-related, the definition is found in Wikipedia [17]:

[...] Agility or nimbleness is the ability to change the body's position efficiently and requires the integration of isolated movement skills using a combination of balance, coordination, speed, reflexes, strength, and endurance. Agility is the ability to change the direction of the body in an efficient and effective manner [...]

This definition, although unreferenced, gives a good high-level view on locomotion-related agility with its manifold of components. Consequently, the agility of a system or a being is hard to grasp, measure and quantify. Hints of how to draw a definition it and build a corresponding benchmark may be taken from a great source of inspiration for technological systems, nature. Here, agility manifests in various species. Furthermore, humans strive to compare and measure themselves and their animal partners throughout various kinds of competitions highlights specific clues towards finding a solution to our benchmark related problem and the physical aspects needed to achieve agile movement in robots.

In this part, we focus on to the agility definition related to the field of multi-legged, terrestrial locomotion. Covering even more areas of locomotion would surpass the framework of this thesis. This section starts our aim of understanding and achieving agile motion by presenting a concise definition of the term agility inspired by the analysis of different natural role models.

chapter 3 will build on this definition to propose a novel benchmarking scheme for multilegged robots.

2.1 Agility in Wildlife

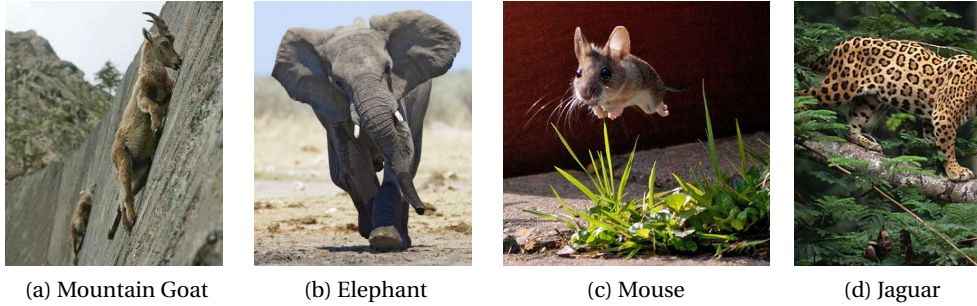


Figure 2.1 – Animals in the wild need to adjust to their environments to survive; example animals of different sizes with their unique adaptation to agility; (a) mountain goat climbing extreme slopes [18], (b) Elephant charging with up to 40km h^{-1} [19], (c) Mouse performing a leap of multiple body heights and body lengths [18], (d) Jaguar balancing on a downward slope (tree) [20]

Animals that do not live in captivity need to be self-sustainable, which means to be able to find food, reproduce, evade predators or be themselves the predator. Especially the last two points force animals to have a large variety of motion-patterns, such as crawling, sneaking, jumping, running, climbing and many others. Animals, in general, are not specialized in one task, although it might seem like it for some of them. The cheetah as the fastest sprinter for example ($v_{max} = 120\text{km h}^{-1}$ [21]), surely seems specialized in speed but is amongst others also capable of sneaking or crawling. An elephant appears to be specialized in long distance slow motion, but when threatened it can run up to 40km h^{-1} and execute sharp turns [21]. An interesting aspect to look at is thus, how agility can be correlated to the scale of a system or animal. If you would compare a mouse with an elephant for instance, which one is more agile? An animal, in general, adapts its agility to the environment and the conditions it is living in. So what is agility in animals? Is it just speed or just ability to climb or crawl? We believe that it is a combination of all the locomotion related tasks and that they are firmly coupled to each other, especially when looking at how animals adapt their physical form to minimize energy consumption while maximizing their agility. Agility is thus not a single feature of locomotion but a group of complex motion patterns and should be related to the respective energy cost. Also, agility is not something fixed to ground locomotion, but also flying, swimming and diving. As previously mentioned we will concentrate for this thesis on terrestrial locomotion.

2.2 Agility in Sport

This section will highlight our observations towards defining and benchmarking agility when looking at human- and animal-sports. Observations from sports are generally qualitative but will influence our definition and the benchmarking structure in chapter 3 decisively as can already be seen in the conclusion of this section.

2.2.1 Agility in Animal-Sports

In sports performed in cooperation of human and animal, two examples of extreme agility-demonstration come to mind: dog-agility, where the name already includes the main feature of the sport, and horse-show-jumping, that also provides an impressive demonstration of control and explosive force. The core of both sports is a series of complex movements, executed with a minimal number of mistakes and completed as fast as possible. Like all sports, high amounts of energy are used by the animals, resulting in visible fatigue. This should be further included in our observations. In horse show-jumping, the animal (with the human on the back) has to

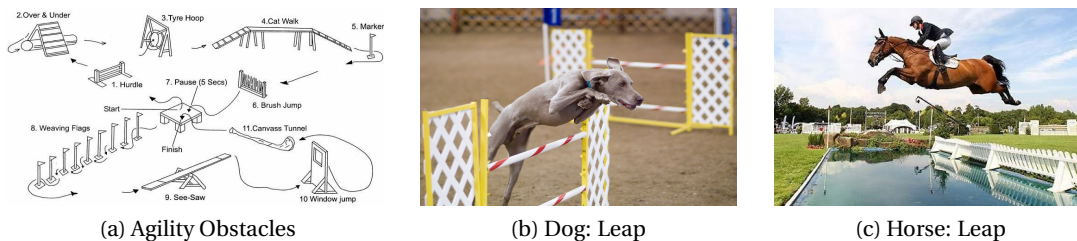


Figure 2.2 – Examples of agile animal sports: (a) Layout of a dog-agility course with high complexity in the path and a multitude of obstacles [22], (b) Dog performing a high-jump during a dog-agility competition [23], (c) Horse performing a jump during horse show jumping [24]

perform a series of leaps over differently shaped obstacles in combination with a pre-defined path, including accelerations and sharp turns. This sport demands from the horse the ability to precisely follow the commands of its rider and to explosively execute difficult jumping and turning tasks in succession of each other. Time and precision are of the essence. A scoring scheme also includes a penalty system taking into account failures in execution of any task (e.g. knocking down a rail).

Dog agility, on the other hand, varies even more in the complexity of tasks at hand. The dog has to follow a specific course of jumps, ramps, balancing-boards, and other obstacles as fast as possible, with specific stops to test control, making the perfect run even more difficult. The dog-trainer is allowed to give directional commands, as guidance. The decision on how to

fulfill these is up to the dog but also influenced by lengthy and intense training beforehand. The quick and fault-minimal fulfillment of the course is taken as the grading measure of this sport.

Our observation showed that agility in animal sport is focused mainly on precision and speed. The best reference is dog-agility as the task-space is vast. It serves additionally as a guide to draw a baseline for comparison and normalization in subsection 3.2.1.

2.2.2 Agility in Human-Sports

[25] intensively analyzed the role of agility in human sports by a literature review of different sports scientists. The findings of their work are summarized below and concur widely with the observations we had from our animal analysis. Criteria for agility are:

1. Must involve the initiation of body movement, change of direction, or rapid acceleration or deceleration.
2. Must involve whole-body movement.
3. Involves considerable uncertainty, whether spatial or temporal.
4. Open skills only (meaning skills that do not require a pre-learned stimulus to be activated; one could say: natural behavior).
5. Involves a physical and cognitive component, such as recognition of a stimulus, reaction, or execution of a physical response (the skill must be activated by recognizing its need due to outside factors, e.g., leg retraction induced by hitting an obstacle with the foot).

Agility in their opinion should incorporate the whole body with changes of direction executed in a reactive rather than a planned manner. Reactive behaviors show the bodies general readiness to cope with uncertain situations and thus react nimbly or with agility. Preplanned behavior can make use of motion patterns one would not naturally use for the task at hand, but which can give (especially in sports) the overall best performance in this specific task. On the other hand, they exclude preplanned skills like straight and steady running from the term agility. Some of these banned skills, like fast forward running, might in our opinion still be valid to include in the agility definition as performing them shows excellent value for locomotion itself. Another interesting approach is presented in [26]. Here not agility in human sports per se is researched, but a benchmark for human-likeness of bipedal robots is defined. Although there is no time factor involved in the referenced work, many different tasks are described, that the robot has to fulfill to get a good score. The idea of separating behaviors is very interesting and concurs with our views on how to define agility (see chapter 3).

2.3 Agility in Legged, Terrestrial Robotics

This section shows our observations towards defining agility when looking at it from a more technological perspective. Agility as a term is used in a manifold of robotics papers. Hereby it is often characterized only as a synonym for forward speed, maneuverability (e.g., the ability to do controlled change in movement or direction) or is just mentioned as a term symbolizing high performance of a robot or animal [27–36]. Forward speed is undoubtedly a critical factor in agility and thus often used for comparison of many robots with significant variance in size (see Table 4.1), but in our opinion not sufficient to describe an agile system to its fullest.

2.4 Conclusion for Agility Definition

From our observations in the animal kingdom and the legged robotics world, we draw the following conclusions, which are summarized in a definition of agility

2.4.1 Conclusion from Wildlife, Human- and Animal-Sports

To conclude our observations of nature, there are some key aspects of locomotion that can be seen as main features to describe agility sufficiently and simple enough for further quantification:

1. Agility is not the result of execution of a single skill, but a complex set of motion patterns as well as the possibility to rapidly switch between them.
2. Ideally, reactive execution of known skills with minimal prior planning
3. Agility varies from one species to another and thus should, at least, be defined differently in terrestrial, aerial and aquatic locomotion (in case of interest in aquatic robots, please refer to [37]).
4. Precision in task execution is one of the key aspects.
5. Speed of the task execution is another key aspect.
6. Agility is related to the scale of the system or animal. Thus it should be normalized to attempt a comparison.
7. The energy-cost to execute a task should be part of benchmarking a system's agility.

2.4.2 Conclusion from Agility Definitions or Evaluations in Robotics

The realm of robotics did not yet produce common methods to define agility. Speed (non-dimensional and dimensional) is well researched, and some attempts to benchmark other tasks are made. Besides the general understanding, that agility stands for high performance or maneuverability, there are, to our best knowledge, no other attempts in its definition. The topic of measuring agility will be continued in section 3.2, where a new and general benchmark for legged systems is presented.

2.4.3 Definition of Agility for Legged, Terrestrial Robots

We close this section with a high level definition of agility, that we followed in our work.

Agility is representing a previously acquired and size dependent set of locomotion skills, executed in a precise, fast and ideally reflexive manner to an outside stimulus.

3 Agility Benchmark

In this chapter, we present a novel and practical approach towards benchmarking agility, defined in chapter 2. We focus on terrestrial, legged locomotion in the field of quadruped robotics. We define agility as the ability to perform a set of different tasks executed in a fast and efficient manner. A review of existing characterization and benchmarking methods in robotics is done and added to the final evaluation of the usefulness of the proposed benchmark. The actual normalized benchmarking values are defined, and measuring methods, as well as an on-line database for agility number collection and distribution, are presented. To provide a baseline for agile locomotion, various videos of dog-agility competitions were analyzed and agility numbers calculated where applicable. Finally, a validation and first implementation of the benchmark is done with different robots directly available to the authors. Robots used are the mammal-like, cat-sized robots Cheetah-Cub, Cheetah-Cub-S, Cheetah-Cub-AL, and Oncilla as well as the amphibious robot Pleurobot, modeled after a salamander. In conclusion, our benchmark will enable researchers not only to compare existing robots and find out strengths and weaknesses in different design approaches but will also give a tool to define new fitness functions for optimization or learning processes and future robot developments. We hope to contribute to establishing new ways of how robots and their natural role models are measured and thus intensify the links between biology and technology even further.

3.1 Introduction and Review on Characterization and Benchmarking Methods

Movements of a bio-inspired robot can be characterized and often evaluated easier than artificial structures/robots by comparing to their natural counterparts. As many of these systems try to replicate their role models to a certain degree, methods from decades of biological research can be applied for characterization. In locomotion related robotics this includes mainly the characterization of the gait in its different facets. Additionally, newer techniques

and characteristic numbers can help to quantify robot or animal performance. This section will review a selection of such aspects and close with a conclusion drawn for the development of our benchmarking method.

3.1.1 Gaits

A general gait description and factors used for characterization will be shown in this part. The understanding, characterization, and analysis of familiar patterns is a basic tool used since the times of Hildebrand and Alexander [38, 39]. Up to today, this method of gait-definition is used as a first benchmark to assess the quality of a gait.

A gait can be defined as

"..an accustomed, cyclic manner of moving in terrestrial locomotion." [38]

Animals and humans use different kinds of gaits to move with various speeds in a controlled and metabolically cost-efficient way [40]. These locomotion patterns are influenced and characterized by different factors, which vary from species to species, such as actions of the head, spine, tail or legs. Another strong factor that also varies the gait is the number of legs; we differentiate between bipedal, quadrupedal gaits, etc. To describe different gaits, Hildebrand and other researchers used mainly the timing of the footfalls and the duration of the contact between feet and ground or the duration of the flight phase. In general, there are two classes of quadrupedal gaits, asymmetrical and symmetrical ones. They can be further divided into specific movement patterns, that will be described in the following paragraphs [38, 39, 41–44].

Characterization of Gaits

While naming the gaits themselves is essential, having the primary terminology that allows the characterization on a general basis is advantageous. The following section will show the usually applied criteria as well as give an overview over quadrupedal gaits.

Symmetrical Gaits The trademark of a symmetrical gait is that girdle paired legs are exactly one-half cycle out of phase between left and right legs, regardless of the relative timing of forelimbs and hindlimbs. The symmetry is referring to a kind of mirror-symmetry in time. [38, 41–43]. Although not perfectly symmetric, the lateral sequence walk is generally considered to fall into this category. One could see the bound as a symmetric gait if looking at the fore-hind-symmetry of the movement, but historically the convention is only considering symmetry of girdle paired legs. In consequence bound is an asymmetric gait. Symmetric gaits are mostly

3.1. Introduction and Review on Characterization and Benchmarking Methods

employed for relatively low to medium speeds [39, 43]. The category includes: a) pace b) walks c) running walks d) trots

In Figure 3.1 examples of the footfall patterns in relation to the stride time are given by a gait diagram after Hildebrand [38, 41].

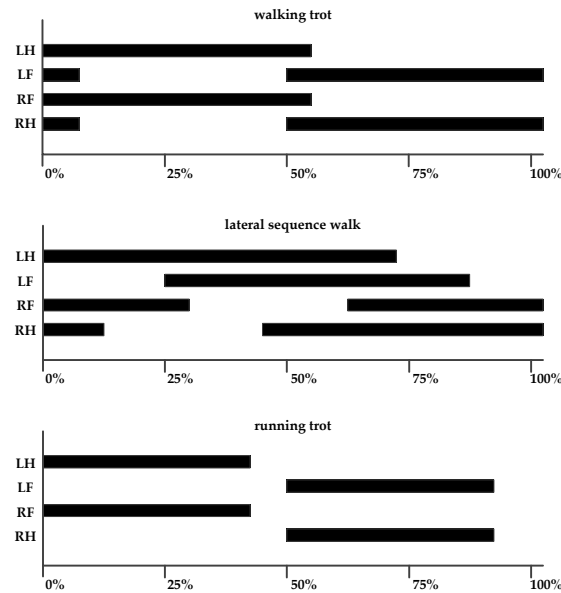


Figure 3.1 – Examples for symmetrical quadrupedal gaits (only qualitative for illustration)

Asymmetrical Gaits For moderately high and fast terrestrial locomotion most animals use asymmetrical gaits, that make up any gait, not being symmetric [38, 41–43]. Examples for asymmetrical gaits are as follows (see Figure 3.3): a) half-bounds b) pronk c) gallops d) bounds



Figure 3.2 – Rotary gallop of a cheetah illustrating large flight-phases in this highly dynamic gait [40]

In most high-velocity gaits, flight phases, that means phases in which the animal moves ballistically forward without ground-contact, are parts of these asymmetrical gaits. The heavy usage of the elastic back during that movement can be seen in Figure 3.2 for the rotary gallop of a cheetah [40] and may be explained through energy advantages by passive elastic movement.

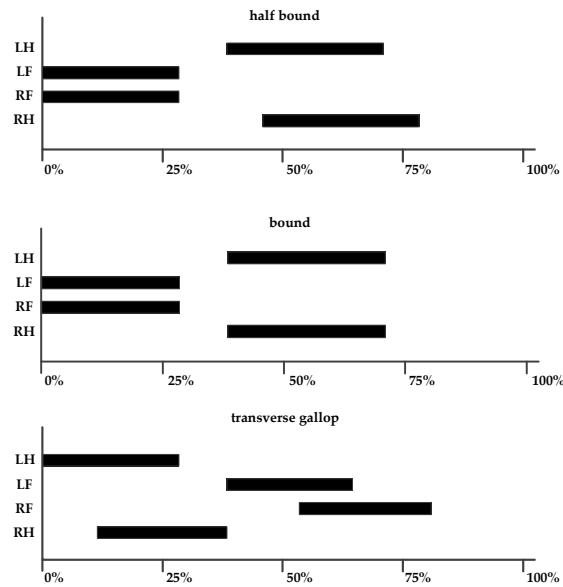


Figure 3.3 – Examples for asymmetrical quadrupedal gaits (only qualitative for illustration)

Stride As a stride, we define one completed moving-cycle and thus making the stride-frequency, the number of strides per unit time. The stride length is described as the distance traveled in one stride (e.g., from one-touch-down to the next) [39, 43].

Duty factor - DF Another factor that can help determine the nature of a gait is the duty factor, a unit-less number. It describes the fraction of the stride duration that one foot is in contact with the ground and thus determining the relation of swing- to stance-phases of a gait. Walks usually have a $DF \geq 0.5$, while gaits with flight phases, like the bound, show $DF \leq 0.5$ [3, 45].

Lead Sequence In any gait, the first foot of a pair to touch the ground in a stride is named trailing foot; respectively the second one to touch, the leading foot. The definition of high-velocity gaits, especially the gallop, requires one other factor, which is the lead sequence. This sequence allows the differentiation into transverse (forefeet have the same lead as the hind-feet) and rotary motion patterns. Different combinations of footfalls mark different gaits (Figure 3.3). The simultaneous footfall of the front and hind feet, for example, terms the gait as a bound, while a simultaneous hind footfall and a definitive fore lead characterize the gait as a half-bound.

Fast runners as the cheetah (*Acinonyx*) or the antelope and gazelle (*Gazella*) prefer hereby the

3.1. Introduction and Review on Characterization and Benchmarking Methods

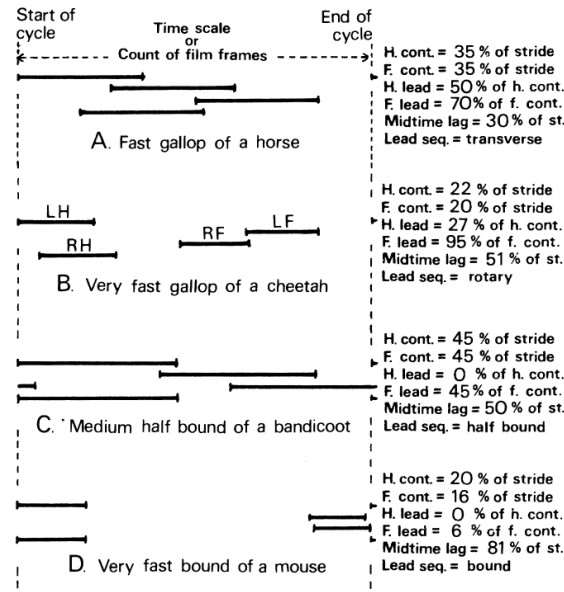


Figure 3.4 – Different gaits with their respective lead-sequence after Hildebrand [38]

rotary sequence over the transverse (Figure 3.4). Bound and half-bound are mostly used by small and agile mammals, like mice or bandicoots [38].

3.1.2 Dimensionless Numbers

Well defined scores, like the Froude number used by [39] or the normalization of robot speed to body-lengths per second (BL/s) in combination with the Cost of Transport (COT) [46] are accepted throughout the legged robotics community. In our opinion, this acceptance has its basis in the ease of use of these scores. One only needs simple geometrical measurements as well as energy- and speed-data for their generation. This ensures accessibility and easy understanding for a broad audience. Both scores quantify straight forward or backward locomotion and thus are not sufficient for entire broad feature set of agile locomotion.

Froude number

To be able to compare dynamical motion during similar gaits in different sized animals the Froude number (FR) was introduced [3, 39, 43]. It is again a unit-less number calculated with the use of earth's gravity (g), the hip joint height from the ground (h) and the mean forward

velocity \bar{v} , combined in the following formula:

$$FR = \frac{\bar{v}^2}{g \cdot h} \quad (3.1)$$

A Froude number $FR > 1$ is considered a threshold indicator for dynamical, terrestrial locomotion. [3, 43]

Cost of Transport

Cost of Transport, or short COT, is often employed to put systems with different masses and actuation styles into relation. It symbolizes the energy or power cost a robot needs to run at a certain mean velocity. This value is often presented with a unit, although a unit-less notation is possible as well. The COT only includes the locomotion related energy consumption (P_{el}), excluding standby consumption of motors or electronics, robot weight (m), gravity (g) and mean velocity (\bar{v}):

$$COT = \frac{P_{el}}{m \cdot g \cdot \bar{v}} \quad (3.2)$$

3.1.3 Benchmarking Environments and other Robot Benchmarks

As the previously mentioned comparison and characterization approaches were not sufficient for all applications, some scientists developed benchmarking methods by introducing performance matrices or setting up standard environments to evaluate their robots. As an example of implementation of test areas within specific scenarios, the framework of search and rescue operations, such as "NIST standard Test Bed for Urban Search and Rescue", is often chosen. As a result of this the primary measure is not the agility of a robot itself, but amongst others, the number of victims found in a cluttered terrain [47–50]. Of course, navigation through an almost realistic disaster terrain is very demanding for a robot and may even not yet be possible, but this method gives no quantitative and comparable values for the desired specific agility benchmarking. Other benchmarks that are task driven can be found with the DARPA robotics challenge and generally military fitness tests. Here, many tasks besides the pure locomotion related components are evaluated. The general measure is success and speed of the execution, which can be related to our later proposed benchmark, although we will specialize on locomotion aspects. Additional to the approach above, analysis of acceleration capabilities in the framework of dynamic capability equations can be used to identify the performance of a robot [51, 52]. This method is rather complex and thus not very attractive for

3.1. Introduction and Review on Characterization and Benchmarking Methods

us, as we aim for an easy-to-use benchmark. [53] proposed a framework for benchmarking versatility in comparison to the robots complexity. Although this approach showed many interesting ideas, a big challenge is the complexity of the method itself. It includes comparisons of land, water and aerial robots in one framework, which makes it easy to get confused. A key factor in their proposed method is a weighting system. The weights are chosen without clear background data. Unfortunately, this makes agreeing with and following the proposed method difficult. The next attempts on measuring agility we want to mention is shown for the case of the leaping quadruped Canid [54]. [55] introduced a coefficient for specific agility during stance using the mass-normalized change in extrinsic body energy. They argue that the change in extrinsic body energy, especially during leaping, reflects the effect of an agile movement on the robot best. This specific agility score is not dimensionless and thus scaling effects have to be taken into account when comparing different robots. Another leaping metric can be found in [56]. Here frequency and velocity of consecutive jumps are brought into relation with each other. The metric itself resembles our approach strongly as it takes the time for the maneuver as well as the height into account. The main differences are the non-dimensionless nature of the proposed score and the fact of taking an average speed of multiple jumps instead of putting emphasis on repeatability. Positioning these approaches as a valid alternative to our method, especially when performing jumps, we acknowledge the strong influence of the robot energetics and thus will try to incorporate an inspired value. Another interesting approach is presented in [26]. Here not agility per se is researched, but a benchmark for human-likeness of bipedal robots is defined. Although there is no time factor involved in the referenced work, many tasks are defined that the robot has to fulfill to achieve a good score. The idea of measuring behaviors separately and referencing it to a baseline is very interesting and concurs with our views on how to define agility.

3.1.4 Conclusion for Benchmarking Methods

The realm of robotics did not yet produce common methods to benchmark agility. Speed (non-dimensional and dimensional) is well researched, and some attempts to benchmark other tasks are made. The most used benchmarking scores are very easy to use, only requiring little experimental data and utilizing geometrical measurements of the robots to scale between platforms. The approach of setting up a test bench is also valid, but unfortunately, very time consuming, expensive and complex. Concluding from our observations, our proposed method should be easy to use, with as little experimental data as possible and incorporate robot energetics, if applicable.

3.2 Agility Benchmark

This section is depicting our efforts on the generation of a certain agility benchmark, taking the findings from existing benchmarks and our agility definition into account.

3.2.1 Proposed Method for Benchmarking Agility

As agility, in general, is highly related to the speed of how a task can be done, all scores proposed are normalized and dimensionless speeds, guaranteeing comparability between different robots and animals. Normalization and dimensionless scores are achieved by employing the scaling method of Hof [57]. As described in the following, there are thirteen scores which should, in the authors' opinion, form the core concept of agility in legged terrestrial systems. The higher the scores for turning (A_{ts} and A_{tr}), leaping (A_l , A_{lv} and A_j), slope running (A_{s1} , A_{s2} and A_{s3}), standing up (A_{st1} , A_{st2}), sidestepping (A_{ssstep}) as well as forward and backward locomotion (A_{fl} and A_{bl}) are, the better the agility is. The lowest possible score is zero. Although negative scores are possible, we disregard them as they only show how bad a system is in achieving a motion. This badness-score may nevertheless give researchers clues for their robot improvement to reach an agility score higher than 0. To take the quality regarding precision and repeatability into account, certain variance factors will be introduced for each score. Furthermore, an overall weighted agility score as the sum of the components is proposed and also correlated with the cost of agility (COA). The scores are kept as simple as possible (see Table 3.1 and respective description paragraphs) to allow easy experimental implementation. To provide a baseline for agile locomotion, various videos of dog-agility competitions were analyzed and agility scores calculated where applicable. For the rest of the scores, intuitive values were chosen, or different means were applied. The exact baseline-method is presented later on in this section. Distribution and publication of the agility scores will be facilitated by an open-access online database hosted on the EPFL network [agility.epfl.ch].

Measurement of Geometrical Values

To allow uniformity when defining the geometrical values for robots with different shapes and number of legs, the following scheme should be applied. Robot length l_R is to be measured from the first hip axis to the last one with fully elongated body. The width w_R is defined as the distance between the outer edges of two opposite legs at hip level. The last value, robot height is taken as distance from ground to hip-axis in an upright standing posture. The same position is used when defining the height of the center of mass (COM), h_{COM} , also including the mass of the legs.

Table 3.1 – Summary of benchmarking calculations

Number	Variance	Calculation
Turning with a radius	$q_{tr} = 1 - \left(\frac{\Delta r}{0.25 \cdot r} \right)$	$A_{tr} = q_{tr} \cdot \frac{h_R}{r} \cdot \frac{p}{t} \cdot \sqrt{\frac{h_R}{g}}$
Turning on the spot	not needed	$A_{ts} = \frac{p}{t} \cdot \sqrt{\frac{h_R}{g}}$
High-jump	$q_j = 1 - \left(\frac{\Delta h_j}{0.25 \cdot h_j} \right)$	$A_j = q_j \cdot \frac{h_j}{h_R} \cdot \frac{1}{t} \cdot \sqrt{\frac{h_R}{g}}$
Leap out of stance	$q_l = 1 - \left(\frac{\Delta l_l}{0.25 \cdot l_l} \right)$	$A_l = q_l \cdot \frac{l_l}{h_R} \cdot \frac{1}{t} \cdot \sqrt{\frac{h_R}{g}}$
Leap out of motion	$q_{lv} = 1 - \left(\frac{\Delta l_{lv}}{0.25 \cdot l_{lv}} \right)$	$A_{lv} = q_{lv} \cdot \frac{l_{lv}}{h_R} \cdot \frac{1}{t} \cdot \sqrt{\frac{h_R}{g}}$
Slope up	$q_s = 1 - \left(\frac{\Delta w_s}{w_R} \right)$	$A_{s1} = q_s \cdot i_{s1} \cdot \frac{h_{com}}{h_R} \cdot \frac{l_s}{h_R} \cdot \frac{1}{t} \cdot \sqrt{\frac{h_R}{g}}$
Slope down	$q_s = 1 - \left(\frac{\Delta w_s}{w_R} \right)$	$A_{s2} = q_s \cdot (-i_{s2}) \cdot \frac{h_{com}}{h_R} \cdot \frac{l_s}{h_R} \cdot \frac{1}{t} \cdot \sqrt{\frac{h_R}{g}}$
Slope side	$q_s = 1 - \left(\frac{\Delta w_s}{w_R} \right)$	$A_{s3} = q_s \cdot i_{s3} \cdot \frac{h_{com}}{h_R} \cdot \frac{h_R}{w_R} \cdot \frac{l_{s3}}{h_R} \cdot \frac{1}{t} \cdot \sqrt{\frac{h_R}{g}}$
Standing up 1	$q_{st} = \frac{m_{succes}}{10}$	$A_{st1} = \phi \cdot \frac{1}{t} \cdot \sqrt{\frac{h_R}{g}}$
Standing up 2	$q_{st} = \frac{m_{succes}}{10}$	$A_{st2} = q_{st} \cdot \frac{1}{t} \cdot \sqrt{\frac{h_R}{g}}$
Side-stepping	$q_{step} = 1 - \frac{\Delta l_s}{0.25 \cdot l_R}$	$A_{step} = q_{step} \cdot \frac{w_s}{h_R} \cdot \frac{1}{t} \cdot \sqrt{\frac{h_R}{g}}$
Forward locomotion	$q_{fl} = 1 - \frac{\Delta w_{fl}}{w_R}$	$A_{fl} = q_{fl} \cdot \frac{l_{fl}}{h_R} \cdot \frac{1}{t} \cdot \sqrt{\frac{h_R}{g}}$
Backward locomotion	$q_{bl} = 1 - \frac{\Delta w_{bl}}{w_R}$	$A_{bl} = q_{bl} \cdot \frac{l_{bl}}{h_R} \cdot \frac{1}{t} \cdot \sqrt{\frac{h_R}{g}}$

Turning with a Radius

The first values, time taken for the maneuver t [s] and number of turns achieved in that time p form the core of the equation. After Hof [57] this is implemented by division of the time through the square root of robot height (h_R [m]) divided by gravity (g [m s^{-2}]). In addition, a term for normalization of the turning radius r [m] with the robots height h_R [m] is added. The last term is the variance of the turn q_{tr} [%]. The variance is describing how well the robot can perform an ideal circle and is measured by the distance (orthogonal to the movement direction) of starting point to endpoint after **10 consecutive turns**. If the robot's deviation from the ideal circle is larger during the turn (e.g. irregular circle, ellipse etc.) and coming back to the starting point, the larger distance should be chosen to calculate the turning variance. We define a variance larger than one quarter of the mean turning radius to mark highly unreliable behavior and thus set the agility value to zero. In case of on-the-spot turning, this value would become 1 and the radius 0, resulting in a non-solvable equation. Thus the formula for A_{ts} applies in this special case.

$$q_{tr} = 1 - \left(\frac{\Delta r}{0.25 \cdot r} \right) \quad (3.3)$$

$$A_{tr} = q_{tr} \cdot \frac{h_R}{r} \cdot \frac{p}{t} \cdot \sqrt{\frac{h_R}{g}} \quad (3.4)$$

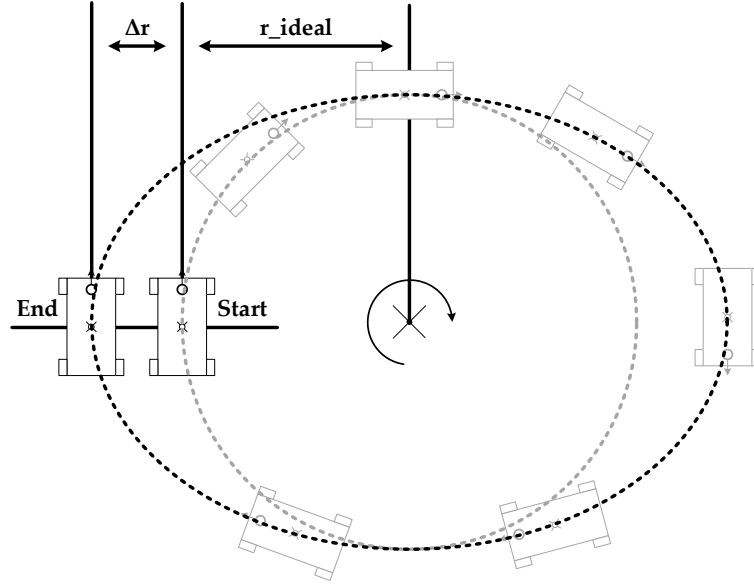


Figure 3.5 – Illustration of the turning behavior of a 4-legged robot with an ideal radius r_{ideal} difference between start and end point Δr

Turning on the Spot

A_{ts} is chosen if the robot's rotational axis is exactly in the geometric middle, otherwise turning with a radius applies. A robot capable of spot turning will always achieve higher turning agility, than a robot that can only turn with a radius, if these skills are not separated as the radius is equal to 0. On the other hand, if the robot shows both skills, higher overall agility should be achievable. The main features of the on-the-spot turn are the time needed to complete the turning procedure t [s] and the number of turns p around the robot middle axis, which results in angular speed. A variance or quality of the turn is not needed as any diversion from the rotation around the middle axis results in a turning with a radius and the respective score applies. The only normalization with respect to the robot that is needed is a dimensionless time.

$$A_{ts} = \frac{p}{t} \cdot \sqrt{\frac{h_R}{g}} \quad (3.5)$$

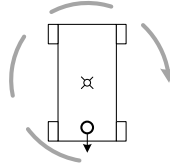


Figure 3.6 – Illustration of spot turning behavior of a 4-legged robot

Jumping and Leaping

Both movements are very agile and explosive, but pose a risk for robots as damage can occur. Successful execution is thus a sign for high capability and should be represented in our benchmark. Jumping has no or only little horizontal movement as it is describing how high the robot can jump, whereas one focuses on the horizontally traveled distance in air when talking about leaping. Both scores include the time for the maneuver t [s], scaled dimensionless, the height of the jump h_j [m] (measured as distance from the hip when standing and at apex height) and the length of the leap l_l [m] (measured at the hip before and after the leap on the first contact with the ground) normalized with the robots' hip height h_R [m]. The variance factors $q(j)$ [%], $q(l)$ [%] and $q(lv)$ [%] give a notion of the repeatability and precision by giving the mean deviation Δh_i [m] in percent of the overall mean jumping height h_j or leaping length l_l [m], measured from **10 repetitions**. Again one quarter of the respective mean value will be the boundary of failure for an agile robot. Leaps out of a running motion should logically

increase A_l through the initial thrust. We encourage users of our benchmark to acknowledge the fact with an index at the score A_{lv} . This score is not different from A_l but gives an indicator of the motion the robot was in, when the leap occurred. The initial velocity should be noted as a remark.

$$q_j = 1 - \left(\frac{\Delta h_j}{0.25 \cdot h_j} \right) \quad (3.6)$$

$$q_l = 1 - \left(\frac{\Delta l_l}{0.25 \cdot l_l} \right) \quad (3.7)$$

$$q_{lv} = 1 - \left(\frac{\Delta l_{lv}}{0.25 \cdot l_{lv}} \right) \quad (3.8)$$

$$A_j = q_j \cdot \frac{h_j}{h_R} \cdot \frac{1}{t} \cdot \sqrt{\frac{h_R}{g}} \quad (3.9)$$

$$A_l = q_l \cdot \frac{l_l}{h_R} \cdot \frac{1}{t} \cdot \sqrt{\frac{h_R}{g}} \quad (3.10)$$

$$A_{lv} = q_{lv} \cdot \frac{l_{lv}}{h_R} \cdot \frac{1}{t} \cdot \sqrt{\frac{h_R}{g}} \quad (3.11)$$

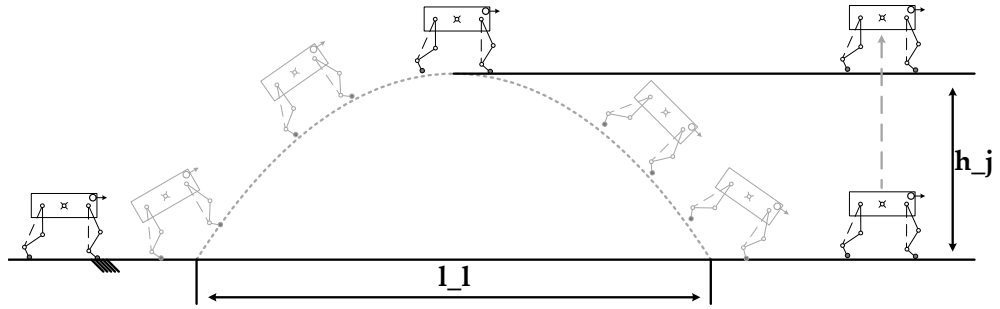


Figure 3.7 – Illustration of leaping and jumping behavior of a 4-legged robot with the jumping height h_j and the leaping distance l_l

Slope Running

Navigation on slopes (climbing would be an exceptional case where the inclined surface is at least orthogonal to the ground) needs almost the biggest variety of parameters to be defined sufficiently. Slopes up- and downwards, with the same calculation but one working with and one against gravity, as well as slopes inclined towards the sagittal plane of the robot and thus orthogonal to the movement direction should be considered. This will be implemented by setting the respective inclination i_{s1} , i_{s2} and i_{s3} in [%], whereas i_{s1} and i_{s3} are positive,

opposing the negative i_{s2} . Geometrical measurements and time are used for calculation of the score. Normalization is taken into account with the height of the robot's center of mass h_{com} [m], its width w_R [m] (especially important as robots with a wide or sprawling posture, have a strong advantage in the side-slope task due to the smaller possibility of falling to the side) and robot height h_R [m]. To receive a dimensionless speed value for the agility representation, the time for the maneuver t [s] and the distance traveled l_s [m] are scaled by the robot height h_R [m] and gravity (as seen before). The variance of the performance influences the measure with q_s where the percentile deviation from a straight path after a distance of **10 body-lengths** in respect to the robot width is calculated. More than one robot width will be seen as too large of a variance and thus considered as not precise enough, setting the agility score to zero.

$$q_s = 1 - \left(\frac{\Delta w_s}{w_R} \right) \quad (3.12)$$

$$A_{s1} = q_s \cdot i_{s1} \cdot \frac{h_{com}}{h_R} \cdot \frac{l_s}{h_R} \cdot \frac{1}{t} \cdot \sqrt{\frac{h_R}{g}} \quad (3.13)$$

$$A_{s2} = q_s \cdot (-i_{s2}) \cdot \frac{h_{com}}{h_R} \cdot \frac{l_s}{h_R} \cdot \frac{1}{t} \cdot \sqrt{\frac{h_R}{g}} \quad (3.14)$$

$$A_{s3} = q_s \cdot i_{s3} \cdot \frac{h_{com}}{h_R} \cdot \frac{h_R}{w_R} \cdot \frac{l_{s3}}{h_R} \cdot \frac{1}{t} \cdot \sqrt{\frac{h_R}{g}} \quad (3.15)$$

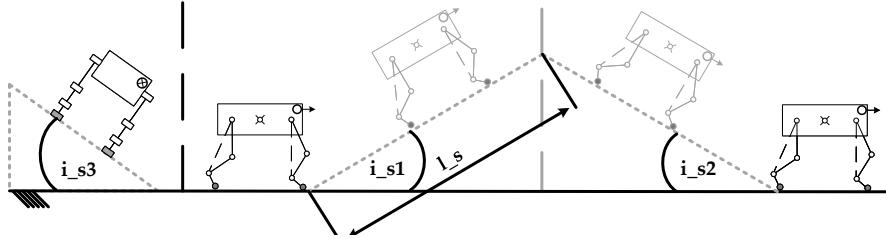


Figure 3.8 – Illustration of the slope running behaviour of a 4-legged robot with the lateral slope on the right (inclination upwards i_{s1} and downwards i_{s2}), the travelled distance on the slope l_s and the slope in the sagittal plane with its inclination i_{s3} on the left

Standing up

Standing up is mostly related to the time t [s] needed to get up from a crouched posture with the trunk touching the ground. This basic behavior is sometimes hard to stabilize and thus worth being considered in our benchmark as score A_{st2} . Even higher skill and agility is needed if the robot is lying on the side or even upside down. This is represented by the angle the robot's sagittal or transversal plane has in the lying position to the normal vector of the flat

ground ϕ [rad]. The variance is given by the percentage of successful, stable lifts $m_{success}$ in respect to the total number of **10 trials**. A successful lift is defined by the robot not falling over for a period of minimum 5s after reaching its standard locomotion posture.

$$q_{ts} = \frac{m_{success}}{10} \quad (3.16)$$

$$A_{st1} = \phi \cdot \frac{1}{t} \cdot \sqrt{\frac{h_R}{g}} \quad (3.17)$$

$$A_{st2} = q_{st} \cdot \frac{1}{t} \cdot \sqrt{\frac{h_R}{g}} \quad (3.18)$$

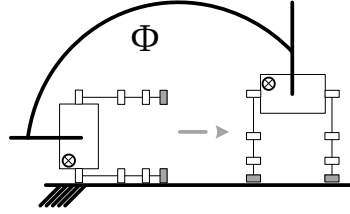


Figure 3.9 – Illustration of the standing up behaviour of a 4-legged robot with the angle between the standing and lying sagittal planes ϕ

Sidestep (non-holonomic)

Moving sideways is defined through the width of one step w_s [m] normalized by the robot height h_R [m] and the time needed to perform the maneuver t [s] in its dimensionless form. q_{sstep} [%] describes the variance of the sidestep by relating the deviation from a straight path Δl_s [m] in terms of robot length l_R [m] after **10 steps**. A variance of more than a quarter of the robot length is defined as not precise and thus not agile.

$$q_{sstep} = 1 - \frac{\Delta l_s}{0.25 \cdot l_R} \quad (3.19)$$

$$A_{sstep} = q_{sstep} \cdot \frac{w_s}{h_R} \cdot \frac{1}{t} \cdot \sqrt{\frac{h_R}{g}} \quad (3.20)$$

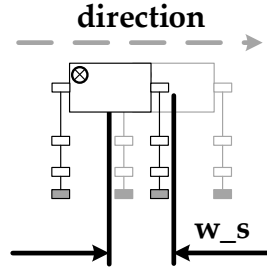


Figure 3.10 – Illustration of the side stepping behaviour of a 4-legged robot with the achieved stepping distance w_s

Forward and Backward Locomotion

The last part of the agility scores is related to the most known locomotion type in mobile robotics, straight forward and backward locomotion. To calculate, we need the respective distance traveled forwards l_{fl} [m] and backwards l_{bl} [m] normalized with the robot height h_R [m] and the measured time of the respective movement t [s] in the dimensionless form. The variance is again the deviation from a straight path with respect to robot width w_R [m] after a distance of **10 body-lengths**.

$$q_{bf} = 1 - \frac{\Delta w_{bf}}{w_R} \quad (3.21)$$

$$A_{bl} = q_{bf} \cdot \frac{l_{bl}}{h_R} \cdot \frac{1}{t} \cdot \sqrt{\frac{h_R}{g}} \quad (3.22)$$

$$A_{fl} = q_{bf} \cdot \frac{l_{fl}}{h_R} \cdot \frac{1}{t} \cdot \sqrt{\frac{h_R}{g}} \quad (3.23)$$

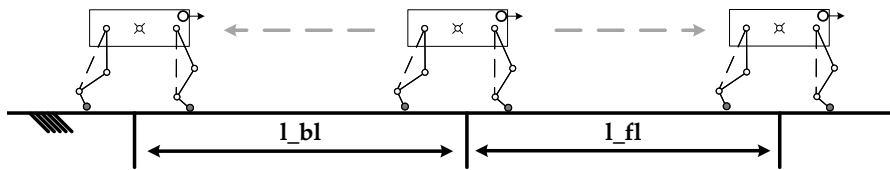


Figure 3.11 – Illustration of the running behavior of a 4-legged robot with the traveled distances forwards l_{fl} and backwards l_{bl}

General Agility

As all of these scores describe agility in a certain manner and we encourage evaluating them separately, as this shows the qualities of the different characteristics clearly. Nevertheless, it is interesting to combine them with a global overview of the system's agility besides looking at them separately. The weighted average agility ($A_{gav\%}$) of all agility-elements allows us to compare different systems which cannot perform the same tasks fairly easy. This is based on our view, that a robot should be called agile not only if it can manage to excel in one task, but also if it can execute various tasks with lower performance. The normalization with our exemplary dog-data gives weight to the different scores and thus allows a fair comparison.

$$A_g = \sum_i A_{task_i} \text{ where } i = \text{number of scores achieved} \quad (3.24)$$

$$A_{gav\%} = \frac{\sum_i \frac{A_{i-robot}}{A_{i-dog}} \cdot 100\%}{j} \text{ where } j = \text{number of scores in benchmark} \quad (3.25)$$

Baseline Values

Even with the scores established, it remains challenging to find a good reference frame. Again, inspiration and observation from nature might help to handle this task. Dog-agility competitions are highly standardized (e.g., obstacle length and height, weight classes of the dogs) and video analysis can serve as a valuable tool for measuring time during the run of a competitor. In our case, the frames until completion of each task were counted and through the video recording frequency, the respective time was calculated. The physical parameters of the participating dogs were taken as a mean of the size-classifications in the dog-agility rulebook and by evaluating the standard measurements for the respective race. The height of the center of mass was approximated as 100% of the hip-height. This follows from [58] where the authors placed weights at the hip height, claiming it to be close to the center of mass. The size of the respective obstacle to the agility-task performed is taken from the dog-agility rulebook as well [59, 60]. All these factors in mind, Table 3.2 shows scores that, in the author's opinion, stand for exceptional agility and can serve to norm the previously defined agility scores. Thus the values of the aggregated dog agility in Table 3.3 represent a value of 100% for each respective agility score. Quality is always seen as the highest, meaning 1. Unfortunately, dog-agility does not cover all of the proposed agility-scores or combines them within fluid transitions which let the need for other sources arise. This concerns (1) on the spot turning, (2) leaping out of stance, (3) side slope running, (4) side-stepping (5) forward and (6) backward locomotion. On the spot turning can be found in some other video sources where dogs of different sizes perform tricks. The turn itself happens (seemingly independent of size) very fast and is thus approximated as a duration of $t = 0.3[s]$.

Table 3.2 – Baselines for agility scores extracted from dog-agility competitions; mean values for 3 winners of the competition in different size classes, geometries taken as mean of the performing dogs

	Large	Medium	Small
dog-size [m]	$h_{dl} = 0.53$	$h_{dm} = 0.39$	$h_{ds} = 0.3$
	$l_{dl} = 0.63$	$l_{dm} = 0.53$	$l_{ds} = 0.43$
	$w_{dl} = 0.35$	$w_{dm} = 0.3$	$w_{ds} = 0.25$
A_{tr}	0.064	0.0469	0.032
A_j	0.397	0.381	0.394
A_{lv}	1.055	0.874	0.643
A_{s1}	0.486	0.484	0.663
A_{s2}	0.486	0.484	0.663
A_{fl}	5.877	6.186	6.529
A_g	8.365	8.455	8.924

Conclusive leaping data out of the stance is sparse and will thus be approximated as half the running-leap value. Pure side slope running is rarely noted in nature as the animal would most likely change direction to either descent or climb the slope. We hypothesize that a possible side-slope-running cannot be performed faster than normal slope ascent. Consequently, we assign the same value. As before side-stepping rarely occurs in nature but can be seen in trick shows like Dog Dance [61]. The movement itself can be achieved and performed relatively fast after training. The measured value from [62] gives a time of $t \approx 0.2[s]$ per step with step widths of half a body width.

Table 3.3 – Baselines for agility scores extracted from dog-agility competitions and merged with intuitive values to reach the 'aggregated dog'; length is representing the radius for the turning score, the inclination is calculated from height and length of the obstacle

	Dog Aggregated				
dog-size [m]	$h_{ds} = 0.41$	$l_{ds} = 0.53$	$w_{ds} = 0.3$		
	t [s]	l_o [m]	h_o [m]	q	Nr []
A_{ts}	0.3		$p = 1$	1	0.679
A_{tr}	1.18	0.97	$p=0.5$	1	0.036
A_j	0.61		0.48	1	0.394
A_l	0.53	0.48	0.305	1	0.453
A_{lv}	0.53	0.97	0.305	1	0.916
A_{s1}	0.9	2.89	0.914	1	0.531
A_{s2}	0.9	2.89	0.914	1	0.531
A_{s3}	0.9	2.89	0.914	1	0.531
A_{st1}	0.5		$\Phi = 1.57$	1	0.639
A_{st2}	0.25			1	0.814
A_{sstep}	0.2	0.175		1	0.438
A_{fl}	1	12.2		1	6.108
A_{bl}	1	3.05		1	1.527
A_g	13.597				

Forward speed can be found from literature on animal locomotion and the specifics of different animal species. In our case, often performing dog breeds were investigated and speed-values for the respective breed (Border collie, Shetland Sheepdog, Jack Russel terrier) were used [63]. Backward locomotion is unnatural to many animals as they would rather use a fast turning motion and their forward locomotion skills in combination. Videos for dogs show, again after training or in situations with no other option, backward stepping with low to medium speeds, especially compared to forward speed [64]. In our case a representative value, approximated to be one quarter of the maximum forward speed, can be found in the baseline-table for the aggregated dog (Table 3.3).

Cost of Agility

As we want to be able to compare different systems with each other, it can be useful, but not necessary, to include the cost of performing the above-measured tasks. For this purpose the power consumption of each single task P_{task} [W] is used. This power results from the difference of the standby power consumption and the one during execution of the task. The robot weight m_R [kg], which strongly influences the difficulty to perform certain tasks (e.g., jumping or leaping) is an additional factor. In combination with the specific agility score A_{task} we introduce a power density that can be compared between different systems. This Cost of Agility resembles the often used and well-established Cost of Transport, that was introduced to further quantify forward locomotion [46].

$$COA = \frac{P_{task}}{A_{task} \cdot m_R} \quad [\text{Wkg}] \quad (3.26)$$

The Cost of Agility cannot yet be included in the baseline-values derived from nature as measuring metabolic cost throughout the required task execution in animals is not possible for the authors, and only insufficient data can be found in published articles [65]. Besides, this value is also directly coupled to the respective agility score, which is already standardized. We thus propose using it as-is and building a conclusive database of different cost-values over time.

Open Database for Agility Benchmarking

As part of this publication, we propose an online framework to enable researchers to share their experience with the agility-benchmark. The agility-database can be found on the EPFL hosted website [agility.epfl.ch] and is open access. We hope to encourage researchers to share and compare their robot's performance to other systems in the database. Additionally, we hope developers can find new robots through this benchmark, that include features they might be interested in and thus make their innovations more efficient.

Experimental Setup

Due to the simplicity of the proposed method, getting good and reliable data from the experiments does not impose the need for high technology. We propose two different setups, which deliver sufficient accuracy to derive the needed parameters. Table 3.4 gives an overview of the generally needed equipment in the minimal setup. The equipment does not include the actual slopes or other installations one would choose for the experiments.

Table 3.4 – Experimental equipment needed for the setups 1 and 2 (suggestion)

Equipment	Setup 1	Setup 2
Motion capturing system	X	
High speed camera top-view		X
High speed camera side-view		X
High power lights		X
Scale for height of jump		X
Scale for length of jump/run		X
Scale for angle of slope		X
Scale for weight of the robot	X	X
Energy-measurement-system	X	X

Having a professional motion capturing system makes recording the needed data from experiments easier. Nevertheless, it is advised, especially for illustration and comparison purposes, to record the experiments with high-speed cameras. One camera should be mounted in top-down-view and the other one from a side view. If setup two is chosen, a scale for the respective movement should be in the picture-frame of the camera, so the achieved movement can be quantified. The time can be extracted by counting the recorded frames and bringing them in correlation with the respective frame-rate of the recording-system or using the time stamps of the recording.

3.2.2 First Experimental Implementation

With the agility-benchmark being defined, implementation of existing robotic systems is the logical next step. As we have a broad range of different legged robots in the Biorobotics laboratory, we can implement a proof-of-concept directly. A general comparison of the agility scores can be found in Table 3.5.

Overview over the Selected Robots

The first series of robots we applied our new benchmark to, come from the mammal-like quadruped family starting with Cheetah-cub [3] with its under-actuated advanced spring loaded pantographic legs and good passive perturbation stability, then Cheetah-Cub-AL, a

reviewed version of the aforementioned quadruped, and Cheetah-Cub-S, a robot with the same leg but actuated spine design for steering [4]. Another pantograph-driven robot, Oncilla, closes the mammal-like starters with a high level of sensor integration (inertial measurement unit, joint-position, 3D-force-sensors in the feet) and respective closed-loop control, employing stumbling-correction, posture-control, and leg-extension-reflexes [5]. As a contrast to these cat- or dog-like robots, we also tested our sprawling posture robot Pleurobot. It features a highly actuated spine in combination with an extremely low COM (center of mass) as found in its biological counterpart, the salamander [66]. All robots are characterized in Figure 3.12 and Table 3.5.

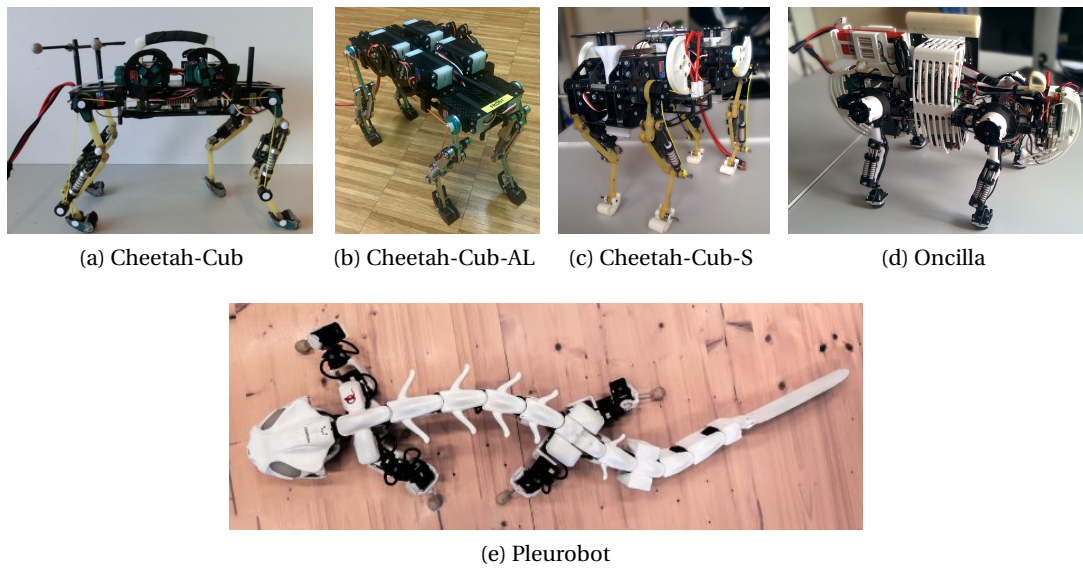


Figure 3.12 – Robots, selected for an initial test of the benchmark

Experimental Results and Discussion

Depicted in Table 3.5, the robots used in the lab are far less agile (at least in the global score) than our baseline dogs (Table 3.3). Nevertheless strong points of the robots become evident, and one can see the whole skill set they can use. Pleurobot and Oncilla clearly show the most skills and Cheetah-Cub the highest agility when it comes to pure speed. Turning is present in multiple of the cat robots and is a factor of 4 to 20 less than the turning scores of dogs. Oncilla shows good turning scores that start coming visibly closer to the ones of dogs. Oncilla also is the only one able to turn on the spot. This table is but a first start as visualization and proof of concept, as the searchable online database can provide even easier and more visible access to the information. This proof-of-concept implementation illustrates the relatively easy use

of our benchmark, even without generation of new experimental data. Cheetah-Cub-S, for example, does not exist anymore, but data gathered in previous experiments was easily reused in our benchmark.

Table 3.5 – Agility scores for selected robots, the optional COA was added where data was available, as some of the robots are out of commission and already existing experimental data was used

	Dog	Cheetah-Cub			C-C-AL			C-C-S			Oncilla			Pleurobot		
m_R [g]		1100			1100			1160			5050			5000		
h_R [m]		0.1			0.1			0.1			0.180			0.12		
w_R [m]		0.1			0.1			0.105			0.245			0.38		
l_R [m]		0.205			0.205			0.205			0.394			0.53		
Setup		1			1			1			1			2		
		[%]		$[\frac{W}{kg}]$	[%]		$[\frac{W}{kg}]$	[%]		$[\frac{W}{kg}]$	[%]		$[\frac{W}{kg}]$	[%]		$[\frac{W}{kg}]$
A_{ts}	0.679										0.014 2					
A_{tr}	0.036	0.02	5	n.A.	0.02	5.6	n.A.	0.02	4.3	n.A.	0.08	21.6	n.A.	0.001	3.8	n.A.
A_j	0.394															
A_l	0.453															
A_{lv}	0.916															
A_{s1}	0.531										0.007	1.2	n.A.	0.04	7.5	n.A.
A_{s2}	0.531										0.044	8.3	n.A.	0.05	9.4	n.A.
A_{s3}	0.531													0.048	9	n.A.
A_{st1}	0.639															
A_{st2}	0.814															
A_{sstep}	0.438															
A_{fl}	6.108	1.434	23.5	94.46	0.687	11.2	n.A.	0.606	9.9	n.A.	0.474	7.8	41.7	0.463	7.6	n.A.
A_{bl}	1.527	0.404	26.4	n.A.	0.353	23.1	n.A.	0.303	19.8	n.A.	0.587	38.4	49.5	0.459	30	n.A.
$A_{gav\%}$	100	4.2			3.1			2.6			6.1			5.2		

3.3 Conclusion

Starting in the introduction, we tasked ourselves to understand the concept of agility, its definition, and quantification. In this part, we strive to give one possible answer in the form of the qualitative definition of a previously not-clearly defined robot performance trademark, agility and hope to inspire more development towards a better understanding of nature and robotics. We aim at generating a better understanding of new and existing robotic systems, by putting forward means to benchmark them further. Nevertheless, the acceptance of the proposed agility-benchmark is not easily predictable. We hope to generate a means for the focused development of new and agile robot, based on the found agility-qualities. The agility scores could be used as fitness functions for the optimization of mechanisms and their

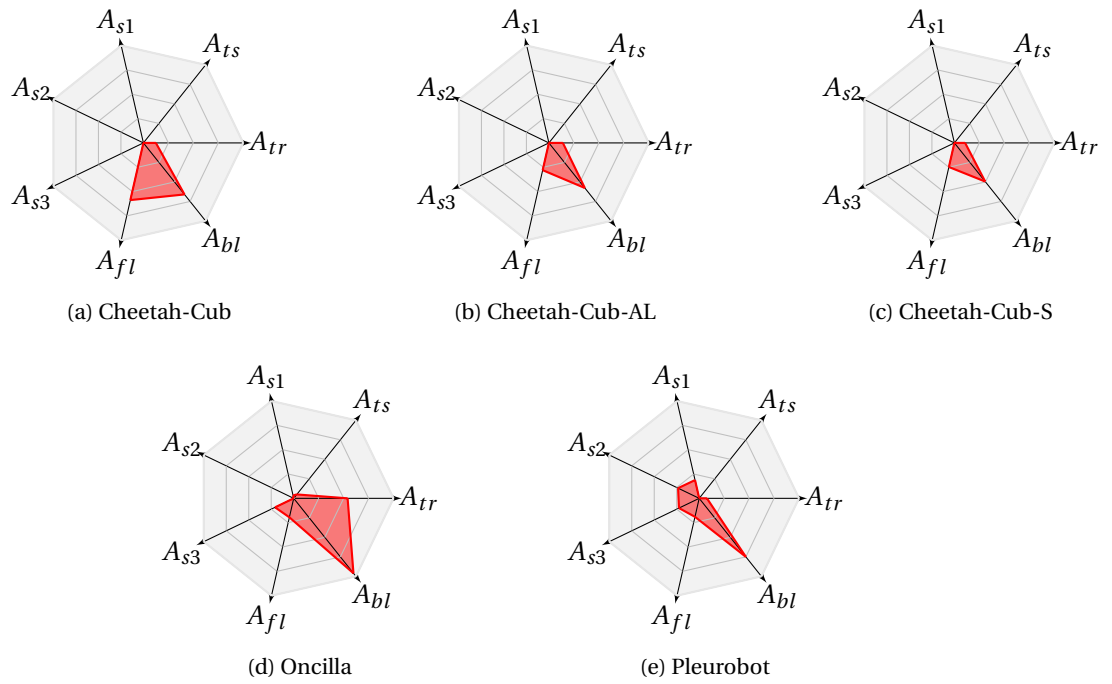


Figure 3.13 – Strength-plots for agility of different robots in % of aggregated dog scores; maximum radius present 40% relative agility for each score; individual scores in red.

respective control, including learning approaches. With these primary outcomes, we propose a real means for robot development in the future and help to bring legged robotics one step closer to complex applications. As researchers discover and implement new robot features (such as transition capability between tasks), the agility benchmark should be extended as well, building on the open-source nature of our method. This parallel evolution of robot and benchmark will hopefully give rise to better and safer performing robots that can benefit society.

Achieving Agility with Small, Low-cost Quadrupedal Robots

Part II

4 Introduction

As a roboticist the logical aim is to build and/or simulate one or multiple robots, that can fulfill all the aspects of our agility definition. Starting from a general overview on some existing robots in the literature and the platforms already available or being developed at the time of my arrival in BIOROB, this chapter will give a high-level view on how our development process was structured and why we chose to do so.

4.1 State-of-the-Art: A General and non-exhaustive Overview

In this state of the art, we wish to introduce a selection of important quadrupedal robots, which influenced the robotics development over the last years. This section is by far not exhaustive and presents only a high-level overview to bring the performance of the developed robots into a context. We will partially discuss mechanisms, electronics, and control strategies in more detail in later chapters. Besides this generalized overview, we will introduce Cheetah-Cub, Bobcat and Oncilla, all robots developed in BIOROB. These robots present in part the starting point and experimental platforms for my work. Consequently, they were continuously maintained or/and improved throughout my PhD.

4.1.1 Agile Legged, Terrestrial Robots

Terrestrial legged robots appear in very different shapes and sizes. This ranges from insect scale up to large systems the size of a small horse [5, 67–69]. Another important feature to take into account is the number of legs and thus related the preferred locomotion pattern. In this state-of-the-art our focus is on locomotion shown by different quadrupedal robots highlighted in Table 4.1 and Figure 4.1 and their relation to agility. Classifying existing robots in our agility benchmark, however, is difficult, as only information from previous publications is available. We could calculate an approximate score for forward locomotion (with $q = 1$) for nearly all

robots to bring standard measures in relation to our work. Often included in publications is the absolute or relative speed, geometric measures and sometimes slope-inclinations or jump-heights. Different authors also described their robot's capabilities for turning, but often without the necessary information to calculate our agility scores. In consequence, we refrain from generally extracting scores with this limited information, as we would need to make too many assumptions (e.g. q -values) to present a coherent overview. Instead, we propose in Table 4.2 a hypothetical analysis, which agility-scores could be achieved and calculated by the robot developers. We group robots according to their mass (Group 1: $m \geq 50kg$, Group 2: $20kg \geq m > 50kg$, Group 3: $10kg \geq m < 20kg$, Group 4: $10kg > m$), evaluating them on a qualitative level. Table 4.1 highlights some classical measures used to compare different legged machines initially.

Group 1

Robots like BigDog, HyQ, HyQ2Max, and Spot perform relatively agile rough terrain locomotion with a strong focus on balance, a medium relative speed, and sophisticated, often model-based, locomotion control. HyQ2Max is additionally able to righten itself from different lying positions. Compromising light-weight for robust and very powerful hydraulic actuation, with its drawback of high energy consumption, is characteristic in all four robots. Off-board supply is often used to lighten the load in experimental setups. The strong actuation in combination with a two-segmented leg design and sturdy build is allowing these robots generally to locomote over challenging terrain, mount heavy equipment (manipulators, sensors), and be very robust to perturbations (high body inertia results in high forces needed for disturbance). There are two major difficulties, working with robots of this size: (1) mainly influenced by the robot dimensions and weight, they are difficult to handle and need a team of operators, supply staff, and large experimental space. (2) Due to their very powerful actuation, they are dangerous for the robot handlers. If the control does not work correctly, health risks are inevitable (e.g., getting kicked by the robot). Consequently, time and space consuming safety measures have to be taken and use as an educational tool is almost out of the question. References to the robots, mentioned in the following subsections can be found in Table 4.1

Group 2

In the next group, consisting of Raibert's Quadruped (RQ), MIT-Cheetah I+II, ANYmal, Spot-Mini, StarLETH and Scout II, a trend away from hydraulics towards electrical actuation is becoming prominent (besides RQ, whose development date was before the appearance of efficient electric motors). The robots' size and weight reach realms, feasible to employ customized electric actuation with or without passive series elastic elements, e.g., high-power-density in MIT-Cheetah and highly integrated SEA actuators in ANYmal. SpotMini is in the unclear,

as not much detail about its technical structure is published. This group of robots is often specialized for different purposes reaching from navigation and spatial mapping in cluttered terrains, mobile manipulation to very high dynamic locomotion. The available payload allows for a high variety of perception sensors to be equipped and used in model-based, closed loop control schemes. Another important aspect is the possibility to handle the robot with less than two handlers, making the robots very well suited as sturdy experimental platforms, also for questions other than locomotion. Restrictions for morphological research is present due to the weight. Filigrane passive compliant structures, like toes, or a partially passive compliant spine are complicated to implement with current technical means, as the employable compliance can often not support the robot's mass. This scaling related effect, is most visible in MIT-Cheetah, switching from an actively bendable spine in Version I to a completely rigid trunk in Version 2. Although already much safer to handle, robots in our second group, still possess very strong actuation. This makes the need for high safety guidelines necessary to avoid accidents.

Group 3

The only robot in our third category is Canid. Relying on electrical actuation with compliant, whleg-like legs and an actuated flexible spine, we observe here the boundary to include flexible trunks into robots. Canid is also capable of jumping, indicating the use of high power density, but now commercially available, electric actuation. The robot weight of roughly 11 kg allows it to be handled by a single person and in a small experimental environment. In our opinion Canid also provides a level of compliance that increases safety strongly. The downside is decreased payload capacity and space, available on the robot. This restricts the applicable periphery and computation power if everything should be integrated on the robot. Subsequently, research with smaller robots has to focus on a specific area, may it be locomotion, or morphology related work, or using the robot as a specific sensor carrier. All-round-robots, like in group 2, are capable of a broader application range.

Group 4

Small robots, here even under 5 kg, represent the last and most influential group for the work presented in this thesis. Besides robots from BIOROB, that will be presented more detailed in subsection 4.1.2, we selected Tekken 1 and 2, Puppy I and II as well as the Takuma quadruped (Takuma-qp). For this class of robots, a different development scheme can be employed. Additional to a general light-weight approach, very high cost-reduction becomes feasible. As the robot's weight decreased, so does the necessary torque to induce movement, enabling the use of purely commercial actuation technologies down to high-grade RC-servo-motors. Most robots presented use passive elastic elements in legs or trunk to minimize the used active

actuation and research more morphology-related aspects of locomotion. This includes the use of spring-loaded pantographic leg-structures inspired by [70] and control methods (like CPGs) not relying on precise sensor feedback or torque-control. Nevertheless, as shown already in Tekken 1 and 2, stable locomotion, even on relatively rough terrain remains possible. Losing the capability to carry heavy sensory equipment, e.g., LIDAR (needed for quick and precise spatial mapping) is compensated with ease of use as experimental platforms for template (basic principles) research. Small robots can be handled safely by a single operator, even after very basic training. Cost-efficient production allows for groups without a high budget to copy, maintain and use small robots as physical simulators and thus increases options to verify theoretical or simulation work.

Table 4.1 – Comparison of selected quadruped robots: table data taken from [3] and [85], and extended; mass, robot height at hip-level, robot length, maximum speed, Froude number ($FR = \frac{\bar{v}^2}{g \cdot h}$), body lengths/second, type of gait, presence of a flexible spine and the foot shape. A_{fl} estimated with $q_{fl} = 1$; $A_{fl\%}$ is the percentage of the agility-dog-value of 6.108

Robot		m_{rob} kg	h_{hip} m	l_{rob} m	v ms^{-1}	FR	BL/s s^{-1}	A_{fl}	$A_{fl\%}$ %	Gait	Spine	Foot shape
BigDog	[71]	109	1	1.1	3.1	0.98	2.8	0.99	16.2	bound	rigid	ball
HyQ	[72]	91	0.789	1.0	≈ 2	0.52	≈ 2	0.72	11.8	trot	rigid	ball
HyQ2Max	[88]	80	0.724	0.887	1.5	0.32	1.7	0.56	9.2	trot	rigid	ball
Spot	[74]	75	0.94	(?)	(?)	(?)	(?)	(?)	(?)	trot	rigid	half cylinder
Quadruped	[75]	38	0.56	0.78	2.9	1.53	3.7	1.24	20.3	bound	rigid	ball
MIT-Cheetah	[76]	33	0.5	0.7	6	7.34	8.57	2.71	44.4	gallop	flexible	half cylinder
MIT-Cheetah II	[77]	33	0.5	0.7	4.5	4.13	6.43	2.03	33.3	gallop	rigid	half cylinder
ANYmal	[78]	30	≈ 0.4	≈ 0.5	0.8	0.16	1.6	0.4	6.6	walk	rigid	ball
SpotMini	[79]	30	0.84	(?)	(?)	(?)	(?)	(?)	(?)	trot	rigid	half cylinder
StarLETH	[80]	23	≈ 0.5	0.5	0.75	0.12	1.5	0.34	5.5	trot	rigid	ball
Scout II	[81]	20.865	0.323	0.552	1.3	0.53	2.4	0.73	12	bound	rigid	ball/cylinder
Canid	[54]	11.3	0.39	0.288	1.38	0.67	1.97	0.71	11.6	bound	flexible	wheg
Oncilla	[5]	5.05	0.18	0.4	0.63	0.25	1.6	0.47	7.8	trot	rigid	ball
Tekken 2	[82]	4.3	0.25	0.3	0.95	0.37	3.2	0.61	9.9	trot	rigid	half cylinder
Tekken 1	[83]	3.1	0.21	0.23	1.1	0.59	4.8	0.77	12.5	trot	rigid	half cylinder
Puppy I	[84]	1.5	0.2	0.17	0.5	0.13	2.9	0.36	5.8	bound	rigid	half cylinder
Cheetah-Cub	[3]	1.1	0.158	0.205	1.42	1.30	6.9	1.14	18.7	trot	rigid	half cylinder
Bobcat	[85]	1.03	0.125	0.166	0.78	0.5	4.7	0.7	11.5	bound	flexible	half cylinder
Takuma-qp	[86]	0.55	0.1	0.34	0.03	0.001	0.09	0.03	0.5	walk	rigid	half cylinder
Puppy II	[87]	0.273	0.075	0.142	0.5	0.34	3.5	0.58	9.5	bound	rigid	half cylinder

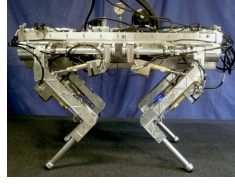
Conclusion

The presented state-of-the-art clarified for us two main aspects: (1st) Visible from our qualitative analysis and Table 4.2, we can state that researching agility, in general, is possible with any size of quadrupedal robot. The distinction has to be made if a more all-round robot (groups 1 and 2) or a more specialized system (groups 3 and 4) are desired. (2nd) The iterative approach,

4.1. State-of-the-Art: A General and non-exhaustive Overview



(a) BigDog [71]



(b) HyQ [72]



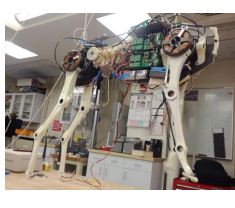
(c) HyQ2Max [73]



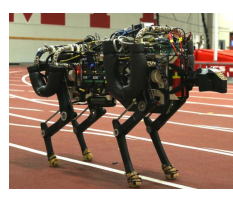
(d) Spot [74]



(e) Quadruped [75]



(f) MIT-Cheetah I [76]



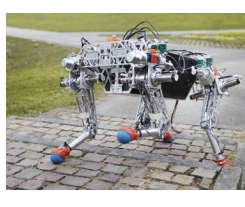
(g) MIT-Cheetah II [77]



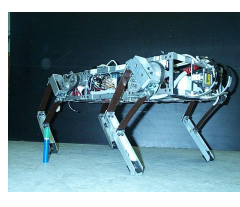
(h) ANYmal [78]



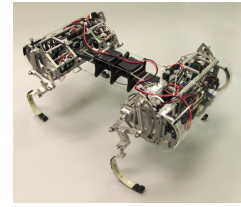
(i) SpotMini [79]



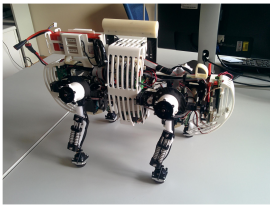
(j) StarLETH [80]



(k) Scout II [81]



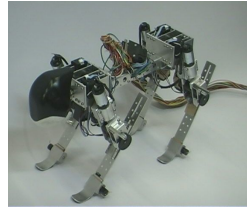
(l) Canid [54]



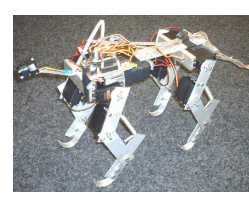
(m) Oncilla [5]



(n) Tekken 2 [82]



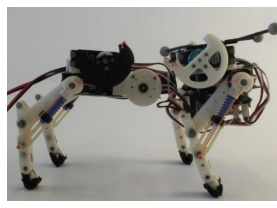
(o) Tekken 1 [83]



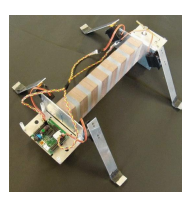
(p) Puppy I [84]



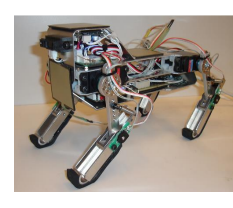
(q) Cheetah-Cub [3]



(r) Bobcat [85]



(s) Takuma-Qped [86]



(t) Puppy II [87]

Figure 4.1 – Multiple quadruped and bio-inspired robots forming a non-exhaustive state-of-the-art in quadruped robotics; (a-d) Group 1: $m \geq 50\text{kg}$; (e-j) Group 2: $20\text{kg} \geq m > 50\text{kg}$; (l) Group 3: $10\text{kg} \geq m < 20\text{kg}$, (m-t) Group 4: $10\text{kg} > m$

Table 4.2 – Hypothetical analysis, which agility-scores could be achieved and calculated by the robot developers

Robot	A_{fs}	A_{tr}	A_j	A_l	A_{lv}	A_{s1}	A_{s2}	A_{s3}	A_{st1}	A_{st2}	A_{sstep}	A_{fl}	A_{bl}
BigDog	X	X				X	X	X		X	X	X	X
HyQ	X	X				X	X	X		X	X	X	X
HyQ2Max	X	X	X		X	X	X	X	X	X	X	X	X
Spot	X	X	X		X	X	X	X		X	X	X	X
Quadruped	X	X	X	X	X	X	X	X		X	X	X	X
MIT-Cheetah	X	X				X	X	X		X	X	X	X
MIT-Cheetah II	X	X	X	X	X	X	X	X		X	X	X	X
ANYmal	X	X	X	X		X	X	X	X	X	X	X	X
SpotMini	X	X	X	X	X	X	X	X	X	X	X	X	X
StarLETH	X	X				X	X	X		X	X	X	X
Scout II	X	X				X	X			X		X	X
Canid	X	X	X	X	X	X	X			X		X	X
Oncilla	X	X				X	X	X		X	X	X	X
Tekken 2	X	X				X	X			X		X	X
Tekken 1	X	X				X	X			X		X	X
Puppy I	X	X				X	X			X		X	X
Cheetah-Cub	X	X				X	X			X		X	X
Bobcat	X	X				X	X			X		X	X
Takuma-qp		X					X					X	X
Puppy II	X	X				X	X			X		X	X

we chose for our robot development towards an agile and highly bio-inspired system, is more feasible with small quadrupeds, as cost- and time-investment is lower. Furthermore, our intent to use the robots as educational research platforms (in MA-thesis and student projects), implies safety and ease of use to be of the essence. These are also prominent features of group 4. The next subsections will lead closer towards the development work done in this thesis and give an overview of the developed robots.

4.1.2 Previously existing Quadruped Robots of BIOROB

Our development work in BIOROB did not start from zero but was to my advantage already on the way for a short period. Mainly three robots, Cheetah-Cub, Bobcat, and Oncilla were already developed or reached the stage of the first hardware iterations. These cat-like systems indicate the closer state-of-the-art that we adapted and in which succession we continued our developments.

Cheetah-Cub

Cheetah-cub (4.2a) is a quadruped robot with advanced spring loaded pantographic legs, developed at the BIOROB-laboratory by Spröwitz and Vespignani [3]. Its actuation consists

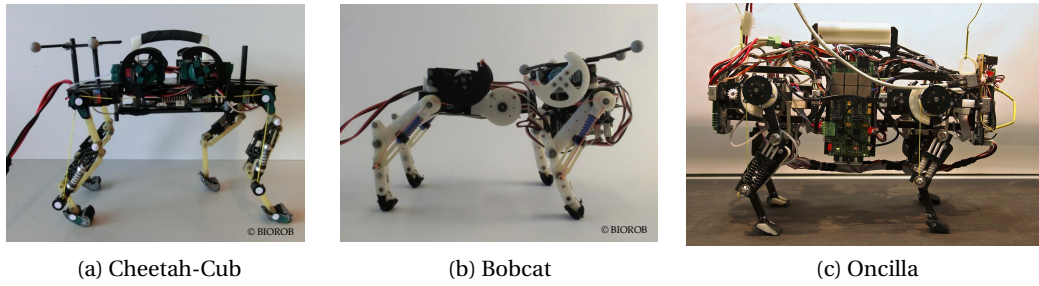


Figure 4.2 – Previous existing quadruped robots of BIOROB, from a side view

of 8 Kondo KRS2350 ICS, which are positioned on the robot's stiff trunk and are powered, through a cable connection, by a DC power supply. The materials used are mostly CNC milled carbon and glass fiber plates, CNC milled POM and 3D printed ABS parts. This material combination makes the robot very robust and at the same time very lightweight ($m = 1.1\text{ kg}$). A RB110 control board with Linux installed as the operating system runs the pre-defined CPG network as an open loop control (no sensors on the robot). Cheetah-cub can reach fast forward locomotion of 6.9 Bl/s and can do step downs of 20% of its leg length with high success rate. Additional tests (see Cheetah-Cub-S, subsection 9.2.2) showed also turning capability in low speeds.

Bobcat

The compliant, quadrupedal robot Bobcat is a cheap and easy to produce experimental platform for dynamic locomotion. With the actuation design based on the Cheetah-Cub, it was developed in BIOROB extending morphology research with an active and compliant spine. The leg design features a 2-segmented compliant leg with an additional springy toe. The width between fore- and hind-shoulders is different to enable overlapping feet (often seen in the fast motion of animals, see Figure 3.2). The spine actuation is achieved with a single RC servomotor, positioned in between fore and hind trunk-segment. Its movement range is $\pm 35\text{ deg}$ in the sagittal layer. A fully connected CPG-network resembling the one implemented on Cheetah-cub is used to control the robot. An additional oscillator node expands it for the spine actuation. Electronic hardware and power-supply are the same as in Cheetah-Cub. [85]

Oncilla

Oncilla is a compliant, quadruped robot developed during the FP7 European project AMARSi (Adaptive Modular Architectures for Rich Motor Skills, project start March 2010, project duration 48 months). The goal of the AMARSi project was to improve the richness of robotic

motor skills. Oncilla is a highly sensorized robot with pantographic legs (ASLP legs) as well as an abduction/adduction (AA) mechanism. The sensorization features encoders on each joint and motor, force and moment sensing at the hips, and IMU as well as new ground contact sensors in the feet (3d force-sensors). The research done with the BIOROB team focuses around closed loop rough terrain locomotion and richer motor behaviors. [5]

4.1.3 Overview of built Robots during the Thesis

The chapters following the introduction are describing our domain-specific development towards Serval, our newest robot, which integrates its predecessors' features. To facilitate the understanding of our design-choices, we highlight in this subsection the purpose of the constructed robots.

Lynx

Lynx is a compliant quadruped robot with the focus on three modular spine designs and a pantograph leg design. It was mainly built out of milled carbon- and glass fiber plates as well as 3D-printed ABS-pieces. The actuation is realized with RC-Servomotors (Kondo KRS2350 ICS, stall torque 2 Nm at 6 V) that are controlled by an RB110-electronics board with integrated Linux-OS. The robot has 9 actuated degrees of freedom (DOF), two per leg and one in the spine. It consists of two trunk segments of that the front one is slightly heavier (about 40 g) caused by the location of the RB110, the legs and an active spine that connects the trunk elements. The spine-versions (SV) are all actively actuated but differ in their use of the compliant elements as well as a "single point of rotation" (the strongest abstraction from nature) vs. "multiple points of rotation" (a less strong abstraction from nature). The design is completed by a passive tail-like structure, that acts like a 5th-leg-stabilizer of the system in case of high pitching motion induced by bad gaits (it prevents the robot from falling backward). In these cases, the compliant elements in the structure will push the robot in the opposite pitch-direction. This results in the establishment of ground contact with all four legs. This tail-like structure represents a non-bio-inspired part, as animals (except the Kangaroo and some small mammals) seem not to use their tails for active pitch support during ground locomotion (ongoing research).

Cheetah-Cub-S

Cheetah-Cub-S is a hybrid robot that combines the pantographic leg design of Cheetah-Cub with a flexible spine. It thus gains the ability to steer. The spine can bend laterally much like a spine of lizards and is actuated by a single motor located in the middle between fore and hind trunk segments. Cheetah-Cub-S can turn with a radius of 0.5 m and a speed of 0.35 ms^{-1} with

a non-optimized gait, taken from Cheetah-Cub. Higher turning-speeds should be achievable with the optimization of the slipping behavior. The steering is not limited to one fixed radius at the time, that was confirmed by letting the robot run a slalom with different turning radii. Additional experiments classified the payload capacity of the robot. Another comparison study with Cheetah-Cub was done in which steering without a spine and abduction/adduction was investigated.

Cheetah-Cub-AL

Cheetah-Cub was not fundamentally altered from its early development days. Some major changes are introduced with Cheetah-Cub-AL. The leg was redesigned and features now a (to the sagittal plane of the leg) symmetric diagonal spring, canceling unwanted bending behavior present in previous Cheetah-Cub-versions. Additionally, making use of classical CNC-manufacturing techniques with aluminum in combination with ball-bearings in every joint, friction was reduced, alignment of the axis and repeatability of experiments were improved. The changes to the trunk are little but feature now easy access to the control board for development purposes. Another major change is the switch to a new operating system, Jokto, that improves stability and ease of use. Tuleu implemented inverse-kinematics of the legs for control purposes. This allowed to tune gaits much faster and more intuitively. The robot was featured recently in Prof. Ijspeert's talk in TED Global Geneva.

Serval

Serval, the last in a line of robot iterations, is meant to serve as a quadruped for agile movement. We use the previously researched mechanisms, control structures and gained knowledge in the electronics development to build a combined and hopefully higher performing robot. Serval consists of an active 3-DOF spine (combining advantages from Lynx and Cheetah-Cub-S), leg units with adduction/abduction mechanism and a scaled ASLP-version of Cheetah-Cub-AL. All motors (Dynamixel MX64R and MX28R) are combined with in-series elastics to protect the somewhat sensitive gear-boxes from harm in different load scenarios. The robot is equipped only with a minimal sensor set, consisting of a low-cost, medium-grade IMU. Collaborations started close to the end of this thesis will provide contact and GRF sensing with capacitive sensors as well as a sensitive skin for physical guidance. Control is realized through inverse kinematics for the legs, (for now) offsets in the spine and an underlying CPG-network for pattern generation. Reflexes, like in *Oncilla*, were not yet implemented, but are ongoing and future work.

Chapter 4. Introduction

Table 4.3 – Characteristic values of quadruped in BIOROB; Robots built prior to this thesis: Cheetah-Cub (CC), Bobcat; built prior and in the first months of this thesis by the author: Lynx; Robots built in collaboration with major contribution from the author: Oncilla, Cheetah-Cub-S (CCS); Robot built solely by the author: Serval, Cheetah-Cub-AL (CCAL); Geometric measures extracted from CAD, additional information extracted from publications and data-sheets; DS-Diagonal Spring, PS-Parallel spring,FS-Foot spring, PR-Protraction/Retraction, FE-Flexion/Extension, AA-Adduction/Abduction, SBC-Single Board Computer; Iterations-Iterations until the final design, BT-Blue-tooth, G-Gear, Ko-Kondo, Dx-Dynamixel, Ma-Maxon, AJE-Absolute joint encoder; geometric measures rounded to the [mm], hanging in air

	Unit	CC	CCAL	CCS	Lynx	Bobcat	Oncilla	Serval
Height: Max	[mm]	233	264	217	288	(?)	357	390
Height: Ground-Hip	[mm]	166	164	166	160	125	201	228
Width: Max	[mm]	124	128	132	129	(?)	245	247
Width: Leg-leg	[mm]	89	91	96	101	97-127	138	211
Length: Max	[mm]	246	248	271	438	(?)	468	563
Length: Hip-Hip	[mm]	207	206	206	226	166	223	378
Mass: Total	[g]	1100	1200	1160	1200	1030	5050	3560
Mass: Electronics	[g]	560	560	608	608	608	2845	2167
Mass: Mechanics	[g]	540	640	552	592	422	2205	1393
Stiffness: DS	[N/mm]	2.33	3.6	2.33	2.33	2.33	5.8	7.76
Stiffness: PS	[N/mm]		4.8/ 2.33			(?)	7.4	9.06
Stiffness: FS	[N/mm]		1.98			(?)	Sensor	1.98 (x2)
Stiffness: AA	[Nm/rad]						253.2	
Stiffness: Spine	[N/mm]					(?)		8.4/ 52
DOF: Actuated		8	8	9	9	9	12	15
ROM: PR fore	[°]		+122/-40			(?)	±34	+76/-50
ROM: PR hind	[°]		+70/-90			(?)	±34	+84/-64
ROM: FE	[mm]		69			(?)	70	93
ROM: AA	[°]						±8	+90/-70
ROM: Spine	[°]			±10	±30/ -15	±35		±90/±30
Motor: Servo					Ko KRS2350 ICS			Dx MX28R/64R
Voltage: Servo	[V]				9-12			10-14.8
Stall torque: Servo	[Nm]				2 (6V)			2.5/ 6 (12V)
No load speed: Servo	[°/s]				375 (6V)			330/ 378 (12V)
Gear ratio: Servo					200:1			193:1/ 200:1
Motor: EC							Ma 323218	
Voltage: EC	[V]						24	
Stall torque: EC	[Nm]						0,639 (45,5A)	
Gear box: G							Ma 370687	
Gear ratio: G+Cus							84:1/ 56:1	
Stall torque: EC+G	[Nm]						7.1/ 4.7 (6A)	
No load speed: EC+G	[°/s]						1164/ 499	
SBC					RoBoard RB-110			Odroid XU4
Connectivity					WiFi			BT, Wifi
Sensors				None			AJE, 3D-GRE, IMU	IMU, (GRE, Skin)
Untethered				No			Yes	
LiPo-Battery				No			3S-4.5Ah-45C	3S-3.3Ah-25C
Iterations		>2	2	1.5	2	1	>3	1.5

5 Domain Specific Design I: Mechanics

The mechanics chapter, as the first domain-specific chapter, will start by summarizing the basic and advanced methods used in lightweight prototyping. Consequently, a general overview of production processes and materials will be presented and their usefulness analyzed. Further on, we highlight the mechanical development of different robots towards our last robot, Serval, that combines mechanisms tested in earlier systems.

5.1 Materials and Methods for Lightweight Structures

For the success of a mechanical design of a legged robot, the use of different materials in the right combination is imperative. Each material has its properties and special difficulties as well as advantages, that are construction-relevant. Based on the construction-boundaries such as:

- Lightweight construction
- Robustness
- Flexibility through compliance
- Higher stiffness for skeleton-parts
- Ease of assembly (modular structure)
- Fast production (prototyping)

A broad range of materials can be chosen to build our robots. To connect the designed parts classical methods like gluing, soldering, screwing with or without inserts and fitting may be

selected, depending on the situation at hand. These connection methods are not specially discussed but may play a part in the material selection.

This chapter deals with the basics of lightweight construction, its elements, materials and functional principles. Also, a brief insight into the theory of engineering mechanics is given. These points form the basis for the design of our systems and are therefore essential for this work.

5.1.1 General Definition

Lightweight construction cannot be considered as an isolated area of mechanics, statics, materials engineering or design theory as it contains insights from all these and other fields. So what is meant by lightweight construction? A definition is provided by Wiedemann [89]:

"Lightweight construction is, first of all, a declaration of intent: for functional or economic reasons, to reduce or minimize the weight, without diminishing the load-bearing capacity, rigidity or other functions of the construction or, finally, in other words: improving the load-bearing capacity without increasing weight."

Three variants are visible in lightweight construction. The cost-driven lightweight construction relies on direct cost savings regarding material and production. In contrast, ecologically-driven lightweight construction depends upon the justification of high manufacturing costs by, e.g., energy saving and maximizing the weight-to-payload ratio. The third variant, giving a purpose of using lightweight construction, is based on mass reduction for the realization of system functions [89]. From an industrial point of view, the combination of the individual variants in a concept that is optimally adapted to the final product is preferred. Taking both ecological and functional aspects into account and striving to be as cost-efficient as possible allows for optimal use of resources when generating a high-quality product, or in our case advanced scientific prototypes.

In a lightweight construction, special structures can be employed to ensure the functionality of a system with the lowest possible weight as well as meeting indispensable requirements for static and dynamic safety. This is made possible by various construction methods, materials and the use of intelligent production technologies. Since lightweight structures are generally somewhat delicate, it is often essential right at the start of a project to integrate strength and stiffness analysis by classical or computer-assisted methods (FEM).

5.1.2 Design Principles

Lightweight structures are generally realized by using thin-walled sheet-designs or frameworks (transforming stresses into compression and tension). On the one hand, by combining multiple trusses, one can obtain a spatial framework and simple frames, or, on the other hand by bent sheets, shell-shaped components, such as hollow shafts can be created. One realizes an intended outer shape depending on the underlying mechanical functionality as the most important aspect.

We differentiate:

- Strain structures: ropes, nets, membranes
- Strain + compression + shear structures: bars, trusses, membrane shells and folding units
- Bending + torsion structures: beams, frames, plates and bending shells

In conclusion, purely tensile-stressed constructions are best suited to lightweight construction, as they do not buckle and their minimum weight is independent of the choice of force paths. However, pure strain constructions can only be approximated in reality, since small secondary forces always occur. These manifest themselves in bending, compression, and torsion loads. In addition, it becomes clear that lightweight construction with smaller wall thickness has to be reinforced through the use of more complex structures to ensure the required strength and rigidity. The prime example of this is the truss, that is constructed only of tension and compression bars and thus nullifies bending loads. However, typical membrane profiles, efficiently distribute the forces occurring over the entire cross-section and can, therefore, ensure stable structures.

Design by classical rules can be extended through the usage of new tools, as computer-assisted design becomes more relevant each day. Methods like FEM-analysis (automatic calculation of stress and displacement of mechanical parts) and dynamics simulations were used in this work. Many tools in commercial CAD-software are available to double-check one's design before production, and if the loads are known in advance. The principles described in the following subsections allow initial design decisions to be taken more comfortable and with a more systematic approach. Consequently, computer-aided analysis tools can be employed more efficiently.

Lightweight Construction

Assemblies, as the name implies, consist of several individual components that must be connected. Joining techniques of various kinds determine the design of the technical structure.

These techniques, here called lightweight construction, can be divided into four generic terms:

- Differential construction
- Integral construction
- Sandwich construction
- Composite construction

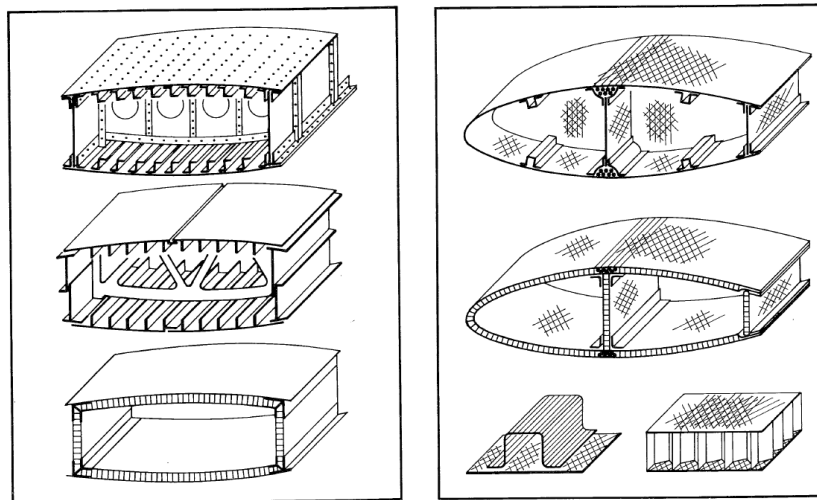


Figure 5.1 – Lightweight construction (left: Differential-, Integral- and Sandwich-construction; right: Composite-construction) [89]

When choosing the optimal construction technique, factors such as fail-safe quality, possibilities for inspection and repair or the aging and fatigue of components and connectors are critical.

In the *differential construction*, parts are selectively connected to each other, e.g., by screws or rivets. This has the consequence that notches and cracks occur more easily, but not immediately run through the entire component, stopping at the next riveted joint. In addition, it is producing a relatively simple assembly with less need for sophisticated machinery and tools. The downside is an increased amount of time for assembly. In contrast, the *integral construction* designates components that are made in one piece. This can be done by CNC or other milling techniques, sheet-metal-bending, as well as technologies such as laser sintering, a rapid prototyping process in the 3D-printing-realm. How exactly this and other methods

work can be found in [90] and will be discussed later-on in section 5.2. Compared to the differential, the integral design is much less susceptible to cracking in general but ruptures quickly run through the entire component unless the designer considered this and integrated features to stop them. Generally, parts made integrally cannot be altered or repaired easily. Connecting individual elements to form an organic entity is called *sandwich construction*. Here, the advantages of the differential are combined with those of integral design. Connections can be realized through an adhesive bond, that is preventing crack propagation by their inherent elasticity, thus achieving a large fail-safe quality. Once the bond is formed, little alteration is possible. Shear is generally an issue when glue is used, as it is weak towards this kind of stress. Countermeasures, like lips or pins, can improve safety. The last considered lightweight construction is the *composite structure*. Materials of various specific properties are combined into laminates in a sandwich construction. The most known example is CFRP (carbon fiber reinforced plastic) also colloquially referred to as carbon. CFRP includes carbon fibers and a connector resin, the matrix, that will be discussed in more detail in the following sections. By combining different materials, outstanding strength values can be achieved with equal or even lower weight than with classical materials. The most prominent drawback, however, is that composite materials cannot be repaired easily and are very difficult to verify for manufacturing imperfections. Besides, classical analysis methods with bar or plate models for sandwich construction may not be sufficient [89]. Composite structures need particular attention when being connected to other parts, as they only partially allow for classical employed connectors due to their material properties. Preferred connection methods are bolting and adhesive bonding. Which lightweight design is used or whether several are combined with each other, must be tailored to the problem at hand and is often subject to iterations. In a mechatronic system, one can often find all methods combined and integrated to form a functioning assembly. In our designs, we mainly employed differential and integral methods. We generally need the adaptability to change our design partially after first tests are executed, that is a strength of differential construction. Integral methods allow to form rather complex parts, that would be difficult or very costly to realize otherwise (3D-printing).

5.1.3 Materials

Lightweight construction means developing systems that have less weight. However, this does not necessarily have to be achieved by economy of material, e.g., by reducing the wall thickness. Other materials may have comparable properties at higher, equivalent or even lower material usage or specific weight. The right material choice in combination with an optimal design approach is decisive for the component's functionality. For example, if a resilient part is to be constructed, no brittle or rapidly plastically deformable material should be used. On the other hand, aspects such as required rigidity and strength have to be taken into account for any part. Classical materials, such as titanium, magnesium or aluminum and their alloys, face

new "creations" of composites and different high-grade plastics. This section is intended to provide a brief insight and compare the most important properties of the materials considered in this work.

Metals

The classic metals, especially high-quality aluminum alloys, remain very important in addition to the newly developed composite materials. This is primarily due to components in integral as well as differential construction, that can be produced easily by conventional methods. Further, the calculation of isotropic mechanical behavior of components with very few data is possible and reliable. Of particular interest is the plastic working power of various alloys, that, in the case of overloading reduces stress peaks and absorbs kinetic energy (but deforms the part permanently). The basis for a correct design with this material are characteristic values extracted from stress-strain diagrams (see Table 5.1) and the consideration of strength and stiffness of various constructions (subsection 5.1.4).

Aluminum Alloys The variety of aluminum alloys is enormous, making this metal interesting for lightweight construction. Thanks to its low specific weight, it is an ideal basis for production of stiff or flexible alloys. Due to this possibility of variation, the alloy can be adapted to the respective application, and thus an optimal design result can be achieved. In the case of highly loaded buckling bars, an AlZnMg alloy is preferred since it has a high yield strength. For notch-prone components, however, an AlCuMg alloy is used, as there is a high elongation at break and low yield strength. The yield strengths are greatly influenced not only by choice of alloying partners but also by the manufacturing method and heat treatment. Depending on the alloy, hardening causes up to a threefold increase in stiffness and yield strength that is up to six times higher than the initial state [91]. We often employ AL-alloys (mostly AL6xxx for structurally stiff and AL5xxx for bending parts) in our robots, due to their easy abrasive machinability, low cost and relatively lightweight.

Titanium and Magnesium In addition to aluminum, titanium, and magnesium alloys are also suitable for use in lightweight construction. The disadvantage of warm-tempered magnesium alloys, although possessing a very low specific weight, is the behavior in the compression test. Here a low yield occurs with the tendency of disintegration, which can lead to component failure. In the tensile test, the behavior is similar to the one of aluminum alloys. They cannot be machined easily by abrasive techniques, as precautions due to their high flammability have to be taken. This makes the use of our prototyping facilities difficult. Titanium, which has a higher specific weight than aluminum, is recommended for high-temperature applications due to the high melting point. A combination of other elements is also a way to increase

its strength significantly. The peculiarity of titanium alloys lies in a very high elongation before breakage, which increases significantly with increasing temperatures, until almost ideal elastic-plastic behavior is to be expected [91]. Usage of titanium-allowes can be interesting for their elastic behavior, see subsection 5.1.3. The otherwise relatively high weight and difficult manufacturing (tough material) are preventing wide-range employment in our robots.

Nitinol NickelTitanium, NiTi, or Nitinol is a metal alloy with special and unique properties. Classically used as a shape memory alloy (SMA) it is also capable of a phenomenon called super- or pseudo-elasticity. In our case, the shape memory properties are less important, as forces are generated relatively slow and with strong temperature dependency. This prevents us from using the SMA as an actuator. The super-elasticity on the other hand (with 10-30 times the value of an ordinary metal) is of great interest as bending structure, springs, and other parts may benefit greatly from this. High elasticity is reached by the local transformation of the crystal structure within the alloy. When bending, the Nitinol changes (locally) from austensite to martensite state and the other way around without being restrained by plastic deformation, see Figure 5.2. The stiffness can be calculated with classical means using E and G moduli as well as the shape of the Nitinol piece, see Figure 5.4.5. The right choice of the modulus remains a question as the transformation is local, and not the whole structure changes at once, remaining thus not homogeneous at all times. Additionally, Nitinol exhibits a drastic change in properties depending on the temperature/crystal-state. For approximate calculation, we assume a full homogeneous transition to austensite state and use its modulus. We employ Nitinol in different robots as "omnidirectional" leaf-springs and other bending elements, that allow our robots to be flexible but also durably robust over long experimental periods.

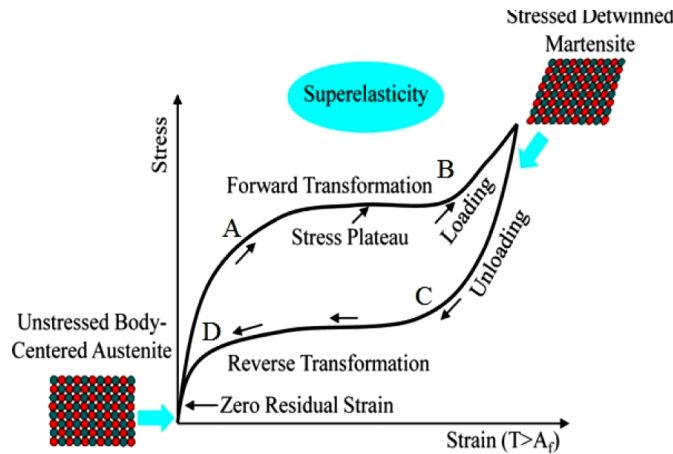


Figure 5.2 – Stress-Strain behavior of Nitinol depicting the transformation during super-elasticity between martensite and austensite states; hysteresis depending on transformation direction is visible and adds difficulties to numerically classify the material, adopted from [92]

Plastics

Plastics are artificially produced materials by combining different chemical elements. The variety of plastics and their characteristics seem almost infinite. The availability of specific characteristics with relatively cheap prices for standard engineering plastics make these valuable for prototyping and lightweight construction. We will introduce only three selected plastics in this section, that were used almost constantly throughout our development process.

ABS Acrylnitril-Butadien-Styrol is a plastic, that is used in different rapid prototyping-procedures, such as FDM-3D-printing. It is easily formable in different shapes due to its sensitivity to temperature (melting between 95 – 110°C). The price and ease of use make this material interesting for first prototype implementation. Long-term parts that are exposed to sunlight should not use this material, as it degrades over a relatively small amount of time in from of becoming brittle. Additionally, one should be aware that it is not strong enough to hold a screw-connection and is sensitive to different chemicals that can be found in commercial glues.

PA2200 PolyAmide 12 in its powdered form is called PA2200. It is a multi-purpose plastic used in SLS-3D-printing. The general high chemical resistance and good durability especially when looking at impact absorption make this material interesting. It is easily bonded by gluing, tapping is not advised, as the screw thread will rip quickly if tightened too much, due to the powder as a base.

POM PolyOxyMethylen is a plastic that can be bought in plates of different measurements and pre-defined extrude-shapes. Processing by abrasive machining, e.g., milling is easy. The main advantage with POM is the low friction which makes it ideal for self-built gears and bearings. It is very pressure and tension-stable but is vulnerable to bending, because of quick plastic deformation. Another difficulty with POM is its low surface energy which makes it hard to glue. Special glue with an additional primer allows a successful bonding. POM is ideal to support skeleton-structures or serve for connection-pieces, which do not hold high loads (sandwich-construction).

Fiber Composites

The term composites describes the combination of different materials into a new component with properties adapted to the application at hand. This area of material technology is specifically rich in application when different fibers and certain bonding resins are combined forming so-called fiber composites. In addition, ceramic and metal composites complement

the variety of materials. In this work, however, particular attention is put on fiber composites, as we will show their value for lightweight construction [91].

Fiber-Plastic-Composites A fiber-plastic-composite consists of a Duromer (plastics, that cannot be deformed after their hardening) which forms a matrix into that different fibers are integrated. The matrix, with its high specific volume, provides flexural rigidity, that is enhanced by the fibers along with an increase of strength. The combination possibilities of fibers and resins are enormous [93] and consequently we discuss only the following particularly popular compounds:

- CFRP: Carbon Fiber Reinforced Plastic
- GFRP: Glass Fiber Reinforced Plastic
- AFRP: Aramid Fiber Reinforced Plastic (e.g., Kevlar)

All fiber composites share two important aspects. They are modeled after wood and therefore are also anisotropic (directional) in their properties. For multi-axial stresses, tissue build from unidirectional layers is required. The second aspect is the fiber density. The more fibers there are, the higher the stiffness and strength will be. The fiber composite construction is a separate design in itself and should therefore not simply replace isotropic materials. Due to its anisotropic behavior, it requires different structural concepts than metal, which can lead to problems (e.g., different properties of matrix and fiber make calculation difficult), but also to advantages (e.g., very lightweight with high stiffness) [91]. The mechanical properties of typical fiber and matrix combinations can be found in Table 5.1.

Glass fibers generally possess high strength and are elastic whereas carbon fibers are available in different versions:

- HM: High modulus (high rigidity)
- HT: High Tenacity (high strength)
- IM: Intermediate Modulus (medium stiffness)
- UT: Ultra Tenacity (very high strength)
- UM: Ultra modulus (very high stiffness)

The organic fiber Aramid lies with its characteristics between glass and carbon fibers. More detailed considerations of the specific fiber and matrix materials would go beyond the scope of this work. The interested reader is encouraged to check these details in [89, 93].

Unidirectional Fiber Laminates In a unidirectional laminate (UD), fibers, embedded parallel to each other in the resin, take over the function of a supporting structure. Multi-axial load requires the combination of multiple unidirectional layers to create a multi-directional fiber web or tissue. Fiber laminates are orthotropic sheets (direction-dependent elasticity properties, but no coupling between strain and shear distortions). An analytical description is not trivial but can be found in [91], if necessary for the design. As we need to consider loads from all directions, we cannot only employ UD-laminated but are forced to consider tissues. This increases the complexity if, e.g., 3D-printed parts, have to be reinforced with UD-laminates. Special design software, mainly for aerospace industry, lately came available to define the optimal routing of fibers depending on the expected load [94]. This process is far from trivial in design as well as production and thus has to be critically evaluated before used in the construction of a robot. A good alternative is presented by half-ready laminates (e.g., as plates), or tissue and resin separately. These can be used to reinforce parts rather easy, but without the exact knowledge if optimal strain distribution is achieved. For us, only expecting small loads, the second approach seems sufficient and less time-consuming. Considerations on failure modes and the stresses required for fiber tissues are given in the section subsection 5.1.4.

5.1.4 Strength and Stiffness Considerations: Classical and Computer-assisted Methods

Strength and stiffness are basic restrictive factors in the design of components. Through various entry-points, different loads are generated, that the components must endure. Common methods for calculation and analysis of such factors as well as computer-assisted methods are presented in this section.

Stress-strain Behavior Lightweight constructions are mostly verified according to static aspects, which includes the control against kinking and buckling or complete material failure. Priority is given to the analysis of the material properties up to the breaking point, that can be determined by carrying out the uniaxial tensile test. The resulting curves are in almost all classical material cases already present and can be consulted right away. It should be noted that the tensile test corresponds to a standard in which no disturbing influences, such as cross-strains like shear or torsion are included. As isotropic material reacts in the same way, not depending on of the strain direction, this is generally seen as sufficient information.

Different important characteristics are extractable from the resulting curves and are used for strength calculations in classical, as also computer-aided methods. The modulus of Elasticity (Young's Modulus) describes the slope of Hook's line, the Secant modulus the stress-strain ratio in the nonlinear range, and the Tangent modulus the ratio of increasing strain. The structural

analysis primarily uses the Tangent and Elasticity modulus. In addition to the longitudinal strain ϵ_x , there are also proportional transverse strains, which are described by the transverse contraction number, also called Poisson's constant. $\epsilon_y = \epsilon_z = -\nu \cdot \epsilon_x$ [91]. These values are used to verify the strength and stiffness of employed materials, as described in the subsections below:

Classical Methods

Isotropic Materials Materials whose properties are independent of the direction are called isotropic. For components with these properties quite simple formulas of strength-theory can be applied to verify their design. They can be found, e.g., in [95] or in the textbooks of the Department of Machine Elements of the TU Ilmenau [96]. The considered load types and the corresponding numerical verification are for:

- Tension / Compression
- Bending
- Shear
- Torsion
- Combinations of it

If initial analysis of the structure suggests the problem of kinking or buckling, Euler kinks [97], bending kinks [93] or analysis methods of buckling for parts different from beams should be considered [93]. To determine the respectively acting forces and force entry points the usual methods of technical mechanics are used [97, 98]. We generally applied this method for simple parts, which could be quickly verified. For more complex parts we usually used computer-assisted methods.

Fiber Laminates (anisotropic) Since fiber laminates do not consist of only one material, i.e., are inhomogeneous, the individual components must also be considered in the strength analysis. Accordingly, a distinction is made between fiber and resin (matrix) breakage and a combination thereof, the intermediate fiber breakage. Experimental and analytical information and tables for different material combinations can be found in [91]. In layer composites, elastic isotropy can be assumed if three or four equal layers are arranged at $60deg$ or $45deg$ to each other. For such laminations, as well as for three-layer ($0deg/ + 45deg/ - 45deg$) and cross-laminated, we summarize the most prominent values in Table 5.1.

Computer assisted Methods

The most famous computer-assisted method to verify a mechanical part is called FEM, Finite Element Method. Integrated into almost all commercial CAD-software this, in its core rather complex, method allows the end-user to obtain stress, deformation, and safety-factor analysis practically immediately. The definite advantage is the simulation of static or sometimes even dynamic load scenarios without a physical prototype and, due to high automation, in a very short amount of time. As in any simulation software, the results can only be as reliable as the inputted data itself. Most important in this regard is the right choice of loads and material properties that correspond as closely as possible to the ones applied on the physical part. If these loads are not entirely understood or predictable, errors in the FEM-results become inevitable. Nevertheless, even without precisely corresponding results, most FEM analysis on the part level, can give a valuable insight if the design choices were right before physical testing is used to validate. We employed this method on different critical parts (see examples in Figure 5.26 for deformation analysis of NiTi-spring-assembly), whose complexity was too high for quick "analog" verification or where our calculations had to be confirmed before implementation. A major challenge for using FEM in legged locomotion is the knowledge about applied forces and their directions, as these are seldom precisely known and often hard to predict.

Comparison of Materials

This section provides an overview clarifying advantages and disadvantages of individual materials by presenting their characteristic properties and their usage in BIOROB's robots. In the case of metals, only exemplary values for alloys used in this thesis are given. The tensile strengths of fiber-reinforced plastics should primarily be seen as examples as well since different values result from the structure of the laminate and fiber content. In addition, as described in section subsection 5.1.4, a distinction must be made according to the direction of applied stress and the nature of failure (fiber or matrix breakage). The values shown represent the worst-case scenarios, depicting loads perpendicular to the functional direction of the laminate.

As can be seen from Table 5.1, fiber laminates can certainly keep up with classical lightweight aluminum, especially if they are loaded according to their anisotropic operating direction. They offer the advantage of a very low specific weight. Disadvantages that do not occur in the case of isotropic metals are, above all, the stress values that can only be determined by sophisticated methods, or nowadays with analytical software, and the time-intense production of complex structures. Hence, a combination of these materials is advantageous, as optimization of both economic and functional aspects is possible.

Table 5.1 – Useful characteristics of different materials: Metals (Al6061, pure Ti, pure Mg, pure NiTi); Plastics (ABS (Acrylnitril-Butadien-Styrol, amorphous and thus no true melting point, value used for 3D-printing), POM (Polyoxymethylen), PA2200 (Polyamide 12), Isotropy depending on manufacturing method; Fiber composites (CFRP (Carbon-fiber reinforced plastic), GFRP (Glass-fiber reinforced plastic), AFRP (Aramid-fiber reinforced plastic) [91] and various material data-sheets, tensile strength is divided in FB (fiber breakage) and MB (Matrix breakage); Robots using the respective material are indicated in the end of the table

Parameter	Unit	Metals				Plastics			Fiber composites							
		Al	Ti	Mg	NiTi	ABS	POM	PA	AFRP HM		GFRP E		HT		CFRP	
									Tissue	UD	Tissue	UD	Tissue	UD	UD	UD
Density	$[g\,cm^{-3}]$	2.7	4.51	1.74	6.5	1.06	1.43	0.93	1.37	1.46	2	2.03	1.55	1.55	1.6	1.8
Young's modulus	$[kN\,mm^{-2}]$	68.9	102.81	44	40(M)/75(A)	2.24	2.9	1.7	29	76	22.8	46.2	67.23	138	155	380
Yield strength	$[N\,mm^{-2}]$	275	275.6	115	70-140(M)/195-690(A)	20	68.2		414	100	463	1070	524	1447	2200	880
Tensile strength (FB/MB)	$N\,mm^{-2}$	310	344.5	180	895 (annealed)	29.6	67.5	48	270/200	230/30	690/90	700/40	880/250	1200/35	n.A.	1500/35
Poisson ratio		0.33	0.36	0.35	0.33	0.38	0.39	0.394					0.39	0.39	0.39	0.39
Melting point	$[^{\circ}C]$	≈ 600	1668	650	1310	230	175	≈ 175	dependent on matrix material							
Thermal conductivity	$[W\,mK^{-1}]$	167	16.44	150.6	18	0.16	0.16	0.127	dependent on matrix material							
Conductive (electric)		yes	yes	yes	yes	no	no	no	yes							
Isotropic		yes	yes	yes	yes	no	yes	yes	quasi	no	quasi	no	quasi	no	no	no
Bobcat		X				X	X				X		X			
Lynx						X	X						X			
Oncilla		X				X	X	X					X			
Cheetah-Cub							X				X		X			
Cheetah-Cub-S		X			X	X	X				X		X			
Cheetah-Cub-AL		X				X	X						X			
Serval		X			X		X									

5.1.5 Conclusion

The right choice of materials and design method, according to the task at hand, pose one of the most important basics of mechanical design. Special emphasis is placed here on the choice of materials, as this has a significant effect on design and methodology. Materials that do not have good rigidity are not suited for parts under high pressure. Likewise, brittle materials are unfavorable for integral construction as they show a tendency to crack under load. The best advice when planning a design is to keep all construction methods and materials in mind, select the seemingly appropriate ones and do a clear verification, may it be with computer-assisted or classical analysis tools, or by implementing physical prototypes. For us, this resulted in the choice of differential and integral construction, as we aimed to build a system that can be repaired or modified easily. As prototype-designers, this liberty is necessary for us to adjust our robots almost on-the-fly with slight modifications towards achieving more robust mechanics. Furthermore, differential construction allows a broader range of research questions to be addressed in a shorter amount of time (e.g., limb amputation, different foot designs, the impact of leg stiffness, modular and compliant spine - yes or no, exchangeable sensor-sets for optical navigation and path planning or "blind" locomotion with reflexes). In the same spirit, we explore different material combinations to minimize weight, increase robustness and durability or just for the sake of learning about the pros and cons of new material and production technologies.

5.2 Manufacturing Methods for Prototyping

In a robotics environment, where many unknown factors force implementation of a simulated or physical test-platform, one is often obliged to produce multiple robot-iterations, before a functioning system can be obtained. In the hardware-environment production time is of the essence, as it plays a major part of the development process (as can be seen in chapter). Rapid prototyping is used for a long time for this reason and developed over the last years into two major branches, abrasive/subtractive prototyping and additive prototyping, that will be described in the following sections.

5.2.1 Abrasive/Subtractive Prototyping

Subtractive prototyping is based on the simple principle of removing material from a basic block or rod to create the designed part. This form of prototyping is well established in the industry for multiple decades and nowadays mostly represented by computer-guided (CNC-)machining, may it be with a router, lathe, or a combination of both, called turning-center. With these methods, almost any outer form of a part can be build, although enclosed hollow structures may remain difficult or unachievable, due to unacceptability with the milling tool.

5.2. Manufacturing Methods for Prototyping

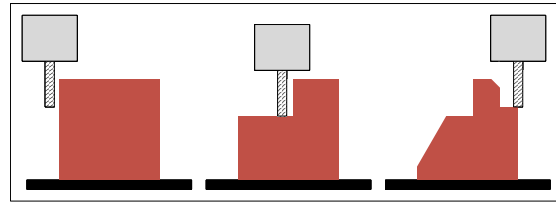


Figure 5.3 – Illustration of subtractive prototyping, adapted from [99]

The most common milling techniques for small prototyping include 3-axis CNC-router-milling and 2-axis CNC-lathe-milling, also available in the prototyping workshops of BIOROB and EPFL. Restrictions on the design due to smaller machining-dimensionality was acceptable due to this direct availability and very affordable pricing. Another, although not strictly abrasive process, is laser cutting, where thin or medium-thick plates are cut in a 2D-plotting manner to receive the desired form. This fast process is of value for any flat part needing only medium precision and quick production time. Table 5.2 highlights the most critical aspects of the three techniques, including an excerpt of the vast material range available. When to employ CNC-machining and significant advantages as well as disadvantages of the method are presented in the comparison Table 5.4 along with a statement which of or robots was built using these classical approaches.

Table 5.2 – Summary of selected abrasive technologies, adapted with information from [99]

Technology	Typical Materials	Dimensional Accuracy	Speed	Cost
CNC-milling	AL, Brass, Stainless Steel, ABS, PA, POM, Woods, Fiber Plastics and more	$\pm 0.025\text{mm}$ to $\pm 0.125\text{mm}$	+	\$\$
CNC-lathe	AL, Brass, Stainless Steel, ABS, PA, POM, Woods, and more	$\pm 0.025\text{mm}$ to $\pm 0.125\text{mm}$	+	\$\$
CNC-laser	AL, Stainless Steel, ABS, PA, POM, Woods, and more	depending on material thickness	++	\$

5.2.2 Additive Prototyping

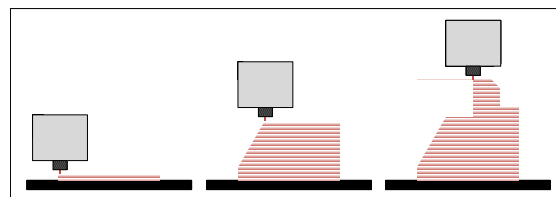


Figure 5.4 – Illustration of additive prototyping, adapted from [99]

When it comes to additive prototyping, the underlying principle is as simple as its subtractive counterpart. The material is bonded/printed together layer by layer and forms the desired and

often complex 3D-structure, thus being called 3D-printing. Due to specific needs for the bonding of different materials, a high variety of printing techniques developed over the last years and is continuing to increase very fast. Our selected processes, whose characteristics are described in Table 5.3, are FDM (Fused Deposition Modeling), SLA/DLP (Stereo-lithography/Direct Light Processing), SLS (Selective Laser Sintering), Material Jetting, Binder Jetting and DMLS/-SLM (Direct Metal Laser Sintering/Selective Laser Melting). As a detailed description of the principles behind these techniques surpasses the scale of this work, we would like to reference the interested reader to [99, 100], where excellent explanations can be found. For our work, we employed mostly FDM and SLS, mainly motivated by ease of availability in our research institutes workshops and the still reasonable pricing for our low-cost robots. The comparison in subsection 5.2.3 is putting these, still novel, methods in relation to classical machining and showing their application in our robots.

Table 5.3 – Summary of selected 3D-printing technologies, adapted with information from [99]

Technology	Typical Materials	Dimensional Accuracy	Layer height	Support	Cost
FDM	PLA, ABS, PETG, PA, PEI, ASA, TPU	$\pm 0.5\%$ ($\min \pm 0.5mm$); $\pm 0.15\%$ ($\min \pm 0.2mm$)	50 – 400 μm	Not always required	\$
SLA/DLP	Different Resins	$\pm 0.5\%$ ($\min \pm 0.10mm$); $\pm 0.15\%$ ($\min \pm 0.05mm$)	25 – 100 μm	Always required	\$\$
SLS	PA, TPU	$\pm 0.3\%$ ($\min \pm 0.3mm$)	80 – 120 μm	Not required	\$\$
Material Jetting	Different Resins	$\pm 0.1\%$ ($\min \pm 0.05mm$)	16 – 30 μm	Always required	
Binder Jetting	Stainless Steel, Sand, Ceramics	$\pm 0.2mm$ ($\pm 0.3mm$ sand)	100 μm	Not required	\$\$\$
DMLS/SLM	Stainless Steel, Ti, Al	$\pm 0.1mm$	30 – 50 μm	Always required	\$\$\$\$

5.2.3 Comparison and Conclusion

In our opinion, both manufacturing methods, CNC and 3D-printing, show great potential and our reasoning behind seeing them rather as complementary technologies than competitors will be explained in the following. The information extracted to Table 5.4 points towards classical machining if high accuracy, very high mechanical strength with purely isotropic behavior and a wide material range are needed, whereas complexity of the parts should be kept low to medium. If one needs a complex, almost organic, design or a lightweight structure with hollow enclosures, build in different plastics, 3D-printing is a valuable option. The designer should keep the anisotropy and dimensional inaccuracy in many printing technologies in mind to avoid failure or too many part iterations. Metal printing should only be considered if the price does not play a role and the part cannot be simplified for CNC-milling, i.e., a highly integrated hydraulic actuator like [101]. Additionally, NC-machining requires a skilled technician to handle programming, tool selection, and process observation, whereas 3D-

Table 5.4 – Comparison of selected 3D-printing technologies with classical subtractive machining including advantages and disadvantages for mechanical prototyping, adapted with information from [99, 100], 1 (very bad) to 5 (very good); *Depending on material; **Depending on part complexity

Aspect	FDM	SLA/ DLP	SLS	Material Jetting	Binder Jetting	DMLS/ SLM	CNC-Router	CNC-Lathe	CNC-Laser
Available Materials	3	3	3	3	2	2	5	4	4
Dimensional Accuracy	1	4	2	4	3	4	5	5	4
Part Strength	2	2	3	2	2	4		*1-5	
Grade of isotropy	1	3	4	4	4	4		*1-5	
Surface-quality (untreated)	2	4	3	4	2	3	5	5	4
Part service life	2	3	4	3	4	5		*2-5	
Production Speed				**3-5			***3-5		5
Cost	\$	\$\$	\$	\$\$\$	\$\$\$	\$\$\$\$	\$\$	\$\$	\$
Excess material recycling	1	5	2	5	5	5	5	5	/
Advantages	Inexpensive	Good accuracy	Mechanical properties	Accuracy	Build speed	Hollow structures	High range of materials		Very fast
	Build speed	Build speed	Less anisotropy	Surface quality	Multi-material	High accuracy	Very good mechanical properties		
		Surface quality		Surface quality	Low temp	Mechanical properties	Very high accuracy		Not very expensive
Disadvantages	Rough surfaces	UV sensitive	Rough surfaces	Limited mechanical properties	limited strength of parts	Very expensive	No hollow structures		Cuts conic
	Degradation with time	Material change cult	Poor re-usability of powder		rough surfaces	Few materials	Complexity limit: Axis-NR		Mostly 2D
	Accuracy	Mechanical properties				Rough surface	High tool usage/variety		
	Edge-warping								
Bobcat	X						X	X	
Lynx	X						X	X	
Oncilla	X		X				X	X	
Cheetah-Cub							X	X	
Cheetah-Cub-S	X						X	X	
Cheetah-Cub-AL	X						X	X	
Serval							X	X	X

printing is almost plug-and-play without much prior knowledge. A certain level of post-processing is required in both technologies and is thus excluded from our comparison.

5.3 Application in existing Robots in BIOROB

This section is highlighting mechanical design aspects of previously existing robots in BIOROB, already introduced in subsection 4.1.2 and analyzing their pros and cons for our following design choices. A summary of robot specifications (geometric measures, weight, actuation etc.) can be found in Table 4.3.

5.3.1 Cheetah-Cub

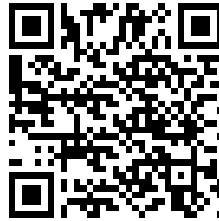


Figure 5.5 – Please find here a 3D-PDF for detailed illustration of the robot: <https://go.epfl.ch/3DPDFCheetahCub>

Cheetah-Cub as one of the first quadruped robots developed in BIOROB, set our "gold-standard" regarding leg-mechanism-design for small **and** dynamic robots on even and mostly level ground. The principle of the pantographic leg, an approximation of a cat's or dog's leg proposed by [70, 102], was implemented, also keeping the ratio for different leg segments to its biological counterparts. We will present the resulting Advanced Spring Loaded Pantograph leg (ASLP leg) in this subsection on a high level and discuss pros/ cons of the mechanisms mechanical design resulting from our experience with the robot. The CoM of Cheetah-Cub is located in the sagittal plane and the middle between fore and hind hip axis, as motors and electronics are situated proximally on the trunk and presenting by far the highest mass contribution. The interested reader is referenced to [3], where a detailed description of the original Cheetah-Cub is presented.

Main Design Contribution: The ASLP-leg

The design of the ASLP leg in Cheetah-Cub and resulting locomotion behavior resembles the one of a natural leg well. Relying on a pre-compressed and additionally, gravity loaded diagonal spring, the leg is kept under tension and is opposing a motor (located proximally on the trunk) that is responsible for active knee flexion via a cable mechanism. Extension and

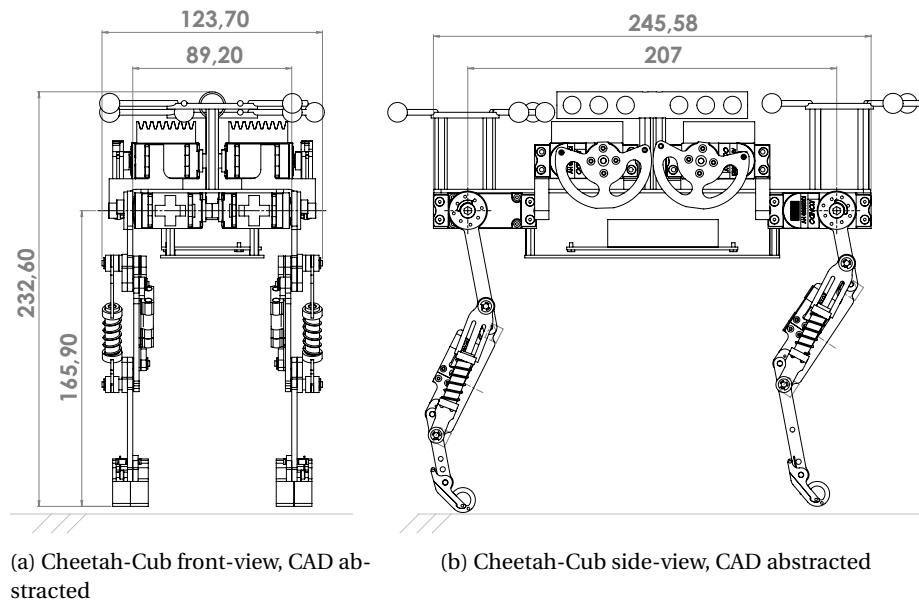


Figure 5.6 – (a-b) front and side view of Cheetah-Cub with characteristic measurements, abstracted CAD from SolidWorks

Flexion of the hip are directly induced by a motor connected to the hip-joint. The second, parallel spring is absorbing major impact from the ground contact by allowing the flexion of the l3 segment, partially storing its energy and releasing it to support the lift-off-phase of the gait as well as stabilizing after step-downs. The spring mechanism is translating a tension into compression for a linear spring. This allows a mechanical stop to be implemented, when the leg is fully extended (l1 and l3 are parallel) A passive compliant foot with a cylindrical end shape is the interface between ground and robot, thus responsible for transmission of propulsion forces, see Figure 5.7. The springs compliance partially opposed by internal friction in the leg's joints, acting as a damping element. This design approach and the choice of mostly GFRP, CFRP or POM for the legs' structural parts, results in an extremely lightweight and consequently low-inertial leg.

Advantages and Disadvantages in Cheetah-Cub

Advantages The general mechanism of the leg is very interesting when looking at straight-forward or backward locomotion on level and even ground, representing a major step towards agile locomotion, as almost all other tasks rely on this ability as a sub-feature. Here the leg is performing optimally when the right spring stiffness is chosen, so that the robot is propelled forward with enough propulsive force and at the right time (controller coordination see subsection 7.2.1). Additionally, its low inertia is allowing high frequency of locomotion,

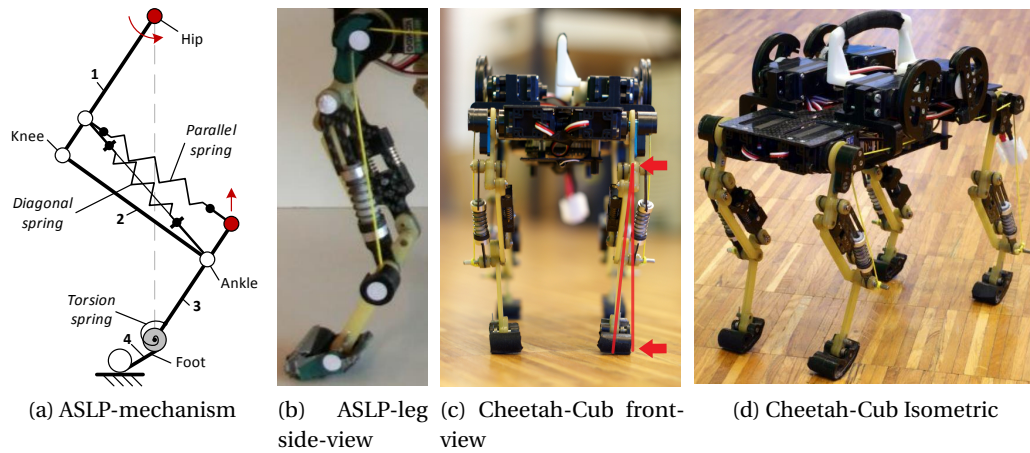


Figure 5.7 – (a) Four-segment advanced spring loaded pantograph: l1 → Scapula, l2 → Humerus, l3 → Radius, l4 → Foot, Red - Actuation, Parallel and Diagonal springs for shock absorption and leg extension; adapted from [3, 4]; (b) ASLP-leg from a side-view; (c) Cheetah-Cub from a front-view; (d) Cheetah-Cub from an isometric view

without relying on powerful actuators. The compliance in the leg, especially through the foot- and parallel springs, enables stable locomotion with a broad range of control parameters in open loop as well as very high relative speeds [3]. The design of the leg is kept rather simple and scalable, resulting in a relatively easy implementation of design changes. Simplicity in production and assembly of the trunk lead to small time investment for its construction and makes easy repair in case of breakage a possibility.

Disadvantages The main issue, occurring after a relatively high number of experiments, is related to wear-and-tear of the legs, resulting in a significant stability and performance drop. The diagonal spring was placed one-sided due to geometric constraints, resulting in a generation of parasite torques on the legs joints. These induce hole-widening at the joint axes (although sliding-bearings where used) and plastic deformation of the leg-segments, seen in Figure 5.7 (red arrow). Additionally, as there is no abduction/adduction (AA) in Cheetah-Cub, this permanent bending cannot be compensated through the robot control. Consequently, there are also changes in the ground contact area and angle, increasing the risk of falling to the sides. Bending introduces a minor increase of friction forces in the joints, putting a higher strain on the knee actuation and bearings. Another issue lies within the material selection. Fiber materials alone cannot easily be integrated with a differential construction (preferred method for prototyping due to flexibility, see subsection 5.1.2), tapping into the material and screwing parts together. The assembly of different components is mostly performed through integral construction by gluing. Especially for high-precision alignment, this method

is somewhat tricky, presenting "from-the-start" error sources in the legs. In case of failure of the glue connection (generally weak towards shear-forces), a reproduction of the involved parts usually becomes necessary, as cleaning the often permanently damaged surfaces and perform a reliable repair can become more time-consuming than replacing the parts. The leg is performance-wise ideal for level locomotion and shock absorption, due to the decoupled and spring-loaded knee-motor mechanism. This decoupling is forcing the leg to rely on passive extension against gravity and limits its performance, e.g., for jumping, where active extension with more force than provided by the springs is necessary. Another, still to be optimized, feature is the form and material of the robot's feet. Rounded feet as in Cheetah-Cub present a good starting design but still lack traction, especially before toe-off, where most of the propulsion is produced. Different foot shapes could perform better and should be explored. Pairing the shape with the right material is the next aspect to be researched. As Cheetah-Cub exhibits (positive) slippage due to the early touchdown of its feet, too high friction material is not advised. On the other hand, in propulsion we want higher friction to transmit forces better. One alternative to explored in the future is anisotropic material, allowing slippage in pro- and high friction in retraction.

Conclusion

The ASLP leg provides an excellent starting point for the mechanic leg development with clearly improvable aspects concerning material choice and durability due to different spring-placement (in Cheetah-Cub-AL, subsection 5.4.4). Performance wise, there is little need to improve the mechanism for our goal agility. Adding one more active degrees of freedom for adduction/abduction to each leg will enable to adapt to material fatigue and help with agile robot control, see chapter 7.

5.3.2 Bobcat

Bobcat, the first quadruped robot of BIOROB to be equipped with a flexible trunk and employing 3D-printing (FDM) with ABS filament for multiple of its parts, was designed as a tool to research the influence of trunk motion on the bounding gait (see subsection 3.1.1 for a detailed description of the bounding gait). The rest of the body and legs was constructed with CFRP, GFRP, and POM. Its legs were partitioned into two spring-loaded leg- and one spring-loaded foot-segment, actuated via a cable mechanism, the same way as Cheetah-Cub. The forelegs are farther apart than the hind legs, to facilitate possible overlapping during the movement, see [85]. No CAD is available, and consequently, no 3D-PDF is included in this work.

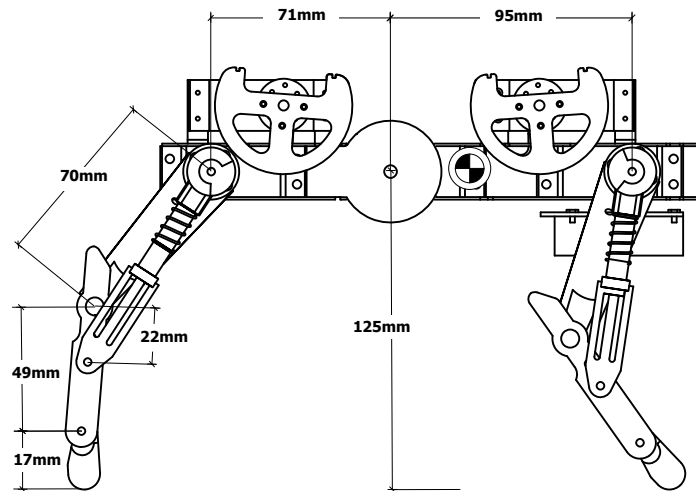


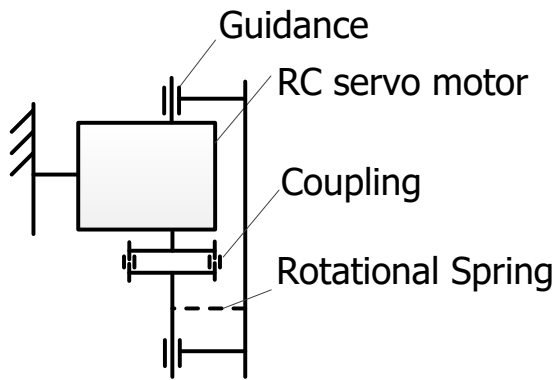
Figure 5.8 – side view of Bobcat with characteristic measurements, abstracted CAD from SolidWorks, adapted from [85]

Main Design Contribution: The Rotational Spine

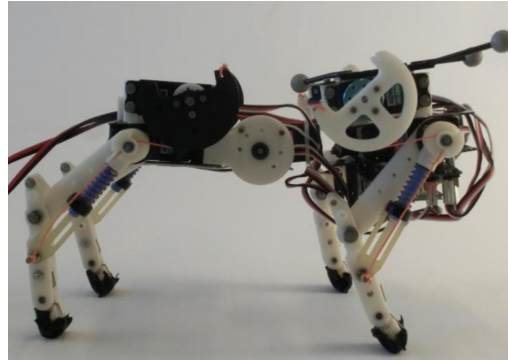
The rotational spine of Bobcat is located 71mm behind the fore hip axis and connects fore and hind trunk roughly 7mm in front of the robots CoM. Its actuation by a single servo motor allows a range of motion of $\pm 35^\circ$ from the horizontal and in the sagittal plane. Additionally to the motor, a mechanically lockable in-series-elastic element is available. The spines position and motion are aimed towards lengthening the available step-size without shortening the overall robot length significantly.

Advantages and Disadvantages in Bobcat

Advantages As can be seen in large animals like horses or cows in comparison to small and more nimble ones, like cats or rats, the spine stiffness increases with size and weight. This logical correlation has its basis in the need to support the bodies weight during motion and standstill alike without relying on constant muscle tension throughout the whole body. Bobcat is leveraging its overall size being small and lightweight, allowing for the implementation of a flexible spine and achieving agile bounding. The approximation of the spine to a single rotational joint located slightly towards the hind-trunk seems to be enough for this robot to achieve the desired behavior. Especially the ease of implementation is favorable for this design approach.



(a) Bobcat: spine mechanism front



(b) Bobcat: side-view

Figure 5.9 – (a) schematic of the spine-mechanism from top view; (b) Bobcat robot from a side-view, two-segmented legs with knees pointing backwards, rotational spine (active with in series elastic) in positioned 71 mm (/95 mm) from the hip (/shoulder) joint in between of fore and hind trunk; adapted and modified from [85]

Disadvantages Implementing only a two-segmented leg, Bobcat lost the advantage of self-stabilization through the parallel spring in case of perturbation. Additionally, the 3D-printed parts were not optimal in all load scenarios. Especially in cases of hard impacts or shear on the legs, these tended to break rather easily. Long-term effects of the general wear-and-tear and material fatigue on the 3D-printing could not be observed, as the Bobcat-project was running for less than one year and only indoors.

Conclusion

Bobcat confirmed the usefulness of a rotational spine, improving the replication of a bounding gait with close characteristics to the natural counterpart, and proved the value of 3D-printing as a very rapid prototyping method for geometrically complex parts. Most important is the result that weight and size should be kept to a minimum if one wants to use the flexibility of the trunk (later also confirmed by the MIT-Cheetah team, switching from a flexible trunk to a rigid one, see Figure 4.1). The impact in changing the level of bio-mimicry, especially concerning the level of abstraction from a real vertebrate spine while using the ASLP leg was tested in a later robot, Lynx, see subsection 5.4.2.

5.3.3 Oncilla

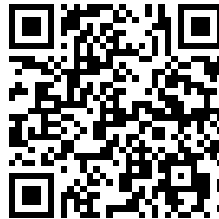


Figure 5.10 – Please find here a 3D-PDF for detailed illustration of the robot: <https://go.epfl.ch/3DPDFOncilla>

Oncilla, a robot built for closed-loop control and untethered operation, was strongly inspired by previous work with Cheetah-Cub. Its legs feature the same principle with the ASLP at its core. Due to size, weight, payload and performance expectations of the robot, stronger brushless dc-motors (including homemade planetary gears for the knee actuation) and stiffer springs where needed and forced the design to become more rigid, while keeping the base weight as low as possible. The robot thus relies on differential construction using CNC-milled as also 3D-printed parts. POM, CFRP-plates, ABS and later also PA2200 were used as main materials. Sensors were integrated through gear mechanisms to give accurate joint-position feedback. Additionally, an adduction/abduction (AA) mechanism was added to the modular design, increasing the end-effectors range of motion (ROM) and allowing richer locomotion skills, see chapter 9. The higher load and experience with Cheetah-Cub also led to the use of high-duty ball-bearings for the all robot axes, resulting in a large reduction of overall friction. A more detailed description of the robot is also presented in [5].

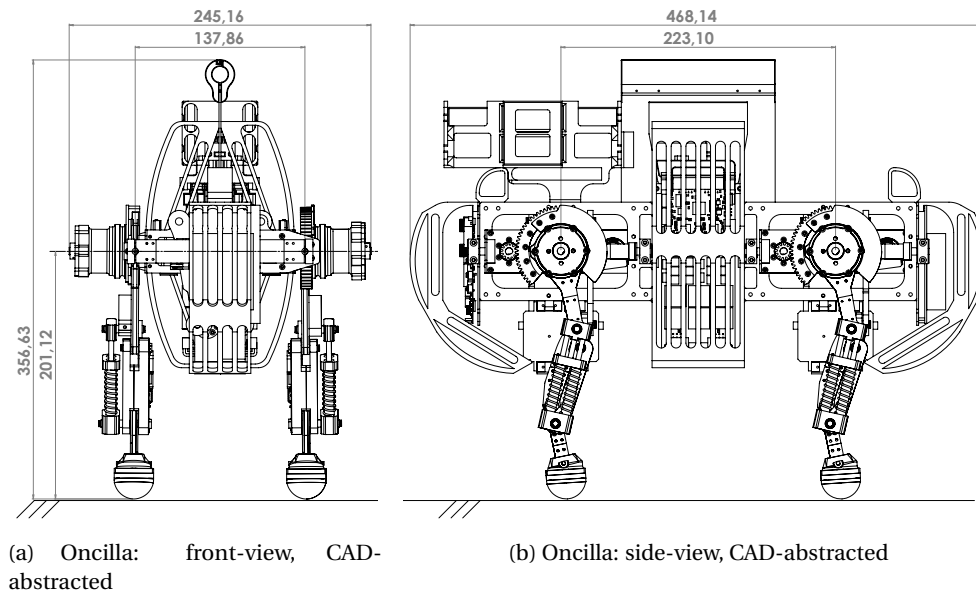


Figure 5.11 – Oncilla from front and side view, abstracted CAD-model with general measurements annotated, adapted from [5]

Main Design Contribution: The Adduction/Abduction Mechanism and Modular Design

Oncillas' design is highly centered on keeping the mechanics' weight and size of the robot as low as possible, as expected load by motors and electronics are significant, see subsection 6.2.2. Subsequently, the integration of relatively large EC-motors posed a challenge to the mechanical design. A possible solution was proposed with a modular design approach, separating the robot in three main trunk-units and four leg-units, whereas fore and hind trunk are of the same design. Each leg-unit was constructed is also identical in terms of parts, but not left-right-symmetrical for the assembly. This generally results in a reduction of production cost and effort. These leg-units which include a small servo motor placed on the robot belly increases the lateral ROM of about ± 8 deg through a four-bar-mechanism.

Original Design Contributions to Oncilla

Together with our lab technician, Francois Longchamps, we performed several iterations on different subparts of the robot, maintained and built five robot copies for BIOROB and project partners. After following a decision not to use the hip-force sensors, we replaced the leg-units' mounting apparatus with a fast clamping mechanism, decreasing the time needed to mount and amount said unit. This allowed faster performance when maintaining the robot. We iterated on the choice of materials, moving away from FDM printed ABS towards SLS

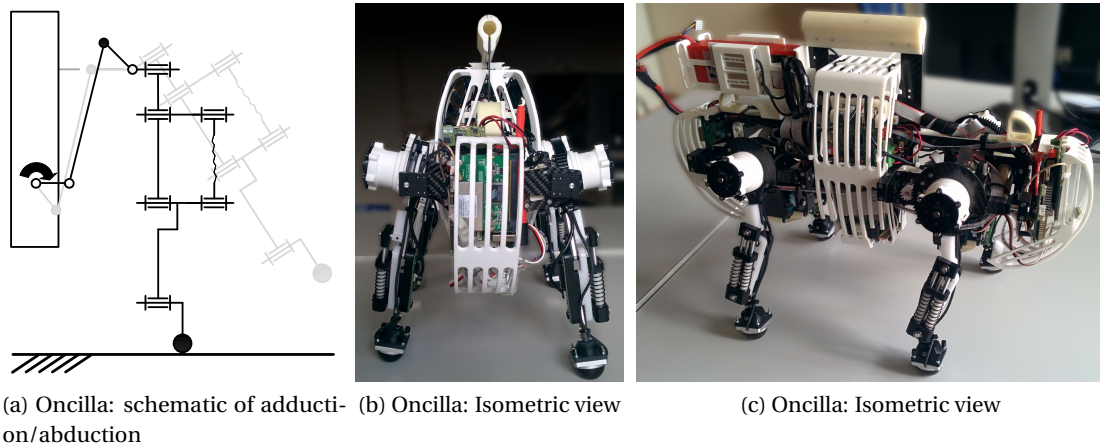


Figure 5.12

printed PA2200 due to better durability and almost isotropic material behavior. The legs, as before, were built in a differential method (with CFRP and ABS), using screws, connected to press-fitted inserts and nuts as tappings are not possible in the used materials. We changed geometry where necessary due to unwanted friction or contacts and used CNC-milled POM instead of ABS for higher precision and ease of assembly. The spring-guidance was iterated on to avoid unwanted disassembly during experiments ("explosion of the mechanism") that was endangering the users. In addition to these changes, we designed a cable management system, battery housing and protective grills for the electronics as well as modular feet, to switch between GRF-sensor and spring-loaded foot rapidly. For the latest Oncilla update, done before a large exhibition with expected long-endurance testing, we implemented fore and hind leg with equal segmentation, see Figure 5.11. This allowed us to skim down the number of different parts and have pre-assembled replacement legs, that would fit fore and hind, realizing a quick repair if needed. Impact on the gait was minimal on flat ground and could be adapted with minor parameter tuning. In total five Oncilla copies were produced, assembled, tested and maintained by the BIOROB-team and certain partners in AMARSI.

Advantages and Disadvantages in Oncilla

Advantages The modular architecture of Oncilla has proven in principle to be very beneficial when it comes to production. Generally re-using the same parts in multiple places and generating symmetries where possible allows for a small stock of spare parts to be sufficient for constant maintenance. Additionally, failure of one part did not mean to re-build a full unit from scratch, and the resulting improvement was beneficial and easily implemented in the rest of the units. In case of very distributed design, such synergies are often not usable. The

adduction/abduction mechanism is moving the whole leg-unit including the motors allowing for rigid connection between leg and actuation without additional masses to be moved by the legs motors. The rugged geometry and placement of heavy components close to the ground made the robot inherently very stable, as the COM was rather close to the ground, improving the usability as an experimental platform for intensive testing strongly.

Disadvantages Oncillas first iterations were designed, assembled and distributed under great time pressure. As the ARMARSI-deliverables stated early distribution to partner laboratories, time to thoroughly test and iterate on the design was missing. Integration of many components into a small work-space make assembly and production very time-consuming and complex. A tracked time for a trained technician to assemble one leg-unit was measured to be at least one hour and respectively for the full robot mechanics roughly 6 hours. This gave rise to concerns how well maintenance outside of BIOROB, e.g., by the other partners of ARMARSI, could be realized and if a complex platform like this is suited for Open-source distribution. Another major drawback is the precision needed in the production, especially concerning parts that hold the robot's joint position sensors. Due to the sensor technology (hall effect, discussed in subsection 6.2.2) less than a tenth of a millimeter precision was needed for alignment. This also proved to be a vital drawback during experimentation as sensors would sometimes randomly stop working because they got misaligned through vibrations and impacts. Oncilla was and is still used as an experimental platform, and thus results and analysis of long-term employment effects are feasible. Already improved through the iterations described above, but still present is the aging of 3D-printed materials. This is manifesting in breakage of parts due to UV-rays (Sun), chemical reaction with different glues, or mechanical wear-and-tear in many parts. This should be improved as regular, and depending on the concerned part, expensive as well as time-consuming maintenance is necessary for the robot to perform satisfactorily. The positioning of the robots adduction/abduction actuation was in hindsight not ideal. Placing them at the robot's belly improved the position of the COM (the lower, the better, as better stability) but drastically reduced the ground-clearance of the robot making, for example, high step-downs an issue. The same comment is applicable for the placement of the motor-driver-boards although here not much could have been done simply due to their size in comparison to the robot as a whole. The ROM of the adduction/abduction was very small, although sufficient for adaptation to different perturbations [12]. This was mainly due to the long EC-motors that passed through the robots' sagittal plane. When the adduction/abduction was engaged, the motors would hit mechanical stops. This could be improved by increasing the trunk height or widening the distance between the hip-axes, leading in both cases to possible stability-issues due to possibly increased rolling angles in certain scenarios.

Conclusion

Oncilla's mechanical design showed that a modular approach can be beneficial when it comes to cost and efficient production. Too many parts make the assembly complex but also allow relatively fast maintenance (if the parts are connected with differential methods). A compromise should be found in this regard. Again, as seen in Bobcat, the choice of FDM printing with ABS had not proven to be a sustainable approach, and SLS printing was more suited to our applications. Following the needed precision for sensor integration, advantages of classical CNC-milling over the (at the time) emerging 3D-printing-technologies for exact component dimensioning were observed.

5.4 Mechanical Development towards Serval

Serval, the latest robot, that was constructed during this Ph.D. thesis, is the last of an iterative development line. Most of its features were separately implemented, tested in different robots, and integrated into Serval's final form. This section is describing this iterative process and analyzing pros and cons in the different robots, clarifying the occurring variations in the Serval design.

5.4.1 Mechanics needed for Agile, Legged Robots

When looking at dogs or cats moving through their environment, they show enormous skill balancing and adapting to unforeseen circumstances. Nevertheless, they often trip, fall or run into their surroundings. As we hypothesize not being able to reach a better level of control and environmental sensing, than our role-models, our robots needed at least a sturdiness somewhat close to the animals'. This includes first and foremost compliant element in key positions, protecting the robots' hardware from harm. Further, a sturdy, but very lightweight skeleton should build the mechanical core, resulting in a low inertia system, enabling fast reaction without high strain on the actuation. If these measures fail to enhance the movement and protect our robot, repairs are facilitated by a modular design approach.

5.4.2 Lynx



Figure 5.13 – Please find here a 3D-PDF for detailed illustration of the robot: <https://go.epfl.ch/3DPDFLynx>

Lynx is a compliant quadruped robot with the focus on multiple modular spine designs (doable as robot size allows for strongly under-actuated flexibility in the trunk) and a pantograph leg design (Figure 5.14). It is mainly built out of milled CFRP- and GFRP plates as well as 3D-printed ABS-pieces. The legs are differently constructed than in Cheetah-cub but realize the ASLP mechanism again as the functional principle. The actuation is realized with RC-Servomotors in a similar manner to Cheetah-Cub. The robot has 9 actuated degrees of freedom (DOF), two per leg and one in the spine. It consists of two trunk segments of which the front one is slightly heavier (about 40 g) caused by the location of the control board, the legs and an active spine that connects the trunk elements. The spine-versions (SV) are all actively actuated but differ in their use of the compliant elements (see Figure 5.4.2, Figure 5.4.2 and Figure 5.4.2) as well as a "single point of rotation" (the strongest abstraction from nature) vs. "multiple point of rotation" (less strong abstraction from nature/ closer to the actual S-shape of a cat-spine (full spine, locomotion relevant without the head could also be seen as C-shaped)). The design is completed by a passive tail-like structure, that acts like a 5th-leg-stabilizer of the system in case of high pitching motion induced by bad gaits (it prevents the robot from falling backwards). In these cases, the compliant elements in the structure will push the robot in the opposite pitch-direction. This results in the establishment of ground contact with all four legs. This tail-like structure represents a non-bio-inspired part, as animals (except the Kangaroo and some small mammals) seem not to use their tails for active pitch support during ground locomotion (ongoing research, see also [7]).

Main Design Contribution: Active and Inter-changeable Spines

Spine-design Version 1 (SV1) Similarly, to the spine used in Bobcat [85] SV1 implements a purely rotational spin, a simple way of implementing a spinal undulation in the sagittal plane (upwards and downwards actively). It is actuated by one motor at its center and has an in-series glass fiber rod as the compliant element. This compliance prevents the motor to receive too high impacts during its oscillating motion and thus prolongs the lifetime of the motor. Important to know is that the rotatory joint (here axis of the servo) is close to the front

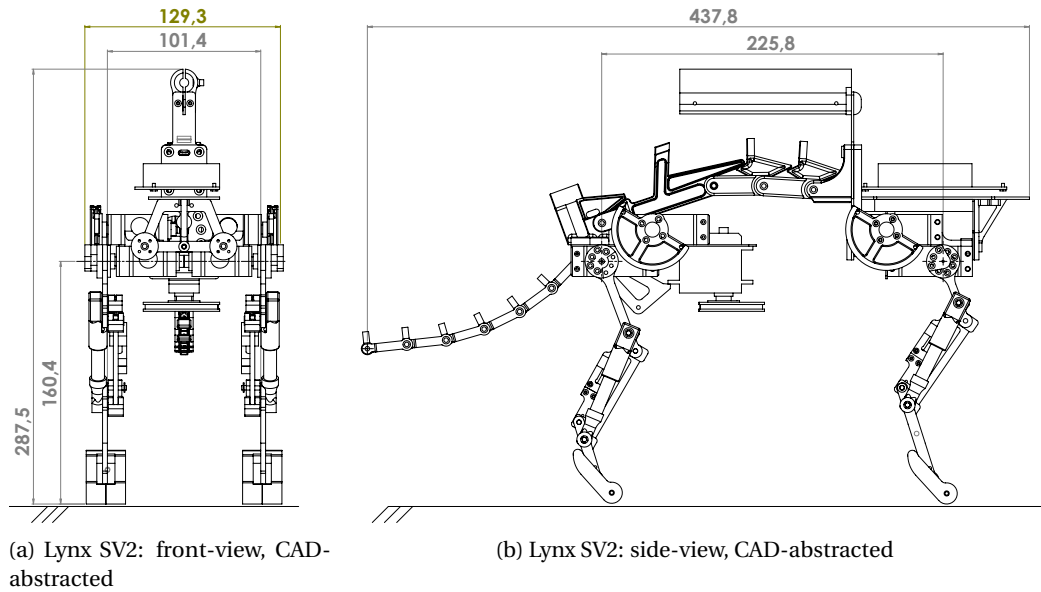


Figure 5.14 – Side view of Lynx with fore-, hind-trunk and all three exchangeable spine-modules, from top to bottom: SV1, SV2, SV3 and front-view of Lynx; with characteristic measurements extracted from SolidWorks

body segment. This stands in contrast to the animal world, where deflection over the whole length and not at a single rotational joint can be observed [40]. The exact point of rotation is subject of ongoing research. Thus it is our interest to see if a very simplified spine can achieve the desired motion. [103] recently studied the influence of the rotation axis and concluded that a position more to the rear could be beneficiary for dynamic robot locomotion.

Spine-design Version 2 (SV2) The second spine design (Figure 5.15) is purely composed of 3D-printed ABS pieces that are connected through steel axes. The structure seems more like that observed in nature because of the modular segments (equivalents of the "vertebrae"). It can move in the sagittal layer downwards actively (with RC-motor as flexor) and upwards until the blocking point passively (compliant rod as extensor). The specific shape allows a pre-bending of the compliant element, again a glass fiber rod, which acts antagonistically to the actuation. The difference of this design in comparison to SV1 lies in the passive reverse motion achieved through the spring element.

Spine-design Version 3 (SV3) SV3 is a multi-segmented spine build out of ABS (Figure 5.15), with structural similarities to SV2. Its passive elasticity consists of two glass fiber rods, in parallel. The rods are, due to the shape of the spine (mechanical stops at the equivalents of

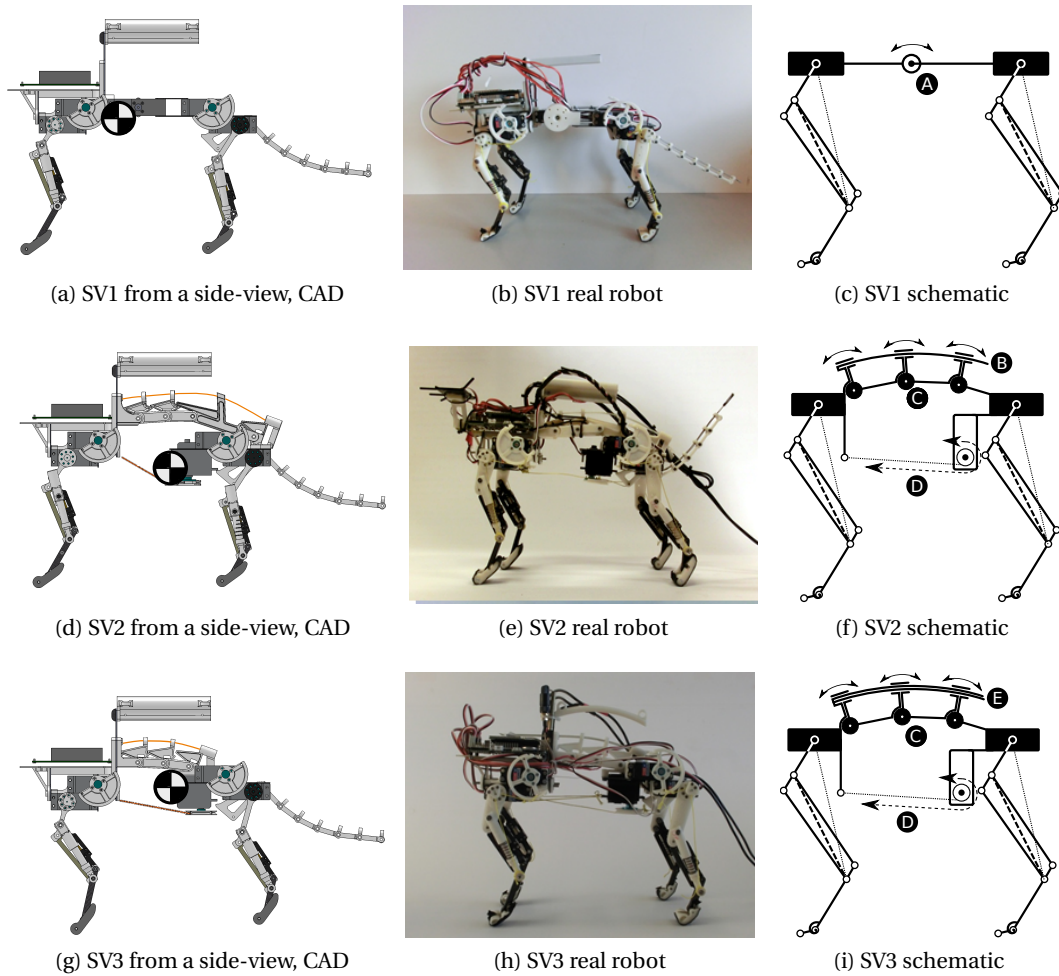


Figure 5.15 – Schematic presentation of Lynx-robot spine configurations, side-view, front to the left, computer-design (left), real robot (middle), and schematic view (right). From top to bottom: SV1, SV2, and SV3. The markers on the computer design indicate the centre of mass for each configuration. (A) Single, rotatory, actuated joint of SV1. (B) Single leaf-spring, mounted in a pre-stressed fashion. (C) Multiple, passive, rotatory hinge joints of spine design SV2 and SV3; joints have limited range of rotation: only downwards, not upwards. (D) Antagonistic actuation based on pulley and cable mechanism, this actuation produces a flexing-torque of the SV2/SV3 spine. In case of external flexing forces, the cable mechanism goes slack. (E) Spine design SV3 applies two glass-fibre leaf springs in-parallel, and has a higher stiffness compared to SV2 (B). The symbol in the middle shows the position of the centre of mass (from CAD-model)

"vertebrae"), pre-bent and thus apply an upwards force. The actuation is achieved by one RC servo motor, that acts antagonistically to the glass fiber rods, by pulling via a string on a lever opposite to its mounting position. It is driven over a pulley to achieve straight alignment and prevent the spine from bending sideways, influencing stability. Differences to SV2 are the stiffness of the spine, which is doubled, its length as well as the position of the contact with the hind trunk-segment.

Advantages and Disadvantages in Lynx

Advantages The overall built time of the robots was very fast (e.g., compared to Oncilla). Using FDM and minimal machining, allowed for very rapid implementation (about three months) of one early-up-prototype (not mentioned in this thesis) and three follow up spine-versions. The modularity, only having to produce the trunk once and exchanging the spines, was contributing as well. The robots were able (with repairs) to perform a very high number of experimental runs in a small amount of time, generally confirming, that 3D-printing is plausible to be used for robot prototyping.

Disadvantages The pre-bent glass-fiber-rod of SV2 and SV3 increased friction massively due to strong and sharp contacts with its guidance system. Consequently, energy got dissipated to overcome friction and was not usable for the actual movement generation. The vertebrae block movement upwards in the spine, that could be problematic in gaits like the rotary gallop, where a small extension of the spine can also be observed. Additionally, multiple vertebrae and leg-parts broke due to the anisotropic nature of the used FDM-ABS, when stressed from different directions.

Conclusion

The key message from Lynx would be to use modularity in design as much as possible, as it allows for rapid repair, experimentation, and specialized configurations. The use of 3D-printing is contradictory in this work, as it has pros and cons alike. On the one hand, it allowed straightforward implementation of the parts without manual machining. On the other, many pieces broke during experiments, resulting in a large effort to keep the robot running, hindering continuous experimentation. Experience gained from this project, how to design when using anisotropic FDM is one valuable outcome from this mechanical construction. Another is the positioning and number of vertebrae, needed to allow for natural motion, see subsection 9.2.1.

5.4.3 Cheetah-Cub-S



Figure 5.16 – Please find here a 3D-PDF for detailed illustration of the robot: <https://go.epfl.ch/3DPDFCheetahCubS>

Cheetah-Cub-S firstly introduced a spine for steering on the Cheetah-Cub basis. The robot consisted of two trunk/leg-units and a lateral bending spine-unit. Each trunk unit housed two ASLP-legs. The legs were adapted from the role model Cheetah-cub and paired via a CFRP plate to create fore and hind trunk modules, forming a small-footprint structure. In principle, this structure could incorporate strain-gage sensors. After problems encountered in Oncilla (see subsection 6.2.2), this idea was abandoned and never implemented.

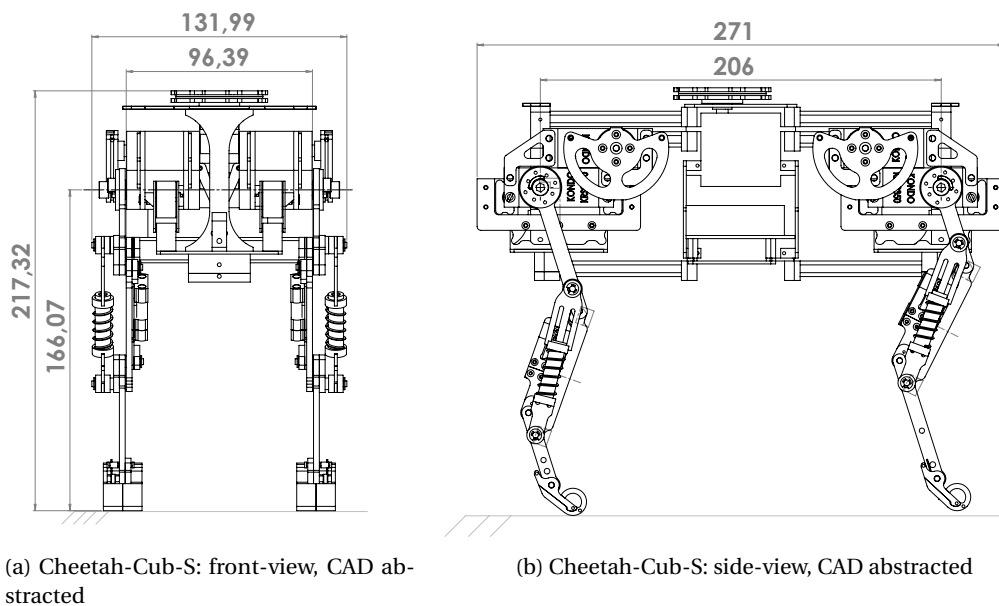


Figure 5.17 – (a-b) front and side view of Cheetah-Cub-S with characteristic measurements, abstracted CAD from SolidWorks

Main Design Contribution: Spine for Steering

The spine is located symmetrically between the trunk-modules and is composed of an active and compliant joint, see Figure 5.18. Deflection can be determined actively while external loads are partially absorbed by the compliant element. The motor, placed in the center of the robot flexed both fore and hind trunk synchronously and equally towards one side. Torque was initially transmitted via a cable mechanism (dashed lines) but exchanged due to an instability of transmission in the prototype (slack of cables) against a bar mechanism. The original version with a spring-loaded cable mechanism was implemented later and performed well. One leaf spring (first POM, later NiTi) (green line) was attached to each side of the motor. The overall turning radius is reduced compared to having only one spring on a particular side, but synchronous bending seemed beneficial, as the leaf-springs could be dimensioned shorter, thus just holding half of the robot's gravity each. In principle, only lateral bending is allowed. Furthermore, to decrease externally induced torsion, two leaf springs were mounted in parallel on the robot's belly.

Each spine segment bends to ± 5 deg which corresponds to a total spine deflection of ± 10 deg.

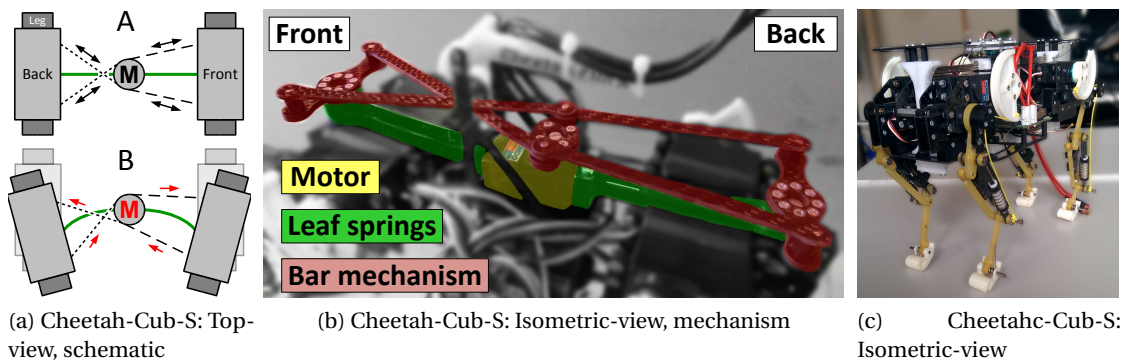


Figure 5.18 – Detailed figures of Cheetah-Cub-S; (a) Schematic depicting the steering mechanism with constant stress on the cables in case of active turning; (b) Rigidified steering structure with bar-mechanism; (c) Isometric view, showing the replicated ASLP leg and the modular leg unit.

Advantages and Disadvantages in Cheetah-Cub-S

Advantages The most prominent advantage of the steering-spine is its simplicity of the principle behind the mechanism. One single active degree of freedom adds the capability of directional movement. This, in contrast to more complex steering principles, e.g., via adduction/abduction, is a cheap and relatively efficient use of resources.

Disadvantages The spine segments were not able to prevent external torsion sufficiently which always resulted in unsuccessful locomotion. Figure 5.19 shows examples of manually produced spine twists.

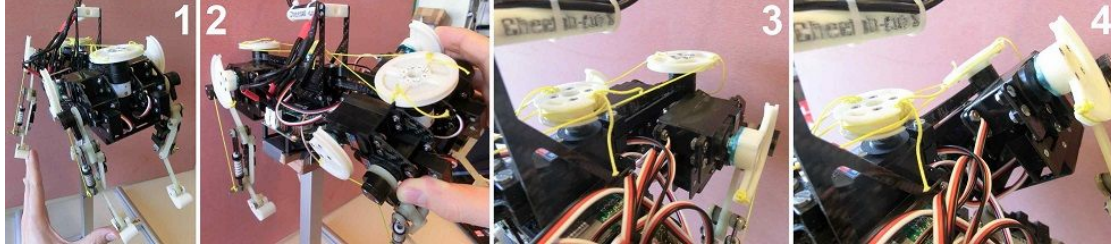


Figure 5.19 – Examples of high spine torsion: 1 - front and back pushed by hand, 2 - front only, 3 and 4 - Comparison back part

The first picture shows the situation with both parts rotated against each other. To minimize torsion, the overall height and stiffness of the leaf springs were increased by implementing a third one in parallel. The segment was added at the bottom of the robot to prevent extensive redesign. The amount of torsion was reduced significantly which improved the overall performance. The original idea of steering via cables was suboptimal due to missing structures for keeping tension at all time. The cables sagged which led to an undesired backlash. Instead of implementing additional components, the cables were replaced by four rigid bars and the pulleys by simple levers. Due to the small range of the spine angle, the rigid bars never go into a singularity. As a side effect, we could observe additional stiffening against torsion whereas manual flexion of the spine was very much reduced. One downside, besides unexpected behavior through the compliance, is the space, that the mechanism requires.

Conclusion

The principle behind the steering-spine is very effective (small radius with little control alteration) and can be implemented mechanically with little effort. Concerning the transmission of motor torque to the trunk units, it is possibly favorable not to use a cable mechanism but couple the steering motor directly (through a compliant element, protecting the motor from impacts) to the rest of the robot. Adding a flexible element opposite of this (semi) rigid connection can keep unwanted torques or forces in check.

5.4.4 Cheetah-Cub-AL



Figure 5.20 – Please find here a 3D-PDF for detailed illustration of the robot: <https://go.epfl.ch/3DPDFCheetahCubAL>

Cheetah-Cub was not fundamentally altered from its early development days. A new and parameterized (easily scalable) leg-design introduced in Cheetah-Cub-AL featured a (to the sagittal plane of the leg) symmetric diagonal spring, canceling unwanted bending behavior present in previous Cheetah-Cub-versions, see subsection 5.3.1.

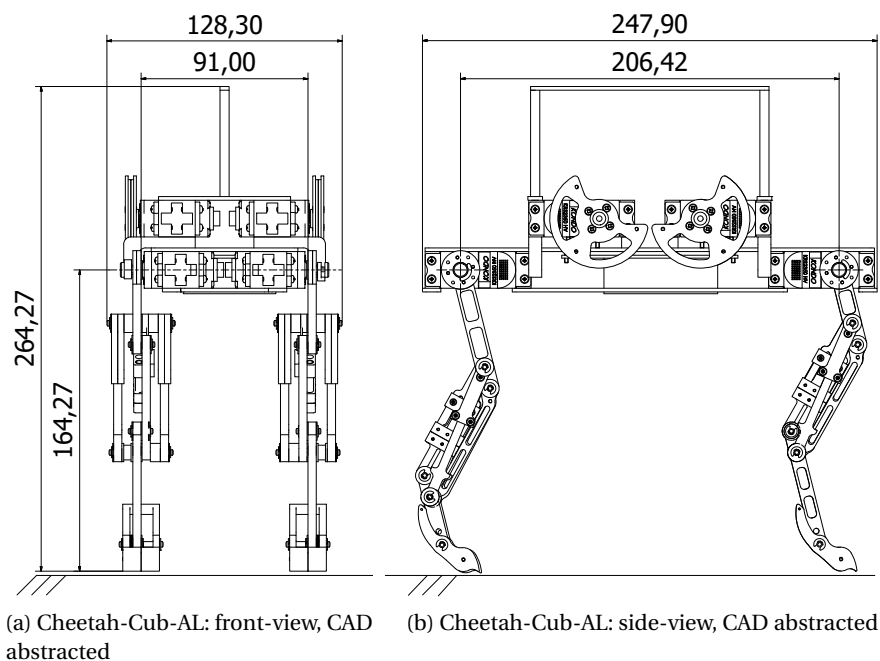


Figure 5.21 – (a-b) front and side view of Cheetah-Cub-AL with characteristic measurements, abstracted CAD from Autodesk Inventor

Drawing benefits from classical CNC-manufacturing with aluminum in combination with ball-bearings in every joint, internal friction was reduced, alignment of the axis and repeatability of experiments were improved. The changes to the trunk are little but feature now an easy access

to the control board for development purposes and a slimmer design, for easy transportation. Overall dimensions of the leg segments were slightly altered to allow for easier production. Leg-length was kept constant. This easy to assemble structure is ready for quick modification, e.g. to test the impact of spring placement on agility [28].

Main Design Contribution: Double-spring and Material Selection

The symmetric diagonal springs are guided on an AL-bar with a rectangular profile, that slides inside an Al-housing. Aluminum is cheaper and easier to machine than CFRP and can simply be connected in a differential approach by reliably tapping and screwing into the material. Additionally, to screw connection, the leg's parts were "stacked" together on the joint-axes and fixed by spring-lockers at their ends. The stiffness of the springs was slightly adapted and experimentally optimized to accommodate an increased robot weight. The compression cable of the ASLP-mechanism could not be routed exactly through the leg's sagittal plane but was placed as closely as possible.

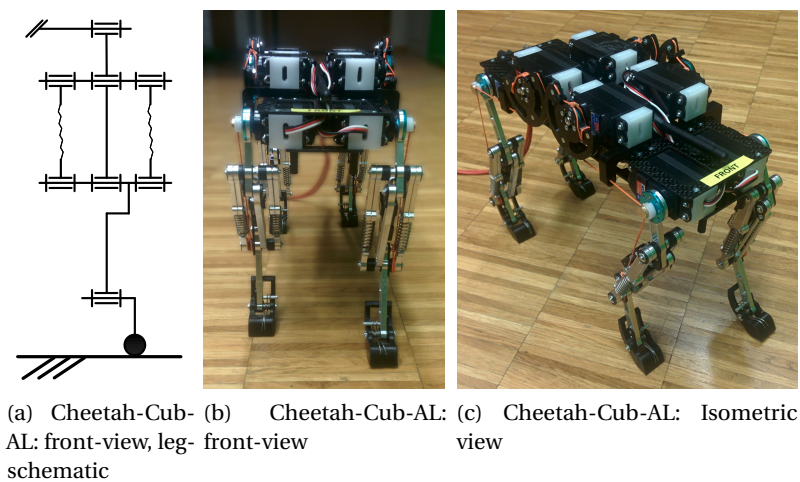


Figure 5.22 – Detailed views on Cheetah-Cub-AL; (a) showing the symmetric double-spring structure from a front view; (b,c) front and isometric view after first assembly; no bending effect on the legs are visible.

Advantages and Disadvantages in Cheetah-Cub-AL

Advantages The symmetric spring construction made the robot more reliable after long-term experimentation. Being able to assemble without the need for gluing, the design is highly adaptable and reparable. One leg can be assembled in under 8 minutes and without specialized equipment.

Disadvantages The guidance of the springs is not optimal, as AL glides on AL, resulting in an abrasion on different edges and surfaces of both guidance pieces. Consequently, a higher play was observed after a while (not enough to make a repair or replacement necessary, but visible when moved manually). Another (minor) disadvantage of the new design is the increased weight of 20% in comparison to the original ASLP.

Conclusion

The success in changing material and double-spring mechanism should replace the original ASLP leg implementation. Attention has to be given to the material combination for the guidance, as any unwanted play is lowering the reliability of a design. This might become more prominent as it had in Cheetah-Cub-AL as soon as the design is scaled to a larger size (small play at the end of the guidance can result in strong displacement at the beginning).

5.4.5 Serval



Figure 5.23 – Please find here a 3D-PDF for detailed illustration of the robot: <https://go.epfl.ch/3DPDFServal>

Mechanical development in Serval presents a combination of tested mechanisms from previous robots with the goal of enhancing their advantages whereas canceling out as many disadvantages as possible. The resulting robot consisted of a somewhat modular design built around pre-defined servo-motors (Dynamixel MX64R/MX28R) as a differential and symmetrical assembly. One can distinguish three reusable main units: (1) trunk, (2) leg and (3) spine unit, illustrated in Figure 5.27, Figure 5.28, and Figure 5.29. These units integrated and extended with a new foot design as well as in-series elastics for motor and mechanics protection from impacts were designed to enable agile locomotion. Dimension-wise the robot is settled on a similar scale as Oncilla, with focus on reaching an as lightweight as possible construction. To this end and with ease of implementation in mind, the robots' skeleton was mainly built from lightweight AL, Steel (only for axis) and POM, machined with classical CNC-milling, CNC-Laser, and bending techniques as well as using only two different screw sizes (M2, M2.5).

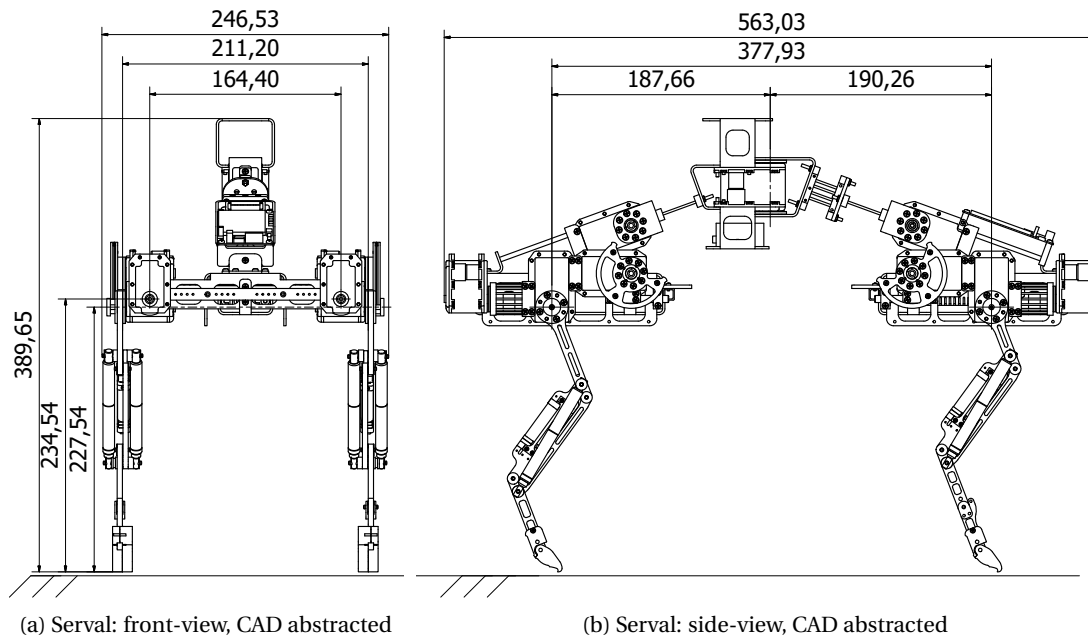
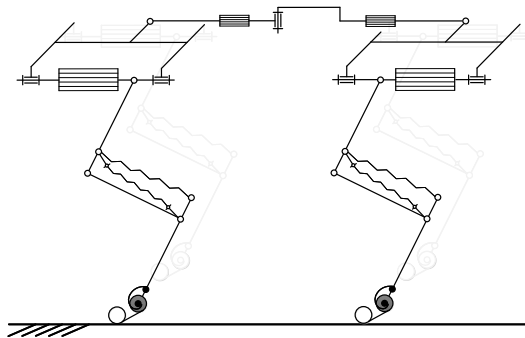


Figure 5.24 – (a-b) front and side view of Serval with characteristic measurements, abstracted CAD from Autodesk Inventor

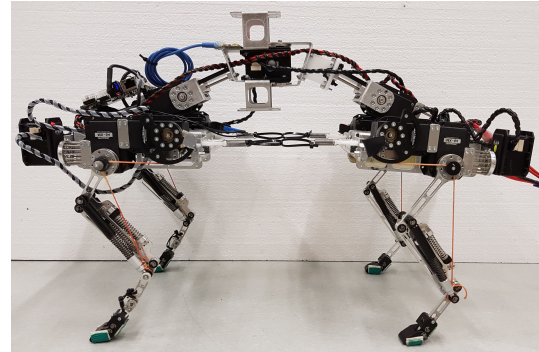
Main Design Contribution: Systems-integration, In-Series-Elastics, Flexible Toes

Serval was built by combining four leg-units with two trunk- and one spine-unit, which were designed around the actuation and using the motor-chassis as frame-elements to keep weight at a minimum. These specialized units will be discussed in the following paragraphs.

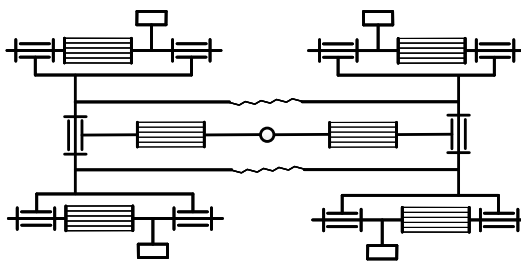
Leg-unit The leg-unit incorporated at its base an ASLP-leg in the design of Cheetah-Cub-AL, see description in Figure 5.27. Due to the size of the robot and thus the legs' dimensions and resulting lever arms, a drastic increase in spring stiffness had to be undertaken, see Table 4.3. ASLP segmentation (fore and hind differ) was kept as a scaled version of Cheetah-Cub-AL to re-use as much of the previous design as possible. Additionally, an additional passive-compliant carpal-joint (wrist joint) was added to the forelegs, to test the possibility of small-step-ups without sensory feedback. The leg unit was iterated once, as the diagonal spring-mechanism with rectangular guidance caused the following issues due to (mainly) manufacturing (in)precision and material combination: The guidance's inner part was able to scratch on sharp edges of the outer guide (both AL). This in the beginning unnoticeable wear-and-tear worsened quickly during the first experiments resulting in a full blockage of the ASLP-mechanism. After exchanging the guidance with a turned AL-inner- and POM-outer-



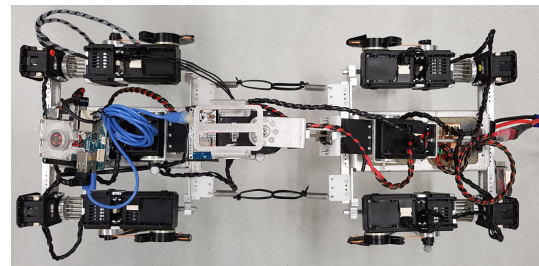
(a) Serval from a side-view, schematic



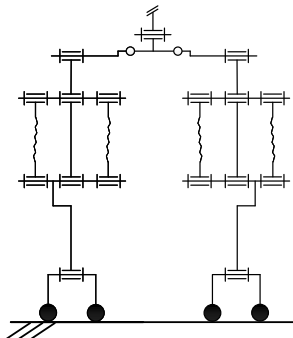
(b) Serval from a side-view



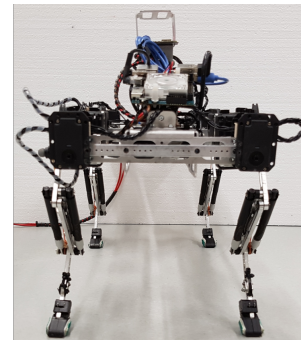
(c) Serval from a top-view, schematic



(d) Serval from a top-view



(e) Serval from a front-view, schematic



(f) Serval from a front-view

Figure 5.25 – Detailed views on Serval: (a,b) Side view with ASLP mechanism and in series elastics in legs and spine; (c,d) Top view, steering DOF in the middle, symmetrie of the design is visible with 4 leg-, two trunk- and one spine-unit; (e,f) Front view depicting the double-spring ASLP and seperated spring loaded foot, AA-DOF is aligned with the hip axes.

guide, repetition of this error was never observed again. Between robot adduction/abduction (AA), with direct actuation located roughly on the hip axis height, an in-series torsion tube-like mechanism was mounted. This tube consisted of 16 circular arranged NiTiNol-wires of $d = 1.5\text{mm}$ thickness. Flexion of the leg due to external forces resulted in a torsional displacement, reducing direct impact propagation to the AA-actuation. This mechanism could be combined with a rotational damper to dissipate impact energy instead of just smoothing the peak forces. After testing different designs, we decided to include a segmented, spring-loaded foot with two rounded, claw-shaped toes. We hypothesized the need for ground adaptation due to the large AA-capability of the robot (changing the lateral angle to the ground) and hoped for better grip on rough terrain.

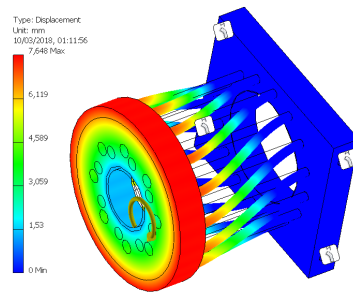


Figure 5.26 – Example of a deformation analysis using FEM for the AA-compliance, resulting in a visualization and numerical values for defined parts; Precision and correctness is only as good as the inputted data.

For approximate calculation, we assume full homogeneous transition to austensite state and use its Young's modulus and Poisson's ratio, see Table 5.1. The resulting approximated torsional stiffness had to be calculated as torsion rod with hollow core and diameter resulting from a closed shell of NiTiNol wires. The calculation is as follows:

$$\Phi = \frac{M_t \cdot l}{G \cdot I_t} = \frac{M_t}{k_t} \quad (5.1)$$

$$G = \frac{E}{2 \cdot (1 + \nu)} = \frac{75}{2 \cdot (1 + 0.33)} = 28.2 \quad [\text{kN mm}^{-2}] \quad (5.2)$$

$$I_t = \frac{4 \cdot A^2 \cdot d}{U} = \frac{4 \cdot 800.9 \cdot 1.5}{24} = 200.2 \quad [\text{mm}^4] \quad (5.3)$$

$$U = 16 \cdot d = 24 \quad [\text{mm}] \quad (5.4)$$

$$A = 16 \cdot 0.25 \cdot \Pi \cdot d^2 = 28.3 \quad [\text{mm}^2] \quad (5.5)$$

$$k_t = \frac{G \cdot I_t}{l} \approx \frac{28.2 \cdot 200.2}{22.3} \approx 253.2 \quad [\text{Nm rad}^{-1}] \quad (5.6)$$

The resulting values help us to define length, number and diameter of the employed NiTiNol

rods in a way to achieve deflection in case of unwanted perturbation, but only very small deflection during "normal" locomotion. The new foot design features two spring-loaded toes, flexibly adaptable to the ground when AA is engaged. After many experiments and design iterations, we decided to use a rounded claw instead of a cylindrical shape. This should allow better traction in granular media as often encountered outside a lab environment.

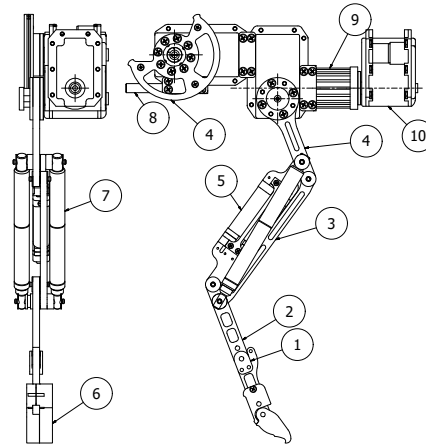


Figure 5.27 – Serval's leg unit from a side and front view: (1) carpal joint, (2) l3-segment (parallel to l1), (3) l2-segment, (4) l1-segment (parallel to l3), (5) parallel spring (uncompressed), (6) compliant foot (2 toes), (7) diagonal springs (symmetric to saggital plane of the leg), (8) rotary fixation for the leg-unit, (9) AA-in-series-elastic, (10) AA-motor with axis slightly displace from hip axis, higher ground-clearance when moving to the outside, smaller to the inside

Trunk-unit Depending on its position in the fore or hind, the trunk unit is housing the SBC or LiPo-battery in its bent AL-shell. Subsequently, to allow the needed plastic deformation without cracking, the AL-alloy used had to be quite soft. To give rigidity to the assembly and allow flexible mounting of auxiliary equipment like sensors, a head or tail unit, tapped bars were added to the leg units suspension. Up to four leg units could be exchanged or turned around (to narrow the robots leg-to-leg width) within a few minutes and with a minimal tool-set, by opening the suspension-clamp (fixed-loose-connection) on one and three screws on the other side (fixed connection).

Spine-unit Three active DOE, one for rotation in the transversal and two for rotation in the saggital plane, were forming the core of the spine including a small handle and IMU-connector on the middle motor. The elements were connected through bent AL-pieces and leaf-springs made of four NiTiNol wires in parallel. The hind elastics were connected in a cross shape, stiffening the spine in one direction and enabling compliant behavior in the orthogonal other to comply with the in-series load for their respective motor. The overall arrangement

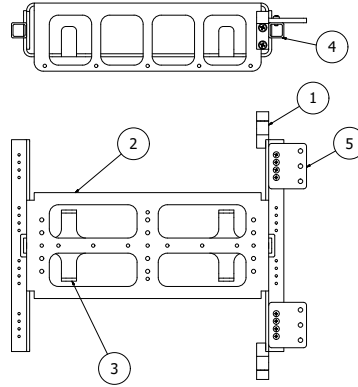


Figure 5.28 – Serval's trunk unit from a side and top view: (1) removable fixation for the leg-unit, (2) main body (single bend AL-piece), (3) Battery/ SBC fixation, (4) reinforcement and attachment bar, (5) attachment for tension springs, keeping the trunk level on ground contact

of the springs is approximating a classical rectangular leaf spring. This results in different overall behavior of the springs depending on the direction of the applied forces, inducing a small displacement in one and larger in the orthogonal direction. For adjustment of the allowable deflection and stiffness of the springs, clamps can be added to the spring-fixations, shortening the free length of the mechanism. Stiffness is also reducible by removing wires from the set. The resulting stiffness for the leaf springs is calculated per wire and added up to a parallel placement of four wires in total (k_{x1} -long elements, front and back, k_{x2} short elements, middle):

$$s = \frac{F \cdot l^3}{3 \cdot E \cdot I_x} = \frac{F}{k_x} \quad (5.7)$$

$$c = \frac{3 \cdot E \cdot I_x}{l^3} \quad (5.8)$$

$$I_x = \frac{\Pi \cdot d^4}{64} \quad (5.9)$$

$$k_{x1} = \frac{3 \cdot 75 \cdot \frac{\Pi \cdot 1.5^4}{64}}{30^3} \approx 2.1 \quad [\text{Nmm}^{-1}] \quad (5.10)$$

$$l_{x2} = \frac{3 \cdot 75 \cdot \frac{\Pi \cdot 1.5^4}{64}}{16 \cdot 2^3} \approx 13 \quad [\text{Nmm}^{-1}] \quad (5.11)$$

$$k_{x1-total} = 4 \cdot k_{x1} = 8.4 \quad [\text{Nmm}^{-1}] \quad (5.12)$$

$$k_{x2-total} = 4 \cdot k_{x2} = 52 \quad [\text{Nmm}^{-1}] \quad (5.13)$$

For our spine, we desire relatively stiff connections enabling the direct transmission of forces in the steering direction and softer springs for saggital movement. We believe that a certain amount of compliance as the opposite of stiffness in the spine is necessary when impacts, e.g., from falls, are too large to be absorbed by the legs' compliance alone. This hypothesis as yet to be tested (as we did not yet dare to let our robot fall from heights overpowering Serval's legs)

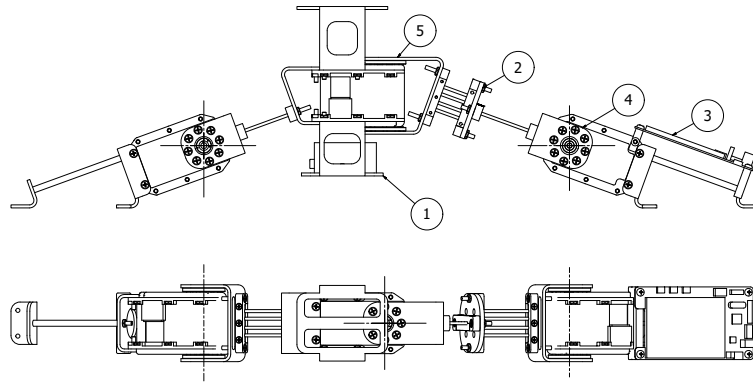


Figure 5.29 – Serval's spine unit from a side and top view: (1) IMU fixation, (2) Cross-joint with Nitinol-leafsprings, (3) screen for basic HMI, (4) up-down DOF, (5) steering DOF

Advantages and Disadvantages in Serval

Advantages Serval presents a symmetric and modular approach, including different interchangeable parts and fast production. The robots' design optimizes positive effects of previous robots without repeating the mistakes made, e.g., very large ROM, direct steering spine and AA. Mechanical tuning options for all springs (stiffness change/ employing different pre-compressions/ removing or blocking) are included and make experimental adaptation and optimization towards a more agile system possible. All parts are fully parametrized and can be scaled by changing few key values, allowing for implementation of smaller or larger robots in the future. Machining is exclusively done in AL and POM, fully isometric materials, giving the option of quality control through classical and simple FEM analysis. Enough space and pre-defined connections are implemented to modify and add, for example, the sensory equipment to the robot. Besides these advantages, we managed to keep the mechanics' cost to a minimum, see Table 8.1.

Disadvantages Optimizing the robot's skeleton for weight, left us at the lower boundaries, of what is possible with classical methods and AL. If we need to lighten the load in the future even

more, e.g., to allow for heavy sensor equipment to be present while keeping the same actuation, we will have to switch to novel composite material reinforcement. We can imagine a metal skeleton, for precision and connectivity with specially reinforced structures in a sandwich design (much like in *Oncilla*). Further, the spine is not rigid enough to keep the robot's fore and hind trunk level, as soon as the legs touch the ground. We had to add tension springs in between the trunks to counteract these forces. Unfortunately, this might interfere with the very efficient use of the spine DOFs in their full range of motion. Although providing good adaptability, our feet are tiny. This hindered us in finding a suitable sensor for GRF-sensing. To the end of this thesis, a new collaboration arose, with capacitive sensors, small and flexible enough for plausible usage on our robot's feet. This has yet to be integrated. Additionally, we still did not find a very sturdy material to produce the feet from. POM, used in our prototypes, is wearing out relatively fast due to abrasion.

Conclusion

From the mechanical side, Serval has the potential for agile locomotion. Relatively stiff legs allow for good shock absorption in a higher weight-range and possibly fast extension (explosive behavior) in low load cases. Modular design and adaptability of spring-stiffnesses enable experimental tuning for our agility tasks efficiently. Turning and locomotion in difficult terrain are in principle possible via different strategies, leveraging the high ROM in AA, spine, and legs.

6 Domain Specific Design II: Electronics

Electronics are kept rather simple in all our robots, except Oncilla, relying on mainly off-the-shelf components, if possible. Due to the high availability of different components on the market, we needed to selectively decide on their ease-of-use and functionality. The first half of this chapter is dedicated to a general overview of electronic components considered to be used in our robots as well as a high-level summary of actuator technologies and their benefits. We conclude by highlighting the chosen components of our robots and their application in the second half of this chapter.

6.1 General Introduction of Electronics used in Quadruped Robots

Besides the robots' mechanics, electronics make up a large portion of the robot's hardware. These include actuators based on different force or torque generation principles, one or several single board computers (SBC) that execute the robots' controllers, custom printed circuit boards (PCB) in different functional ranges, and lastly sensors, to identify internal and external robot states as well as to gather data for closed-loop control. This section is dedicated to an overview of a set of electronic components often used in mobile, legged robots. Specific selections for our robots are shown in section 6.2 and section 6.3

6.1.1 Common Actuators used in Legged Locomotion

Choosing the right primary actuator technology for the application at hand is one of the first steps when designing a robot. Almost all decisions in the development process follow this step. Generally one can select between three technologies, electric, hydraulic or pneumatic actuation, or a combination of these. More detailed, they can each produce motion linearly or rotationally, both valid options for legged walking machines. Table 6.1 is highlighting these technologies with main advantages and disadvantages.

Our vision of an untethered, but quite small, robot is leaving us with two choices for actuation, electric and pneumatic, as hydraulics are too powerful for our lightweight robots and rely on very heavy support equipment. Battery driven micro-pumps and reservoirs have been successfully implemented as a sub-part for actuation, but not as the main driving force behind the locomotion in small, legged robots, e.g., in [104–106] with the usage as adaptable feet. The most reasonable technologies to use are DC and EC (Brush-less DC) motors with their use also in servo-motors. The integration of low-level control, electronics, and communication employs servo-motors with the easiest implementation, but also with low efficiency due to usually high spur-gear reductions.

Table 6.1 – Summary of selected actuator technologies in legged locomotion, adapted and extended from [107] and [108]

	Electric	Hydraulic	Pneumatic
Energy source	Electric power-supply	Electric or combustion	Electric or combustion
Energy storage	batteries	accumulator	reservoir
Energy cost	Low	Moderate	High
Linear actuator variants	Via mechanical conversion or linear EC	Cylinders	Cylinders/ muscles
Rotary actuator variants	DC, EC, AC, Servo	mechanical conversion	mechanical conversion
Max. Available torque/force	Medium	Very high	Medium
Max. Speed	High	Medium	High
Size	Very small to large	Medium to very large	Small to very large
Main Advantage	Safe to operate	High strength	Passively compressible
Main Disadvantage	High losses through gearing	Heavy support equipment	Reservoir needed for speed
Size of Quadrupeds	Small to medium	Large	Medium
Bobcat	X		
Lynx	X		
Oncilla	X		
Cheetah-Cub	X		
Cheetah-Cub-S	X		
Cheetah-Cub-AL	X		
Serval	X		

6.1.2 Common Control Boards used in Legged Locomotion

Having the aim of producing a (semi-) autonomous and compact mobile system, one necessity is the presence of a highly integrated control board on the robot itself. This SBC should be powerful enough to handle the control of motion, sensor-integration, and communication with the user through a wireless interface. In our considerations, we excluded microcontrollers with too little computational power or low connectivity/ interfacing options (to connect

6.1. General Introduction of Electronics used in Quadruped Robots

desired sensors and actuators) from the beginning.

Table 6.2 – Characteristics of selected control boards (SBC) used in legged robots; information is extracted from respective datasheets

		Raspberry Pi 3B	Odroid XU4	RB110
Processor speed	[Ghz]	1.2	2	1
Processor type		Broadcom BCM2837 64bit	Samsung Exynos5422 ARM Cortex-A15	DM&P Vortex86DX
Nr. of cores		4	4	1
Memory	[MB]	1024	2048	256
USB 2.0		4	1	1
USB 3.0		0	2	0
Micro SD slot		Yes	Yes	Yes
PWM		0	0	16
GPIO		40	30	specialized
Graphics		HDMI	HDMI	none
Bluetooth		4.1	No (USB dongle)	No
WiFi		802.11 bgn	No (USB dongle)	No (PCI-card)
Ethernet		10/100	10/100/1000	No (adapter)
Voltage	[V]	5	5	5
Power Consumption	[W]	1.2	3	2
Weight	[g]	42	38	40
Size	[mm ³]	85 x 56 x 17	83 x 59 x 18	96 x 56 x 18
Price	[CHF]	37	70	254
Bobcat				X
Lynx				X
Oncilla				X
Cheetah-Cub				X
Cheetah-Cub-S				X
Cheetah-Cub-AL				X
Serval			X	

A comparison of two main SBCs used in our robots can be seen in Table 6.2. Raspberry Pi 3B is added to the comparison due to its popularity. The relatively new Odroid XU4 is leading mainly in computation power, whereas the Raspberry Pi (2016 model) is providing a balance between onboard availability of interfaces and computation power. The RB110 (available since 2012) is far less powerful, but presents excellent connectivity, especially if one needs to directly interface many servo-motors that cannot be controlled via a bus. The price is never the less very high in comparison to the newer boards, as one could, for example, buy almost 7 Raspberry Pi for one RB110. Our selections will be justified in the respective design sections.

6.1.3 Common Sensors used in Legged Locomotion

Sensors are needed to enable performance of different closed-loop control tasks, like obstacle avoidance, sensing of the environment for reflex implementation, and adaptation of the control to successfully stabilize open loop gaits against strong perturbations from the outside. For these tasks, a wide variety of sensors are commonly used in legged robots, see Table 6.3.

Table 6.3 – Summary of selected and common sensor technologies in legged locomotion

Technology	Example	Application	Advantage	Disadvantage	Cost	Used in
Optical	Optoforce	3D-GRF	all in one solution	not abrasion resistive high weight for small robots	\$\$\$\$	Oncilla
			3D-force	high weight for small robots		
	Camera	Obstacle-recognition	easy to integrate	light dependent	\$	
			high variety available	computationally intensive post-processing	\$	
	LIDAR	Mapping	rich information in 3D	high weight	\$\$\$\$\$	
			high resolution and accuracy	very expensive		
			made for mapping, professional solutions available	computationally intensive post-processing		
Capacitive	CySkin	Ground contact	cheap	mostly 2D information	\$	Serval
		Artificial skin	relatively robust	mostly binary signals		
			easy treatable signals			
Magnetic	Hall-effect	Joint position	precise measurements	high precision mounting needed	\$	Oncilla
			easy treatable signals	sensitive to magnetic fields (motors)		
			sensor itself small (IC)	commercial versions large		
Electromechanical	Straingages	GRF	very simple signals	abrasion sensitive	\$	Oncilla
			temperature compensation easy (bridge)	mounting sensitive		
			only 1D per sensor-pair	bulky		
	Potentiometer	Joint position	high sensitivity very cheap	only single turn rotation	\$	
Combination	IMU	Heading, Position and	very simple signals rich information in 3D highly integrated	high mechanical wear sensor-drift depending on quality, very high prices	\$ - \$\$\$\$	Oncilla Serval
		Acceleration	small form factor			

As described in subsection 1.3.4, we aim to build small and low-cost robots. Consequently, size, weight, and cost constraints limit the use of certain sensors, like high-end IMUs or LIDAR.

The employed sensors are mentioned again in section 6.2 and section 6.3.

6.1.4 Conclusion

Available technology for actuation, control, and sensing is vast. We suppose almost any robot with a medium to big size can use only off-the-shelf components and satisfyingly realize their locomotion goals. To reach the overall optimum solution (weight, size, energy-consumption, connectability, etc.), off-the-shelf components might not be specialized enough, and robot developers would have to implement their strategies or contract a company to do it. In our case, using comparably small robots, electronics pose different but solvable, issues, mainly concerning size and weight. As industrial grade electronics are mostly employed in stationary systems, size and weight reduction do not have to be a primary design goal. Hence, we have to select our electronics mostly from the realm of RC-modeling for actuation and (in the last years) also in the R&D robotics sections of motor and sensor producers. If the right components cannot be found, there is no other solution to either switch the underlying principle and search again or build de actuator/ sensor/ PCB, etc. ourselves. The following sections will highlight the component-choices and clarify pros and cons, encountered when using them.

6.2 Application in Existing Robots in BIOROB

6.2.1 Cheetah-Cub-Family: (Almost) Sensor-less Robots

Looking at the electronics selection for Cheetah-Cub (-S, -Al, -W), Bobcat, and Lynx, no variations were done over the years. The small and very lightweight robots rely on Kondo KRS2350 ICS RC servo motors directly connected to a RoBoard RB110 embedded Linux SBC. As described before, the RB110 is expensive in comparison to its competitors. In the case of the Cheetah-Cub-Family, the main reason for its initial use was the existing interface option to many Servo-motors, without the need for additional electronics development and unavailability of comparable boards. After several years of successful usage, Odroid and Raspberry Pi became more of interest due to computational power but were not used in the Cheetah-robots in consequence of its specialized control framework, that would have to be changed significantly to work with a new board.

Cheetah-Cub, Bobcat, and Lynx were never planned to be closed-loop platforms, but tools to research and understand the benefits or disadvantages of mechanical compliance and bio-inspired designs for locomotion. Consequently, no sensors, besides the internal position sensing of the servo-motors, were integrated. In the following development and the emergence of the Tegotae control rule [109–111], attempts of equipping the robot with GRF sensors were undertaken but ended with little success. The somewhat disappointing results mainly followed

an unavailability of small, very lightweight and precise GRF-sensors (Optoforce sensors weigh $\approx 50\text{g}$ and thus add almost the full weight of one leg to the feet, resulting in a very high increase of inertia) followed by difficulties producing an experimental sensor in-house [11]. Efforts to implement such sensors may be undertaken in the future thanks to new potential collaborations, see section 11.2.

Advantages and Disadvantages in Cheetah-Cub-Family

Advantages Where there is little, little can break or generate sources of failure. The main advantage is the simplicity the robots' electronics bring about. All servo motors have their low-level power and control electronics integrated and are directly connected to the SBC, allowing for control in real-time [11] in high locomotion frequencies and enabling quick readiness of the robot for experiments.

Disadvantages Besides the high price of the robot control board, the missing sensorization is the strongest disadvantage. Without any sensors, neither the internal states of the robot are traceable, nor can the environment be perceived, rendering closed-loop control impossible. The motor connectors got worn out rather quickly due to vibration and shocks, as well as by frequent exchange of motors after overheating rendered them unusable. The connection between the components got lost, and experiments had to be suspended until the issue was handled. The problem of vibration also caused the power-connectors on the board to loosen, thus resulting in several power-cuts and the necessity to restart the Linux-system. This problem was hard to find out, as it was not visually perceivable. Before switching out the RB110, multiple cables were exchanged in an attempt to solve this issue. The electronics of the Kondo-RC-Servos themselves caused another problem. Unfortunately, heat-transfer to the environment is very inefficient in the motors' design. Hence, several internal boards burned if excessive heat was not detected early enough. After some time of trial and error, a maximum number of gait-cycles, which could be safely run before a cooling period, was found and no more motors had to be exchanged.

Conclusion

Having a limited set of electronics on the robot is beneficial for overall cost and simplicity, but has a strong downside on the employable control methods. Nevertheless, these robots can move fast in an unperceived flat environment and tolerate a certain level of disturbances through their mechanics. Using a sufficient number of sensors to generate adequate and precise information for closed-loop control, but preventing physical implementation to exceed in complexity is a desirable path to be taken in our robots.

6.2.2 Oncilla: High Sensor Integration

Oncilla features a broad set of printed circuit boards (PCB) and sensors in sharp contrast to the approach used in the Cheetah-Cub-Family. The control board is again an SBC RoBoard RB-110. Due to the development of drivers and architecture in Cheetah-Cub and Oncilla in parallel, this board was the best choice to run the locomotion controllers, described in subsection 7.2.2. Additionally, a custom made power board converts voltage and maximum amperage from a three-cell LiPo (lithium polymer) battery, with a total capacity of 4500 mAh, to the respectively acceptable values for PCBs and sensors. A custom master-control board regulated communication between sensors, motor driver PCBs, and the SBC. Each of the four motor driver PCBs control and connects to two 90W brushless DC motors (EC-motor, two motors per leg) and run a local PID for speed and position and current control. Kondo KRS2350 ICS were used for the four AA-joints and connected directly to the RB-110. To read absolute joint positions, the motor driver PCBs are capable of communicating with and power three custom hall-effect-encoders per leg. Additionally, half-spherical Optoforce 3D-force sensors were used directly as feet and connected to the RB-110 through a USB-hub. Another sensor added in later Oncilla versions was a Microstrain 3DM-GX3-35 IMU to sense posture and accelerations. In the earlier Oncilla versions force-sensors on the hip were present, whose measurements were also communicated to the motor driver PCBs. Later on, these sensors were abandoned, due to problems distinguishing the real-GRF from the measured values, as complex leg-dynamics were also projected in the sensor-readout. With this hardware configuration, a control time step of $2ms$ was achieved.

Advantages and Disadvantages in Oncilla

Advantages Oncilla's high-quality sensors, EC-motors, and mostly well-developed support electronics allow the robot to perform effective and robust over longer experimental periods. As the motors are not as under-dimensioned as the RC-servo-motors of Cheetah-Cub (and family) high oscillation frequencies could be reached without risk of overheating. The sensorization enabled closed-loop control, stabilizing the robot even on rough terrain, see [12].

Disadvantages The high-level of electronics-customization brought, additional to the enormous effort, time and prototyping cost, another distinct disadvantage: To realize communication between the designed PCBs, motors and sensors, drivers had to be written and new protocols constructed. Additionally, motor-drivers (PID for two motors per motor-board) had to be designed and implemented. These are low-level development tasks, already present and debugged in commercial electronics in advance of component-sale. In the Oncilla-project this development work had to be done by the researchers working on the robot, consuming

even more time and resources until successful completion. Further, the motor driver boards allowed for a continuous output of 6.1 A per motor. This is less than what the robot's EC-motors could handle (spikes up to 45 A), and thus limiting the robots' performance. Another drawback is the overall price of the robot. Compared to our previous quadrupeds, the robot is very expensive. As an example, one Cheetah-Cub can be built for two Oncilla motors and its support electronics, allowing the construction of up to four Cubs from the actuator investment needed for one Oncilla, see chapter 8.

Conclusion

Oncilla strongly relied on custom electronics, increasing development complexity tremendously and slowing the design process as a whole. Due to unavailability of small, commercial motor driver boards, this was somewhat inevitable. Now, Maxon-motor produces small enough boards with low weight ($< 80\text{g}$) and high power output, that present a valid alternative to our custom PCBs. Having joint-position sensing allowed for exact control and automated calibration of the under-actuated legs, but was also a constant source of error due to the extreme precision needed for the sensors to work. We have to decide in our robots if the benefit of full state-sensing is necessary to achieve agility and worth the very high mechanical complexity. IMU and GRF sensors are very robust and easy to implement and can be used to support different control approaches, see subsection 7.2.2. We have to decide on the quality of IMU and GRF-sensors used, as they present a very high-cost factor, that might be magnitudes lower if other sensors were chosen. Load sensing on the hips is a very interesting idea to see forces acting on the robots' trunk, but again, custom solutions were not optimal. This leads to the conclusion that if sensors are used, only off-the-shelf components should be considered or a very high amount of development work has to be invested.

6.3 Electronics Development for Serval

6.3.1 Electronics needed for Agile, Legged Robots

Agility, means moving relatively fast over difficult terrain, obstacles of different sizes or even jump, as presented in Part I. From this, it becomes prominent, that overall weight and power-density of the actuators are of the essence. This goes hand in hand with the notion of using as little additional PCBs as possible, especially if not needed for the desired locomotion task. Sensorization should be there to enable adaptive behaviors and stabilize the robot after automated tasks were executed. This includes (at least) the integration of an IMU and GRF-sensing. The SBC used in an agile robot needs to be powerful enough to integrate sensor signals quickly with the underlying control and still have enough available processing power to enable higher locomotion tasks, like navigation.

6.3.2 Implementation

For Serval, we decided to pursue a path in the middle between Oncilla and the Cheetah-Cub-family, regarding motor-quality and sensorization, creating a more powerful system than Cheetah, whereas keeping complexity and cost lower than Oncilla. Our strategy was especially to re-use an existing control framework implemented in [112] with only small modifications. This decision was taken as a consequence of our shrinking development team, as colleagues working on control for quadruped robots finished their work in BIOROB and left the laboratory before Serval was built. Hence, Serval employs two different high-quality servo motors (Dynamixel MX64R and MX28R) in combination with an Odroid XU4 SBC, also used in the already developed control framework. Dynamixel motors consist of a small Maxon EC motor combined with a spur-gear (relatively high gear ratio of 200 : 1) and a servo-motor-board. They are capable of serial communication via an RS485 bus, giving the possibility to daisy-chain them and consequently skimming down the cabling effort. A small PCB was designed to distribute electricity from power-supply or an internal 3-cell to 4-cell Lipo battery to the motors and SBC (two PCBs in total for fore and hind trunk, respectively). The board was also acting as an interrupt in case of motor-communication failure. In this case, the motors control had to be reset by cutting the power-supply. By using the interrupt on the PCB, the power to SBC was kept unaffected from the reset. For the initial setup of Serval, sensorization was kept to an absolute minimum, as primarily mechanical effects on locomotion capability and stability were of interest. Internal leg states (joint positions) could support closed loop control, but were also a source of errors in Oncilla. With Serval we wanted to see whether or not these sensors were necessary for agile movement and control. Besides a low-cost Biscuit-Programmable Wi-Fi 9-Axis Absolute Orientation Sensor (IMU) [113], we foresaw the use of GRF-sensors located on the robot's feet. Due to the weight of available Optoforce sensors used in Oncilla, that amounted to about half of one legs weight ($\approx 50g$), we did not integrate the mentioned GRF-sensors, keeping leg-inertia minimal. Further search for plausible sensors led us to [114, 115], who implemented capacitive sensors in a small and lightweight package. Due to the late discovery of these sensors, we did not yet get the chance to customize and implement them on the robot. Additionally, plans to integrate sensitive skin for physical guidance are being realized [116, 117] in the close future.

Advantages and Disadvantages in Serval

Advantages Servo-motors with serial communication capability and a minimal (off the shelf) sensor set, kept the electronics setup very simple and cost-effective. No specialized drivers had to be written, and motors were hypothesized to be more reliable than cheaper RC-servos. Using the same electronics hardware as our colleagues made collaboration possible. We thus benefit from an already debugged and tested control-architecture possible. An additional

advantage in a simple electronics implementation is the ease of replication, e.g., by other research groups or future team-members of BIOROB.

Disadvantages Serial communication through a bus does not allow for real-time control, as command and read-out cannot be done in parallel and as high control frequencies as in Oncilla. This and the servo-motors speed/torque relations limited the overall locomotion frequency for locomotion to a maximum of 2 Hz. As small animals tend to move in higher frequencies, this could impact on the feasibility of using, e.g., high-frequency gaits like a gallop. Closed loop control is possible in Serval, but in its current development state (without GRF sensors) limited to posture control implementations and physical guidance tasks, see section 11.2.

Conclusion

The overall available electronics in Serval, allow for agile gait implementation, but not as sophisticated control as in Oncilla. Depending on future directions, sensors should be added and integrated into the electronics framework. The effort for communication, low-level control as well as sensor development is kept to a minimum by employing off-the-shelf components and liberates development time for other aspects.

7 Domain Specific Design II: Control

After [11] the staff involved with robots should be divided into two groups, the robot handlers (using the robots to answer scientific questions or achieve certain goals) and the robot maintainers (responsible for development work and operational maintenance). In case of robot control, I was not directly involved with the development part and mainly used or modified parameters provided by the control algorithms to generate locomotion patterns.

For this reason, we strongly reference the interested reader to the thesis of our colleagues Mostafa Ajalloeian [12], Alexandre Tuleu [11], the future dissertation of Tomislav Horvat and MA-thesis of Anja E.M. Schmerbauch [118] who were the minds behind most of the control efforts implemented in our robots. The employed methods will be described on an abstracted level in the specific robots sections of this chapter to facilitate the understanding of how control and experimentation were undertaken.

7.1 General Introduction of High-Level Concepts used for Locomotion Control

Generation of desired control signals and the coordination between existing actuation can be achieved by imposing pre-defined open-loop patterns or relying on sensory feedback to modify the actuator states. The first approach often uses biological (mostly kinematic) data in form of MOCAP recordings for the pattern generation, whereas the second is often characterized by building on template models of locomotion. Agile motion of a robot as a sub-part of locomotion in general is one result of using either method. Both approaches can also be combined as shown in [12], relying on the implementation of a CPG-network with its modulation by sensory feedback (reflexes). In this section, we will define and describe the general control concepts we employed in our quadruped robots.

7.1.1 Central Pattern Generators

Central Pattern Generators, short CPGs, are

"[...] neural circuits found in both invertebrate and vertebrate animals that can produce rhythmic patterns of neural activity without receiving rhythmic inputs." [119]

Also, CPGs generally do not rely on sensory feedback to achieve generation of their signal patterns, although research is indicating, that indeed modulation of rhythmic patterns through reflexes is part of the locomotion control apparatus [12, 120]. The important aspect in decoupling the higher brain functions from routine and periodic performed tasks such as found locomotion control is the freeing of resources available for the higher brain functions. For the locomotion-control-apparatus we can see three main decoupled systems, the spinal CPG, that produce rhythmic signals, the Sensor-cells that introduce fast reaction to local stimuli (like stumbling) and the higher control-centers (motor cortex, cerebellum, and basal ganglia) that modulate these signals to achieve the optimal response to changing environmental states, see Figure 7.1. According to [119] three major advantages emerge:

- Reduction of time delays in the motor control loop (feedback-loops in the spinal cord).
- Reduction of the complexity for the passed down, control signals from the brain to the actual muscle controller.
- Reduction of the necessary bandwidth to transmit control signals from high-level to low-level centers.

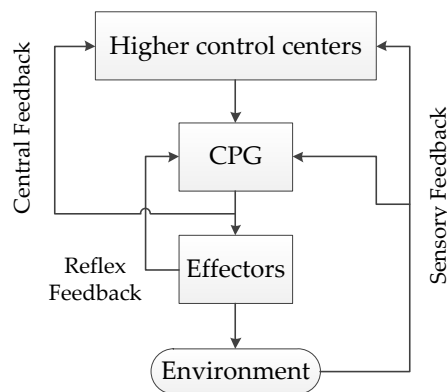


Figure 7.1 – Highly abstracted view on the sensori-motor-connections in animals from a control perspective, adapted from [121]

CPGs for Locomotion Robotics

Besides a high variety of different control approaches (e.g. work of [36, 75, 80, 122, 123], just to mention a few), various CPG models, such as the connectionist models [124], the vector maps [125] and the system of coupled oscillators [126–129] are taken into consideration when controlling bio-inspired robots. Among many other implementations, e.g., in swimming robots [130], the usage of CPGs in quadruped locomotion is widely explored, in particular by Kimura and colleagues [128]. Examples can be found in [119], where several properties identifying CPGs as useful for robot locomotion-control were shown:

- Robustness against perturbations through rapid reactions and return to the normal rhythmic behavior after external interference.
- Use for distributed implementations, e.g., in modular robots
- Few control parameters allow strong modulation of the resulting patterns and thus make large changes in the gait
- Integration of sensory feedback, through coupling terms in differential equations, is achievable and thus provides the possibility of mutual entrainment of mechanical body and CPG [128]
- CPG-models usually provide a good basis for learning and optimization algorithms.

Design of CPGs Firstly, there is to be mentioned that design methods for CPGs vary [119]. Between approaches using learning algorithms and hand-coding, there is not yet a well-established and common design method to be found. The, strongly interconnected, terms to be defined during construction of a CPG are as follows [119]:

- General CPG-architecture (number and type of oscillators, position-/or torque-control)
- Type and topology of the couplings (determine: conditions of synchronization between oscillators and resulting gaits)
- The waveforms: determine the performed trajectories in the gait cycle
- Effect of input signals (Modulation of patterns by, e.g., frequency, amplitude, phase-lags, the correlation between stance- and swing-phase)
- Effect of feedback signals

The detailed mathematical equations that result from this design process can be found in the specific publications listed in chapter and [11, 12].

7.1.2 Reflexes and Posture Adaptation

The detailed methods and background knowledge behind this subsection can be found in [12] and is repeated here on a high-level for clarity of our employed methods.

Reflexes

According to [12] a reflex is biologically defined as an involuntary and almost instant movement as a result to an external stimulus and to be distinguished from preflexes, whose execution is generated intrinsically in the musculoskeletal system and thus with "zero-delay". We use the term reflex rather loosely connected to biology in this work, as it signifies here only a quick reaction to external stimuli. These reactions are meant to prevent our robots from failure in the following three cases.

Stumbling Correction Reflex - SCR Obstacles encountered in the swing-phase of the foot-locus result in stumbling, tipping over or in the best case only changing direction. A typical scenario would be climbing a step in mid-run. The SCR is a simple, but often effective counter-measure, causing the leg to flex more due to direct contact feedback on the leg or feet, opening the possibility to pass the obstacle. This reflex can be integrated as a fixed height offset or cumulative reaction with small steps.

Leg Extension Reflex - LER Guinea fowls (small running birds) extend their legs until they reach the ground or the respective leg is kept fully extended if they miss contact at the beginning of stance phase [131, 132]. This enables the birds to move more stable in unperceived environments. The LER could thus be seen as an inverse of the SCR and can be implemented in the same fashion. In our case, the reflex is active until the ground is sensed or the is "over-written" by other control-events.

Lateral Stepping Reflex - LSR Examples of Spot, HyQ, StarlETH or ANYmal, and many other robots stress the significance of lateral stepping to prevent falling due to large lateral disturbances. In case of impact from the side, the robot should also walk to the side, dispersing the impact energy and returning to a steady motion. Although this might seem simple, the underlying control for robots is not. Exact state and acceleration estimation in combination with enough processing power are needed to allow this kind of quick behavior, that is not always possible, with the minimal sensor set in our robots [12].

Posture Adaptation - PAD

Carlson-Kuhta et al. [133–135] reported in a series of publications a considerable influence of the surface incline on the posture of lab-raised cats. These adaptations allow for stable motion, by modulation of end-effector angle of attack to the ground and level of crouching, as well as keeping the trunk parallel to the inclined surface. This approach is rather trivial to realize in robots, as only the incline has to be known to modify an existing gait with an offset.

7.1.3 Forward and Inverse Kinematics

Our robots' motor signals are generated either by employing forward (command actuator signals directly and derive resulting end-effector motion) or inverse kinematics (command position of the end-effector in 3D and derive actuator signals) for each leg. As the kinematics generation is not a core part of this thesis, we refer to the supplementary material in [5, 11] and Appendix C, where the kinematics equations for Oncilla can be found. Due to the consistent ASLP usage in all our robots, these kinematics are valid throughout our work.

7.1.4 Conclusion

Controlling a quadruped robot is a non-trivial task, that needs knowledge not only of the technological implementation of a controller but also of gaits, sensory feedback integration, simulation and many aspects more. For our robots, and especially for Serval, we employ a control strategy we want to call: as simple as possible, but as sophisticated as needed. Nature, as described in this section, is the inspiration for higher level concepts, e.g., pattern generation through CPGs and superposed reflexive behavior. The finished control implementation should allow easy manipulation of robot gaits and thus enable robot-users (to whom I count myself) to work with the robot, without having to go into the detailed underlying control structure.

7.2 Application in Existing Robots in BIOROB

Generally one has a choice between two approaches to control the motors of a robot. Either a position command or the desired torque is set for the motor to follow. In our small robots, we rely on low-cost motors, which are not or only approximately capable of torque-control (on-going project in BIOROB). Consequently, we tend to rely on position control as laid out in detail in the publications mentioned above. The following subsections describe the control implementation for our quadrupedal robots on a high level.

7.2.1 Open-loop Robots: Cheetah-Cub-Family

The control of the Cheetah-Cub-Family was realized through a parameterized, fully connected CPG-network, running on the RB110 control board. Cheetah-Cub's CPG network consists of eight nonlinear oscillators (hip and knee for each leg) and, although principally possible, does not include any feedback. Robots of the family with an actuated spine add another node to the network. With this control architecture, a variety of gaits can be implemented by modifying three phase lag variables (hip-phase lags). Depending on the employed gait, the phase-lag between hips (and spine) are chosen subsection 3.1.1. The spinal actuation and thus its oscillator, was always phase-coupled to the left fore hip-joint (this was an arbitrarily chosen joint for easy implementation of the control, coupling to a different joint would be as well possible) and was treated as a virtual 5th hip joint with his own complete set of CPG control parameters (phase-lag, frequency, amplitude and offset). This also implies the assumption of a coupling between hip joints and spine movement. To compute the necessary control signals for the motors forward kinematics were implemented, see Appendix C. The CPG network, allows us to easily manipulate the main gait parameters, such as amplitudes and offsets of hips, spine, and knees, duty factor (the time the foot remains in stance respective swing-phase) and the phase-relations of the actuators, see Figure 7.2. By adjusting these key-parameters tests of the robot's mechanics and a search for stable locomotion was conducted.

In Cheetah-Cub-AL, inverse kinematics were implemented for the first time and allowed to simplify gait generation and tuning. Another significant change was the switch to a new operating system, Jokto, that improves stability and ease of use.

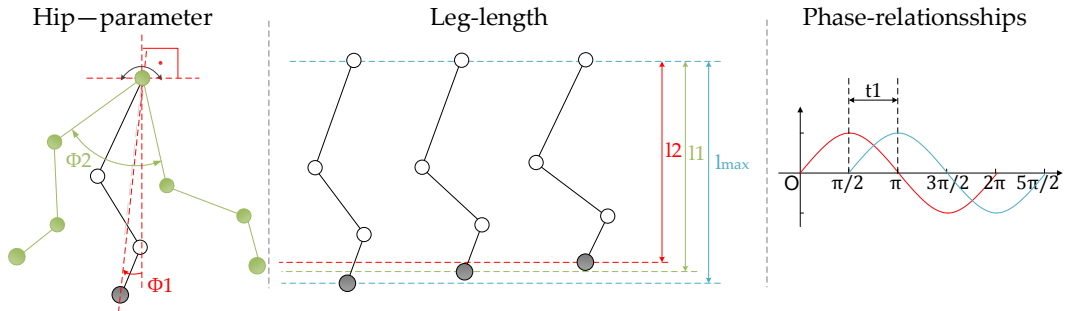


Figure 7.2 – Explanation of CPG-parameters for the legs (forward kinematics): Φ_1 is the hip-offset, Φ_2 the hip-amplitude; l_1 the leg length offset; l_2 the leg length amplitude; l_{max} the maximum unbend leg length; t_1 presents the phase lag between two oscillators, such as the hip- and the leg- or spine-oscillators; these parameters are not accessible with inverse kinematics, as only the foot-locus in 3D and the timing (duty-factor/ frequency are commanded)

Advantages and Disadvantages in Cheetah-Cub-Family

Advantages One major advantage of using a CPG-network is the interconnection of all nodes. This allows the robot to smoothly follow changes in the control parameters and quickly reach a stable limit-cycle behavior (with little computational effort). Forward and inverse kinematics allow a generation of coordinated motion pattern with relatively little effort, and enable an automated gait generation with programs like Matlab (configuration files can be generated and read by the controller), to perform systematic searches for the best parameter configurations directly on the robot hardware. Inverse kinematics have the additional advantage that recorded animal foot-loci can be scaled and replayed on the robot hardware, generating information of how well robots can be compared with their animal counterparts. Lastly, kinematic control does not need any sensory feedback and is thus ideal for our position controlled and sensorless robots.

Disadvantages The direct control of the motors instead of commanding the foot-locus is not very intuitive from the start, causing the empirical exploration of parameter-combinations to be challenging. After experience with the robot and acquiring a feeling for the different parameters impact on the motion, this method is nevertheless acceptable. Kinematic control (with position commands) does not allow direct implementation of force-feedback, like kinematic control (with torque commands) would. With our robots, other ways have to be found to superpose feedback on the existing control structure, see subsection 7.2.2 and subsection 7.1.2.

Conclusion

Using CPGs and inverse kinematics for our small, position controlled robots seems to be a plausible and relatively easy implementable choice. This is especially the case when research-focus is laid on the impact of the mechanical design on gait or perturbation stabilization rather than a sophisticated control. The issue of feedback-integration has to be addressed when moving away from open-loop flat surface gaits towards control for unperceived rough terrain, where open-loop robots are not enough anymore.

7.2.2 Closed-loop Robot: Oncilla

Oncilla, as the first of our robots to be equipped with a broad range of sensors, had the capability for closed-loop control. To this end, the robot's CPG-network of morphed oscillators was combined with different reflex and posture control mechanisms, as presented in subsection 7.1.2. Morphed oscillators are nonlinear oscillators, which encode arbitrary and stable limit cycles (in our case desired joint trajectories), defined as phase-dependent functions, resulting in smooth trajectory generation, [5, 12].

The gait-design was based on closed-form inverse kinematics, that map the desired foot-trajectory to the joint/ motor command. The inter-limb coordination and thus the resulting gait (see subsection 3.1.1) was dependent on a pre-defined phase-lag. In our case, we often used the running trot as a preferred locomotion pattern.

Besides the usage of an SCR, LER, LSR, and PAD, whose exact implementation can be found in [12], turning was achieved with two different strategies. The first strategy utilized the adduction/abduction joint to induce a rotation around the robots center axis. Commanding a sine-wave with opposite signs to both fore and hind AA-joints turning proportional to the sine-amplitude was achieved. Shortening the stride length asymmetrically was the second proposed strategy. Here the inner legs (closer to the center of the turning circle) have shorter, and the outer legs longer step lengths. If one side of the robot was moving backwards and the other forwards, turning around its central axis was induced.

Advantages and Disadvantages in Oncilla

Advantages Oncilla can show very versatile behavior, made possible through different reflexes, turning and posture control. Advantageous is hereby, that all behaviors are implemented quite modular on top of a stable and simple open-loop controller generating the usually occurring "normal" locomotion. This approach only reaching for more complex modulations of the robots' motion is making computation very cheap.

Disadvantages One disadvantage of the control framework on Oncilla is the lack of phase feedback (possible by construct, as phase dynamics exist). As an example, if the robot is kept completely in the air (a large drop for example), it will still try to "locomote". It might be better to have a phase locking mechanism as in [109] or correction by feedback. Moreover, the current Oncilla controller is not the best choice for slow locomotion or precise foot placement.

Conclusion

Oncillas versatile controller is surely a good example of what closed-loop control can achieve. The equipped reflexes and modularity of the approach should be kept in mind for an agility controller as well, as one can implement basic behavior running the robot in the ideal case, and enforce reactions to disturbances when needed.

7.3 Control Development for Serval

For the goal of reaching agile movement with a robot that features all aspects described in Part I, Serval needed to build upon the experience gained with our previous robots. This section is dedicated to elements that are in our opinion necessary for agile locomotion control and a first implementation strategy on Serval.

7.3.1 Control needed for Agility

Following our definition in Part I and our experience with Oncilla/ Cheetah-Cub-family, our robot control needed to consist of a flexible and modular approach. Formed around an open-loop CPG-controller for basic movement generation, we needed to implement different behaviors, which cohere with our defined agility tasks and can potentially be executed in a quick and possibly automated manner. To enhance overall performance and protect the robot from failure, reflexive mechanisms as in Oncilla, based on appropriate sensory feedback, should be used. If these aspects work together symbiotically with a compliant and relatively powerful mechatronic design, we are confident to be capable of a good grade of agility.

7.3.2 First Implementations

The first implementation towards agile movement with Serval consisted of replaying and modifying of kinematic data from agile dogs. This approach, due to the readiness-state of the robot hardware and control (no sensors integrated at the time), was performed in open-loop and is thus a fundamental control to be extended in current and future work.

Foot trajectory generation for Serval's inverse kinematics control was achieved by analysis and mathematical representation of motion capture data from trained Border Collies (provided by the Institute of Systematic Zoology and Evolutionary Biology (Friedrich-Schiller-Universität, Jena, Germany)). Four dogs' data was available to be processed to obtain kinematic data of different gaits. As we received the recordings for dogs moving on the level ground and not on a treadmill with fixed reference frame, some post-processing was necessary to achieve a floating reference that moves with the dog to receive a static foot-locus. Hindfoot trajectories were obtained by subtracting the lateral foot-marker (left) from the position of the left sacroiliac joint (articulatio sacroiliaca) during forward locomotion. The sacroiliac joint is chosen for its property as less flexible joint and thus served as trust-able reference. In case of the fore-foot trajectory, the left margo dorsalis scapulae, as a relatively rigid joint (at least concerning the available data) presented our reference. Figure 7.3 shows an example for fore- and hind-foot trajectory, illustrating differences in, e.g., vertical displacement as well as distances to hip joint axes.

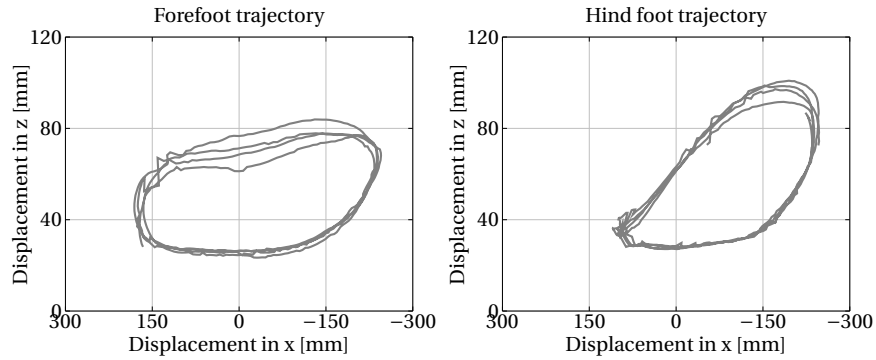


Figure 7.3 – Forefoot and hind foot trajectory for trot of a Border Collie (Ethan); head to the left; rather flat elliptic shape in the fore and angled elliptic shape in the hind (more ground clearance)

Border Collies were all taller than 45cm at withers resulting in the need for scaling of established trajectories to the robot's size. To mathematically recreate the complex shape of a real animal foot-locus, four cubic Bézier curves were fitted to the data. Junction Points have been positioned vertically to the hip axis and on the transition from stance to swing and swing to stance phase. Consequently, inner Bézier points were calculated so that cubic Bézier curves defined the dog's foot loci correctly.

We proposed a parametrization approach using hip height (H) as origin (x_0, z_0) , step height (h), compression factor (c), step length (SL) and length proportion per direction (LR and LL) for trajectory modification in experiments, see Figure 7.4. The use of take-off and touchdown angles, like in Cheetah-Cub-AL's foot-locus parametrization [11], was deliberately omitted to keep the ratios and proportions of foot trajectories imported from animal data intact but keeping adjustment of the general trajectory size a possibility.

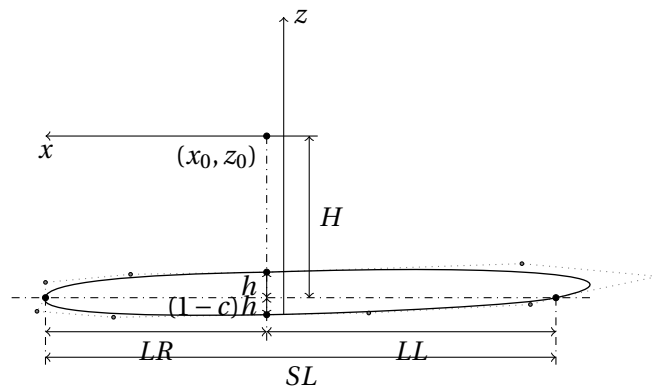


Figure 7.4 – Parametrization of foot trajectory with significant values

Having extracted the foot-loci from cubic Bézier curve interpolation (depending on the leg timing), the data was ready to be "replayed" by Serval. Underlying control was using a strongly adapted framework from Pleurobot [136] (please refer to the mentioned publication for a detailed control description). On a high-level, we used the controller's state machine along with a CPG-network to update the foot-position continually, generating our different motions. Combined with the correct timing of the inter-limb coordination (inter-limb phase-lag in Cheetah-Cub), a specific gait was ascertained.

Through parameter modification of the trajectories, we implemented the following motion patterns and experimentally tested them in open-loop (lying and sitting present pre-programmed behaviors kinematically copied from motion capture data, but strongly adapted to the robot shape), see section 9.3:

- Walk
- Trot (with and without AA)
- Bound (crouched)
- Gallop
- Single and double step-down
- Slope-up with flat ground transition
- Sidestepping
- Turning with a radius
- Fall absorption
- Rough Terrain
- Lying/sitting down and standing up

Additionally, standing up from sitting and lying posture were implemented as hard-programmed motion.

Advantages and Disadvantages in Serval

Advantages With the implementation of an underlying controller that is well-developed and maintained, we gain the capability to use different open loop motion patterns, our expected basis for agile locomotion. Using real animal data allows us to compare the robot to possible

role models and define how much we can use our robot as a tool for biology. The parametrization method is valuable, as it also allows for testing of simple foot-trajectories, like squares, ellipses or circles, that might be sufficient for an artificial system to locomote.

Disadvantages The control implementation needed for agile movement is not yet complete and thus restricting the possible results and added knowledge in this thesis. Reflexive behavior and automated execution of the implemented tasks are still missing, but not far from being achieved.

Conclusion

Even with this still incomplete control, we can manage to test Serval in a laboratory environment and determine its functionalities or limits without closing the control loop, iterate on mechanics if necessary, and draw a baseline to assess future work.

8 Conclusion and Cost-Evaluation

In subsection 1.3.4 we defined our approach synthesizing robots, that can be handled safely and do not need excessive training before usage. The way to achieve this paired with our goal to have cost-effective designs without losing too much experimental flexibility was described in the previous chapters. Following an iterative process (V-model macro-cycle), testing out different mechanisms in four separate robots, we arrived on our latest design, Serval. With its superior ROM, modular, compliant and lightweight structure as well as relatively strong actuation in combination with suitable processing power and a flexibly extendable primary control we can confirm to have build a system following the principle construction boundaries: Lightweight construction; Robustness; Flexibility through compliance; Higher stiffness for skeleton-parts; Ease of assembly (modular structure); and Fast production (prototyping).

Inspiration from biology in design and control led to robots, that can serve as valid platforms testing how to achieve agility in small and quadrupedal robots (described in chapter 9).

Concerning the cost of our robots and thus availability even to laboratories and research centers with a small or medium budget, we were successful. Following Table 8.1 all Cheetah-Cub-Versions and Lynx can be built for less than 2k CHF and Serval for less than 6k CHF. Oncilla, due to high-grade motors and expensive, but qualitatively high-grade sensors, is available for roughly 15k CHF. In comparison to costs of commercially available robots and general expectations for robotics, all our robots are relatively cheap. Concerning maintenance, we can also state, that mechanical hardware repairs are a tiny part. The most expensive portion is caused by failing motors or electronics, which have to be replaced. Subsequently, investing effort in protecting these from physical harm (with, e.g., in-series compliance) is to be considered vital for low-cost robots to succeed.

Table 8.1 – Estimation of cost for production (P) and maintenance (M) of per robot copy (final design) over its project duration in [Swiss Francs - CHF], excluding cost for person hours, smaller side-projects, periphery equipment (and coffee)

Component	Type	Cheetah-Cub		Cheetah-Cub-AL		Cheetah-Cub-S		Lynx		Bobcat		Oncilla		Serval	
		Qty.	Total [CHF]	Qty.	Total [CHF]	Qty.	Total [CHF]	Qty.	Total [CHF]	Qty.	Total [CHF]	Qty.	Total [CHF]	Qty.	Total [CHF]
Mechanics leg	P	4	120	4	150	4	120	4	140	4	100	4	200	4	170
Mechanics trunk	P	1	60	1	80	2	60	2	70	2	60	2	250	2	400
Mechanics spine	P					1	30	3	30	1	20			1	850
Motor EC	P											8	6800		
Motor Servo	P	8	1320	8	1320	9	1485	9	1485	9	1485	4	660	15	4300
Control board	P	1	254	1	254	1	254	1	254	1	254	1	254	1	37
Electronics boards	P											5	750	3	40
Sensors	P											13	6920	1	30
Partial Sum	P		1754		1804		1949		1979		1919		15834		5827
Complete rebuilds mech	M	2	360	0	0	0.25	53	0.25	60	0.1	18	0.25	113	0.1	142
Broken EC	M											1	850		
Broken Servo	M	30	4950	4	660	3	495	4	660	?		0		4	1146
Broken Electronics boards	M											3	450	0	
Broken Sensors	M	2	508	0	0	0		0		0		0		0	
Partial Sum	M		5818		660		548		720		18		1300		1288
Total Sum			7572		2464		2497		2699		1937		17134		7115

9 Experiments and Validation

Validation of our robots, to test their capabilities and grade of agility achieved was conducted throughout the years. We implemented different experimental methods and researched mostly characteristics described in section 3.1. As our agility benchmark was not yet ready when we build the robots, not all of them did participate. We thus explain the experiments and validation done with the robots separately from the previously defined values of the agility benchmark. Where applicable data is available, we display the respective agility scores. For this dissertation we do not explore all possible aspects of comparing our different robots as dynamical systems (full kinetic and kinematic analysis including a variety of perturbation experiments), as this is outside the scope of this work. We will however try to characterize our robots' performance as thoroughly as possible, mainly focusing on the generated motion and the resulting interaction with the environment (GRF).

9.1 Experimental Environments and Tools

This section will describe the soft- and hardware tools as well as environments used to capture data during experiments.

9.1.1 Motion Capture

Fourteen high-speed infrared cameras build by Naturalpoint, Inc. [137] were used to capture kinematic data of the robots. This Motion Capture System, short MOCAP, records the reflection of markers on the robot with $f = 250\text{Hz}$ and thus can give a position in the 3D-space related to the recording time. The relative position to the absolute coordinate base was clarified through a ground plane calibration. The cameras are positioned in a rectangular shape, in a height of 0.7m , 1.5m and 2.5m around the catwalk (Figure 9.1) and thus covering a recording-volume of [$width = 1\text{m}$, $length = 4\text{m}$, $height = 0.5\text{m}$, spacial precision 0.48mm , depending on

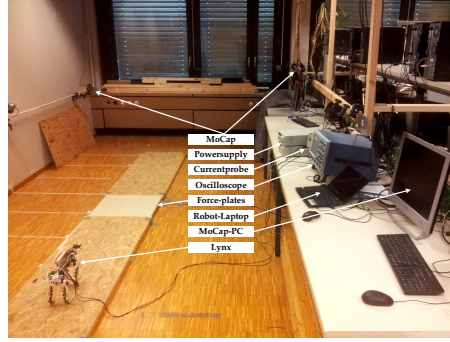


Figure 9.1 – Experimental area (Catwalk, Force-plates and MOCAP) in old laboratory; new setup is equally designed

calibration quality]. Recording and cleaning up of the data was performed with Arena (later Motive) [137]. If necessary, marker labeling could be done with Mokka [138]. The cleaned up data, saved in a c3d-format, was processed using Mathworks Matlab [139] and the b-tk plugin [138] to derive the desired values, such as speed or pitch angle and their respective time-dependent graphs.

9.1.2 Power Consumption

The calculation of the cost of transport (COT, according to [46]) needs the electrical power used for actuation, see equation (9.1). Recorded through a current probe, clamped at the power cable, a digital oscilloscope (LeCroy6100) sampled the amplifier output (Tektronix) with a frequency of $f = 50kHz$. For further processing of the digitally saved data, such as filtering, Matlab was again chosen. The voltage could be read directly with a voltmeter. To get the real power consumption for the actuation the standby power of SBC and servo motors was subtracted.

$$COT = \frac{P_{el}}{M \cdot g \cdot \bar{v}} \quad (9.1)$$

9.1.3 High-speed Video

From previous experiments done in the BIOROB-laboratory, it was shown, that the trajectories of infrared markers mounted on the legs were rather difficult to collect due to interfering signals. As a result, high-speed video recording at a sampling rate of $f = 240Hz$ of optical markers (with different colors) was proposed to capture the movement of the leg joints, if necessary and wished for. The camera (Casio EX-ZR100/ Sony FS700RH) was mounted

sideways to the moving robot, either manually moving on rail or statically, to capture the robot profile. Tracking of the marker-trajectories can be done with Tracker, a freeware program with automated tracking features [140]. The resulting data-tables can be again processed in Matlab [139].

9.1.4 Ground Reaction Forces

The interaction of the robot with the ground can be quantified by the size of the Ground Reaction Forces (GRF). These forces are measured with two force-plates (Kistler, type 9260AA3, [141]), mounted side-by-side and covered with non-reflective tape within the catwalk, see Figure 9.1. The surfaces friction coefficient of wooden plates and force-plates were kept about equal. The resulting signals are sampled by an A/D converter (Kistler Bioware 64ch DAQSystem, type 5695A1) at $f = 1000\text{ Hz}$. Further processing can be done in MatLab. Additional to external force measurement, we were using internal GRF-sensors (Optoforce OMD30) to track the robot's stance phases and forces occurring. This was only possible so far with Oncilla, as the only robot equipped with GRF-sensors.

9.2 Experiments with the Cheetah-Cub-Family and Oncilla

Robots whose build was described in the previous part were tested with different methods, but always towards a common goal, their agility, and display of natural gaits. Although we used Cheetah-Cub on many occasions at the beginning of our work and supervised student projects centered around this robot (see Appendix A), we did not redo or implement fundamentally different experiments than those of the original development team. Hence, we do not present any tests explicitly done with Cheetah-Cub but concentrate on the robots in our development line towards Serval (Lynx, Cheetah-Cub-S, Cheetah-Cub-AL, Oncilla, and Serval).

9.2.1 Lynx



Figure 9.2 – Please find here videos of experiments with Lynx described in this subsection:
<https://go.epfl.ch/ExperimentsLynx>

Although our work with Lynx began as MA-Thesis, we continued with experiments during

the first months of my Ph.D. and concluded in a conference publication. More detailed experimental explanations can be found in [142], as we only present relevant work for our agility approach, published in [2].

Experiments with all spine versions consisted of a grid search per spine with 180 different gaits, performed two times each, to research the influence of different design approaches and parameter combinations on the robots agility and "natural grace". For varied parameters and ranges see Table 9.1. The spine offset for SV1 was set to reach a horizontal spine position, whereas SV2's and SV3's zero position was preventing their actuation cable mechanism from slack while on the ground and in a standstill.

Table 9.1 – First 6 rows: parameter space for the open, tested CPG-parameters. Last 7 rows: fixed CPG-parameter-space. 180 experiments per spine configuration were conducted. Please cp. Figure 7.2 for an explanation of the CPG-parameters.

CPG-parameter	Unit	Values
Fore hip amplitude	deg	40, 50, 60
Hind hip amplitude	deg	30, 40, 50, 60
Fore hip offset	deg	20, 25, 30
Hind hip offset	deg	15, 20, 25
Spine amplitude	-1-0 []	-0.2, -0.3, -0.4
Spine phase lag	rad	0, $\Pi/2$, Π
Frequency	Hz	2.5
Virtual duty factor	[]	0.3
Leg-length-amplitude	0-1 []	0.6
Leg-length stance deflection	0-1 []	0.0
Leg-length offset	0-1 []	0.2
Hip-leg phase lag	rad	2.6
Fore-hind phase lag	rad	Π

Speed

In contrast to gaits with no or even negative speeds ($v_{min} = -0.58 \text{ m s}^{-1}$, Froude-Nr $FR = 0.23$) due to wrong parameter combinations, the best gaits of SV1 produced up to $v_{max} = 0.75 \text{ m s}^{-1}$ / $FR = 0.37$. Gaits having a speed considered $v = 0 \text{ m s}^{-1}$ presented a relatively big part in the results for SV1. It was especially visible for gaits having a spine phase lag of Π . SV2 on the other hand showed in gaits with a positive speed ($v_{min} = 0.04 \text{ m s}^{-1}$ / $FR = 0.001$ to $v_{max} = 0.6 \text{ m s}^{-1}$ / $FR = 0.24$). The last design, SV3 reached a speed range from $v_{min} = 0.05 \text{ m s}^{-1}$ / $FR = 0.002$ to $v_{max} = 0.6 \text{ m s}^{-1}$ / $FR = 0.24$. SV2's and SV3's tendency for positive and higher speeds indicated the systems' ability to locomote with a broad set of control-parameters. SV1 in contrast exceeds very specific parameter combinations to move.

9.2. Experiments with the Cheetah-Cub-Family and Oncilla

Table 9.2 – Varied CPG-parameters of the fastest gaits; F-F/H-Amp/Off amplitudes and offsets of the hips, S-Amp/PL amplitude and phase-lag of the spine; see Figure 7.2 for an explanation of the CPG-parameters.

	F-H-Amp [deg]	H-H-Amp [deg]	F-H-Off [deg]	H-H-Off [deg]	S-Amp [-1-0 []]	S-Pl [0 – Π]
SV1	50	50	30	25	-0.4	0
SV2	60	60	20	15	-0.3	Π
SV3	60	60	20	15	-0.2	Π

Cost of Transport

Figure 9.3 illustrates the decreasing cost of transport with increasing speed in all designs. Negative, as well as speeds considered $v \approx 0 \frac{m}{s}$ are not shown. SV1 had a higher maximal and lower minimal COT than the other designs. In SV2 and SV3, which resemble each other in the design, a clustering of different COTs for the same speed-values can be observed. This is rarely the case for SV1. The clustered gaits experienced a more significant influence of parameter-changes on the power-consumption for the same speed, giving hits for energy- rather than speed-optimized gaits to be found in this region.

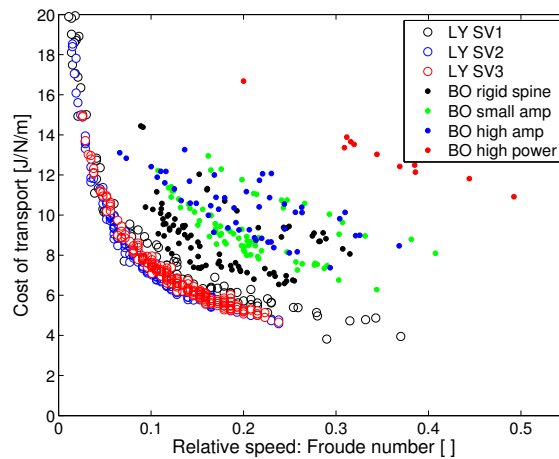


Figure 9.3 – Comparison of cost of transport and speed, of Lynx-robot (LY, empty markers), and Bobcat-robot (BO, full markers). Bobcat-robot values are taken from [85]. Bobcat-robot featured an SV1 spine design, but a two-segmented leg design, other than Lynx-robot’s three-segment ASLP leg design. The plot indicates that Bobcat-robot with its active, single rotatory joint reached a higher maximum robot speed (red markers), also compared to Lynx-robot-SV1 with the same spine configuration. However, within the same relative speed range, Lynx-robot outperformed Bobcat-robot regarding the cost of transport, in all its spine-designs. In “rigid-spine”, Bobcat-robot ran with its spine fixed. All remaining BO-spine modes (small amp, high amp, high power) were conducted as actuated, SV1-spines.

Gait-classification

The classification of "natural looking" animal gaits in robots can be done by considering two major points. First the footfall pattern, that is characteristic for each gait and second the vertical position change of the trunk. Figure 9.6 shows a stride-cycle of the Lynx-Versions' highest speed gaits as well as the respective (qualitatively, from video derived) footfall-patterns in combination with their real duty factors. SV2 has the strongest resemblance with the footfall-pattern seen in Figure 3.1, an animal-like bound. It is followed by SV1, which lacks flight phases and also makes use of the tail-like structure to move at all (making the design less desirable as robustness is questionable). SV3 shows overlapping foot contact with fore and hind feet resulting in a duty-factor over 0.5. This is not the case in an animal-like bound. The results of a motion-analysis confirm these findings, with the lowest average pitch and resulting vertical deflection for SV2 followed by SV3 and SV1 (SV1: $d_{av} = 0.11 m$, SV2: $d_{av} = 0.06 m$ and SV3: $d_{av} = 0.07 m$). Its large pitching motion explains as well, why SV1 was the only version needing to use the tail as a stabilizer.

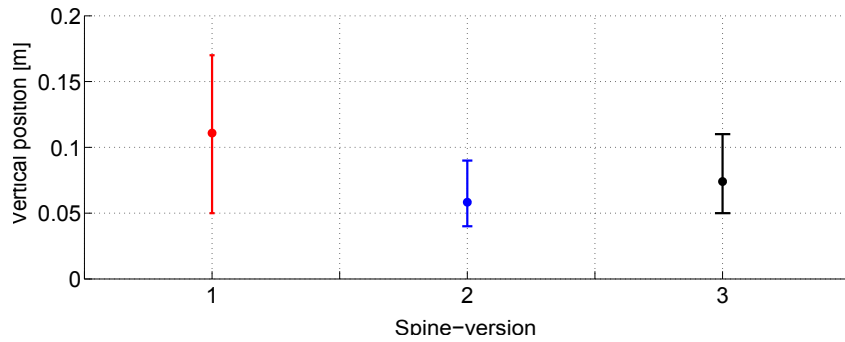


Figure 9.4 – Change of the instantaneous, vertical position of the robot trunk, for the best 10 gaits per spine configuration: (SV1: $d_{av} = 0.11 m$), (SV2: $d_{av} = 0.06 m$) and (SV3: $d_{av} = 0.07 m$). Lynx-robot in SV1 applied gaits with much higher vertical excursion; between 5 cm and up to 17 cm, compared to SV2. The high vertical jumps of SV1 indirectly led to a higher maximum robot speed, but would have completely destabilized the robot without its tail-like structure.

In Figure 9.5 it is visualized, that SV2 has the highest number of natural-looking gaits. SV1 has more gaits with very high pitch angles, able to produce fast movement due to correction effects of the tail-like structure. These gaits, on the other hand, do not resemble a bound as observed in nature, but a kind of artificial gait. SV3 shows gaits appearing quite natural, but due to high spine-stiffness experience even fewer flight phases than the other two. SV2 can adapt to the environment and misalignment of touchdowns during the movement nicely and thus appears as natural in general. In SV2 notably, a wide parameter range can be used to produce feasible gaits, emphasizing the adaptability to sub-optimal control and the adaptability to the environment (through stabilization effects by internal compliance,[3]).

9.2. Experiments with the Cheetah-Cub-Family and Oncilla

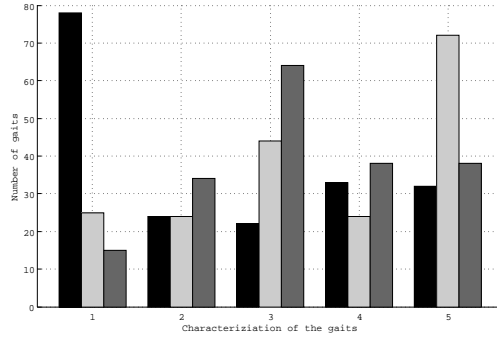


Figure 9.5 – Distribution of "non-natural" and "natural" looking gaits: black|SV1, light grey|SV2, dark grey|SV3; scale (x-axis) from 1 (non-natural) to 5 (natural)

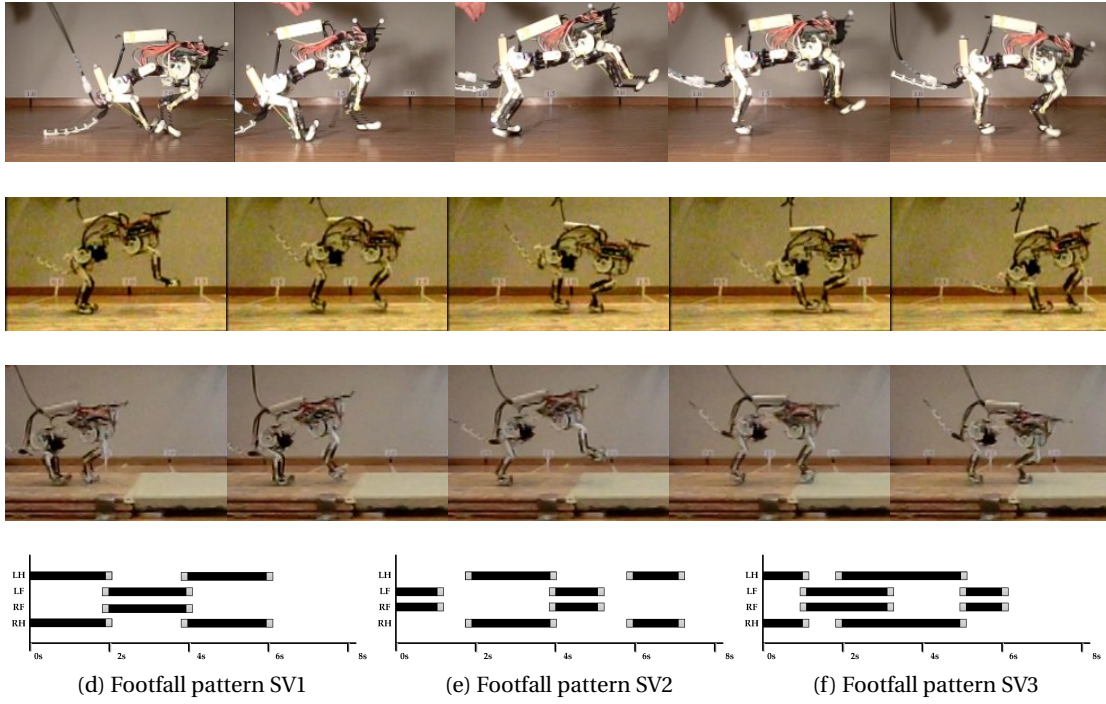


Figure 9.6 – Representative bound-gait snapshots (left) and corresponding qualitative, from video derived, footfall-patterns (right; grey: error-margin due to optical videoanalysis) of the fastest gaits SV1, SV2, and SV3 (from top to bottom, respectively). **SV1**: $v = 0.75\text{m/s}$, SV1 is the only configuration that required stabilization in pitch-rotation, via its tail-like structure preventing falling backwards (visible in the first snapshot/ strong influence on gait), real Duty-factor (relation of stance to swing phase of the legs) $DF_{av} = 0.5$. **SV2**: $v = 0.6\text{m/s}$, and no ground contact of its tail-like structure, real Duty-factor $DF_{av} = 0.4$. **SV3**: $v = 0.6\text{m/s}$, no ground contact of tail-like structure, real Duty-factor $DF_{av} = 0.625$.

Discussion and Conclusion

Table 9.3 – COT-comparison of the best (here fastest not lowest COT) gaits in all version with respective Bobcat-gait; (data taken from [85])

Bobcat	Lynx-SV1	Lynx-SV2	Lynx-SV3
$[\text{JN}^{-1} \text{m}]$	$[\text{JN}^{-1} \text{m}]$	$[\text{JN}^{-1} \text{m}]$	$[\text{JN}^{-1} \text{m}]$
10.9	3.9	4.9	4.7

In terms of COT SV1, SV2 and SV3 differ only minimal (Figure 9.3). Only a clustering to specific speed-values marks differences, indicating that the robots' COT is not very dependent on stiffness if morphology is similar. All spine-versions reach much lower COT-values than Bobcat. This decrease of COT in the active spine gait, although the mass of the robot is increased ($\approx 0.17 \text{ kg}$), is most likely due to the advantages in the passive compliant behavior of the ASLP-leg in contrast to a two-segmented spring loaded leg. The robots show almost the same top speed, whereas SV2 and SV3 are $\approx 21\%$ slower than SV1, and $\approx 25\%$ slower than Bobcat, resulting in a Froude-Nr for Lynx that is overall half the one of Bobcat (due to longer legs). One interpretation would be seeing it as advantageous using a two-segmented leg in combination with a simple, rotational spine as well as the need for more complex spines as soon as the leg design represents biology more closely. The difference in speed is following the implementation of a spine architecture with higher elasticity and thus slower reaction time than direct actuation. -Concerning the shift from a single, to a multi-segmented spine, we can observe an increase in locomotion stability, less dependent on optimized control parameters. As shown in Figure 9.2.1 the multi-segmented spines, with the right level of stiffness, seem to enable motion closer to bound-characteristics found in the literature. These include flight-phases in the footfall-pattern as well as pitch stability and acceptance of a wider range of control parameters. The single-rotation spine in SV1 might thus be too strongly abstracted from a multi-vertebrae spine in the long-spined animal role models and if used in combination with the ASLP-leg (Bobcat-robot manages quite nicely). Although SV3 shows comparable results in the top speed, it differs in the observed characteristics from SV2. The reason for this might be the slower reaction time of the spine, due to higher spine-stiffness, and the resulting delay in the flexion of the spine. Overall performance (speed and stability) could not be improved, when taking Cheetah-Cub as a reference. The direct transmission of the spine movement in SV1 seems (in our case) to be more effective than with a decoupled cable mechanism. We could combine this effect with the stabilizing features (little pitch) achieved through the multi-segmented spines in SV2 and SV3. Based on the observations, new insight into the mechanical design of a compliant spine in combination with ASLP legs was gained and thus should be implemented in further developments. As we used spines with different levels of abstraction (single rotation/ u-like structure), s-like spine implementation and active flexion/extension could be the next step to develop an agile system.

9.2. Experiments with the Cheetah-Cub-Family and Oncilla

Table 9.4 – Speed comparison of the best gaits in all version with respective Bobcat-gait; first: actual speed, second: Froude number (data taken from [85]).

Bobcat		Lynx-SV1		Lynx-SV2		Lynx-SV3	
v [m s^{-1}]	Fr []	v [m s^{-1}]	Fr []	v [m s^{-1}]	Fr []	v [m s^{-1}]	Fr []
0.78	0.5	0.75	0.25	0.6	0.24	0.6	0.24

9.2.2 Cheetah-Cub-S

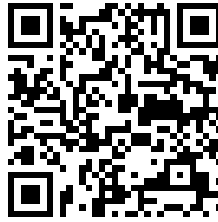


Figure 9.7 – Please find here videos of experiments with Cheetah-Cub-S described in this subsection: <https://go.epfl.ch/ExperimentsCheetahCubS>

Cheetah-Cub-S's steering capabilities were tested in different scenarios and against its predecessor, Cheetah-Cub. First quality and speed of simple circle-turns and secondly rapid direction changes in a slalom were tested. These experiments and our reference methods are described as follows.

Procedure and Radius Calculation

The spine deflection was divided into steps of two degrees, i.e., from -10° to 10° . At each deflection, ten attempts with a minimum of two complete circles were recorded. If the turning radius exceeded the test area, the robot had walked as far as the movement was recordable. Furthermore, attempts were marked as not successful if the robot fell over. To evaluate the experiments, we calculated the theoretical turning radius and used it as a comparison to the real performed one. The calculation of the radius is based on the simplified robot ("Single Track Model" used in automotive construction) and its geometrical constraints. Figure 9.8 illustrates the sketch, used to derive the following equations.

The robot is shown with a bent spine while turning counter-clockwise. The motor (M) separates front and back (c) while the turning radius (R) indicates the curved spine with a deflection (Δw_{ss}). Due to geometrical constraints, the turning angle (θ_t) is four times the spine angle (θ_s). Finally, the turning radius (R) is expressed in radian and calculated by (Equation 9.4).

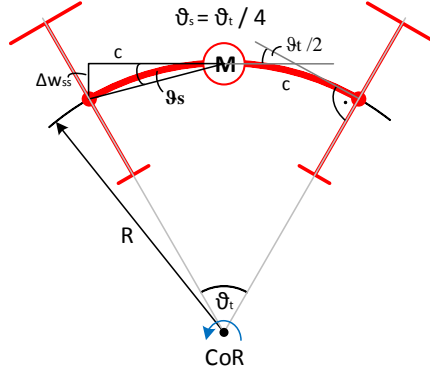


Figure 9.8 – Calculation of radius based on spine angle: M - Motor, CoR - Centre of rotation, R - Turning radius, c - Half shoulder to shoulder distance, Δw_{ss} - Deflection regarding bending force of motor, ϑ_t - Turning angle, ϑ_s - Spine angle

$$\vartheta_t^{rad} = \frac{2 * c}{R}; R = \frac{2 * c}{\vartheta_t^{rad}} \quad (9.2)$$

$$\vartheta_t^{rad} = \frac{2 * \pi * \vartheta_t^{deg}}{360^\circ}; \vartheta_t^{deg} = \vartheta_s^{deg} * 4 \quad (9.3)$$

$$R = \frac{2 * c * 360^\circ}{2 * \pi * \vartheta_t^{deg}}; R = \frac{c * 90^\circ}{\pi * \vartheta_s^{deg}} \quad (9.4)$$

Turning and its Analysis

One of the top markers was used to analyze the turning motion regarding radius and velocity. The experimental radius was calculated by two algorithms with the help of MATLAB (R2014a). First, if at least one full circle was achieved, the center of rotation (CoR) was calculated by the average values for direction x and y. Based on this point, the radius to each point of the trajectory was calculated by the Euclidean distance. The average and standard deviation of all distances were used for the mean radius and its deviation. This was done for high spine deflections: 10°, 8°, 6°, 4° & -10°. Second, if no full turning motion was recorded, the calculation was done by a predefined MATLAB-function (CircleFitByPratt.m [143]) based on Newton's approximation method. The average and standard deviation of all radii were used for the mean radius and its variation. This algorithm was used for all other spine deflections: 2°, 0°, -2°, -4°, -6° & -8°. The mean velocity was calculated by the total distance traveled divided by the observed time frame that was kept constant for all runs at each deflection to simplify the evaluation.

Cheetah-Cub-S trots different circle radii with decreased angles. The test area is not sufficiently

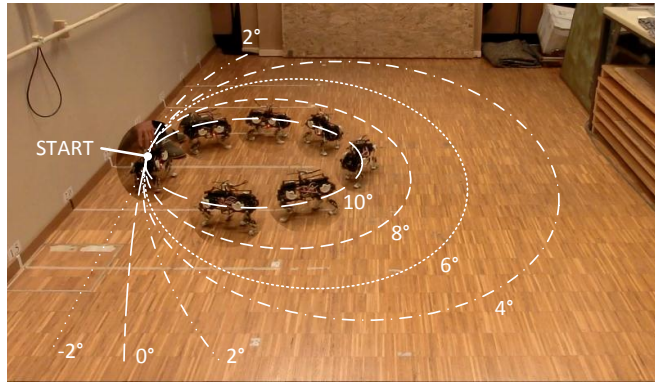


Figure 9.9 – Simplified trajectory of different spine deflections: Full turning up to 4°, negative spine deflections were left out for clarity

big for all the deflections; thus results were approximated with the method mentioned above during the analysis. With a focus on the sharpest turning motion, the robot achieves its minimum radius of 0.51 ± 0.07 m in one run at 10° spine deflection and speed of 0.31 ms^{-1} . Figure 9.10 illustrates an exemplary single attempt of Cheetah-Cub-S with 10° spine deflection. The four turns occur clockwise from start to end position in about 39 s.

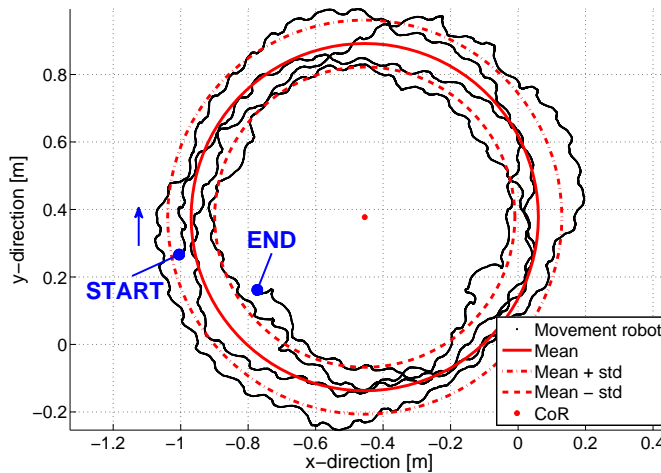


Figure 9.10 – One exemplary single attempt of Cheetah-cub-S with 10° spine deflection, ~4 clockwise turns from start (-1, 0.25) to end (-0.75, 0.15) point; mean value in red

The bidirectional swinging occurred due to the inherent perturbations during the trot gait. The calculated CoR, mean radius and corresponding standard deviation are shown in red. Furthermore, primary parameters (Spine deflection, radius, and velocity) were given to simplify the classification.

97% of all 110 runs were successful because Cheetah-Cub-S fell over only when it hit a wall. This happened mostly at very small spine deflections because the starting point was close to the wall to maximize experimental surface. Due to variations at the touchdown, the robot sometimes tended to walk towards the border. The overall results are illustrated in Figure 9.11.

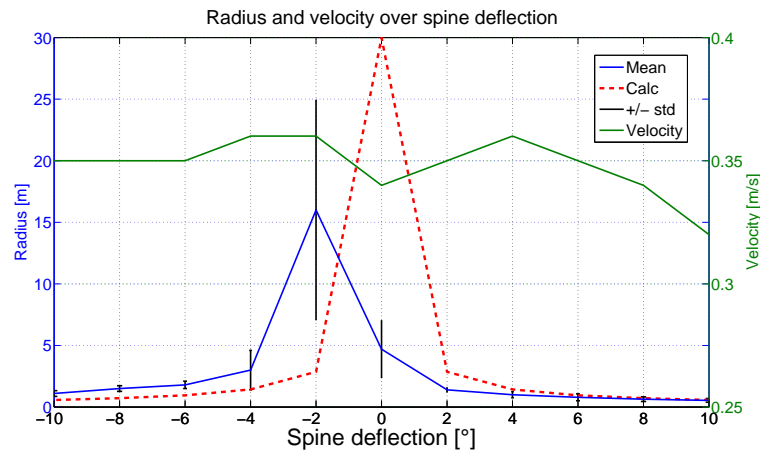


Figure 9.11 – Results of experiments: Radius and velocity over spine deflection: Calc - calculated radii (30 m at 0° represents ∞), std - standard deviation; peak at -2° as a result of material fatigue and plastic deformation of the spine

The radius peaks at -2°, decreases and levels out towards greater spine deflection because the larger the angle, the smaller the radius (see Equation 9.4, p. 134). An asymmetry exists by comparing mean and calculated radii. Induced by small plastic deformations on the leaf spring after many experimental runs, a minor backlash of the steering mechanism was caused, and zero position of the spine was altered. In consequence, the spine experienced a small offset to one side, leading experimental radii to be smaller than the calculated ones for positive deflections.

The maximum velocity of 0.36 m s^{-1} was reached at straight locomotion and decreased slightly with greater spine deflection. The ground had the most determining effect on propulsion because of its structure. Parquet made out of small wood pieces created slight anisotropic friction and thus influenced the overall speed. Also, a tape was used as markers in other experiments done in parallel that changed the friction locally. The low friction between feet and ground as well as a non-optimized gait caused sliding motion that increased with greater spine deflection. Nevertheless, optimization of the gait would have clouded the comparison to the original Cheetah-Cub at the time and thus was only noted in further developments (e.g., work with Serval).

Cheetah-cub's ability to turn, induced by markedly changing the gait parameters, i.e., the amplitude of hip actuation, was tested (ASL [12]). The necessary differences in amplitude of

9.2. Experiments with the Cheetah-Cub-Family and Oncilla

inner and outer leg were calculated based on the distance of each leg towards the CoR. The same phenomenon can be seen by considering a car and its wheels when it drives on a curved path. The outer wheel spins faster than the inner one following or inducing the turn. The calculated amplitude of the inner leg had to be 20 % less than the outer to achieve a radius of 0.5 m. No changes in direction occurred. The reason was the high frequency of the gait, which made it impossible for the servo-motors to reach the desired amplitudes. Small changes did not affect the locomotion. The frequency was not lowered to keep the comparison between our two robots. To achieve similar radius, the inner amplitudes were set to zero and then increased empirically until the desired motion occurred. The following Figure 9.12 shows the result of Cheetah-Cub turning clockwise (R \approx 0.5 m) with an amplitude ratio of 5° (inside) to 50° (outside).

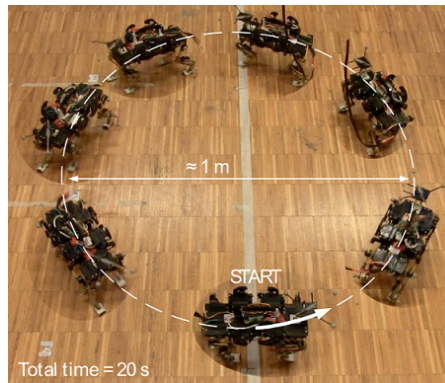


Figure 9.12 – Cheetah-cub turning clockwise with an ASL amplitude ratio of 5° to 50° (inner to outer legs): R \approx 0.5 m

The full circle was completed after 20 s that correlates to $\approx 0.16 \text{ m s}^{-1}$. The velocity was half the one of Cheetah-Cub-S, and the observed gait changed dramatically. The predefined trot transformed into a full contact sliding gait caused by the small amplitudes and made it very sensitive to surface quality. The differences in amplitude of calculation and reality were disproportional. One cause could be the nature of the implemented foot trajectory. The calculated amplitudes correlated to the distance during stance-phase (wheel-model with full-time contact) but in reality, the foot touched the ground less. To achieve the desired ground contact, the foot trajectory has to be controlled and adjusted during locomotion, that is only possible in a closed loop robot.

Slalom-run

An additional task to test the robot's versatility was implemented. Moving around three objects by two clockwise and one counter-clockwise turn, created a slalom of different turning radii. Before this test, none of our quadrupeds ever displayed more than forward locomotion. This was a little closer to a real-life scenario for agility, as full turns happen rather rarely, although

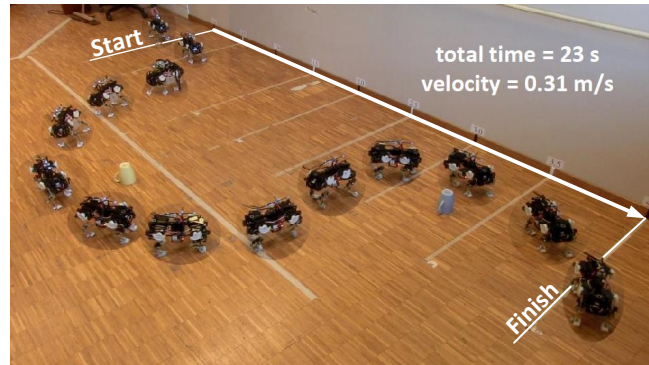


Figure 9.13 – Slalom-Experiment: Recorded movement of Cheetah-cub-S represented by snapshots (without cable), white arrow represents 4 m distance; speed about 0.3m s^{-1}

also important as an agility component. The start and finish line were four meters apart and within turning marks were spread symmetrically. Figure 9.13 shows the recorded movement in snapshots. The robot can be steered by a user to solve a particular task, by merely changing the spine offset. Cheetah-Cub-S succeeded nicely that gives additional weight to the usefulness of a bendable spine for steering.

Discussion and Conclusion

With the help of an artificial spine, the turning radius was reduced to 0.51 m (≈ 2.48 BLs) at 0.31 m s^{-1} . The design allowed a human operator (or a higher-level navigation controller) to modulate the spine deflection and therefore to steer the robot in its environment.

Table 9.5 – Comparison of Cheetah-cub and Cheetah-cub-S

Properties	Cheetah-cub-S	Cheetah-cub
Mass [g]	1160	1100
Height [m]	0.1	0.1
Width [m]	0.105	0.1
Length [m]	0.205	0.205
Max. forward velocity [m s^{-1}]	0.36	1.42
Max. turning velocity [$^{\circ}\text{s}^{-1}$]	34 ⁴	18

In comparison to Cheetah-Cub, dimensions are similar apart from the mass, forward and turning velocity. Although the additional weight of 60 g, caused by the spine actuator, Cheetah-Cub-S can almost turn twice as fast as Cheetah-Cub and keep most of the characteristics of

⁴Min. radius of 0.54 m @ 0.31 m/s

a standard trot gait. For us, it is an excellent trade-off between the increase in maneuverability and maintaining the mechanical and computational complexity low. The forward speed decreased drastically, caused by the non-optimized gait and much lower supply voltage than Cheetah-Cub (9V instead of 14V). Design of a gait adapting to the changed spine morphology should be included for further developments. Nevertheless, Cheetah-Cub-S introduces a reliable approach to enable steering via trunk motion without the consideration of individual foot placement (ASL). We implemented only one additional DOF but increased the maneuverability markedly even though the locomotion is not optimized yet. If we go back now and take a look at our natural role-models, cats, and dogs, we find that a combination of abduction and adduction is actively used for turning. The legs hereby induce the turn, and the flexible spine is used to lower the turning radii and provide more muscle-force for dynamic maneuvers. A combination of these to successful mechanisms into one should improve the agility even further.

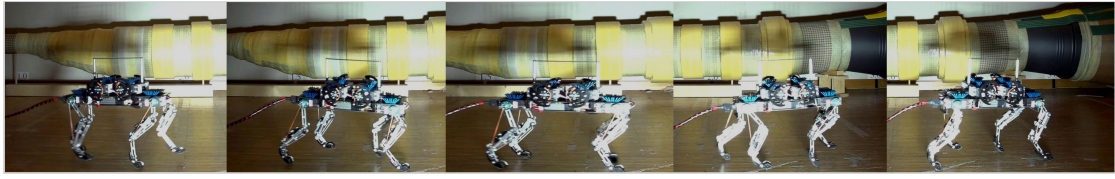
9.2.3 Cheetah-Cub-AL



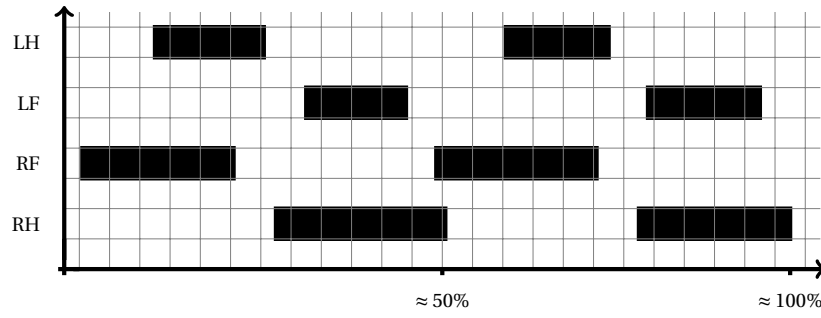
Figure 9.14 – Please find here videos of experiments with Cheetah-Cub-AL described in this subsection: <https://go.epfl.ch/ExperimentsCheetahCubAL>

Cheetah-Cub-AL, a robot for testing the mechanical endurance of an improved ASLP leg design, was used in many small projects as a primary platform, for example in [144] and others. Consequently, we will not show a complete set of experiments, as in other robots, but describe the improved working aspects experienced with the robot and derived footfall patterns of the resulting trot gait from video analysis.

In this footfall and video-analysis, we can see a difference left-to-right, due to perturbations occurring at the beginning of the recording. The mechanics distributed this small disturbance by adapting the stance phase without any controller intervention. Of course, as the robot is fully blind, this led to turning to the left side (smaller stance). This is another example how the mechanical properties of the ASLP leg can stabilize after disturbance or with non-optimal gait parameters (to a certain extent). The derived duty factors are: $DF_{LF} = 0.38, DF_{LH} = 0.37$ $DF_{RF} = 0.66, DF_{RH} = 0.63$ and $DF_{av} = 0.51$, so very close to the commanded value of 0.5. Due to adaptation, the trot pattern becomes a bit too stretched and does not show as many flight-phases as possible at a speed of $\approx 0.7 \text{ m s}^{-1}$. Another factor is here, that video-analysis is



(a) Snapshots of an exemplary gait



(b) Derived footfall pattern, $DF_{LF} = 0.38, DF_{LH} = 0.37, DF_{RF} = 0.66, DF_{RH} = 0.63$ and $DF_{av} = 0.51$

Figure 9.15 – Snapshots and Footfall-pattern for an initial trot gait; typical characteristics of the footfall pattern are visible; left-right difference due to curved path after small perturbation; combined $DF_{av} = 0.54$; speed $\approx 0.7 \text{ m s}^{-1}$

never as precise as GRF-measurements, so these values are rather to be seen as a confirmation of expected robust behavior than quantitative results.

9.2.4 Oncilla

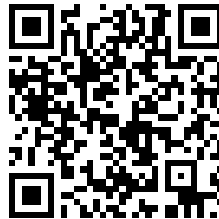


Figure 9.16 – Please find here videos of experiments with Oncilla described in this subsection: <https://go.epfl.ch/ExperimentsOncilla>

Oncilla was tested in different rough, flat and inclined surfaces. Its sensory feedback was used to stabilize open-loop gaits. As an adjustment after preliminary experiments, we added "baby socks" around the robot's foot. In consequence of high surface friction of the employed GRF-sensor and imprecision in the gait execution due to slightly varying runtime-calibrations, we

experienced "stuttering" over the ground. This happened when the robot's foot hit the ground before the actual stance-retraction was commanded [12]. A quick and reliable fix was to put wool-socks around the robot's feet, allowing it to slip slightly. The following experimental results were a collaborative work, with me partially in a supporting role; thus figures and results from [12] and [5] are used as the basis for analysis in this document.

Flat Terrain

The controller used in a Webots simulation of Oncilla was ported directly to the robot. This was made possible by the controller design incorporating simulation from the start [5]. The resulting flat terrain locomotion produced a feasible open-loop gait out of the box, see Figure 9.17. Further, improving the maximum forward and backward locomotion speed to 0.63 and $0.78[\text{m s}^{-1}]$ respectively was achieved through an intuitive parameter optimization. The experiments presented in this section are mostly using a speed of 0.4 to $0.5[\text{m s}^{-1}]$, as the robot is behaving very stable, even without sensory feedback. For flat terrain locomotion, we investigated the influence of posture control (PAD) on the trunk Role-Pitch-Variations (RPV). Illustrated by Figure 9.18 and Figure 9.19 a clear improvement, meaning a smaller RPV, is visible in both cases. Average standard deviation of the roll is 32% and of pitch 13% smaller when using PAD in comparison to open-loop. Although significantly better, the improvement is not as drastic as in the simulated robot, pointing towards reality-gaps from simulation to real hardware and fortifying our opinion from subsection 1.3.3, that a real-world validation is necessary and useful. The interested reader is pointed to [12] for comparison with exact simulation results, as this was not part of my work.

Concerning the robot's COT, we measured $20.4 J/Nm$ at 0.07m s^{-1} and $3.2 J/Nm$ at its top speed of 0.63m s^{-1} . Backwards locomotion reached higher efficiency at lower speeds ($9.6 J/Nm$ at $FR=0.01$) and a lower one at the robots maximum speed ($3.8 J/Nm$ at 0.63m s^{-1}), compared to forward motion.

For the turning on flat ground, we implemented two approaches. First, moving with asymmetrically shortening the stride length (ASL) by scaling foot trajectories (also used in Cheetah, see subsection 9.2.2) and second, superposing side-stepping via the hip AA joints on forward and backward locomotion.

The robot can turn in-place safely as fast as $45[\text{deg/s}]$, and up to a maximum rate of $90[\text{deg/s}]$, although becoming very unstable and prone to tipping over. Small speed losses of about 20% to 30% occur when turning only using AA (radius 0.23m to 0.46m).

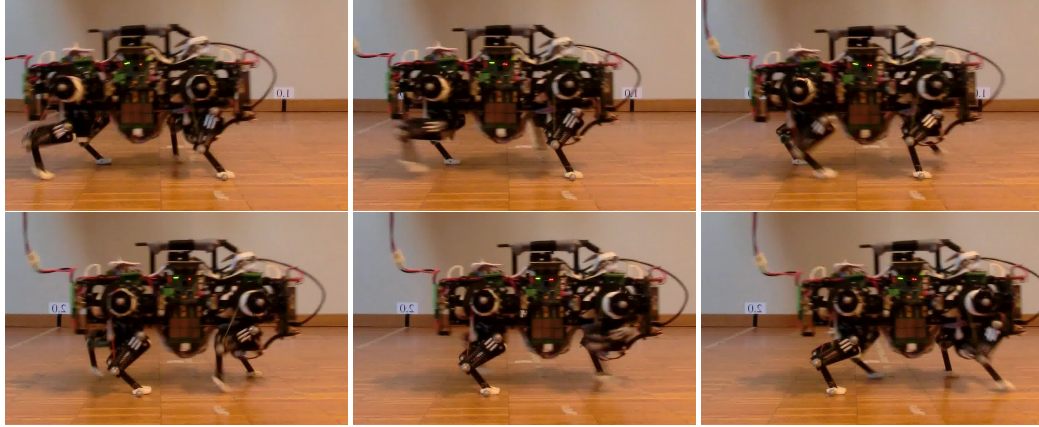


Figure 9.17 – Snapshots of Oncilla trotting forward at about $0.5[\text{ms}^{-1}]$ open loop; tethered; spring-loaded foot; reading direction left to right, top to bottom

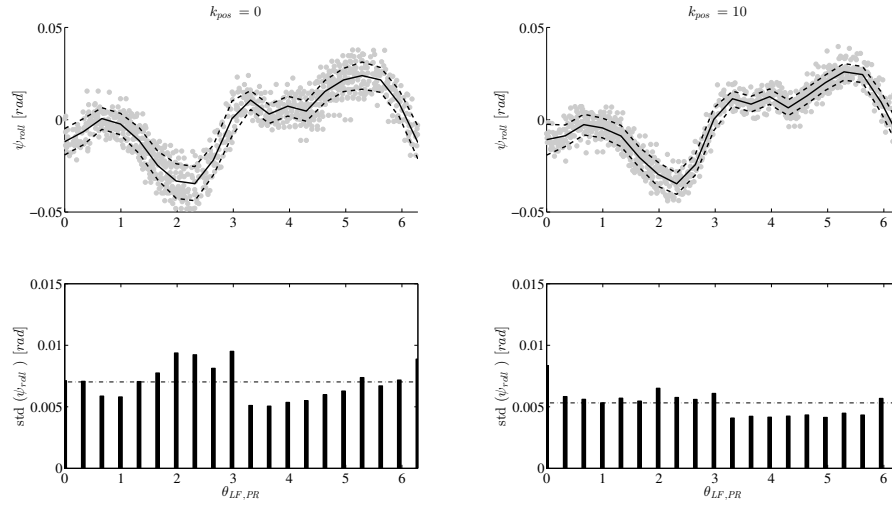


Figure 9.18 – Exemplary trunk roll variation; *Top*: gray markers represent collected data, the solid line is the mean across the cycles, and the dashed lines are showing the standard deviation; *Bottom*., values of the standard deviation; dashed line shows the average standard deviation; *Left*: open-loop; *Right*: closed-loop controller; average roll deviation is 32% smaller for closed loop

Asymmetric Load Carriage

PAD is not only used for pitch correction and, as will be shown later, on slopes, but can also correct posture in case of an asymmetric payload. This important feature is vital if sensors or other equipment, too bulky to be placed in the robots sagittal plane has to be transported. In the experiment, the robot was charged with first 0.5kg , 0.3m right of the sagittal plane, resulting in a continuous rolling torque of 0.15Nm . In case of active PAD, we observed a roll,

9.2. Experiments with the Cheetah-Cub-Family and Oncilla

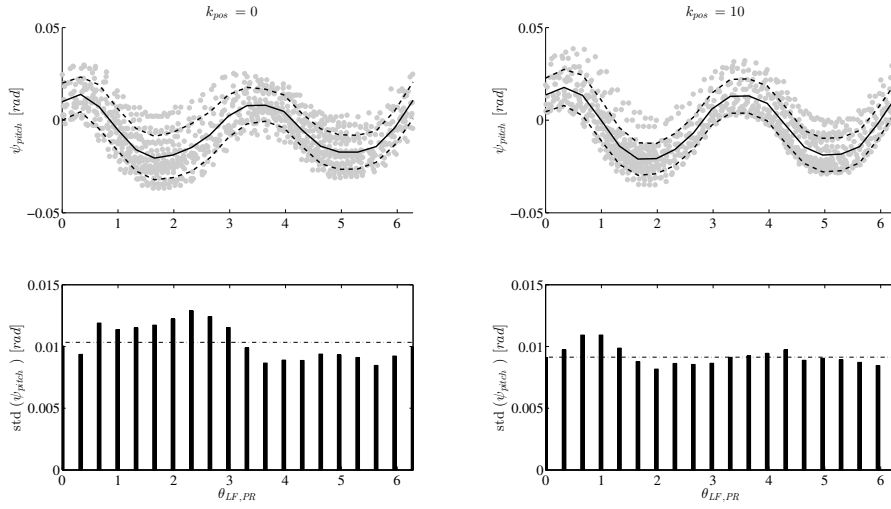


Figure 9.19 – Trunk pitch variations; *Top*: gray markers represent collected data, the solid line is the mean across the cycles, and the dashed lines are showing the standard deviation; *Bottom*., values of the standard deviation; dashed line shows the average standard deviation; *Left*: open-loop; *Right*: closed-loop controller; average pitch deviation is 13% smaller for closed-loop

about two times smaller compared to open-loop control. In absolute values, we measured a maximum roll angle for inactive PAD of $0.18rad$ and active PAD of $0.11rad$. After adding 200g of asymmetric weight, we observed the failure of the open-loop controlled robot (tipping over) and a highly unstable, but working closed-loop control.

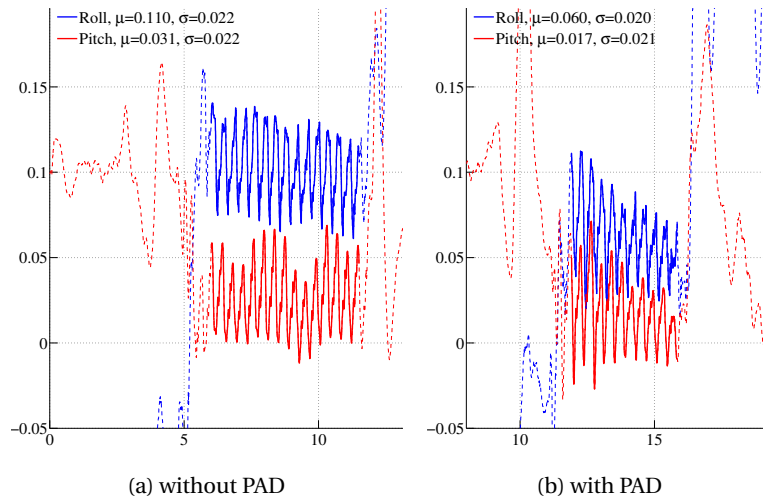


Figure 9.20 – Asymmetric load carriage with and without PAD; dashed lines - robot is in the air/ to be ignored; solid lines - robot is freely trotting with ground contact; (a) no feedback; (b) feedback activated, resulting in average trunk angles about two times smaller

External Lateral Perturbations

Lateral stepping as a response to sideways perturbations is already a proven and implemented concept in many robots. It is based on the lateral stepping reflex (LSR) and usually demonstrated by "kicking" the robot from the side, see section 4.1 and thus creating a one-sided impulse. For our experiments and as the robot is magnitudes smaller than other systems we used a force of about 5N (10% of robot weight) by "slapping" the robot on its handle. Higher forces would exceed the adaptation capability of our AA-ROM and were thus excluded. The LSR was immediately activated and dispersed the impact by moving sideways, see Figure 9.21. The robot was hit at roughly $t = 17.6s$, creating a higher hip AA amplitude as a response and returning to its usual limit cycle behavior after one stride period.

9.2. Experiments with the Cheetah-Cub-Family and Oncilla

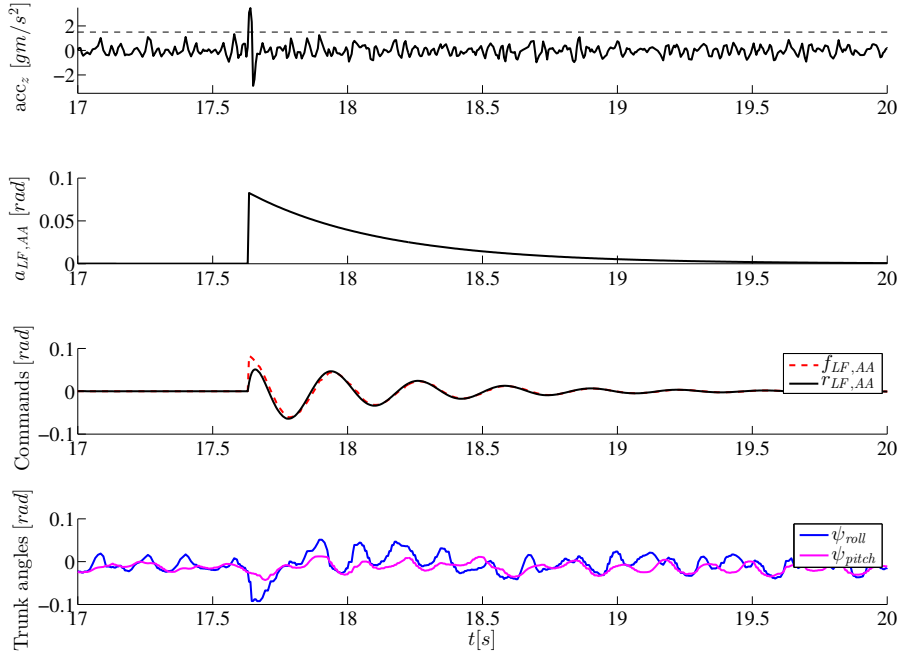


Figure 9.21 – LSR activation after perturbation at $t \approx 17.6$ s; lateral impulse force of ≈ 5 N; *Top:* lateral acceleration with dashed line representing LSR activation threshold; *Middle top:* hip AA amplification signal $a_{LF,AA}$ to respond to impact; *Middle bottom:* hip AA limit cycle $f_{LF,AA}$ is changed, but motor command $r_{LF,AA}$ remains continuous and smoothly converges to $f_{LF,PR}$. *Bottom:* trunk roll angle show rolling anticlockwise, and then recovery

Inclined Surfaces

We already verified Oncilla's agility by testing its turning and perturbation adaptation capabilities on flat terrain. Another important feature is the ability to walk up and down slopes. Our verification was done on a maximum slope of 15° upwards (about 27% inclination).

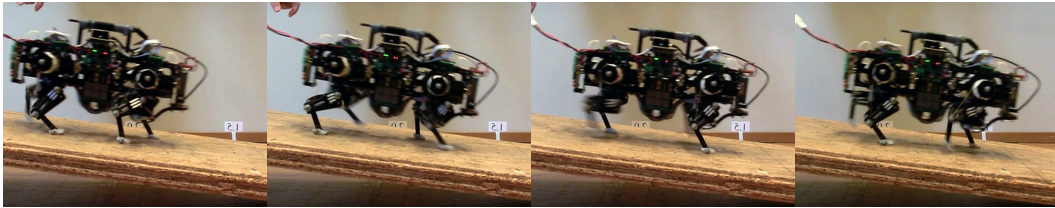


Figure 9.22 – Snapshots of Oncilla descending a slope in forward direction; little slippage occurred due to gravity supporting the movement; no loss between commanded and real speed

In open-loop the robot was only able to climb slopes of $\approx 4\%$ successfully and showed strong difficulties staying on a straight path on steeper slopes. Once the feedback-controller was activated and controlled the feet's angle-of-attack to the estimated ground inclination, we reached significantly longer travel before deviation from a straight line, see Figure 9.23. Adding a heading control by the operator allows for successful slope-ascend in a continuous straight fashion. Descending a slope was possible with and without feedback activated, as gravity supported to movement and the passive dynamics of the legs springs were able to stabilize against high impacts, see Figure 9.22.

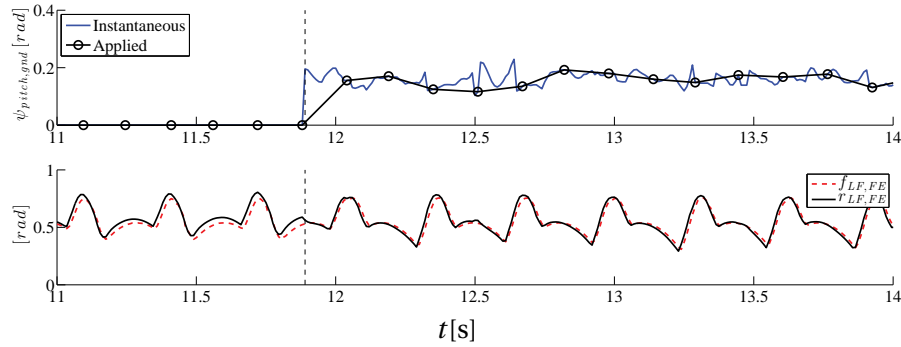


Figure 9.23 – Oncilla climbing an upwards 15° slope; *Top*: Continuous estimation of ground inclination during all stance phases; Controller update to the swinging legs in mid swing; *Middle*: Limit cycle update (calculated from shift in foot-trajectory and IK) with changing ground inclination

Vertical Obstacle

The ASLP leg showed previously robust locomotion, even when encountering step-downs. One of the most prominent failures with the Cheetah-Cub-Family was stumbling or falling due to small step-ups encountered at the end of the leg's swing-phase. Oncilla is employing an SCR to cope with such scenarios. Our verification experiment had the goal of successfully passing a vertical obstacle of about 5% leg length on flat ground. In initial runs, the robot was not able to pass the step, with or without feedback. The reason behind was a large SCR-activation time (0.010s) in comparison to the time needed for a full swing (0.150s) at our experimental speed of 0.5ms^{-1} .

Once the GRF-sensor hit the obstacle, activating the SCR, the leg already pushed the robot backwards, resulting (in the best case) in a direction change and passing the obstacle on the second or third attempt. This being unsatisfactory, we changed locomotion speed to 0.3ms^{-1} with a swing time increase to 0.25s and a "stop" signal preventing the push-back, see Figure 9.24 for an example of SCR activation at $t = 26.5\text{s}$ and successive return to cyclic behavior. Following the successful initial passing of the obstacle, we performed a comparison

9.2. Experiments with the Cheetah-Cub-Family and Oncilla

between open and closed loop during five obstacle passes. Open-loop succeeded in 20% and closed-loop in 100% of the runs. Additionally noticeable is the robot's capability to pass vertical obstacles backwards with higher speeds than forwards. The ASLP's parallel spring enables the leg to compress slightly and bridge the 10ms "gap" between contact and reflex activation.

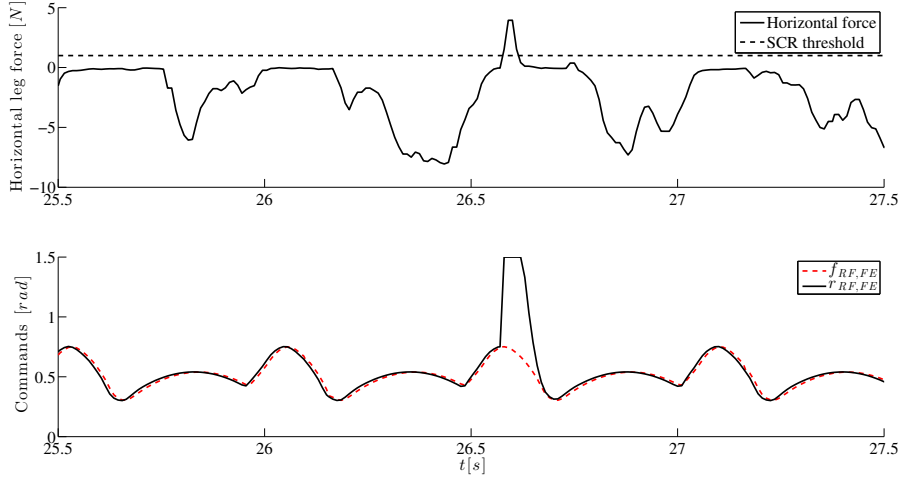


Figure 9.24 – Activation of SCR; *Top*: Contact with obstacle at $t = 26.5$ s (right-fore-foot); *Bottom*: SCR activation, inducing reaction in the oscillator; smooth convergence back to encoded limit cycle after passing the obstacle

Uneven Terrain

Integration of the separate skills to fulfill complex locomotion is one of our defined agility goals. With Oncilla we investigated this approaches feasibility by passing an obstacle course build from flat parquet, stairs, uneven tatami, step down into a pebble-bath with borders and finally rough wooden patches, see Figure 9.25. As described earlier, SCR activation was possible at higher speeds, when moving backwards; thus we preferred this locomotion direction at 0.4ms^{-1} also for this uneven terrain experiment. Again, the results showed the superiority of closed-loop over open-loop control in 10 runs. Without feedback, the robot failed five times completely and became very unstable in 2 additional runs, leading to a success rate of only 30%. Closed-loop control with PAD and SCR allowed 90% of the runs to be completed satisfactorily. In the remaining run, we had to correct the robot's heading manually after abrupt direction change following an obstacle-crash. An illustration of recorded sensor and control signals during one run can be found in Figure 9.26.



Figure 9.25 – Rough terrain setup for Oncilla; Locomotion direction: parquet, two stairs up of $0.010m$ and $0.015m$, rough tatami, step down into pebbles and fixed wooden obstacles (maximum height: $0.03[m]$ ($\approx 16\%$ of the leg length) between footholds

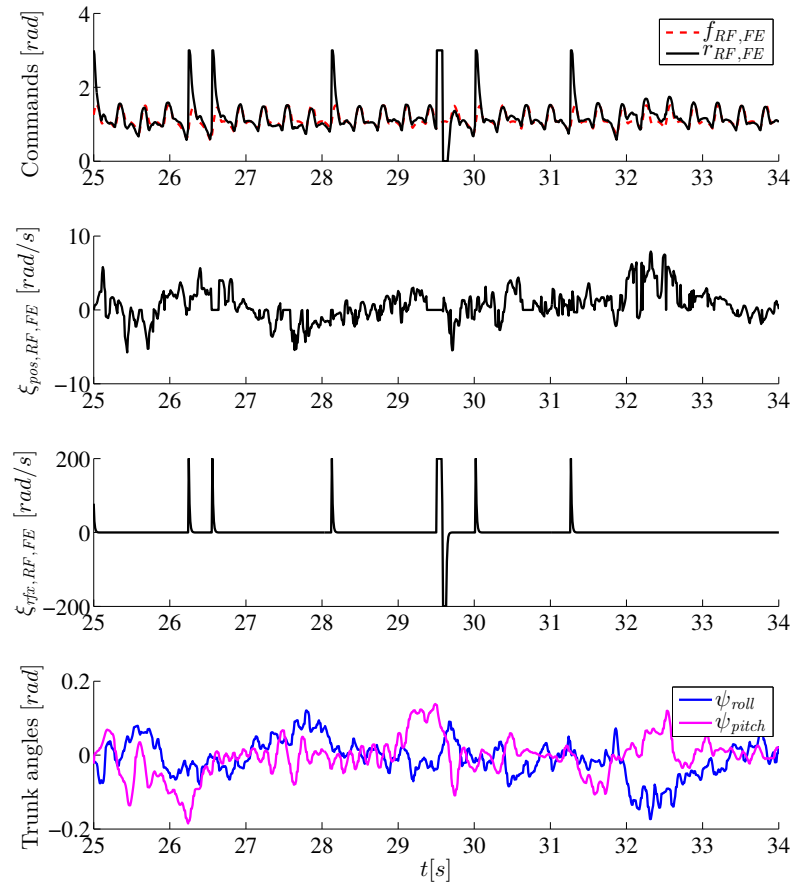


Figure 9.26 – Closed-loop control on rough terrain; control signals for the right-fore knee FE; *1st row*: commands generated by the CPG, visible continuous and momentary feedback; *2nd row*: PAD-feedback; *3rd row*: SCR (multiple) and LER (at $t \approx 29.6s$) activation; *4th row*: trunk angles; *General*: passing from parquet to stairs is visible by two consecutive SCR in between of $t = 26s$ and $t = 27s$; Trunk roll is corrected by PAD by employing knee FE; After $t = 33s$ almost no PAD feedback and no reflex activation, indicating flat surface locomotion

Discussion and Conclusion

Hardware and control validation of Oncilla was largely successful, as we could achieve stable locomotion in many scenarios. The open-loop control (CPG) enabled relatively fast locomotion on flat ground as well as partial success in other scenarios and provided an excellent basis for the superposition of reflexes. SCR, LSR, and PAD advanced the robot's rough-terrain, asymmetric load carrying, turning, perturbation and slope ascending capabilities markedly. Besides being able to locomote with relatively high speed, we achieved the verification of Oncilla's advanced skill-set in comparison to other robots of BIOROB, providing evidence to call it an agile robot.

Nevertheless, our experiments also showed room for improvement, as we needed to reduce speed and increase swing time to enable the SCR to pass a vertical obstacle while moving forwards. Locomotion backwards, and exploiting the fact that Oncilla's legs are compliant in the aft-fore direction is an alternative solution to allocate extra time for SCR activation. Another possible solution is the integration of a carpal-join, able to flex passively, to smoothen the impact on the forelimbs and allocate time for the SCR. Another lesson learned from our experiences with Oncilla is the need for repetitive and precise calibration if a closed loop controller is to be used successfully. In cases of qualitatively low calibration, reflexes can activate too early, late or not at all. The underlying open-loop locomotion is not very sensitive to this (although directional changes can occur if legs don't have the same standard length), supporting the use of a robust sensor-less gait as a reasonable basis for locomotion, rather than relying only on closed-loop control in every occasion.

In conclusion, to implement stable locomotion, with limited performance needs and a controlled environment, an open-loop controller is sufficient, quick and less complex. Using reflexes for closed loop, on the other hand, improves performance by adding more skills for adaptation to the environment, but on the cost of needing a repetitively precise calibration.

9.3 Experiments with Serval

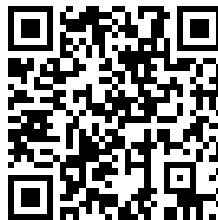


Figure 9.27 – Please find here videos of experiments with Serval described in this subsection: <https://go.epfl.ch/ExperimentsServal>

The first implementation towards agile movement with Serval consisted of replaying adapted kinematic data from agile dogs (Border Collies) and motion pattern derived from cats. The scaled implementation of respective foot trajectories was tested in different scenarios. This approach, due to the readiness-state of the robot hardware and control (no sensors integrated, no closed loop implementation), was performed in open-loop and is thus to be extended in current and future work. Performed experiments are to be seen as a proof-of-concept for hardware and control in a continuously developed robot.

Most of the here presented experiments do not yet employ active trunk movement. For debugging purposes, we decided to block the spine with two POM plates and free it, after initial investigations were completed, e.g., for use in turning maneuvers. All tests presented here were done tethered. After preliminary adaptation of the scaling to match our dog-data to the robot's geometry, we focused on a set of skills/tasks to test robot mechanics and its suitability for agile locomotion:

- Walk
- Trot (with and without AA)
- Bound (crouched)
- Gallop
- Sidestepping
- Turning with a radius
- Slope-up with flat ground transition
- Single and double step-down
- Fall absorption
- Rough terrain
- Lying/sitting down and standing up

Peaks and increasing forces are visible, e.g., at a time of 1 s on the left side (Figure 9.32 or at 0.3 s (Figure 9.33) that were caused by the hind feet obtaining high traction at that moment that led to higher compensation forces in the diagonally opposite foot. Video analysis has identified it. Results for a transverse gallop (Figure 9.37) are influenced profoundly by side-slip of feet.

9.3.1 Flat Terrain

Walk

The first gait implemented on Serval was a standard lateral sequence walk (with $h = 0.001m$, $SL = 0.155m$ and $F = 1.0Hz$, see Figure 7.4) resulting in the foot trajectories presented in Figure 9.28.

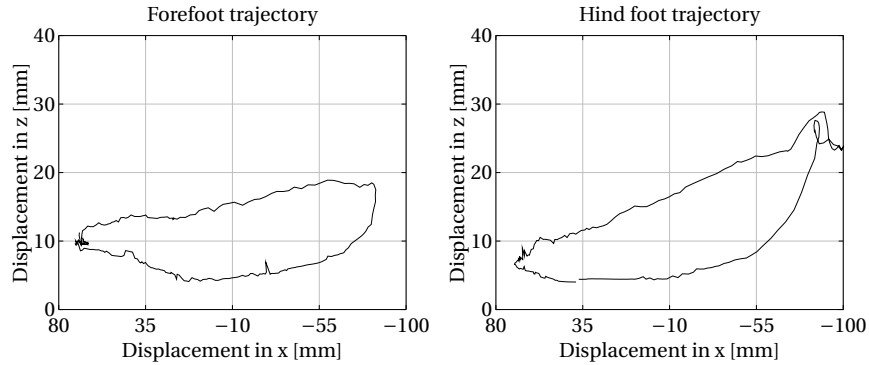


Figure 9.28 – Recorded fore and hind foot-trajectory from walking gait on the ground, using $h=0.001\text{ m}$, $SL=0.155\text{ m}$, $f=1.0\text{ Hz}$, head to the left

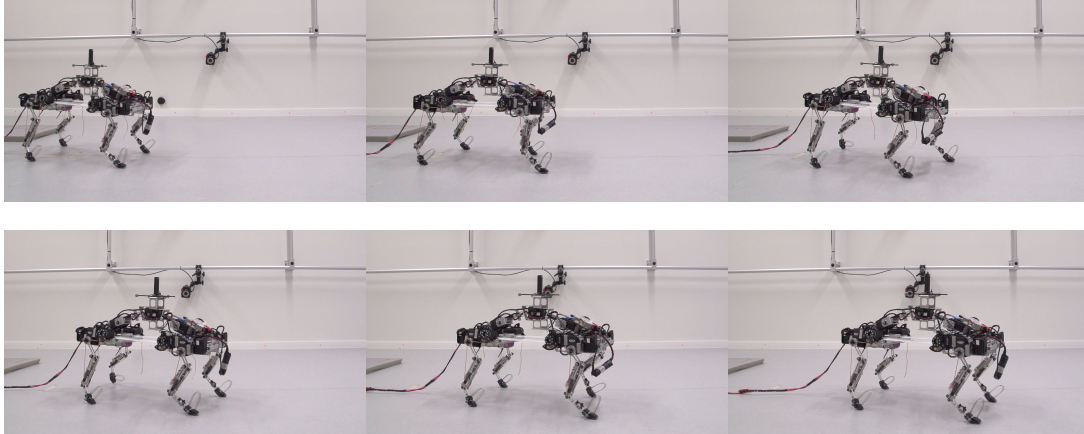


Figure 9.29 – Snapshots of Serval walking; almost no foot lift off visible; sliding is prominent

The robot mechanics, as was already the case for Cheetah-Cub and Oncilla, are tuned for dynamic locomotion, meaning that leg-stiffness is rather high. This leads to expected difficulties when using a relatively slow and static gait, as already observed in Cheetah-Cub. The most prominent drawback visible from Figure 9.29 and the respective video file, was the lack of foot-clearance from the ground. This resulted in an almost complete sliding gait, only

applicable on smooth surfaces. As we did not achieve much lift off, even after a small, intuitive parameter tuning, we decided neither to record GRF, nor to proceed in further analysis of the gait, but move on to the next skill. One other possible reason is the wide posture of the robot needed for high AA-ROM, but resulting in increased roll-motion during low-frequency gaits. A PAD-reflex could diminish this effect.

Trot

Following the gaits, often observed in animals, the running trot was tested ($h = 0.03m$, $SL = 0.15m$ and $F = 1.5Hz$), see Figure 9.30 for foot-trajectories and Figure 9.31 for snapshots. We used two different settings for the AA. When moving on flat ground, the hind legs were flexed towards the sagittal plane and forelegs extended in the opposite direction. This posture is observed in dogs when moving in medium to high speeds to possibly enable overlapping of their feet during motion. This way, the hind legs can provide most of the propulsion whereas the fore legs stabilize the robot. For other tasks, like step-downs or backward trot, we set the AA straight. This decreased variation in the robot's roll-angle when perturbed and was thus useful in cases, where self-stabilization was the top priority. An example of GRFs can be found

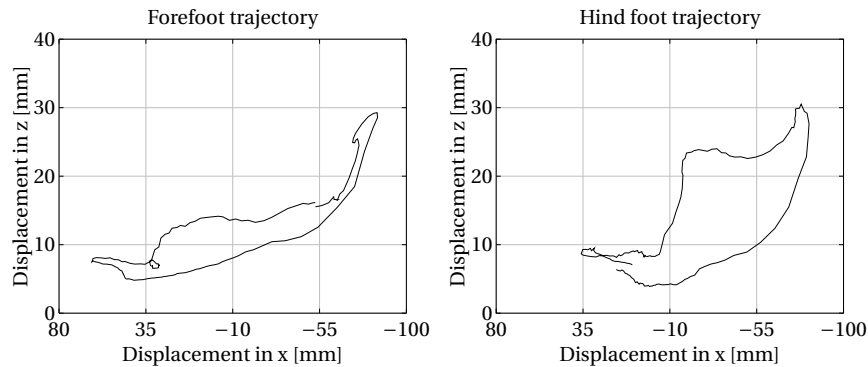


Figure 9.30 – Recorded fore and hind foot trajectory from trot gait, using $h=0.03m$, $SL=0.15m$, $f=1.5Hz$

in Figure 9.32 and confirms the visual impression from Figure 9.31. The robot was able to show main characteristics of a trot-pattern repetitively. This phenomenon, already observed in *Oncilla* and *Cheetah-Cub* can be described by non-optimal controllability of the ASLP leg and the use of slippage to compensate early touch down of the feet. Further, as we were using a gait, not tailored specifically to the robot, but stemming from kinematic recordings, a mismatch is possible. From a mechanics point of view, we see the need for new materials with anisotropic friction to enhance propulsion in one and allow for slippage in the other direction. Nevertheless, the trot gait was very stable, out-of-the-box and enabled the robot to locomote at a speed of $0.83ms^{-1}$ ($FR=0.32$) with a visible trot footfall pattern and without major gait

optimization.

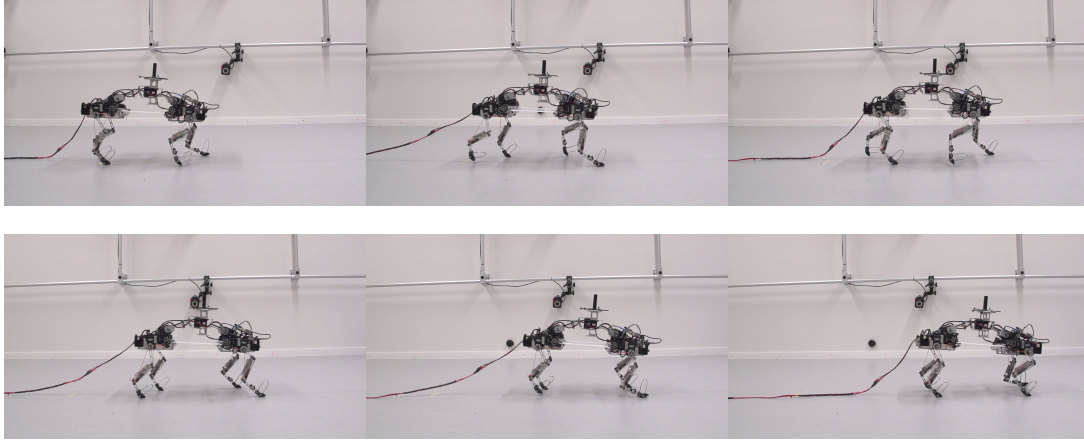


Figure 9.31 – Snapshots of Serval trotting; dynamic movement with characteristic footfall patterns; sliding at touch-down and toe-off, decreasing efficiency; speed at 0.83m s^{-1}

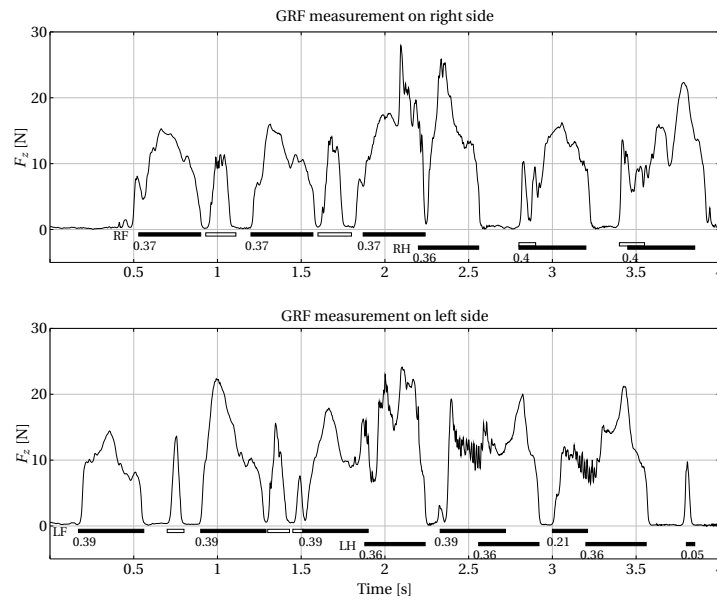


Figure 9.32 – GRF measurements for a trot gait, footfall patterns indicated in black with expected characteristic appearance, foot sliding is represented by white boxes and individual duty factors are marked, mean duty factors: $DF_{LF} = 0.36, DF_{LH} = 0.37, DF_{RF} = 0.37, DF_{RH} = 0.39$ and $DF_{av} = 0.37$; GRF patterns are similar to Cheetah-Cub, with never the full robot weight (33N , without battery) on one single foot; Peaks are visible, e.g., at 1s on the left fore foot that was caused by the hind foot obtaining high traction leading to higher compensation forces in the diagonally opposite foot

Bound (crouched)

The crouched bound, as a symmetric gait, is used by cats to climb very steep slopes over 50% inclination, see subsection 7.1.2, but is also a useful gait when testing active spine movement (Lynx, Bobcat). For us, as we did not yet free the spine, the crouched bound was used mainly for slopes, as described later. Nevertheless, a feasible gait was also becoming apparent when running on flat terrain. Walking foot-loci with changed inter-limb timing was used to achieve the motion.

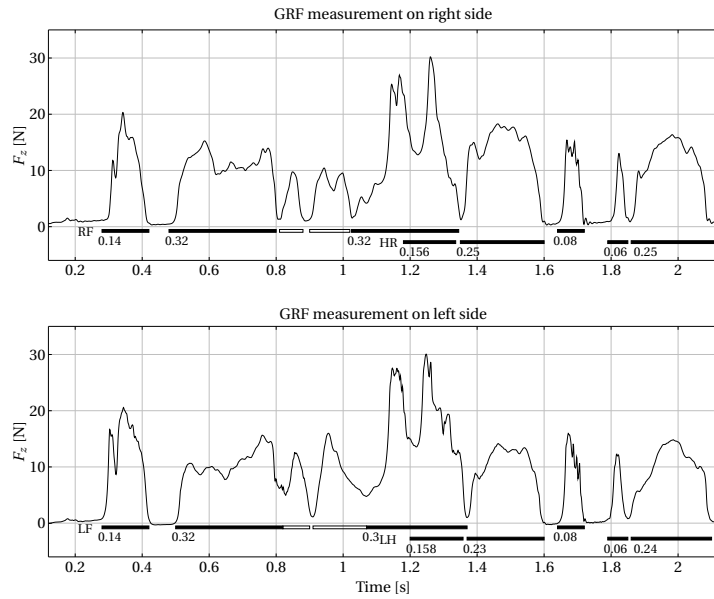


Figure 9.33 – GRF measurements for a bounding gait using a crouched posture; footfall patterns indicated in black with almost exact representation of characteristic distribution; foot sliding is represented by white boxes and individual duty factors are marked; mean duty factors: $DF_{LF} = 0.38, DF_{LH} = 0.34, DF_{RF} = 0.39, DF_{RH} = 0.36$ and $DF_{av} = 0.37$; robot weight is evenly distributed on two sagittally opposite feet (left-right-symmetry); the peak at $\approx 1.3s$ is an example of all feet touching the ground at the same time, resulting in application of the robot's full weight as vertical force

Bounding showed the good directional stability, visible from Figure 9.34 and an almost perfect representation of the desired footfall pattern, illustrated in Figure 9.33. At seldom occasions stick-slip is visible. We hypothesize that improvement towards a non-slip gait is possible when freeing the spine (see subsection 9.2.1) and improving ground contact with anisotropic friction material on the feet.

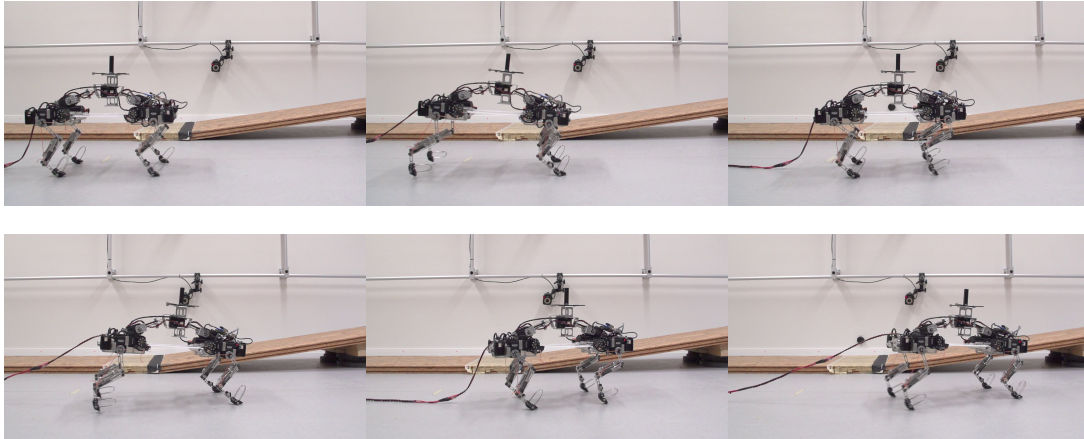


Figure 9.34 – Snapshots of Serval performing a crouched bound; dynamic movement with characteristic footfall patterns (left-right-symmetry); sliding prominent at toe-off; small turning to the left

Gallop

Transverse gallop was the last tested gait with Serval ($h = 0.016m$, $SL = 0.15m$ and $F = 2.0Hz$) and resulted in foot-trajectories displayed in Figure 9.35. As a high-speed gait in animals, we expected faster, dynamically stable movement from the robot. Both aspects could not be

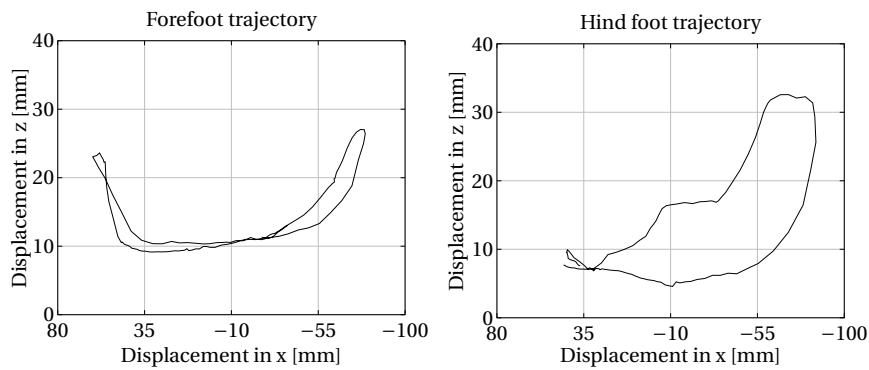


Figure 9.35 – Recorded fore and hind foot trajectory from galloping gait, using $h=0.016$ m, $SL=0.15$ m, $f=2.0$ Hz

observed. Besides the timing between the legs (visible from video), the commanded gait led to sliding in pro- and retraction almost at all times, see Figure 9.37 and Figure 9.36. Characteristic flight phases could not be achieved. Speed varied slightly around our tested trot-gait and thus cannot be seen as highly dynamic, another important characteristic of this gait in nature. This may be due to lack of actuator speed for this gait (only 2Hz max) and the blocked spine,

preventing the necessary energy to be transmitted throughout the whole robot for propulsion. The very low isotropic friction of the ground contact is reducing propulsion, making it very difficult to overcome the system's inertia towards a dynamic gait.

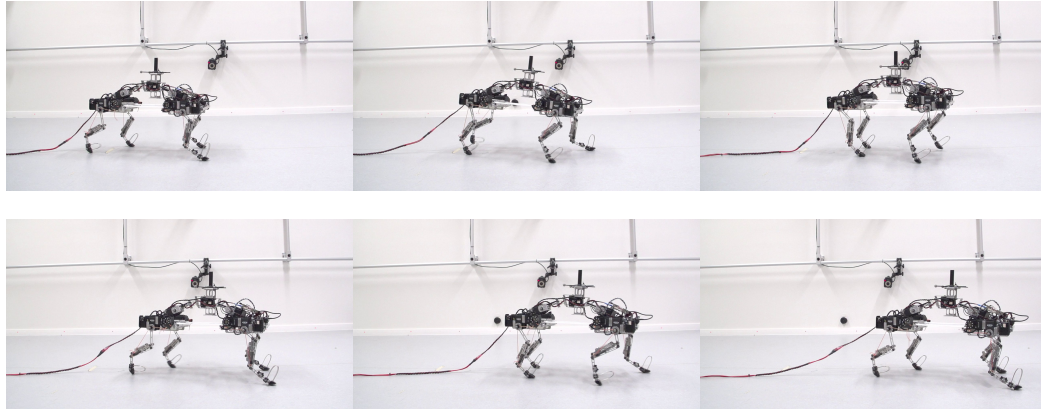


Figure 9.36 – Snapshots of Serval galloping; no dynamic movement; characteristic footfall patterns not noticeable; full contact sliding, no flight phases

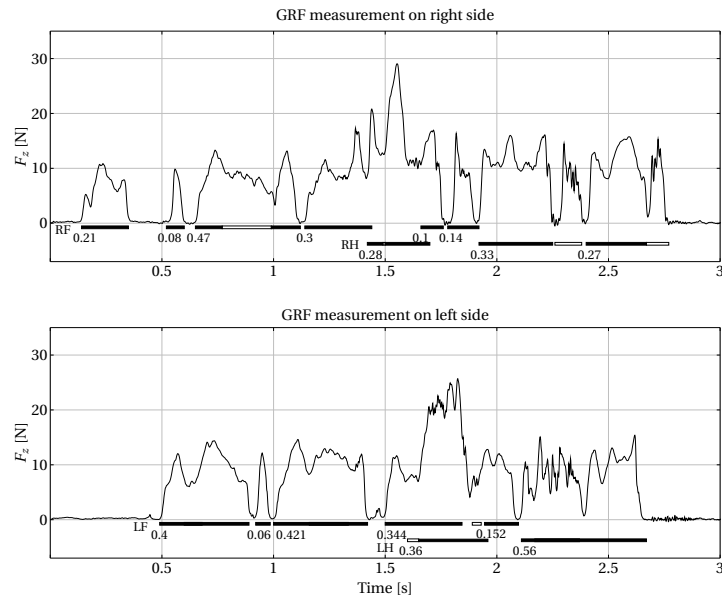


Figure 9.37 – GRF measurements for a galloping gait, foot sliding is represented by white boxes but could almost never be distinguished for the remaining stance-periods; individual duty factors are marked; the average duty factor is close to 1, as we observed almost no lift-off between in the strides, but full contact sliding, thus we refrain from calculating average values

Side-stepping

Lateral side-stepping as preparation for later execution of LSR was included in our initial experiments. The movement was generated, by commanding a spatial 8-figures to the robot's feet, hence using the AA to push the robot to one side and shifting body weight away from the side whose feet should be in swing-phase.

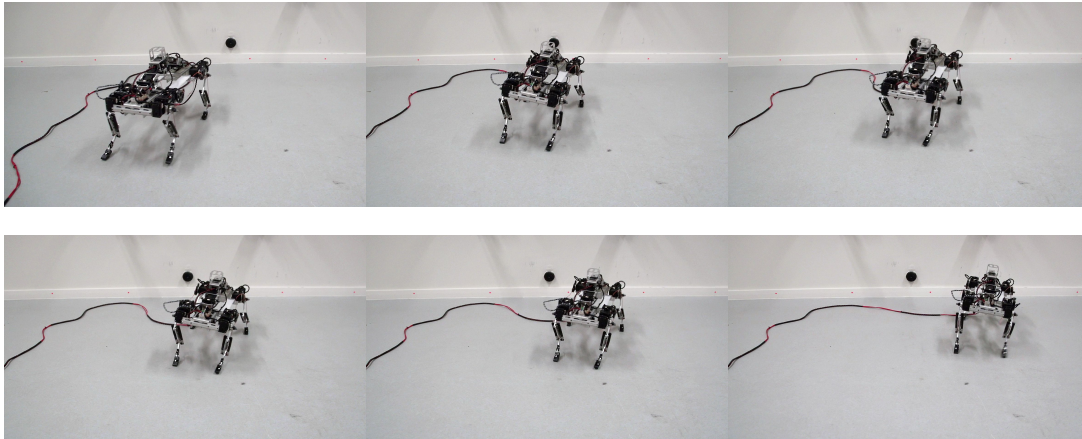


Figure 9.38 – Snapshots of Serval performing side-stepping; movement lateral combined with backwards motion, thus holonomic; stick-slip and stuttering due to foot-geometry and small ground clearance during swing

Without touching the ground Serval was able to perform the task, but as soon as in contact, stick-slip with the feet's hard edges due to little ground clearance made a movement impossible. The snapshots in Figure 9.38 demonstrate an alternative, artificial gait using AA, allowing for lateral-aft motion. A pure lateral movement might be difficult to achieve, if posture is not kept balanced through a PAD-reflex, allowing the swing legs to execute their movement without touching the ground. Future LSR implementation is not possible with only this motion pattern, as it differs strongly from normal gaits, like trot or bound. Oncilla's strategy to LSR remains the most favorable one.

Turning with a Radius

The last movement on flat ground essential for an agile system is the ability to turn. Here a combination of ASL and spine-deflection (like in Cheetah-Cub-S) was used. The resulting turn was again somewhat perturbed by slippage, but with a minimum radius of $0.58m$ tiny, for a robot of Serval's length, see Figure 9.39.

Adding the AA-movement to the two previously mentioned strategies should improve slippage

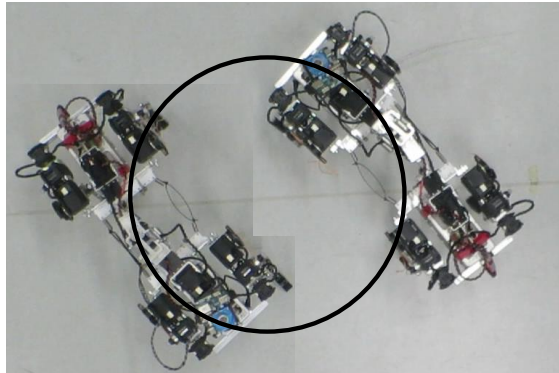


Figure 9.39 – Arranged figure of Serval turning using ASL and spine; Merged snapshots and approximated tuning circle centered on the "head"; movement anti-clockwise; radius $\approx 0.57m$

and make turning more repeatable.

Conclusion

Our study of flat terrain locomotion demonstrated the potential of our robot. Serval was able to achieve multiple motion patterns, only by replaying parameterized dog-foot-locii. Further investigation of optimal gaits and patterns tailored to the robot should improve the existing patterns. Here is to investigate in the future if bio-inspired, but artificially generated patterns, like in the Cheetah-Cub-Family and *Oncilla*, have an advantage over replaying kinematic data.

We see additional mechanical and control challenges, to be addressed: (1) anisotropic friction, geometry, and stiffness of the feet have to be investigated to allow optimal propulsion in all desired directions; (2) the spine-controller has to be implemented to be used in high energy gaits and PAD; (3) Reflexes and the needed sensorization have to be integrated, if step-ups and posture stabilization are to enrich Serval's motor-skills.

A general conclusion for agility is drawn at the end of the section.

9.3.2 Inclined Surfaces

Slope-up

Using a bound and crouched posture adaptation, presented in subsection 7.1.2, experiments have been performed to identify the maximum slope Serval is able to climb up, see Figure 9.40. The maximum inclination feasible with an open-loop gait amounted to 20° ($\approx 36.4\%$) with a transition from flat ground to the slope. Without heading-correction, substantial slippage in the feet in the propulsion phase of the toe-off and drift to the side could be observed. Serval

could repeatedly move on a 16° ($\approx 28.7\%$) slope with little drift. Smaller inclinations could also be achieved with our trot-gait. Locomotion down-slope was also possible, with the same effects visible as in Oncilla. Lateral inclinations were not tested, as we did not have the time to design an appropriate test setup.

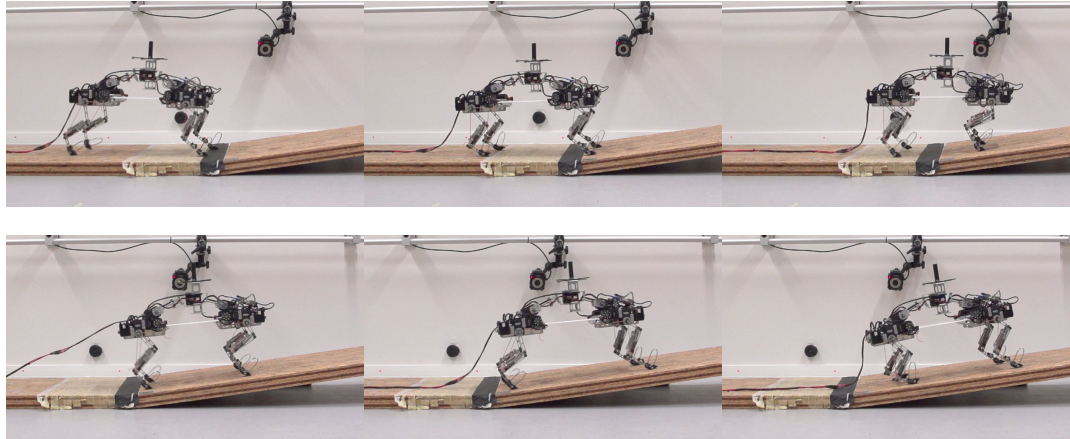


Figure 9.40 – Snapshots of Serval bounding upslope at 16° inclination ($\approx 28.7\%$); the implemented gait is a crouched bound; transition from flat to inclined terrain is visible and successful; heading remains relatively straight.

Conclusion

Serval's capability for ascending slopes in open-loop is very promising. It already improved markedly in comparison to Oncilla (with PAD). In further work and with PAD as well as better surface friction included, even steeper slopes will be feasible.

9.3.3 Perturbed Surfaces and Stability

Single and double Step-down

The corresponding experiments were included to demonstrate self-stabilizing behavior of the robot and the gait robustness (Figure 9.41 and Figure 9.42). The goal of these tests was the determination of the maximum step height which the robot can go down in open-loop while reliably using its legs' compliance. The applied gait was an unchanged trot. The requirements for a successful try was the continuation of a stable gait for at least $2m$ after step-down. At least ten runs were performed per step-height.

With the reliability of 100% Serval adapted to step-downs of 53mm that amounts to $\approx 25.2\%$ of its leg length. The largest step of 63mm ($\approx 30\%$ of leg length) resulted in a success-rate of 70%.

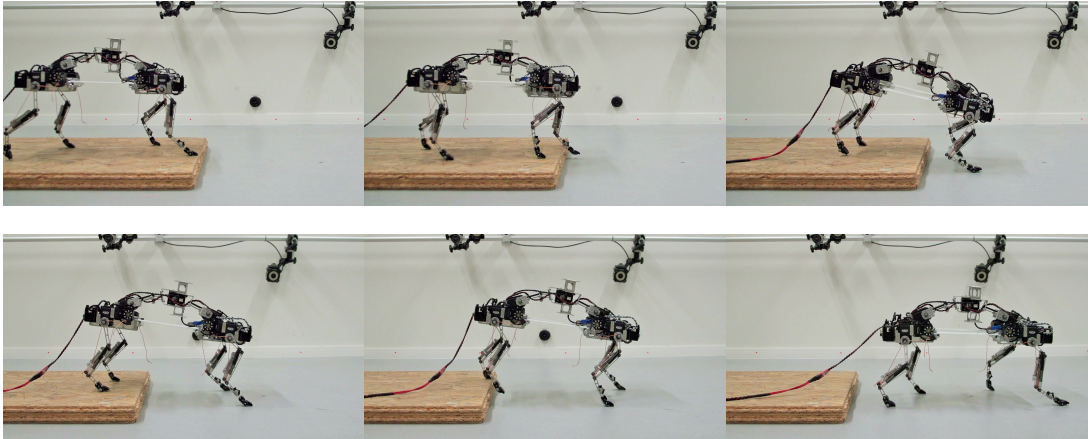


Figure 9.41 – Snapshots of Serval trotting down a single step of 63mm ($\approx 30\%$ of leg length); success-rate of 70%; bending and shock absorption through the parallel spring is visible.

Double step downs that can be seen in Figure 9.42 were successfully performed in 90% of the cases.

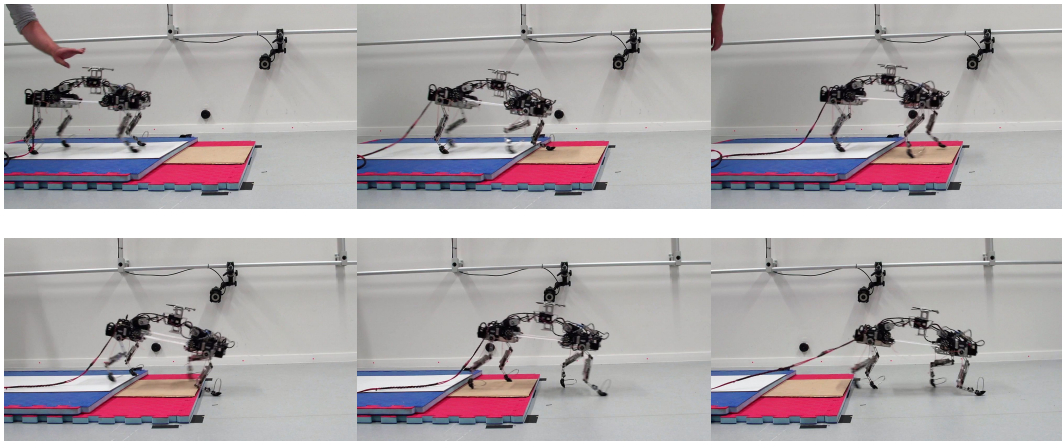


Figure 9.42 – Snapshots of Serval trotting down a double step of 26mm ($\approx 12.5\%$ of leg length); success-rate of 90%; bending and shock absorption through the parallel spring is visible but less prominent than in higher steps.

Concerning stepping down, Serval showed remarkable results and thus followed up on the success in Cheetah-Cub, even increasing the percentile maximal step height by 10% and success-ratio by 50%. The next logical step is to improve maneuverability by implementing step-ups through reflexes.

Fall Absorption

Robustness is key, as agile motion can lead to falls and failures rather quickly. Dropping the robot from a maximum height of 70% leg length while running with a trot showed that it was possible to overcome impacts and continue locomotion in this idealized scenario, see Figure 9.43. Visible in the first images after touch down is the strong deflection of all leg-springs and the resulting push-off. A critical point is presented by the touch-down of the leg's middle segment and respective full compression of the parallel spring, already for this drop height. However, the robot was always able to regain a steady trot after some motion cycles.

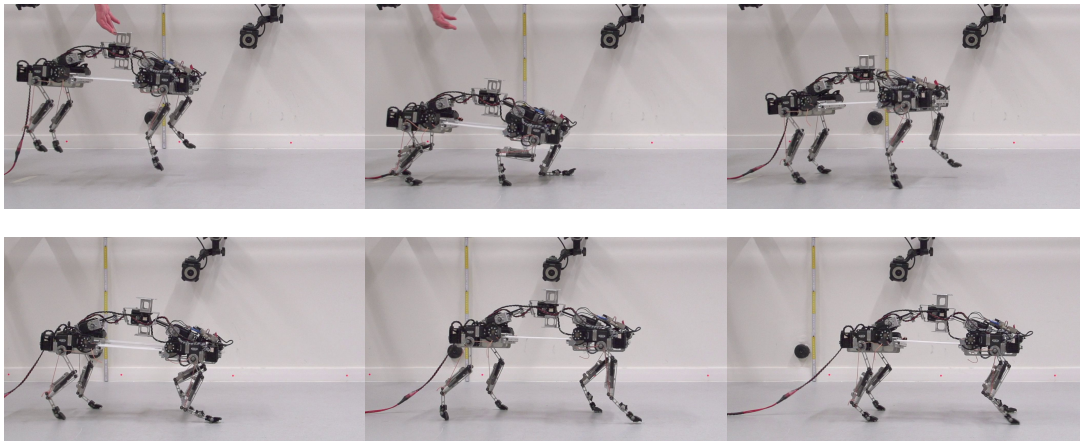


Figure 9.43 – Snapshots of Serval falling from a height $\approx 70\%$ of leg length while trotting; success rate $> 90\%$; complete flexion of the parallel spring and touch down of the knee motor are visible; passive flexion of the very stiff diagonal springs is also visible

This result is encouraging, as it shows robustness as long as the force is transmitted in a way that the leg-compliance is able to disperse the impact. Additional tests from other angles and heights should be performed to characterize the robot further and test the new in-series implementation in AA and spine joints.

Rough Terrain

Moving over sharp vertical obstacles, using only open-loop, was already found to be almost impossible in our experiments with Oncilla. As an additional test of Serval's stability, we decided to let it run on a smooth, but bumpy GFRP rough terrain after a small step-down, see Figure 9.44. Without controlling the heading, the robot was sliding to different sides, moving backwards, but in the end finishing the distance over the plate. This highly irregular behavior cannot be implemented in real scenarios, but again, underlines the robots stability due to its compliance. Heading and posture control may build on this stability to enable new application

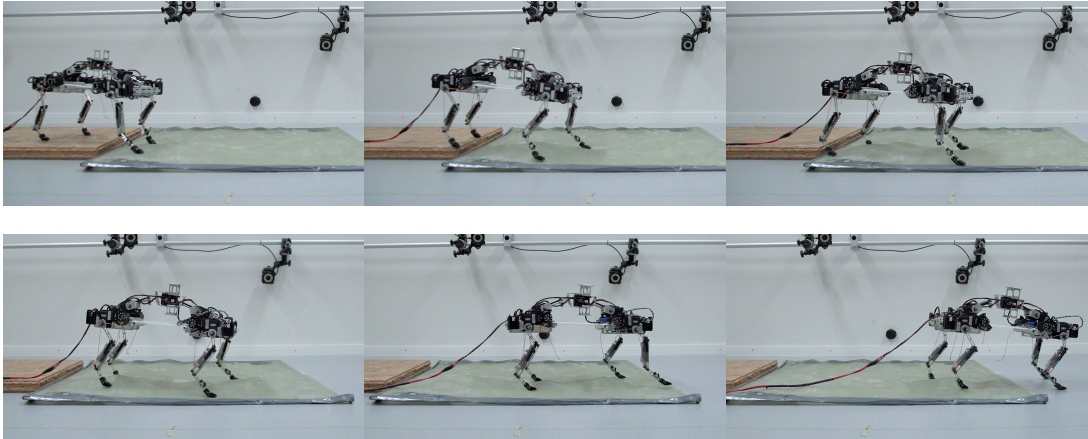


Figure 9.44 – Snapshots of Serval trotting on a smoothed bumpy terrain after an initial step-down; deviations from straight path and uncontrolled movements are present.

environments and increase the robot's real world capacity.

Conclusion

Both rough terrain locomotion, as well as fall absorption, were handled repeatedly well. This is a valuable proof-of-concept of robot-robustness and the importance of passive compliance in small quadrupedal robots. This passive adaptability is providing an important fail-safe if more sophisticated control (to be implemented in the future) might fail.

9.3.4 Artificial Behaviors

Lying/ Sitting down and Standing-up

We defined the transition from sitting/lying to a normal standing posture as a part of agility. Consequently, these behaviors were implemented and tested. Kinematic data for the robot joints was extracted from MOCAP of border collies, and the movements were implemented as hard-coded motion-sequences [118], see Figure 9.45 and Figure 9.46.

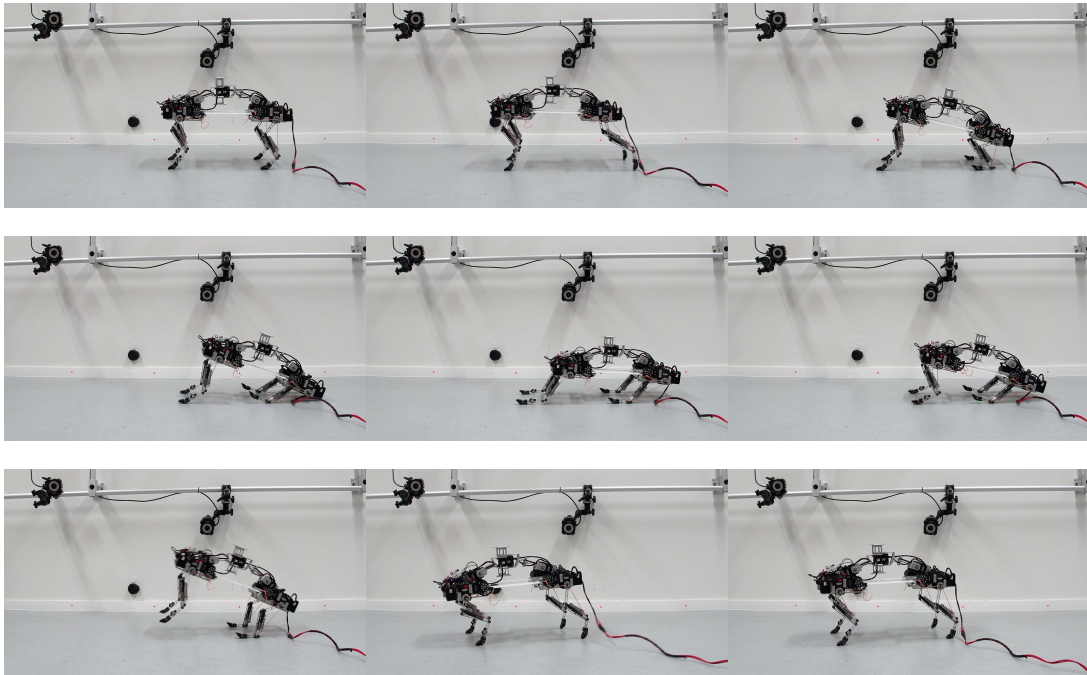


Figure 9.45 – Snapshots of Serval lying down and standing up; fully hard-coded motion-sequence inspired by dogs.

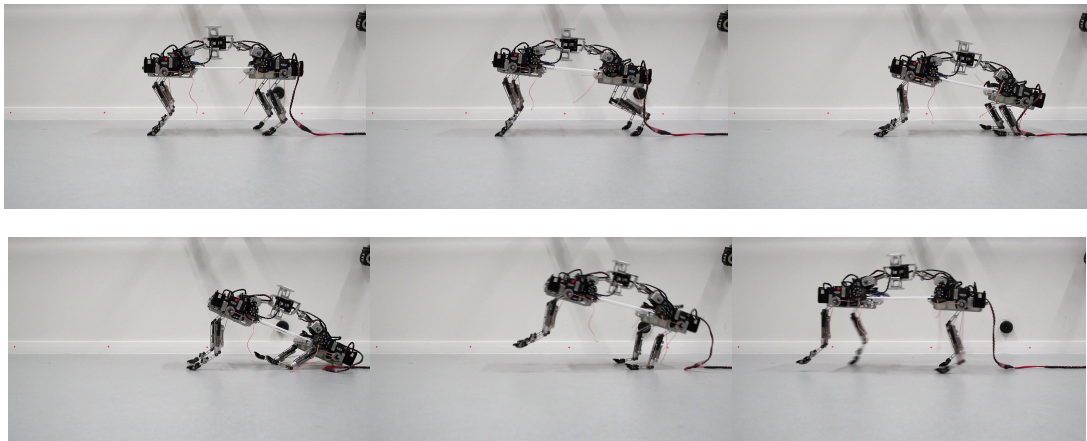


Figure 9.46 – Snapshots of Serval sitting down and standing up; fully hard-coded motion-sequence inspired by dogs.

Conclusion

Both motions were achieved in ideal conditions, on flat ground without any inclinations of the robot body or even lying on its back. The robot was able to repeatedly move from one posture to the other and start trotting afterward. To further enhance the motion-sequences, especially when not in an ideal position (e.g., on the side), further sensorization with an IMU as well as an active spine are needed.

9.3.5 Conclusion for Agility

Serval presented a high level of mobility at medium speeds. With the number of successfully implemented skills, using a basic kinematics-duplication, we debugged the robot hardware, found out strengths to emphasize (compliance and adaptable feet), weaknesses to correct (friction of ground contact and stiffness of spine/AA) and made it ready for future attempts to achieve agile locomotion. All in all the initial tests were a great success and valuable insights towards hard- and software development were gained. We compared Serval with our agility dog in the frame of the agility benchmark, see chapter 3, Table 9.6, and in a strength plot in Figure 9.47

Table 9.6 – Agility scores for Serval in comparison to our agility dog; q- variance values; sidestepping is not counted as no purely lateral movement could be achieved

	Dog	Serval		
		q	Score	[%]
A_{ts}	0.679			
A_{tr}	0.036	0.913	0.003	8.3
A_j	0.394			
A_l	0.453			
A_{lv}	0.916			
A_{s1}	0.531	0.465	0.038	7.2
A_{s2}	0.531	0.400	0.076	14.3
A_{s3}	0.531			
A_{st1}	0.639			
A_{st2}	0.814	1	0.731	89.8
A_{sstep}	0.438			
A_{fl}	6.108	0.51	0.297	4.9
A_{bl}	1.527	0.05	0.016	1
$A_{gav\%}$	100			9.7

Serval achieved an overall average agility of 9.7%, with sitting up having the strongest contribution and being restricted due to a comparably slow gait and medium variance values. This can surely be improved by closing the loop, allowing for higher precision in task execution, as well as a further exploration and tuning of gaits. Nevertheless, our small, safe and low cost robot is able to perform 5 (including side-stepping 6) agility tasks out of 13 with the potential to reach more after some additional control development (A_{ts} , A_{st1} , A_{s3} , A_{sstep}). Jumping

and leaping might be out of the scope for this robot, as active leg-extension or at least more explosive propulsion force is needed. Additionally to the agility tasks, Serval is able to cope with step-downs, smooth rough terrain and falling vertically.

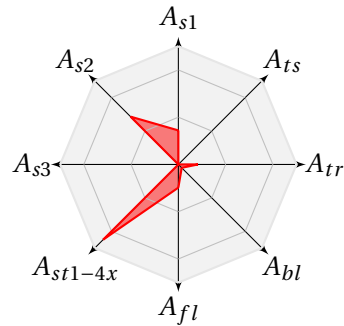


Figure 9.47 – Strength-plot for agility of Serval in % of aggregated dog scores; maximum radius present 25% relative agility for each score; individual scores in red; A_{st1} scaled by 0.5 for better readability of other scores.

Conclusion and Outlook

Part III

10 Conclusion

Agile quadrupedal locomotion is yet to be fully understood, quantified or achieved. An intuitive notion of agility exists, but neither a concise definition nor a common benchmark can be found. Further, it is unclear, what minimal level of mechatronic complexity is needed to realize agile locomotion. In this thesis we addressed and partially answered two major questions:

Question 1: What is agile legged locomotion and how can we measure it?

To answer our first question, we defined agility for robot and animal alike, building a common ground for this particular component of locomotion and introduced quantitative and dimensionless measures to enhance robot evaluation and comparison. Our definition as a particular part of locomotion,

Agility is representing a previously acquired and size dependent set of locomotion skills, executed in a precise, fast and ideally reflexive manner to an outside stimulus.

is based on and inspired by features of agility observed in nature, sports, and suggested in robotics related publications, such as:

1. Agility is not the result of execution of a single skill, but a complex set of motion patterns as well as the possibility to rapidly switch between them.
2. Ideally, reactive execution of known skills with minimal prior planning
3. Agility varies from one species to another and thus should, at least, be defined differently in terrestrial, aerial and aquatic locomotion.
4. Precision in task execution is one of the key aspects.

5. Speed of the task execution is another key aspect.
6. Agility is related to the scale of the system or animal; thus it should be normalized to attempt a comparison.
7. The energy-cost to execute a task should be part of benchmarking a system's agility.

Using the results of this observational and literature review, we build a novel and extendable benchmark of thirteen different tasks that implement our vision of quantitatively classify agility. The scores include: turning (A_{ts} and A_{tr}), leaping (A_l , A_{lv} and A_j), slope running (A_{s1} , A_{s2} and A_{s3}), standing up (A_{st1} , A_{st2}), sidestepping (A_{ssstep}) as well as forward and backward locomotion (A_{fl} and A_{bl}). All scores are calculated from simple measures, such as time, distance, angles and characteristic geometric values for robot scaling. We normalized all scores unit-less to reach comparability between different systems [57]. In an extension of this core, we added an averaging method for general agility, using a baseline (in our case the aggregated dog from different agility competitions) again to compare a robot's relative performance against. Consequently, if a consistent baseline is used, all agility scores have the same weight inside the average agility. This way, solving the important task of enabling comparison between robots with different skills and morphologies, became a reality. Moreover, a COA, strongly inspired by the COT is added to give a quantification of size-related energetic agility cost. An initial implementation with available robots and real agility-dogs as baseline finalized our efforts of answering the first question. Our robots were able to perform relatively few agility tasks, with low scores, leaving the relative averaged agility under 10% of a real dog. This, on the first glance, grounding result is not very surprising, as an already qualitative comparison of animal and robot visualizes the reality gap still to overcome. Nevertheless, with our new developments, we were able to perform many of the benchmarked tasks, which demonstrates our robots' versatility, which has the potential to become agility in the future.

The acceptance of the proposed agility-benchmark is not easily predictable. We hope to generate a means for the focused development of new and agile robot, based on the found agility-qualities. The agility scores could be used as fitness functions for the optimization of mechanisms and their respective control, including learning approaches. With these main outcomes, we propose a means for robot development in the future and help to bring legged robotics one step closer to complex applications. One possible use for agile robots could be the field of search and rescue robotics, where versatility and robustness have to be combined with a certain degree of agility. In this area of application, it is crucial not only to fulfill given tasks but also to do it dynamically, such that rescuers can react to situation changes rapidly or have enough time and information to decide on a profound intervention plan. Agility is needed to protect the robotic system from harm (for example fast recovery from a fall) when operating it in areas that are too dangerous for humans.

As researchers discover and implement new robot features (such as transition capability between tasks), the agility benchmark should be extended as well, building on the open-source nature of our method. This parallel evolution of robot and benchmark will hopefully give rise to better and safer performing robots that can benefit society.

Question 2: How can we make agile legged locomotion with a robot a reality?

Bio-inspired designs introducing and benefiting from morphological aspects present in nature allowed the generation of fast, robust and energy efficient locomotion. We used engineering tools and interdisciplinary knowledge transferred from biology to build low-cost bio-inspired robots able to achieve a certain level of agility and as a result of this addressing our second question. This iterative process led from Lynx over Cheetah-Cub-S, Cheetah-Cub-AL, and Oncilla to Serval, a compliant robot with actuated spine, high range of motion in all joints. Serval presents a high level of mobility at medium speeds. With many successfully implemented skills, using a basic kinematics-duplication from dogs, we found strengths to emphasize, weaknesses to correct and made Serval ready for future attempts to achieve even more agile locomotion. Serval performed an overall average agility of 9.7% (of the aggregated dog), with sitting up having the most substantial contribution and being restricted due to a comparably slow gait and average variance values. This can surely be improved by closing the loop, allowing for higher precision in task execution, as well as a further exploration and tuning of gaits. Nevertheless, our last iteration of small, safe and low-cost robots can perform 5 (including side-stepping 6) agility tasks out of 13 with the potential to reach more after some additional control development (A_{ts} , A_{st1} , A_{s3} , A_{sstep}). Jumping and leaping might be out of the scope for this robot, as active leg-extension or at least more explosive propulsion force is needed. This performance positions Serval above any of its predecessors with Oncilla reaching 6.1%, Cheetah-Cub 4.2%, Cheetah-Cub-AL 3.2% and Cheetah-Cub-S 2.6%.

Did we succeed? - The contribution of this thesis

Once arrived at the end of the Ph.D., it is time to draw a line and evaluate the outcomes mentioned above, asking ourselves the question: Did we succeed in addressing our research questions?

Concerning locomotion related *agility*, its *definition* and plausible *quantification*, the answer is a clear **yes**. Our agility definition is founded on a broad observational and literature basis and is for the first time giving concrete feature-based wording to a broadly used terminology. The following benchmark, if accepted, worked with and extended by the legged robotics and locomotion biologists communities should help the fields to advance towards better understanding and achieving of agility.

Our robot development could only partially mirror this success. We managed to produce different very safe, low-cost and easy to handle robots, using biological templates and researching their place in legged locomotion. Nevertheless, we have to admit, that we **could not** achieve very agile locomotion yet. We **could** however identify key features when employing a flexible trunk (scaling to body size and needed DOF for natural motion) contributing to animal-like locomotion (Lynx, Cheetah-Cub-S, Serval), research different reflex behaviors and their impact on perception-based rough terrain locomotion (Oncilla) and provide further knowledge on a robust design methodology for small quadruped robots (Cheetah-Cub-AL, Serval). This development work is an excellent basis for future explorations, described in the last chapter.

11 For Those Who Follow - Outlook

11.1 How to build on this work

Thanks to the multiple reviews of my thesis we received, I want to add the following section, describing some subjective evaluations and hints how to build on my work or how to build the next, agile robot.

The agility benchmark can be a valuable tool to use if one wants to build a new robot or compare an existing one to the competitors (if accepted by the community). My take would be to search the agility-database for robots that are capable of precisely the skills that are desired for a new platform and take those as a starting point, improve their design, control, and electronics, finally adding value to the new system.

The agility values can be valuable for simulations, to broaden the available fitness-functions. Optimizations can show similarities or differences in a mechanism depending on what aspect of agility is used. This could potentially answer new questions concerning the evolution of different species and common traits between them.

When it comes to hardware and control, there are many pros and cons of any mechanism or method. It strongly depends on the application at hand. I will describe when and why I would use the previously presented concepts: **Low-cost robots** are a great tool to quickly explore many *different* questions as one can quickly build a new robot to adapt to the hypothesis at hand. If one particular research question or goal is in mind, it might be worth investing in a more high-tech solution and explore the question's aspects in greater detail.

Small robots are safe and can thus be used, stored, experimented with and transported without significant infrastructure investment. The downside is the unavailability of many high-power actuation and different sensors for these robots due to the size- and payload requirements nowadays. The trend in these industries is towards miniaturization, and I

believe small robots will benefit strongly leading to a higher performance in the future.

Materials, design- and production methods are highly depending on the desired robot. A look at this dissertation can help to get started on one's development process.

The (unsensorized) ASLP-Leg is a very efficient mechanism when the task calls for dynamic movement without the need for complete controllability. The under-actuation and lack of active extension in the knee make it difficult to see the ASLP-leg in a robot aimed for, e.g., inspection tasks, where foot-placement has to be accurate, or perturbations exceed the adaptability through passive compliance.

The flexible spine is very valuable for small robots to improve perturbation stability, ranges of motion, explore the dynamics of different gaits, have a close comparison to nature and other features I am not yet aware of. The major drawback is the complexity it adds to the robot regarding mechanics and control. My suggestions, especially if one wants to use a medium sized quadruped robot as sensor carrier in different terrains, would be to think twice about integrating a spine, as the added value might not be high enough to justify the added complexity.

Servo-motors are very easy to use and exchange. They are the perfect match for a starting control engineer. If one has more experience or is willing to acquire it, BLDC motors have high performance and durability advantages to consider, for a much higher cost.

A minimum sensor-set should be included as soon as more sophisticated behaviors (such as reflexes) are wished for. The best sensors to start with are in my opinion: IMU, GRE, joint-position, stereo-vision and tactile skin. If possible, industrial grade, off the shelf components should be chosen.

CPG and reflexes build a fantastic basis on which locomotion can start. I believe having both as the underlying controller and superposing more sophisticated planning etc. on top can make a robot control ready for agile behavior. Where precision is an absolute requirement, other methods, more in the realm of optimal control should be looked at.

Take home messages (subjective)

1. The ASLP leg is capable of stabilizing dynamic locomotion.
2. Antagonistic actuation with passive elasticities limits the range of locomotion patterns and applications of a robot but can make control considerably more lightweight.
3. The ground contacts, the feet, are the most sensitive parts to tune in an open-loop and dynamic robot.

4. An actuated spine is very complex, but adds many capabilities/ performance improvements, if build and controlled correctly.
5. Small and low-cost robots will only be able to move in real life environments if they are high performing (jumping, rough terrain) and mechanically robust to falling.
6. A purely open-loop control is not enough to achieve stable, agile locomotion. Reflexes are needed. Planning can be advantageous.
7. Tuning an open-loop CPG control correctly can reinforce positive aspects of the robot's dynamics, increasing performance and stability. Wrong tuning will result most of the times in failure.

11.2 Outlook

We will shortly describe future exploration directions and already started work with our quadrupedal robots:

Theory

Concerning the agility benchmark, extensions of scores, e.g., with rough terrain, step-ups and -downs, etc. should be undertaken. It is also to see if integration with bi-pedal robot benchmarking is feasible, e.g., the Eurobench project [145].

Mechanics

The main issue, limiting performance in our robots is the lossy transmission of generated forces to the ground. Slipping, stumbling and other kinds of negative effects are hindering the generation of propulsive forces, needed for agility. Hence, the most important mechanical improvement we propose for future explorations is a detailed research on highly integrated and sensorized robot feet. Through the modular mechanical design, Serval is ready to exchange body parts and be used to research, e.g., the influence of leg-geometry and spring placement on COT or stability, as also researched in a larger scale system in [28].

Electronics

All our robots, besides Oncilla, are "under-sensorized." We do not or only partially know internal and external states. Equipping our robots with different sensors, integrating them into the communication network and using the resulting information for more sophisticated control (reflexes and other perception), can increase our robots agility. In this context, a

conclusive study on what information quality and quantity is needed to close the loop reliably should be performed. Parts of this work are already started by integration of sensitive skin and an IMU on Serval to enable physical guidance and perception through touch.

Control

Robots, as physical simulators, should be used to test different control strategies and complex scenarios. We mainly see three future control developments: (1) Closing the loop for reliable physical guidance; (2) Adaptation of locomotion strategies after limp-amputation and (3) Closed loop locomotion for agility with a minimal sensor set. The advantage of small robots is the possibility to interact with them, safely. This should and is being leveraged at the moment to guide Serval on flat terrain. Guiding features are based on a real-time trajectory control depending on physical interactions with humans (IMU; inertial information; guidance rope; sensitive skin), as a natural and intuitive method of interfacing with a robot. We imagine the advantage in the proposed approach in the use of less expensive and lighter sensors than the often implemented laser scanners (LIDAR). In addition, time- and computation-expensive vision-based analysis and planning can be avoided, making it especially attractive in small-scale robotics. The second approach is centered around animals' astonishing capability to adapt to limb-loss within weeks after recuperation. An approach to robot-in-the-loop learning, much like in [146] should be feasible with our robust and easy to modify hardware. The last direction is concerning our robots' capability for agility. Especially Serval's control needs to be extended by reflexes like in *Oncilla*. This measure in combination with a systematic search for optimized gaits (artificial or bio-inspired) will improve performance and realize higher levels of relative agility.

Appendix Part

A Side Projects

Additional and often true for many researchers, not only the core topics were pursued, but a not neglectable amount of time was invested in the development of different and scientifically exciting projects. This chapter is a representation of said side-projects. In case that the project lead to a publication, I will only summarize the aim of the project by including the abstract and an illustration from said article, so the interested reader might address him or herself to the original publication (which I strongly suggest). My contribution to these articles can be found in chapter . The projects that did not lead to a publication will also be summarized in the last sections.

A.1 Friction and Damping of a Compliant Foot based on Granular Jamming for Legged Robots



Figure A.1 – Please find here videos of experiments with Oncilla and a granular jamming foot described in this section: <https://go.epfl.ch/ExperimentsOncillaGranular>

This project is presented in full in Hauser et. al [105].

Moving away from simple foot designs of current quadruped robots towards a more bio-inspired approach, a novel foot design was implemented on the quadruped robot Oncilla. These feet mimic soft paw-pads of dogs and cats with high traction and underlying soft tissue.

Appendix A. Side Projects

Consisting of a granular medium enclosed in a flexible membrane, they can be set to different pressure/vacuum conditions. Tests of general properties such as friction force, damping and deformation were completed by proof of concept tests on the robot. These included flat ground locomotion as well as ascending a slope with different inclination. Comparison tests with the previous feet were performed as well, showing that the new feet have high friction and strong damping properties. Additionally, the speed of flat ground locomotion is comparable to the maximum speed of the robot with the previous feet while retaining the desired trotting gait. These are promising aspects for legged locomotion. The jamming of granular media previously has been used to create a universal gripper which in the future also opens up opportunities to use the feet both in locomotion and simple object manipulation (although the manipulation is not tested here).

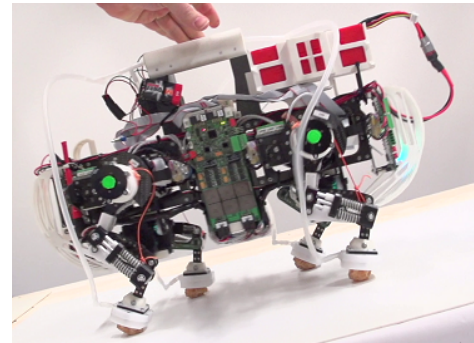
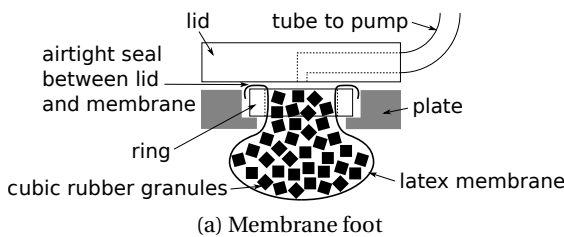


Figure A.2 – A.2a Schematics of the membrane foot. A latex membrane is filled with cubic rubber granules and wrapped around a plastic ring. The plate presses the ring against the lid and forms an airtight seal. A silicone tube connects the membrane to the vacuum pump. A.2b Snapshot of Oncilla running backwards on a slope with 14° inclination; used foot configuration is GMV

A.2 The Swimming Cheetah - a Comparative Study between Robot and Animal

This project is presented in full in Andreoli et al. [8].

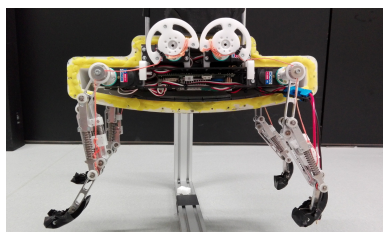
Amphibious robots are designed and developed to function in different environments adapting their morphology and mobility behavior to the specific habitat. To this end, biology and robotics could come together and cooperate with each other providing theories and experimenting technological solutions with the use of bio-inspired robots. This project proposes to enlarge the operational space of innovative terrestrial quadruped robots, adapting them

A.3. MAR - An Energy Efficient Anguilliform Swimming Robot; a Design, Control and Experimental Study

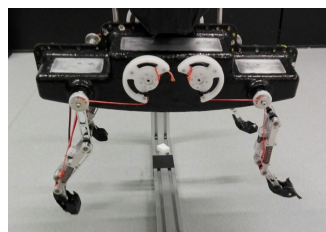


Figure A.3 – Please find here videos of experiments with Cheetah-Cub-W and a granular jamming foot described in this section: <https://go.epfl.ch/ExperimentsCheetahCubW>

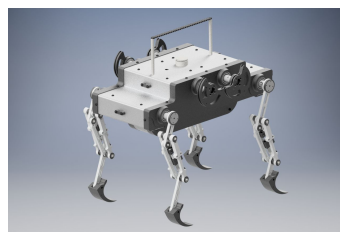
to the aquatic environment. Analysis of swimming animals has shown that the evolution from quadrupedal terrestrial mammals to fully aquatic mammals is based on quadrupedal and bipedal paddling modes. Moreover, different morphological, physical and behavioral changes characterized this transition dramatically from drag-based to lift-based propulsion, particularly concerning locomotion. In this scenario, a small, cat-like, quadruped robot, the Cheetah-Cub-AL, has been used as a testing platform able to mimic but also explore animal gaits. A controller has been built to reproduce both walking and swimming gaits using an intuitive and easily tunable bio-inspired parametrization. Extensive experimental tests together with design solutions inspired by animal adaptation mechanisms allowed to determine an optimal solution concerning foot trajectory and robot configuration. Different locomotion behaviors have been studied considering both quadrupedal and bipedal paddling. Energetic advantages have been found for the latter reflecting swimming mammals evolutionary path. On the other hand, comparing performances in terms of maximum speed and gait stability, diagonal quadrupedal paddling in combination with an enlarged paddle area has resulted in being the optimal choice for the robot.



(a) Cheetah-Cub-W-V1



(b) Cheetah-Cub-W-V1.5



(c) Cheetah-Cub-W-V2

Figure A.4 – Different iterations of Cheetah-Cub-W towards a tether-less and robust swimming and diving design, Version 1, 1.5 and 2



Figure A.5 – Please find here videos of experiments with MAR described in this section: <https://go.epfl.ch/ExperimentsMAR>

A.3 MAR - An Energy Efficient Anguilliform Swimming Robot; a Design, Control and Experimental Study

This project is presented in full in Strübig et. al [9].

Propulsion in surface and underwater robots is primarily dominated by rotating propellers due to high thrust but at the cost of low efficiency. Due to their inherently high speed turning motion, sharp propeller blades and resulting noise, maritime ecosystems are disturbed or endangered. Our work presents a bio-inspired approach to efficient and eco-friendly swimming with moderate to high thrust. This paper describes the concept, development and experimental validation of the novel anguilliform robot *MAR*. With 15 elements making up the 0.5 m long propulsive section and driven by a single, speed-controlled EC-motor, the robot creates a smooth continuous traveling wave for propulsion. Steering and autonomy are realized by a head with integrated batteries (front-rudder) and a tail (hind-rudder). *MAR* accomplished very high thrusts at moderate power consumption in first performance tests. The achieved maximum velocity and the speed related efficiency did not fulfill the expectations in the first tests (in comparison to commercial rotary thrusters), which can be attributed mainly to the spatial limitations and imperfect test setup. Never the less, the potential towards highly efficient and high thrust propulsion is visible and will be exploited in future efforts.

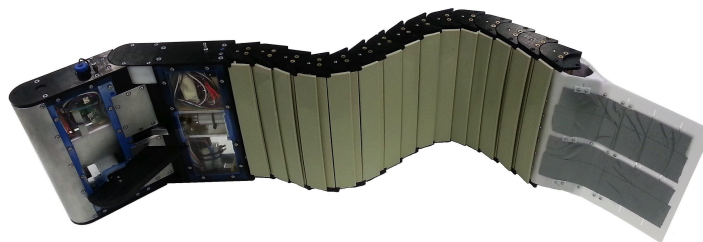


Figure A.6 – An overview of MAR consisting head unit, the motor module, the helix hidden by the elements, and the flexible tail.

A.4 On Designing an Active Tail for Legged Robots: Simplifying Control via Decoupling of Control Objectives

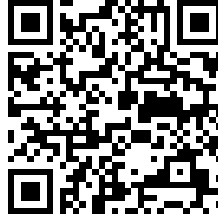
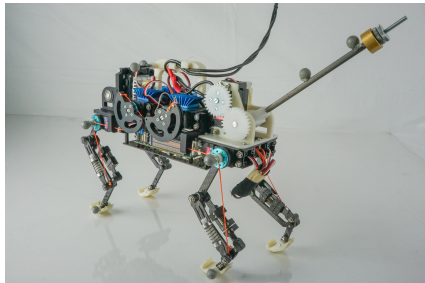


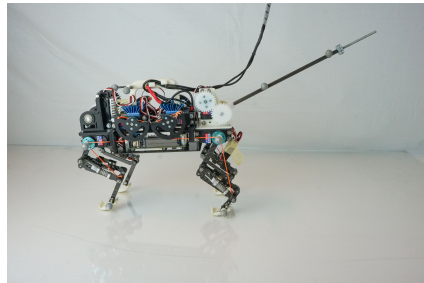
Figure A.7 – Please find here videos of experiments with Cheetah-Cub-T described in this section: <https://go.epfl.ch/ExperimentsCheetahCubT>

This project is presented in full in Heim et. al [7].

This work explores the possible roles of active tails for steady-state legged-locomotion. A series of simple models are proposed which capture the dynamics of an idealized running system with an active tail. The models suggest that the control objectives of injecting energy into the system and stabilizing body-pitch can be effectively decoupled via proper tail design: a long, light tail. Thus the overall control problem can be simplified, using the tail exclusively to stabilize body-pitch: this effectively relaxes the constraints on the leg-actuators, allowing them to be explicitly recruited for adding energy into the system.



(a) Cheetah-Cub-T short-heavy



(b) Cheetah-Cub-T long-light

Figure A.8 – Experiments were conducted using a newly built version of the Cheetah-Cub robot ([3]), with an added 1 degree of freedom tail module. Shown are two different tails, a short-heavy (left) and long-light (right) tail. Both tails have the same moment of inertia around the tail axle. Brightness in the photographs was digitally enhanced.

We show in simulation that models with long-light tails are better able to reject perturbations to body-pitch than short-heavy tails with the same moment of inertia. Further, we present the results of a one-degree-of-freedom tail mounted on the open-loop controlled quadruped robot Cheetah-Cub. Our results show that an active tail can greatly improve both forward

velocity and reduce body-pitch per stride while adding minimal complexity. Further, the results validate the long-light tail design: shorter, heavier tails are much more sensitive to configuration and control parameter changes than longer and lighter tails with the same moment of inertia.

A.5 Force Sensor Setup for Human Machine Interaction using a Stretcher

The developed stretcher contributed to the following publication [10]

The goal of this development was the integration of an Optoforce 3D-force sensor inside each handle of a human-sized stretcher. The construction had to be as rigid as possible and was thus built from industrial standard Strut-profiles. The sheet-metal-bent handle-enclosure is running on POM-sliders and encapsulating the Optoforce sensor. The slider construction is blocking x- and y-direction of the sensor, only allowing z-sensing in tension and compression. As the sensing deflection is limited to 3mm, I implemented mechanical constraints to protect the sensor from over-straining.

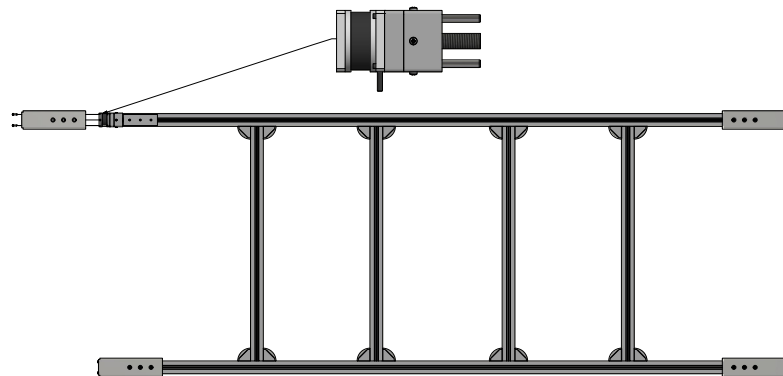


Figure A.9 – Design of a sensorized Stretcher for the Cogimon project

A.6 A Preliminary Head for the COMAN Robot

The developed head did not contribute to any publication but was used in multiple semester projects.

The goal of the development was to integrate a set of sensors and a mini-pc into a compact head, feasible to mount on the Coman robot. The components include:

- 1x NUC DC3217BY

A.6. A Preliminary Head for the COMAN Robot

- 1x Asus Xtion Pro Lite (Kinect like camera)
- 1x XSens 140812MTI10 (IMU)
- 2x FL2-006-R0 (Camera)

The two FL2-006-R0 were placed on manually adjustable mounts to allow the possibility for modification, as they should be used for stereo vision or close environment observation (side-vision) depending on the experimental task. The respective construction was done in CFP due to the low weight requirements and the simplicity of the design.

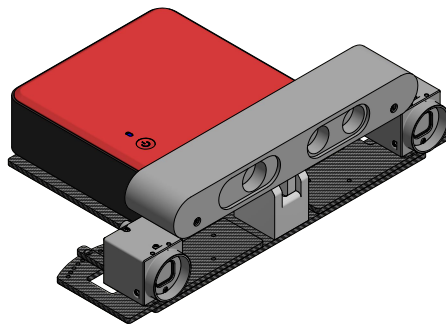



Figure A.10 – Head Design for the bipedal robot Coman

B Thesis-timeplan and misc. documents

ID	Task Name	Start	Finish	Duration	PW invested
1	Lynx	01/10/12	30/01/15	122 wks	30,5 wks
2	First prototype	01/10/12	04/01/13	14 wks	12 wks
3	State of the art and conceptual design	01/10/12	31/10/12	4,6 wks	3,6 wks
4	Mechatronic design	01/11/12	30/11/12	4,4 wks	4,4 wks
5	Partial production and assembly	21/11/12	11/12/12	3 wks	3 wks
6	Experiments and analysis	24/12/12	04/01/13	2 wks	1 wk
7	Second prototype	02/01/13	29/03/13	12,6 wks	11 wks
8	Conceptual iteration of 3 spine versions	02/01/13	10/01/13	1,4 wks	1 wk
9	Mechatronic design	11/01/13	24/01/13	2 wks	2 wks
10	Partial production	31/01/13	20/02/13	3 wks	3 wks
11	Experiments and analysis	21/02/13	29/03/13	5,4 wks	5 wks
12	Publication	01/12/12	30/01/15	113 wks	7,5 wks
13	Masters-Thesis	01/12/12	30/04/13	21,6 wks	4 wks
14	Publication 1 - IROS2014 - Lead author (rejected)	30/04/13	31/05/13	4,8 wks	2 wks
15	Publication 2 - DW2014 - Lead author (accepted)	20/01/13	14/02/13	4 wks	0,5 wks
16	Publication 3 - ICRA2015 - Lead author (accepted)	01/09/14	30/01/15	22 wks	1 wk
17	PhD-Thesis	01/06/13	16/03/18	250 wks	250 wks
18	Overall concept and Candidacy	01/06/13	15/07/14	58,6 wks	12 wks
19	Development Work	01/03/13	03/04/18	265,45 wks	157 wks
20	Agility Benchmark	01/09/13	23/10/17	216,2 wks	32 wks
21	Development of a general Agility benchmark	01/09/13	23/10/17	216,2 wks	24 wks
22	Definition of Agility	01/09/13	07/11/13	10 wks	6 wks
23	Development of the Benchmark	07/11/13	23/10/17	206,6 wks	18 wks
24	Publication	01/09/16	23/10/17	59,6 wks	8 wks
25	Publication 1 - TRO regular paper - revise and resubmit	01/09/16	24/01/17	20,8 wks	4 wks
26	Publication 2 - TRO short paper - pending	02/05/17	23/10/17	25 wks	4 wks
27	Cheetah-Cub-Family	01/07/13	03/04/18	248,25 wks	44 wks
28	Cheetah-Cub	01/01/14	05/02/16	109,6 wks	14 wks
29	Student projects supervision	01/01/15	28/10/15	43 wks	3 wks
30	Student projects	01/01/15	28/10/15	43 wks	3 wks
31	Maintenance	01/01/14	02/11/15	95,8 wks	10 wks
32	Maintenance of original Cheetah-Cub	01/01/14	31/10/14	43,6 wks	2 wks
33	Concept, Production and Maintenance Copy 1	01/11/14	30/04/15	26 wks	4 wks
34	Production and Maintenance Copy 2	01/03/15	02/11/15	35,4 wks	4 wks
35	Publication	01/02/16	05/02/16	1 wk	1 wk
36	Publication - DW2016 - accepted	01/02/16	05/02/16	1 wk	1 wk
37	Cheetah-Cub-S	01/07/13	10/07/15	106 wks	8,5 wks
38	First prototype	01/07/13	31/03/14	39,2 wks	4,5 wks
39	Development of conceptual idea	01/07/13	01/10/13	13,4 wks	1 wk
40	Support for mechatronic design	15/10/13	15/01/14	13,4 wks	0,5 wks
41	Partial production and assembly	06/01/14	19/02/14	6,6 wks	2 wks
42	Support for experiments and analysis	01/03/14	31/03/14	4,4 wks	1 wk
43	Second prototype	01/05/14	06/06/14	5,4 wks	2 wks
44	Conceptual iteration	01/05/14	08/05/14	1,2 wks	0,5 wks
45	Mechatronic design	09/05/14	16/05/14	1,2 wks	0,5 wks
46	Production and assembly	22/05/14	29/05/14	1,2 wks	0,5 wks
47	Feasability tests	02/06/14	06/06/14	1 wk	0,5 wks
48	Publication	01/09/14	10/07/15	45 wks	2 wks
49	Publication 1 - ICRA2015 - rejected	01/09/14	03/10/14	5 wks	1,5 wks
50	Publication - SSRR2015 - accepted	10/06/15	10/07/15	4,6 wks	0,5 wks
51	Cheetah-Cub-AL	01/10/15	30/03/18	130,4 wks	10 wks
52	First prototype	01/10/15	07/12/15	9,6 wks	4 wks
53	Development of conceptual idea	01/10/15	06/10/15	0,8 wks	0,5 wks
54	Mechatronic design	07/10/15	30/10/15	3,6 wks	1,5 wks
55	Production and assembly	25/10/15	18/11/15	3,8 wks	1,5 wks
56	Feasability tests	20/11/15	07/12/15	2,4 wks	0,5 wks
57	Second prototype	12/01/16	01/03/16	7,2 wks	4 wks
58	Development of conceptual idea	12/01/16	15/01/16	0,8 wks	0,5 wks
59	Mechatronic design	15/01/16	04/02/16	3 wks	1 wk
60	Production and assembly	04/02/16	24/02/16	3 wks	1,5 wks
61	Feasability tests	24/02/16	01/03/16	1 wk	1 wk
62	Maintenance	01/03/16	30/03/18	108,85 wks	2 wks
63	Cheetah-Cub-T	01/01/14	01/11/16	147,8 wks	2 wks
64	Publication	01/07/14	01/11/16	122 wks	0,5 wks
65	Publication 1 - Clawar - accepted	01/07/14	03/03/15	35 wks	0,25 wks
66	Publication - Industrial robot - accepted	31/10/14	01/11/16	104,4 wks	0,25 wks
67	Cheetah-Cub-T project support	01/01/14	02/07/14	26 wks	1,5 wks
68	Cheetah-Cub-W	01/10/15	03/04/18	130,65 wks	9,5 wks
69	First prototype	01/10/15	01/02/17	69,85 wks	1,5 wks
70	188 Development of conceptual idea	01/10/15	02/11/15	4,5 wks	0,5 wks
71	Mechatronic design support	01/11/16	25/11/16	3,6 wks	0,5 wks

ID	Task Name	Start	Finish	Duration	PW invested
72	Production and assembly	14/11/16	01/02/17	11,4 wks	0,5 wks
73	Second prototype	01/02/17	01/09/17	30,4 wks	2 wks
74	Iteration of conceptual idea	01/02/17	15/02/17	2 wks	0,5 wks
75	Mechatronic design	15/02/17	01/03/17	2 wks	0,5 wks
76	Production and assembly	01/03/17	31/03/17	4,4 wks	0,5 wks
77	Experiments and analysis support	01/04/17	01/09/17	22 wks	0,5 wks
78	Third prototype	01/09/17	10/11/17	10 wks	4 wks
79	Iteration of conceptual idea	01/09/17	15/09/17	2 wks	0,5 wks
80	Mechatronic design	15/09/17	06/10/17	3 wks	1,5 wks
81	Production and assembly	06/10/17	27/10/17	3 wks	1,5 wks
82	Feasibility tests	27/10/17	10/11/17	2 wks	0,5 wks
83	Publication	31/08/17	03/04/18	30,6 wks	2 wks
84	Publication 1 - Biomimicry - pending	31/08/17	03/04/18	30,6 wks	2 wks
85	Oncilla	01/03/13	22/01/18	255,4 wks	38 wks
86	Oncilla Hardware	01/03/13	22/01/18	255,4 wks	32 wks
87	Student projects supervision	01/06/13	31/12/15	134,8 wks	3 wks
88	Different students with colleagues	01/06/13	31/12/15	135 wks	3 wks
89	Maintenance	01/03/13	22/01/18	255,4 wks	27 wks
90	Co-development of a third design iteration	01/01/14	15/01/15	54,4 wks	4 wks
91	Production of 4 Oncilla copies and spare parts	01/03/13	01/07/13	17,4 wks	10 wks
92	Maintenance of project partner robots	01/01/14	08/05/14	18,4 wks	3 wks
93	Maintenance and Experimentation with Biorob-Versions	01/01/14	22/01/18	211,8 wks	10 wks
94	Publication	01/01/14	22/01/18	211,8 wks	2 wks
95	Publication 1 - IJRR - rejected - ??? Not sure about correct values	01/01/14	06/10/15	92 wks	1 wk
96	Publication 2 - Frontiers - tbd	11/11/15	22/01/18	114,8 wks	1 wk
97	Oncilla-Foot Gripper	01/01/16	07/03/16	9,4 wks	6 wks
98	Development	01/01/16	18/02/16	7 wks	4 wks
99	Hardware development and implementation	01/01/16	11/02/16	6 wks	2 wks
100	Experiments and Analysis	11/01/16	18/02/16	5,8 wks	2 wks
101	Publication	18/02/16	07/03/16	2,6 wks	2 wks
102	Publication 1 - Biorob2916 - accepted	18/02/16	07/03/16	2,6 wks	2 wks
103	Serval	01/10/15	28/02/18	126 wks	37 wks
104	First prototype	01/10/15	03/06/16	35,4 wks	18 wks
105	Development of conceptual idea	01/10/15	15/01/16	15,4 wks	4 wks
106	Mechatronic design	15/12/15	31/03/16	15,6 wks	8 wks
107	Production and assembly	01/02/16	30/05/16	17,2 wks	5 wks
108	Feasibility tests	30/05/16	03/06/16	1 wk	1 wk
109	Second prototype	01/08/16	23/01/18	77,4 wks	15 wks
110	Iteration on the concept	01/08/16	05/08/16	1 wk	2 wks
111	Mechatronic design	01/09/16	23/01/18	72,8 wks	4 wks
112	Production and assembly	01/10/16	22/01/18	68,4 wks	5 wks
113	Experiments and Analysis	01/04/17	22/01/18	42,4 wks	4 wks
114	Publication	01/09/17	28/02/18	25,8 wks	4 wks
115	Publication 1 - SAB2018 - pending	01/09/17	28/02/18	25,8 wks	4 wks
116	MAR	01/02/17	03/04/18	60,8 wks	5 wks
117	Concept and Design support	01/02/17	01/08/17	25,8 wks	3 wks
118	Concept support	01/02/17	02/03/17	4,2 wks	0,5 wks
119	Mechatronic design support	01/03/17	01/06/17	13,2 wks	0,5 wks
120	Production and Assembly	01/05/17	19/07/17	11,4 wks	1,5 wks
121	Experimental and Analysis support	18/07/17	01/08/17	2 wks	0,5 wks
122	Publication	31/07/17	03/04/18	35,2 wks	2 wks
123	Publication 1 - TRO 2018 - Co-Lead-author (pending)	31/07/17	03/04/18	35,2 wks	2 wks
124	Coman-Head	25/05/15	01/09/15	14,2 wks	0,5 wks
125	Mechanical Design and implementation	25/05/15	01/09/15	14,2 wks	0,5 wks
126	Sensor-Stretcher	01/07/15	01/12/15	21,8 wks	0,5 wks
127	Mechanical Design and implementation	01/07/15	01/12/15	21,8 wks	0,5 wks
128	Thesis-writing	22/11/17	16/03/18	16,4 wks	16 wks
129	Misc	28/04/13	15/03/18	254,8 wks	61,5 wks
130	Travel	28/04/13	09/07/17	219 wks	17,8 wks
131	Conference: AMAM 2015	20/06/15	27/06/15	1,4 wks	1,4 wks
132	Conference: AMAM 2017	24/06/17	05/07/17	1,8 wks	1,8 wks
133	Conference: Dynamic Walking 2014	10/06/14	13/06/14	0,8 wks	0,8 wks
134	Conference: Dynamic Walking 2016	03/06/16	08/06/16	0,8 wks	0,8 wks
135	Conference: Dynamic Walking 2017	04/07/17	09/07/17	1 wk	1 wk
136	Conference: ICRA 2015	24/05/15	01/06/15	1,4 wks	1,4 wks
137	Conference: SSR 2015	22/10/15	31/10/15	1,6 wks	1,6 wks
138	Summer School: Shepa 2016	19/06/16	24/06/16	1,2 wks	1,2 wks
139	Update Meeting: AMARSI 2013	28/04/13	02/05/13	1 wk	1 wk
140	Review Meeting: AMARSI 2013	27/06/13	05/07/13	1,4 wks	1,4 wks

ID	Task Name	Start	Finish	Duration	PW invested
141	Review Meeting: AMARSI 2014	13/04/14	18/04/14	1,2 wks	1,2 wks
142	Demonstrations and Talks: London 2013	25/11/13	02/12/13	1,2 wks	1,2 wks
143	Demonstrations and Talks: Bay Area Science Festival 2015	16/10/15	01/11/15	2,4 wks	2,4 wks
144	Demonstrations and Talks: Wien 2015	02/06/15	04/06/15	0,6 wks	0,6 wks
145	Additional Student Projects / Teaching	01/06/13	15/03/18	250 wks	4 wks
146	Administration and Infrastructure	01/06/13	15/03/18	250 wks	4 wks
147	Courses	01/06/13	15/03/18	250 wks	8 wks
148	Vacation + -	01/06/13	15/03/18	250 wks	25 wks
149	Left over	01/06/13	15/03/18	250 wks	2,7 wks

Bio mimicry VS Bio inspiration										modified for printing	
	Available	Time ne	Time ne	Comple	Implem	Value	Value	Value	AHP	Consistency check	
Available Data	1	5	1	1	1	1	1	1	0,176	Consistency OK 3%	
Time needed for concept	1/5	1	2	1/4	1/3	1/7	1/7	1/7	0,040		
Time needed for implementation	1/5	1/2	1	1/5	1/5	1/8	1/8	1/8	0,028		
Complexity of implementation	1	4	5	1	1	1/3	1/3	1/3	0,130		
Implementation with current technology	1	3	5	1	1	1	1	1	0,166		
Value for biology	1	7	8	3	1	1	1	1	0,230		
Value for engineering	1	7	8	3	1	1	1	1	0,230	23,0%	
										credits to: SCB Associates Ltd www.scbuk.com	

Hardware VS Simulation													
	Rapid In	Effective	Total de	Complete	Validati	Freedom	Accessit	Real wo	Validati	Wrong	Translat	Translat	Cost
Rapid implementation of ideas	1	1	1/3	1/3	1/3	1	1/3	1/7	1	1/5	1/3	1/2	3
Effective implementation of ideas	1	1	1/2	1/2	1/2	1	1/2	1/4	2	1/4	1/2	1/2	3
Total development time needed	3	2	1	1	1/3	1	1	1/4	1	1/4	1/4	1/4	2
Complexity of development	3	2	1	1	1/3	1	1/3	1/2	1/3	1/2	1/3	1/3	5
Validation on the system understanding	3	2	3	3	1	1	1/2	1	1	1	1/2	1/2	4
Freedom of exploration / versatility	1	1	1	1	1	1	2	1/3	1	1	1/3	1/3	5
Accessibility of states	3	2	1	3	2	1/2	1	1/5	2	1/3	1/3	1/3	2
Real world validation	7	4	4	2	1	3	5	1	6	1	1	1/4	6
Validation time needed	1	1/2	1	3	1	1	1/2	1/6	1	1/5	1/4	1/4	4
Wrong conclusions from results	5	4	4	2	1	1	3	1	5	1	1	2	5
Translation to hardware	3	2	4	3	2	3	3	1	4	1	1	3	4
Translation to simulation	2	2	4	3	2	3	3	4	4	1/2	1/3	1	4
Cost	1/3	1/3	1/2	1/5	1/4	1/5	1/2	1/6	1/4	1/5	1/4	1/4	1
													AHP
													0,034
													3,4%
													0,043
													4,3%
													0,045
													4,5%
													0,052
													5,2%
													0,082
													8,2%
													0,060
													6,0%
													0,065
													6,5%
													0,143
													14,3%
													0,047
													4,7%
													0,133
													13,3%
													0,143
													14,3%
													0,135
													13,5%
													0,019
													1,9%

modified for printing



credits to:

SCB Associates Ltd

www.scbuk.com

Advantages of Simulations

- **Rapid & Effective implementation of ideas** : Though the implementation can be simple and crude, simulation models allow one to quickly translate ideas into fairly realistic models to observe their response avoiding the need to develop physical models.
- **Validation on the system understanding**: Implementing a simulation model means that a certain level of understanding is obtained regarding the model of interest.
- **Exploration of possibilities** : Simulations provide a platform to extend and explore the various possibilities of a model in scenarios that may be possible/safe to recreate in real world. For example optimization algorithms can be used to reduce the weight of a robot while still keeping its functionality intact
- **Accessibility of states** : To control robots at times the controller depends on states that may not be directly accessible using physical sensors. In such cases simulation models allow computing these states. These are usually hardware-in-the-loop simulation models.

Disadvantages of Simulation

- **Model Validation** : No matter how complex the model is, unless verified and validated against a physical model, results from simulations cannot be assumed to reflect the real world response of the model
- **Complexity in model development** : It is often the case that simulation models are simplified and an idealized case of a physical model. This is so because of the difficulty in mapping and implementing a realistic model. The difficulties may include computational resources, lack of mathematical tools to describe the model, difficulty in modelling physical inaccuracies and external noise. The most challenging part is to find the balance between a simple model which fairly reflects the response of a real system.
- **Wrong conclusions** : Due to the inaccuracies in modelling, the results from a simulation may sometimes lead to wrong conclusions about the system.
- **Translation to hardware** : Often simulation models are developed with the aim to satisfy a task without imposing all the physical constraints. This leads to difficulties in a developing a physical model that at the end can achieve the same performance as a simulation model.

C Leg kinematics

This appendix is a one-to-one copy from [5, 11], and presents the work done by colleagues to implement kinematic control on our robots.

Nomenclature and kinematic variables Leg elements are labeled in Figure C.1, leg segment angles are defined in Figure C.3, and leg length definitions are provided in Figure C.2.

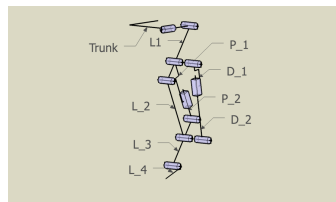


Figure C.1 – Oncilla leg component nomenclature; elements are numbered from proximal to distal. L_i are leg parts of the serial, multi-segment leg. P_i are components of the parallel strut. D_i are components of the diagonal strut. Trunk axes orientations are defined as: X forward, Y upwards, and Z for sideways. We are assuming a right hand base coordinate system.

Reference position and angle orientation This describes the reference positions that are used both in hardware and the Webots simulation (Figure C.5). The reference position is defined by the leg length in its maximum extension, with the L_3 - L_4 axis positioned vertically under the L_0 - L_1 joint. Angle values and ranges are defined in Table C.2.

C.1 Oncilla kinematic

Leg kinematic The kinematic of the leg can be easily computed from figure Figure C.5, if we place the origin at the L_0 - L_1 joint, we have :

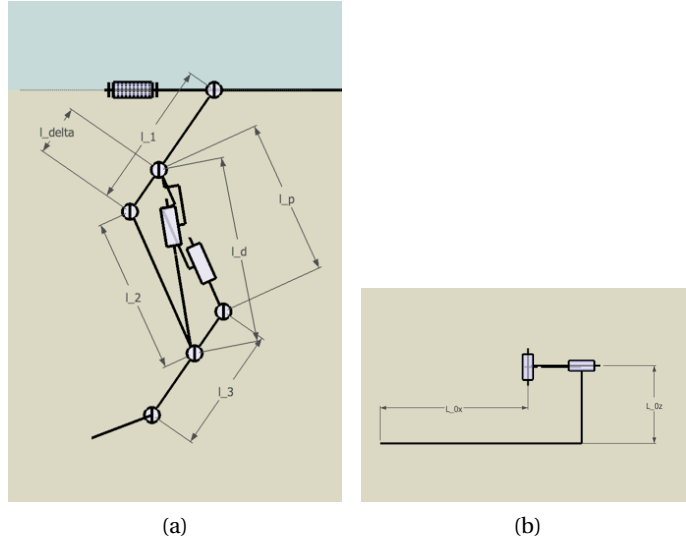


Figure C.2 – Leg length nomenclature. a) Side view, and b) top view.

$$x_{leg} = l_1 \sin(\bar{q}_1) + l_2 \sin(\bar{q}_1 - \bar{q}_2) + (l_3 - l_{\Delta}) \sin(\bar{q}_1 + q_3 - q_2) \quad (C.1)$$

$$y_{leg} = -l_1 \cos(\bar{q}_1) - l_2 \cos(\bar{q}_1 - \bar{q}_2) - (l_3 - l_{\Delta}) \cos(\bar{q}_1 + q_3 - q_2) \quad (C.2)$$

Where $\forall i, \bar{q}_i = q_i + q_i^{ref}$.

For inverse kinematic, since q_3 is not controllable, we simply use for computation $q_2 = q_3$. then we have the relations :

$$x_{leg}^2 + y_{leg}^2 = (l_1 + l_3 - l_{\Delta})^2 + l_2^2 - 2(l_1 + l_3 - l_{\Delta})l_2 \cos(\bar{q}_2) \quad (C.3)$$

$$(C.4)$$

Knee kinematic For both simulation and hardware we would like to know the relation between the angle q_2 , the knee pulley angle θ_M and the diagonal spring length l_d . First we have the relation between the knee pulley angle and the cable length (when in tension), and

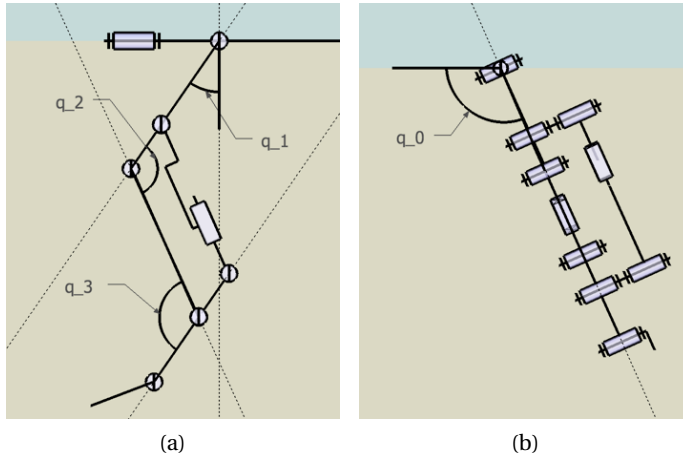


Figure C.3 – Definitions of leg angles in Oncilla robot. a) Side view, and b) front view.

the tangent point angle θ_t :

$$\theta_M = \frac{l_c}{r} + \theta_t \quad (C.5)$$

A “reference angle” was introduced θ_M^{ref} , to control θ in the range of $[0, \theta_M^{max}]$.

Now using law of cosines in triangles (l_Δ, l_2, l_d) and (l_1, l_2) , and Pythagore’s theorem in triangle (r, l_c) , we can have the two relations :

$$l_d^2 = l_2^2 + l_\Delta^2 - 2l_2 l_\Delta \cos(\pi - \bar{q}_2) \quad (C.6)$$

$$r^2 (\bar{\theta}_M^2 + 1) = l_1^2 + l_2^2 - 2l_1 l_2 \cos(\pi - \bar{q}_2) \quad (C.7)$$

The relation between l_d and q_2 follows:

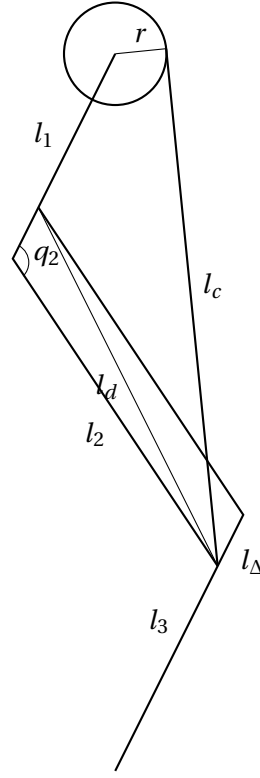


Figure C.4 – Details of Oncilla robot's knee mechanism.

$$l_d = \sqrt{l_2^2 + l_\Delta^2 + 2l_2l_\Delta \cos(q_2 + q_2^{ref})} \quad (C.8)$$

$$q_2 = \arccos\left(\frac{l_d^2 - l_2^2 - l_\Delta^2}{2l_2l_\Delta}\right) - q_2^{ref} \quad (C.9)$$

However we can only easily compute the inverse value for θ_M . Indeed we can separate easily θ_t in two angles with the triangles (l_1, l_2) and (r, l_c) :

$$\tan(\theta_{t,1}) = \frac{l_c}{r} \quad (C.10)$$

$$\tan(\theta_{t,2}) = \frac{l_2 \sin(\bar{q}_2)}{l_1 + l_2 \sin(\bar{q}_2)} \quad (C.11)$$

Table C.1 – Kinematic variable textual definition.

	Desription
q_0	Angle between Trunk and L_0 segment.
q_1	Angle between L_0 and L_1 , also hip angle. Motor and magnetic encoders.
q_2	Angle between L_1 and L_2 , also knee angle. Measured by magnetic encoder.
q_3	Angle between L_2 and L_3 . Measured by magnetic encoder.
q_4	Angle between L_3 and L_4 , also toe angle.
$l_{0,x}$	Forward distance between the geometric center of the trunk and the q_1 axis.
$l_{0,z}$	Sideways distance between the geometric center of the trunk.
l_1	Total length of the L_1 segment, and distances between q_1 and q_2 axes.
l_2	Total length of the L_2 segment.
l_3	Total length of the L_3 segment.
l_Δ	Width pantograph: distance between q_2/q_3 and L_1-P_1/P_2-L_3 junction.
l_d	Length of the diagonal. Variable.
l_p	Length of the parallel segment. Variable.
l_c	length of the cable, from L_0-L_1 to L_2-L_3 junctions.
r	Radius of the knee pulley.

Table C.2 – Reference angles, and angle ranges.

	Fore limb					Hind limb				
	Ref	Hardware		Control		Ref	Hardware		Control	
		min	max	min	max		min	max	min	max
q_0	90.0°	-10°	7°	-7°	7°	90.0°	-10°	7°	-7°	7°
q_1	8.2°	-60°	65°	-50°	50°	11.0°	-70°	68°	-50°	50°
q_2	26.8°	0°	71.5°	0°	???	34.4°	0°	90.9°	0°	N.A.
q_3	26.8°	0°	N.A.	N.A.	N.A.	34.4°	0°	???	N.A.	N.A.

This leads to the following solution:

$$\begin{aligned}
\theta_M = & -\frac{1}{r} \sqrt{l_1^2 + l_2^2 - r^2 + 2l_1 l_2 \cos(\bar{q}_2)} \\
& + \arctan\left(\frac{1}{r} \sqrt{l_1^2 + l_2^2 - r^2 + 2l_1 l_2 \cos(\bar{q}_2)}\right) \\
& + \arctan\left(\frac{l_2 \sin(\bar{q}_2)}{l_1 + l_2 \cos(\bar{q}_2)}\right)
\end{aligned} \tag{C.12}$$

C.2 Inverse Kinematic

In this section we would like to compute the inverse kinematic of the robot. For this purpose since the angle q_3 is not controllable, we simplify equations (Equation C.1) to :

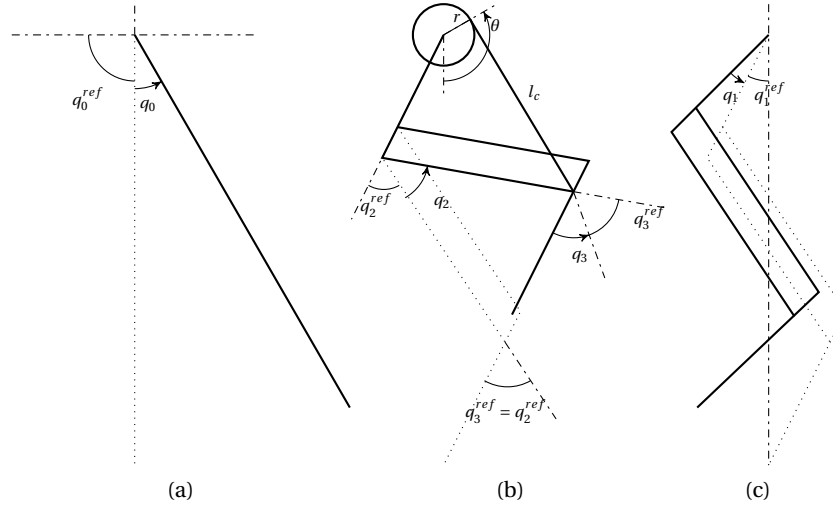


Figure C.5 – Reference position for the oncilla robot. Dotted line represent the reference position of the leg. Angles with arrow are oriented in trigonometric direction. a) q_0 reference angle (front view), b) q_2 and q_3 reference angle (side view), c) q_1 reference angle (side view).

$$x_{leg} = (l_1 + l_3 - l_\Delta) \sin(\bar{q}_1) + l_2 \sin(\bar{q}_1 - \bar{q}_2) \quad (C.13)$$

$$-y_{leg} = (l_1 + l_3 - l_\Delta) \cos(\bar{q}_1) + l_2 \cos(\bar{q}_1 - \bar{q}_2) \quad (C.14)$$

Therefore we can easily relate \bar{q}_2 and the leg length $\sqrt{x_{leg}^2 + y_{leg}^2}$:

$$\bar{q}_2 = \arccos\left(\frac{x_{leg}^2 + y_{leg}^2 - l_2^2 - L^2}{2l_2L}\right) \quad (C.15)$$

Where we set $L = l_1 + l_3 - l_\Delta$ to simplify equations.

To simplify computation of q_1 , we separate it in two angle : q_1^i , the angle “induced” by q_2 and q_1^d the final angle desired for the leg ($\bar{q}_1 = q_1^i + q_1^d$). We find straight forward than :

$$q_1^d = \arctan\left(\frac{-x_{leg}}{y_{leg}}\right) \quad (C.16)$$

$$q_1^i = \arctan\left(\frac{l_2 \sin(\bar{q}_2)}{L + l_2 \cos(\bar{q}_2)}\right) \quad (C.17)$$

After simplification we have the following values :

$$\bar{q}_1 = \arctan\left(\frac{-x_{leg}}{y_{leg}}\right) + \arctan\left(\frac{\sqrt{4l_2^2 L^2 - (x_{leg}^2 + y_{leg}^2 - L^2 - l_2^2)^2}}{L^2 + x_{leg}^2 + y_{leg}^2 - l_2^2}\right) \quad (C.18)$$

D Unfoldables

AA	Abduction/Adduction	DC	Direct current
ABS	Acrylnitril-Butadien-Styrol	DF	Duty factor
AFRP	Aramid fiber reinforced plastic	DLP	Direct Light Processing)
AHP	Analytical Hierarchical Process	DMLS	DirectMetal Laser Sintering
AL	Aluminium	DOF	Degree of freedom
ALSP	Adv. Spring Loaded Panthograph	DS	Diagonal Spring
ASL	Asymmetric stride length	E	Electronics
BI	Bio-inspiration	EC	Electronically commutated
BIROB	Biorobotics laboratory	FB	Fiber breakage
BL	Body length	FDM	(Fused DepositionModeling
BM	Bio-mimicry	FE	Flexion/Extension
C	Control	FEM	Finite element method
CAD	Computer assisted design	FR	Froude number
CC	Cheetah-Cub	FT	Foot trajectory
CCAL	Cheetah-Cub-AL	G	Gear
CCS	Cheetah-Cub-S	GFRP	Glass fiber reinforced plastic
CFRP	Carbon fiber reinforced plastic	GRF	Ground reaction forces
CHF	Swiss franc	HM	High modulus
CNC	Computer numerical control	HT	High Tenacity
COA	Cost of agility	HW	Hardware
COM	Center of mass	IM	Intermediate Modulus
COR	Center of rotation	IMU	Inertial measurement unit
COT	Cost of transport	LER	Leg extension reflex
CPG	Central pattern generator	LHE	Large, high-end
Cus	Custom	LIDAR	Light detection and ranging
		LSR	Lateral stepping reflex
		LiPo	Lithium Polymere

M	Mechanics	RQ	Raibert's Quadruped
MA	Master	S	Safety
MAR	Marine anguilliform robot	SBC	Single board computer
MB	Matrix breakage	SCR	Stumbling correction reflex
MOCAP	Motion capturing	SLA	Stereo-lithography
Mg	Magnesium	SLC	Small, low-cost
N	Necessary	SLIP	Spring loaded inv. pendulum
NiTi	Nitinol	SLM	Selective Laser Melting
O	Optional	SLS	Selective Laser Sintering
P	Price	SMA	Shape memory alloy
PA2200	Polyamide 12	SV	Spine version
PAD	Posture adaptation	Sim	Simulation
PCB	Printed Circuit Board	Ti	Titanium
POM	Polyoxymethylen	UD	Unidirectional
PR	Protraction/Retraction	UM	Ultra modulus
PS	Parallel Spring	UT	Ultra Tenacity
PW	Person weeks	UV	Ultra violet
PWM	Pulse width modulation	VDI	Verein Deutscher Ingenieure
ROM	Range of motion	W	Wished
RPV	Roll pitch variation		

A_{xy}	Agility score	I_{xy}	Moment of inertia
a_{xy}	Amplification	p	Number of full rotations
ϑ	Angle	Π	Pi
Φ	Angle	ν	Poisson's ratio
A	Area	P_{xy}	Power
U	Circumfrence	r_{xy}	Radius
s_{xy}	Deflection	R_{xy}	Radius
d_{xy}	Diameter	G	Shearmodulus
f_{xy}	Frequency	k_{xy}	Spring constant
g	Gravity	t_{xy}	Time
c	Half shoulder to shoulder distance	M_t	Torsionmoment
h_{xy}	Height	q_{xy}	Variance score
i_{xy}	Inclination	v_{xy}	Velocity
l_{xy}	Length	w_{xy}	Width
m_{xy}	Mass	E	Young's modulus

QR-codes for 3D-PDF and experimental documentation for the core topics can be found in the following figure.



Figure 1 – QR-codes and links

Table 1 – Characteristic values of quadruped in BIOROB; Robots built prior to this thesis: Cheetah-Cub (CC), Bobcat; built prior and in the first months of this thesis by the author: Lynx; Robots built in collaboration with major contribution from the author: Oncilla, Cheetah-Cub-S (CCS); Robot built solely by the author: Serval, Cheetah-Cub-AL (CCAL); Geometric measures extracted from CAD, additional information extracted form publications and data-sheets; DS-Diagonal Spring, PS-Parallel spring,FS-Foot spring, PR-Protraction/Retraction, FE-Flexion/Extension, AA-Adduction/Abduction, SBC-Single Board Computer; Iterations-Iterations until the final design, BT-Blue-tooth, G-Gear, Ko-Kondo, Dx-Dynamixel, Ma-Maxon, AJE-Absolute joint encoder; geometric measures rounded to the [mm], hanging in air

	Unit	CC	CCAL	CCS	Lynx	Bobcat	Oncilla	Serval		
Height: Max	[mm]	233	264	217	288	(?)	357	390		
Height: Ground-Hip	[mm]	166	164	166	160	125	201	228		
Width: Max	[mm]	124	128	132	129	(?)	245	247		
Width: Leg-leg	[mm]	89	91	96	101	97-127	138	211		
Length: Max	[mm]	246	248	271	438	(?)	468	563		
Length: Hip-Hip	[mm]	207	206	206	226	166	223	378		
Mass: Total	[g]	1100	1200	1160	1200	1030	5050	3560		
Mass: Electronics	[g]	560	560	608	608	608	2845	2167		
Mass: Mechanics	[g]	540	640	552	592	422	2205	1393		
Stiffness: DS	[N/mm]	2.33	3.6	2.33	2.33	2.33	5.8	7.76		
Stiffness: PS	[N/mm]	4.8/ 2.33				(?)	7.4	9.06		
Stiffness: FS	[N/mm]	1.98				(?)	Sensor	1.98 (x2)		
Stiffness: AA	[Nm/rad]	253.2								
Stiffness: Spine	[N/mm]	(?)						8.4/ 52		
DOF: Actuated		8	8	9	9	9	12	15		
ROM: PR fore	[°]	+122/-40				(?)	±34	+76/-50		
ROM: PR hind	[°]	+70/-90				(?)	±34	+84/-64		
ROM: FE	[mm]	69				(?)	70	93		
ROM: AA	[°]							±8	+90/-70	
ROM: Spine	[°]	±10				±30/-15	±35	±90/±30		
Motor: Servo		Ko KRS2350 ICS						Dx MX28R/64R		
Voltage: Servo	[V]	9-12						10-14.8		
Stall torque: Servo	[Nm]	2 (6V)						2.5/ 6 (12V)		
No load speed: Servo	[°/s]	375 (6V)						330/ 378 (12V)		
Gear ratio: Servo		200:1						193:1/ 200:1		
Motor: EC								Ma 323218		
Voltage: EC	[V]							24		
Stall torque: EC	[Nm]							0,639 (45,5A)		
Gear box: G								Ma 370687		
Gear ratio: G+Cus								84:1/ 56:1		
Stall torque: EC+G	[Nm]							7.1/ 4.7 (6A)		
No load speed: EC+G	[°/s]							1164/ 499		
SBC		RoBoard RB-110						Odroid XU4		
Connectivity		WiFi						BT, Wifi		
Sensors		None						AJE, 3D-GRF, IMU		IMU, (GRF, Skin)
Untethered		No						Yes		
LiPo-Battery		No						3S-4.5Ah-45C		3S-3.3Ah-25C
Iterations		>2	2	1.5	2	1	>3	1.5		

Bibliography

- [1] Peter Eckert and Auke J. Ijspeert. Benchmarking Agility For Multi-legged Terrestrial Robots. *IEEE Transactions on Robotics - in progress*, 2018.
- [2] Peter Eckert, Alexander Sprowitz, Hartmut Witte, and Auke Jan Ijspeert. Comparing the effect of different spine and leg designs for a small bounding quadruped robot. In *Proceedings - IEEE International Conference on Robotics and Automation*, volume 2015-June, pages 3128–3133, 2015. ISBN 978-1-4799-6923-4. doi: 10.1109/ICRA.2015.7139629.
- [3] Alexander Spröwitz, Alexandre Tuleu, Massimo Vespignani, Mostafa Ajallooeian, Emilie Badri, and Auke Jan Ijspeert. Towards dynamic trot gait locomotion: Design, control, and experiments with Cheetah-cub, a compliant quadruped robot. *International Journal of Robotics Research*, 32(8):932–950, jul 2013. ISSN 02783649. doi: 10.1177/0278364913489205. URL <http://journals.sagepub.com/doi/10.1177/0278364913489205>.
- [4] Karl Weinmeister, Peter Eckert, Hartmut Witte, and A.-J. Ijspeert. Cheetah-cub-S: Steering of a quadruped robot using trunk motion. In *2015 IEEE International Symposium on Safety, Security, and Rescue Robotics (SSRR)*, pages 1–6, 2015. ISBN 978-1-5090-1959-5. doi: 10.1109/SSRR.2015.7443021. URL <http://ieeexplore.ieee.org/lpdocs/epic03/wrapper.htm?arnumber=7443021>.
- [5] Alexander Sprowitz, Alexandre Tuleu, Mostafa Ajaoolleian, Massimo Vespignani, Rico Mockel, Peter Eckert, Michiel D’Haene, Jonas Degrave, Arne Nordmann, Benjamin Schrauwen, Jochen Steil, and Auke Jan Ijspeert. Oncilla robot: a compliant, versatile, open-source, quadruped robot with pantograph legs. *in Progress*, 2018.
- [6] Peter Eckert, Anja E.M. Schmerbauch, Tomislav Horvat, Katja Söhnle, Hartmut Witte, and Auke J. Ijspeert. Towards rich motion skills with the lightweight quadruped robot Serval - a design, control and experimental study. In *SAB2018 - The 15th International Conference on the Simulation of Adaptive Behavior - in progress*. SAGE Publications, 2018.
- [7] Steve W. Heim, Mostafa Ajallooeian, Peter Eckert, Massimo Vespignani, and Auke Jan

- Ijspeert. On designing an active tail for legged robots: simplifying control via decoupling of control objectives. *Industrial Robot: An International Journal*, 43(3):338–346, 2016. ISSN 0143-991X. doi: 10.1108/IR-10-2015-0190. URL <http://www.emeraldinsight.com/doi/10.1108/IR-10-2015-0190>.
- [8] Andrea Andreoli, Peter Eckert, Behzad Bayat, and Auke J. Ijspeert. The Swimming Quadruped: an exploratory study of aquatic locomotion. *Bioinspiration and Biomimetics - in progress*, 2018.
- [9] Konstantin Strübig, Behzad Bayat, Peter Eckert, and Auke J. Ijspeert. Design and Development of the Efficient Anguilliform Swimming Robot - MAR. *IEEE Transactions on Robotics - in progress*, 2018.
- [10] Jessica Lanini, Alexis Duburcq, Hamed Razavi, Camille G. Le Goff, and Auke Jan Ijspeert. Interactive locomotion: Investigation and modeling of physically-paired humans while walking. *PLOS ONE*, 12(9):e0179989, sep 2017. ISSN 1932-6203. doi: 10.1371/journal.pone.0179989. URL <http://dx.plos.org/10.1371/journal.pone.0179989>.
- [11] Alexandre Tuleu. *Hardware, software and control design considerations towards low-cost compliant quadruped robots*. PhD thesis, EPFL, 2016. URL <https://infoscience.epfl.ch/record/228969>.
- [12] Mostafa Ajallooeian. *Pattern Generation for Rough Terrain Locomotion with Quadrupedal Robots*. PhD thesis, EPFL, 2015.
- [13] VDI. Richtlinie, V. D. I. 2206: Entwicklungsmethodik für mechatronische Systeme., 2004.
- [14] R J Full, D E Koditschek, and R J Full. Templates and anchors: neuromechanical hypotheses of legged locomotion on land. *The Journal of Experimental Biology*, 2(12):3–125, 1999. ISSN 0022-0949.
- [15] Enrique Mu and Milagros Pereyra-Rojas. Practical Decision Making. (2012), 2017. doi: 10.1007/978-3-319-33861-3. URL <http://link.springer.com/10.1007/978-3-319-33861-3>.
- [16] Andrew Kusiak and David W He. Design for agility: a scheduling perspective. *Robotics and Computer-Integrated Manufacturing*, 14(5–6):415–427, 1998. ISSN 0736-5845. doi: [http://dx.doi.org/10.1016/S0736-5845\(98\)00017-9](http://dx.doi.org/10.1016/S0736-5845(98)00017-9). URL <http://www.sciencedirect.com/science/article/pii/S0736584598000179>.
- [17] Wikipedia. Agility. URL en.wikipedia.org/wiki/Agility.
- [18] R A Wigal and V L Coggins. Mountain Goat, 1982. URL <https://www.quora.com/Which-animals-with-similar-size-weight-are-stronger-climbers-than-humans>.

- [19] Elephant. URL http://www.allposters.es/-sp/African-Elephant-Charging-Etosh-National-Park-Namibia-Posters_i2636378_.htm.
- [20] Tom Brakefield. Jaguar. URL http://content.time.com/time/specials/packages/article/0,28804,2016773_2013947,00.html.
- [21] Homework Help. Speed of Animals, 2013. URL www.speedofanimals.com.
- [22] Agility Club Armbouts Cappel - Histoire de l'agility, . URL http://a.c.a.c.pagesperso-orange.fr/histoire_agility.html.
- [23] Agility-jump, . URL <https://twinkerbird.wordpress.com/tag/kooiker/>.
- [24] Horses - Prime Equine, . URL <http://primeequine.co.uk/ads/horses/>.
- [25] J. Sheppard and W. Young. Agility literature review: Classifications, training and testing. *Journal of Sports Sciences*, 24(9):919–932, 2006. ISSN 02640414. doi: 10.1080/02640410500457109. URL <http://www.tandfonline.com/doi/abs/10.1080/02640410500457109>.
- [26] Diego Torricelli, Rahman S.M. Mizanoor, Jose Gonzalez, Vittorio Lippi, Georg Hettich, Lorenz Asslaender, Maarten Weckx, Bram Vanderborght, Strahinja Dosen, Massimo Sartori, Jie Zhao, Steffen Schüetz, Qi Liu, Thomas Mergner, Dirk Lefeber, Dario Farina, Karsten Berns, and Jose Louis Pons. Benchmarking human-like posture and locomotion of humanoid robots: A preliminary scheme. In *Lecture Notes in Computer Science (including subseries Lecture Notes in Artificial Intelligence and Lecture Notes in Bioinformatics)*, volume 8608 LNAI, pages 320–331. Springer, Cham, 2014. ISBN 9783319094342. doi: 10.1007/978-3-319-09435-9_28. URL http://link.springer.com/10.1007/978-3-319-09435-9_28.
- [27] David A Handelman, Gordon H Franken, and Haldun Komsuoglu. Agile and dexterous robot for inspection and EOD operations, 2010. ISSN 0277786X. URL <http://dx.doi.org/10.1117/12.851251>.
- [28] Andy Abate, Ross L. Hatton, and Jonathan Hurst. Passive-dynamic leg design for agile robots. *2015 IEEE International Conference on Robotics and Automation (ICRA)*, pages 4519–4524, 2015. ISSN 1050-4729. doi: 10.1109/ICRA.2015.7139825. URL <http://ieeexplore.ieee.org/document/7139825/>.
- [29] J. Schmitt and S. Bonnono. Dynamics and stability of lateral plane locomotion on inclines. *Journal of Theoretical Biology*, 261(4):598–609, 2009. ISSN 00225193. doi: 10.1016/j.jtbi.2009.08.019. URL <http://www.sciencedirect.com/science/article/pii/S0022519309003907>.

- [30] Thanhtram Ho, Sunghac Choi, and Sangyoon Lee. Development of a Biomimetic Quadruped Robot. *Journal of Bionic Engineering*, 4(4):193–199, 2007. ISSN 16726529. doi: 10.1016/S1672-6529(07)60032-8. URL <http://www.sciencedirect.com/science/article/pii/S1672652907600328>.
- [31] Uluc Saranli, Martin Buehler, and Daniel E. Koditschek. RHex: A simple and highly mobile hexapod robot. *International Journal of Robotics Research*, 20(7):616–631, 2001. ISSN 02783649. doi: 10.1177/02783640122067570.
- [32] Andrew T. Baisch and Robert J. Wood. Design and fabrication of the Harvard ambulatory micro-robot. *Springer Tracts in Advanced Robotics*, 70(STAR):715–730, 2011. ISSN 16107438. doi: 10.1007/978-3-642-19457-3_42.
- [33] Alessandro Crespi, Daisy Lachat, Ariane Pasquier, and Auke Jan Ijspeert. Controlling swimming and crawling in a fish robot using a central pattern generator. *Autonomous Robots*, 25(1-2):3–13, 2008. ISSN 09295593. doi: 10.1007/s10514-007-9071-6. URL <http://dx.doi.org/10.1007/s10514-007-9071-6>.
- [34] Yunhua Li, Yang Wang, J. Geoffrey Chase, Jouni Mattila, Hyun Myung, and Oliver Sawodny. Survey and introduction to the focused section on mechatronics for sustainable and resilient civil infrastructure. *IEEE/ASME Transactions on Mechatronics*, 18(6):1637–1646, 2013. ISSN 10834435. doi: 10.1109/TMECH.2013.2283537.
- [35] John D. Madden. Mobile robots: Motor challenges and materials solutions. *Science*, 318(5853):1094–1097, 2007. ISSN 00368075. doi: 10.1126/science.1146351. URL <http://www.sciencemag.org/content/318/5853/1094.abstract>.
- [36] Christian Gehring, Stelian Coros, Marco Hutter, Michael Bloesch, Peter Fankhauser, Markus A. Hoepflinger, and Roland Siegwart. Towards automatic discovery of agile gaits for quadrupedal robots. In *Proceedings - IEEE International Conference on Robotics and Automation*, pages 4243–4248. IEEE, may 2014. ISBN 9781479936847. doi: 10.1109/ICRA.2014.6907476. URL <http://ieeexplore.ieee.org/lpdocs/epic03/wrapper.htm?arnumber=6907476>.
- [37] Paul W. Webb. Maneuverability - General issues. *IEEE Journal of Oceanic Engineering*, 29(3):547–555, jul 2004. ISSN 03649059. doi: 10.1109/JOE.2004.833220. URL <http://ieeexplore.ieee.org/lpdocs/epic03/wrapper.htm?arnumber=1353409>.
- [38] M. Hildebrand. Analysis of Asymmetrical Gaits. *Journal of Mammalogy*, 58(2):131–156, 1977. ISSN 1545-1542. doi: 10.2307/1379571. URL <https://academic.oup.com/jmammal/article-lookup/doi/10.2307/1379571>.
- [39] R. Mcn Alexander. The Gaits of Bipedal and Quadrupedal Animals. *The International Journal of Robotics Research*, 3(2):49–59, jun 1984. ISSN 17413176.

- doi: 10.1177/027836498400300205. URL <http://ijr.sagepub.com/cgi/doi/10.1177/027836498400300205>.
- [40] J. E.A. Bertram and A. Gutmann. Motions of the running horse and cheetah revisited: fundamental mechanics of the transverse and rotary gallop. *Journal of The Royal Society Interface*, 6(35):549–559, 2009. ISSN 1742-5689. doi: 10.1098/rsif.2008.0328. URL <http://rsif.royalsocietypublishing.org/cgi/doi/10.1098/rsif.2008.0328>.
- [41] Milton Hildebrand. The Quadrupedal Gaits of Vertebrates. *BioScience*, 39(11):766–775, 1989. ISSN 00063568. doi: 10.2307/1311182. URL <https://academic.oup.com/bioscience/article-lookup/doi/10.2307/1311182>.
- [42] J. J. Robilliard, T. Pfau, and A. M. Wilson. Gait characterisation and classification in horses. *Journal of Experimental Biology*, 210(2):187–197, 2007. ISSN 0022-0949. doi: 10.1242/jeb.02611. URL <http://jeb.biologists.org/cgi/doi/10.1242/jeb.02611>.
- [43] Michael B Bennett and St Lucia. *Tetrapod Walking and Running*. John Wiley and Sons, Ltd, 2001. ISBN 9780470015902.
- [44] H. Witte, R. Hackert, Winfried Ilg, J. Biltzinger, N. Schillinger, F. Biedermann, M. Jergas, H. Preuschoft, M. S. Fischer, N Schilling, F. Biedermann, M. Jergas, H. Preuschoft, and M. S. Fischer. Quadrupedal Mammals as Paragons for Walking Machines. In *Proceedings of Adaptive Motion in Animals and Machines*, page 6 pp., 2000.
- [45] a. a. Biewener. Allometry of quadrupedal locomotion: the scaling of duty factor, bone curvature and limb orientation to body size. *The Journal of experimental biology*, 105(1): 147–171, 1983. ISSN 0022-0949. URL <http://www.biomedsearch.com/nih/Allometry-quadrupedal-locomotion-scaling-duty/6619724.html>.
- [46] A. D. Kuo. Choosing your steps carefully. *IEEE Robotics and Automation Magazine*, 14 (2):18–29, 2007. ISSN 10709932. doi: 10.1109/MRA.2007.380653.
- [47] A. Jacoff, E. Messina, B.A. Weiss, S. Tadokoro, and Y. Nakagawa. Test arenas and performance metrics for urban search and rescue robots. In *Proceedings 2003 IEEE/RSJ International Conference on Intelligent Robots and Systems (IROS 2003) (Cat. No.03CH37453)*, volume 3, pages 3396–3403, 2004. ISBN 0-7803-7860-1. doi: 10.1109/IROS.2003.1249681. URL <http://ieeexplore.ieee.org/document/1249681/>.
- [48] Adam Jacoff, Brian Weiss, and Elena Messina. Evolution of a performance metric for urban search and rescue robots (2003). Technical report, DTIC Document, 2003. URL <http://oai.dtic.mil/oai/oai?verb=getRecord&metadataPrefix=html&identifier=ADA510436>.

- [49] Adam Jacoff, Elena Messina, and John Evans. Performance evaluation of autonomous mobile robots. *Industrial Robot: An International Journal*, 29(3):259–267, 2002. ISSN 0143-991X. doi: 10.1108/01439910210425568. URL <http://www.emeraldinsight.com/doi/10.1108/01439910210425568>.
- [50] a Jacoff, E Messina, J Evans, and Others. Experiences in deploying test arenas for autonomous mobile robots. *NIST special publication*, 1:87–94, 2002.
- [51] Alan Bowling. Mobility and dynamic performance of legged robots. In *Proceedings - IEEE International Conference on Robotics and Automation*, volume 2005, pages 4100–4107, 2005. ISBN 078038914X. doi: 10.1109/ROBOT.2005.1570749.
- [52] Alan Bowling and Shih-Chien Teng. Performance measures of agility for mobile robots. In *Proceedings of the 9th Workshop on Performance Metrics for Intelligent Systems - PerMIS '09*, PerMIS '09, page 188, New York, NY, USA, 2009. ACM. ISBN 9781605587479. doi: 10.1145/1865909.1865949. URL <http://portal.acm.org/citation.cfm?doid=1865909.1865949>.
- [53] Chenghui Nie, Xavier Pacheco Corcho, and Matthew Spenko. Robots on the move: Versatility and complexity in mobile robot locomotion. *IEEE Robotics and Automation Magazine*, 20(4):72–82, dec 2013. ISSN 10709932. doi: 10.1109/MRA.2013.2248310. URL <http://ieeexplore.ieee.org/document/6582554/>.
- [54] Jason L. Pusey, Jeffrey M. Duperret, G. Clark Haynes, Ryan Knopf, and Daniel E. Koditschek. Free-standing leaping experiments with a power-autonomous elastic-spined quadruped. *SPIE Defense, Security, and Sensing*, 8741:87410W, 2013. ISSN 0277786X. doi: 10.1117/12.2016073. URL <http://proceedings.spiedigitallibrary.org/proceeding.aspx?doi=10.1117/12.2016073>.
- [55] J. M. Duperret, G. D. Kenneally, J. L. Pusey, and D. E. Koditschek. Towards a comparative measure of legged agility. In *Springer Tracts in Advanced Robotics*, volume 109, pages 3–16. Springer International Publishing, 2016. ISBN 978-3-540-19851-2. doi: 10.1007/978-3-319-23778-7_1. URL http://link.springer.com/10.1007/978-3-319-23778-7_1.
- [56] Duncan W. Haldane, M. M. Plecnik, J. K. Yim, and R. S. Fearing. Robotic vertical jumping agility via series-elastic power modulation. *Science Robotics*, 1(1):eaag2048, dec 2016. ISSN 2470-9476. doi: 10.1126/scirobotics.aag2048. URL <http://robotics.sciencemag.org/lookup/doi/10.1126/scirobotics.aag2048>.
- [57] At L. Hof. Scaling gait data to body size. *Gait and Posture*, 4(3):222–223, may 1996. ISSN 09666362. doi: 10.1016/0966-6362(95)01057-2. URL <http://linkinghub.elsevier.com/retrieve/pii/0966636295010572>.

-
- [58] D. V. Lee. Effects of mass distribution on the mechanics of level trotting in dogs. *Journal of Experimental Biology*, 207(10):1715–1728, apr 2004. ISSN 0022-0949. doi: 10.1242/jeb.00947. URL <http://jeb.biologists.org/cgi/doi/10.1242/jeb.00947>.
- [59] Agility Shows, Flyball Competitions, Bloodhound Trials, and Field Trials. General Regulations for Agility. Technical report.
- [60] The Kennel Club. Judges ' Guide to Agility Equipment, 2014.
- [61] Dogdance, . URL <http://www.dogdance.info/en>.
- [62] Sidestep Youtube, . URL www.youtube.com/watch?v=qHIRM9bcU8k.
- [63] Dog-breeds, . URL www.dogs.petbreeds.com/stories/5470/fastest-dog-breeds#Intro.
- [64] Backward speed Youtube, . URL www.youtube.com/watch?v=8l4Gj0MO6Gk.
- [65] N C Heglund and C R Taylor. Speed, stride frequency and energy cost per stride: how do they change with body size and gait? *The Journal of experimental biology*, 138(1): 301–318, 1988. ISSN 0022-0949.
- [66] K. Karakasiliotis, R. Thandiackal, K. Melo, T. Horvat, N. K. Mahabadi, S. Tsitkov, J. M. Cabelguen, and A. J. Ijspeert. From cineradiography to biorobots: an approach for designing robots to emulate and study animal locomotion. *Journal of The Royal Society Interface*, 13(119):20151089, jun 2016. ISSN 1742-5689. doi: 10.1098/rsif.2015.1089. URL <http://rsif.royalsocietypublishing.org/lookup/doi/10.1098/rsif.2015.1089>.
- [67] Auke J. Ijspeert. Biorobotics: Using robots to emulate and investigate agile locomotion. *Science*, 346(6206):196–203, 2014. ISSN 10959203. doi: 10.1126/science.1254486. URL <http://www.ncbi.nlm.nih.gov/pubmed/25301621>.
- [68] Ajij Sayyad, B. Seth, and P. Seshu. Single-legged hopping robotics research - A review. *Robotica*, 25(5):587–613, sep 2007. ISSN 02635747. doi: 10.1017/S0263574707003487. URL http://www.journals.cambridge.org/abstract_S0263574707003487.
- [69] Joe Wright and Ivan Jordanov. Intelligent Approaches in Locomotion - A Review. *Journal of Intelligent and Robotic Systems: Theory and Applications*, 80(2):255–277, nov 2015. ISSN 15730409. doi: 10.1007/s10846-014-0149-z. URL <http://link.springer.com/10.1007/s10846-014-0149-z>.
- [70] Hartmut Witte, Rémi Hackert, Karin E. Lilje, Nadja Schilling, Danja Voges, Gertrud Klauer, Winfried Ilg, Jan Albiez, André Seyfarth, Daniel Germann, Manfred Hiller, Rüdiger Dillmann, and Martin S. Fischer. Transfer of biological principles into the construction of quadruped walking machines. *Proceedings of the 2nd International*

- Workshop on Robot Motion and Control, RoMoCo 2001*, pages 245–249, 2001. doi: 10.1109/ROMOCO.2001.973462.
- [71] Marc Raibert. BigDog, the rough-terrain quadruped robot. In *IFAC Proceedings Volumes (IFAC-PapersOnline)*, volume 17, pages 10823–10825, 2008. ISBN 9783902661005. doi: 10.3182/20080706-5-KR-1001.4278.
- [72] C. Semini, N. G. Tsagarakis, E. Guglielmino, M. Focchi, F. Cannella, and D. G. Caldwell. Design of HyQ -A hydraulically and electrically actuated quadruped robot. *Proceedings of the Institution of Mechanical Engineers. Part I: Journal of Systems and Control Engineering*, 225(6):831–849, 2011. ISSN 20413041. doi: 10.1177/0959651811402275.
- [73] Claudio Semini, Jake Goldsmith, Bilal Ur Rehman, Marco Frigerio, Victor Barasuol, Michele Focchi, and Darwin G Caldwell. Design Overview of the Hydraulic Quadruped Robots HyQ2Max and HyQ2Centaur. In *The Fourteenth Scandinavian International Conference on Fluid Power*, number May, 2015. URL https://old.iit.it/images/stories/advanced-robotics/hyq_files/publications/semini15sicfp.pdf.
- [74] Boston Dynamics - Spot, 2016. URL <http://www.gizmag.com/boston-dynamics-spot/36005/>.
- [75] Marc H. Raibert. Trotting, pacing and bounding by a quadruped robot. *Journal of Biomechanics*, 23(SUPPL. 1):79–98, 1990. ISSN 00219290. doi: 10.1016/0021-9290(90)90043-3. URL [http://dx.doi.org/10.1016/0021-9290\(90\)90043-3](http://dx.doi.org/10.1016/0021-9290(90)90043-3).
- [76] Sangok Seok, Albert Wang, Meng Yee Chuah, David Otten, Jeffrey Lang, and Sangbae Kim. Design principles for highly efficient quadrupeds and implementation on the MIT Cheetah robot. In *Proceedings - IEEE International Conference on Robotics and Automation*, pages 3307–3312. IEEE, may 2013. ISBN 9781467356411. doi: 10.1109/ICRA.2013.6631038. URL <http://ieeexplore.ieee.org/document/6631038/>.
- [77] Hae Won Park, Sangin Park, and Sangbae Kim. Variable-speed quadrupedal bounding using impulse planning: Untethered high-speed 3D Running of MIT Cheetah 2. *Proceedings - IEEE International Conference on Robotics and Automation*, 2015-June (June):5163–5170, may 2015. ISSN 10504729. doi: 10.1109/ICRA.2015.7139918. URL <http://ieeexplore.ieee.org/document/7139918/>.
- [78] Marco Hutter. ANYmal - A Highly Mobile and Dynamic Quadrupedal Robot. In *Arbeitsberichte Verkehrs- und Raumplanung, IVT, ETH Zurich*, volume 544, pages 1 – 25, 2009. ISBN 8610828378018. doi: 10.3929/ethz-a-010782581.
- [79] Boston Dynamics | Boston Dynamics. URL <https://www.bostondynamics.com/bigdog%0Ahttps://www.bostondynamics.com/robots>.

-
- [80] Marco Hutter, Christian Gehring, Mark A. Höpflinger, Michael Blösch, and Roland Siegwart. Toward combining speed, efficiency, versatility, and robustness in an autonomous quadruped. *IEEE Transactions on Robotics*, 30(6):1427–1440, 2014. ISSN 15523098. doi: 10.1109/TRO.2014.2360493.
- [81] Ioannis Poulakakis, James Andrew Smith, and Martin Buehler. Modeling and experiments of untethered quadrupedal running with a bounding gait: The scout II robot. *International Journal of Robotics Research*, 24(4):239–256, apr 2005. ISSN 02783649. doi: 10.1177/0278364904050917.
- [82] Hiroshi Kimura, Yasuhiro Fukuoka, and Avis H. Cohen. Adaptive dynamic walking of a quadruped robot on natural ground based on biological concepts. *International Journal of Robotics Research*, 26(5):475–490, 2007. ISSN 02783649. doi: 10.1177/0278364907078089.
- [83] Y Fukuoka and H Kimura. Dynamic locomotion of a biomorphic quadruped Tekken robot using various gaits: walk, trot, free-gait and bound. *Applied Bionics and Biomechanics*, 6(1):63–71, 2009.
- [84] Fumiya Iida and Rolf Pfeifer. Cheap rapid locomotion of a quadruped robot: Self-stabilization of bounding gait. In *Proceedings of the 8th International Conference on Intelligent Autonomous Systems (IAS-8)*, volume 8, pages 642–649, 2004. URL http://people.csail.mit.edu/iida/papers/iida_ias8.cr.pdf.
- [85] M. Khoramshahi, A. Sprowitz, A. Tuleu, M. N. Ahmadabadi, and A. J. Ijspeert. Benefits of an active spine supported bounding locomotion with a small compliant quadruped robot. In *Proceedings - IEEE International Conference on Robotics and Automation*, pages 3329–3334, 2013. ISBN 9781467356411. doi: 10.1109/ICRA.2013.6631041.
- [86] Takashi Takuma, Masahiro Ikeda, and Tatsuya Masuda. Facilitating multi-modal locomotion in a quadruped robot utilizing passive oscillation of the spine structure. In *IEEE/RSJ 2010 International Conference on Intelligent Robots and Systems, IROS 2010 - Conference Proceedings*, pages 4940–4945, 2010. ISBN 9781424466757. doi: 10.1109/IROS.2010.5649134.
- [87] Fumiya Iida, Gabriel Gómez, and Rolf Pfeifer. Exploiting body dynamics for controlling a running quadruped robot. In *2005 International Conference on Advanced Robotics, ICAR '05, Proceedings*, volume 2005, pages 229–235. IEEE, 2005. ISBN 0780391772. doi: 10.1109/ICAR.2005.1507417.
- [88] Claudio Semini, Victor Barasuol, Jake Goldsmith, Marco Frigerio, Michele Focchi, Yifu Gao, and Darwin G. Caldwell. Design of the Hydraulically Actuated, Torque-Controlled Quadruped Robot HyQ2Max. *IEEE/ASME Transactions on Mechatronics*,

- 22(2):635–646, apr 2017. ISSN 10834435. doi: 10.1109/TMECH.2016.2616284. URL <http://ieeexplore.ieee.org/document/7587429/>.
- [89] Johannes Wiedemann. *Leichtbau: Band 1: Elemente*. Springer, 2. auflage edition, 1996.
- [90] R Poprawe. *Lasertechnik für die Fertigung : Grundlagen, Perspektiven und Beispiele für den innovativen Ingenieur ; mit 26 Tabellen*. Springer, 2005. ISBN 35402140629783540214069. doi: 10.1007/b137581.
- [91] Johannes Wiedemann. *Leichtbau: Band 2: Konstruktion*. Springer, 2. auflage edition, 1996.
- [92] Feng Tian, Mohamed Samir Hefzy, and Mohammad Elahinia. A Biologically Inspired Knee Actuator for a KAFO. *Journal of Medical Devices*, 10(4): 045001, aug 2016. ISSN 1932-6181. doi: 10.1115/1.4033009. URL <http://medicaldevices.asmedigitalcollection.asme.org/article.aspx?doi=10.1115/1.4033009>.
- [93] Lüftl Degischer. *Leichtbau : Prinzipien, Werkstoffauswahl und Fertigungsvarianten*. WILEY-VCH, 2009. ISBN 9783527323722.
- [94] Fibersim Overview: Siemens PLM Software. URL <https://www.plm.automation.siemens.com/en/products/fibersim/fibersim-overview.shtml>.
- [95] Schnell, Gross, and Hauger. *Technische Mechanik 2: Elastostatik*. Springer, 6 edition, 1995.
- [96] F G M E TUI. Lehrblätter Maschinenelemente.
- [97] Martin Mayr. *Technische Mechanik*. Hanser, 2. auflage edition, 2008. ISBN 9783446416901.
- [98] Günther Holzmann, Meyer, and Schumpich. *Technische Mechanik*. Springer, 8. auflage edition, 1990. ISBN 978-3-519-16522-4. doi: 10.1007/978-3-322-96779-4. URL <http://link.springer.com/10.1007/978-3-322-96779-4>.
- [99] 3DHubs - Knowledge Base. URL <https://www.3dhubs.com/knowledge-base>.
- [100] Samuel Clark Ligon, Robert Liska, Jürgen Stampfl, Matthias Gurr, and Rolf Mülhaupt. Polymers for 3D Printing and Customized Additive Manufacturing. *Chemical Reviews*, 117(15):10212–10290, aug 2017. ISSN 15206890. doi: 10.1021/acs.chemrev.7b00074. URL <http://www.ncbi.nlm.nih.gov/pubmed/28756658><http://www.pubmedcentral.nih.gov/articlerender.fcgi?artid=PMC5553103>.
- [101] Claudio Semini, Mike Baker, Kulkarni Laxman, Venugopal Chandan, T Maruthiram, Robert Morgan, Marco Frigerio, Victor Barasuol, Darwin G Caldwell, and Gonzalo Rey. A

- Brief Overview of a Novel, Highly-Integrated Hydraulic Servo Actuator with Additive-Manufactured Titanium Body. *IROS Workshop 2016*, pages 4–7, 2016.
- [102] H Witte, R Hackert, M S Fischer, W Ilg, J Albiez, R Dillman, and A Seyfarth. Design criteria for the leg of a walking machine derived by biological inspiration from quadrupedal mammals. In *Climbing and Walking Robots*, pages 63–68, 2001. ISBN 1-86058-365-2.
- [103] Qian Zhao, Hidenobu Sumioka, and Rolf Pfeifer. The Effect of Morphology on the Spinal Engine Driven Locomotion in a Quadruped Robot. In *The 5th International Symposium on Adaptive Motion of Animals and Machines (AMAM2011)*, volume 1, pages 51–52, 2011.
- [104] S Hauser, M Mutlu, P Banzet, and A J Ijspeert. Compliant Universal Grippers as Feet in Legged Robots. *Advanced Robotics*, 2018.
- [105] Simon Hauser, Peter Eckert, Alexandre Tuleu, and Auke Ijspeert. Friction and damping of a compliant foot based on granular jamming for legged robots. In *Proceedings of the IEEE RAS and EMBS International Conference on Biomedical Robotics and Bio-mechatronics*, volume 2016-July, pages 1160–1165, 2016. ISBN 9781509032877. doi: 10.1109/BIOROB.2016.7523788.
- [106] M Mutlu, S Hauser, A Bernardino, and A J Ijspeert. Effects of Passive and Active Joint Compliance and in Quadrupedal Locomotion. *Advanced Robotics*, 2018.
- [107] Difference between Pneumatic, Electrical and Hydraulic Actuators Instrumentation Tools, . URL <https://instrumentationtools.com/difference-between-pneumatic-electrical-hydraulic-actuators/#.WqQSPujOWUk>.
- [108] The difference between: Pneumatic, Hydraulic and Electrical Actuators - HTL Worldwide, . URL <http://www.htl-worldwide.com/the-difference-between-pneumatic-hydraulic-and-electrical-actuators/>.
- [109] Dai Owaki, Takeshi Kano, Ko Nagasawa, Atsushi Tero, and Akio Ishiguro. Simple robot suggests physical interlimb communication is essential for quadruped walking. *Journal of the Royal Society, Interface*, 10(78):20120669, jan 2013. ISSN 1742-5662. doi: 10.1098/rsif.2012.0669. URL <http://www.ncbi.nlm.nih.gov/pubmed/23097501><http://www.pubmedcentral.nih.gov/articlerender.fcgi?artid=PMC3565797>.
- [110] Rui Vasconcelos, Simon Hauser, Florin Dzeladini, Mehmet Mutlu, Tomislav Horvat, Kamilo Melo, Paulo Oliveira, and Auke Ijspeert. Active stabilization of a stiff quadruped robot using local feedback. In *2017 IEEE/RSJ International Conference on Intelligent Robots and Systems (IROS)*, pages 4903–4910. IEEE, sep 2017. ISBN 978-1-5386-2682-5. doi: 10.1109/IROS.2017.8206369. URL <http://ieeexplore.ieee.org/document/8206369/>.

- [111] Dai Owaki, Leona Morikawa, and Akio Ishiguro. Listen to body's message: Quadruped robot that fully exploits physical interaction between legs. In *2012 IEEE/RSJ International Conference on Intelligent Robots and Systems*, pages 1950–1955. IEEE, oct 2012. ISBN 978-1-4673-1736-8. doi: 10.1109/IROS.2012.6385857. URL <http://ieeexplore.ieee.org/document/6385857/>.
- [112] Tomislav Horvat, Konstantinos Karakasiliotis, Kamilo Melo, Laura Fleury, Robin Thandiackal, and Auke J. Ijspeert. Inverse kinematics and reflex based controller for body-limb coordination of a salamander-like robot walking on uneven terrain. In *2015 IEEE/RSJ International Conference on Intelligent Robots and Systems (IROS)*, pages 195–201. IEEE, sep 2015. ISBN 978-1-4799-9994-1. doi: 10.1109/IROS.2015.7353374. URL <http://ieeexplore.ieee.org/document/7353374/>.
- [113] Biscuit - Programmable WiFi 9-Axis Absolute Orientation Sensor [0282] | ameriDroid - ODROID United States and Canada Distribution. URL <https://ameridroid.com/products/biscuit>.
- [114] Alexander Schmitz, Perla Maiolino, Marco Maggiali, Lorenzo Natale, Giorgio Cannata, and Giorgio Metta. Methods and Technologies for the Implementation of Large-Scale Robot Tactile Sensors. *IEEE Transactions on Robotics*, 27(3):389–400, jun 2011. ISSN 1552-3098. doi: 10.1109/TRO.2011.2132930. URL <http://ieeexplore.ieee.org/document/5771603/>.
- [115] Perla Maiolino, Marco Maggiali, Giorgio Cannata, Giorgio Metta, and Lorenzo Natale. A Flexible and Robust Large Scale Capacitive Tactile System for Robots. *IEEE Sensors Journal*, 13(10):3910–3917, oct 2013. ISSN 1530-437X. doi: 10.1109/JSEN.2013.2258149. URL <http://ieeexplore.ieee.org/document/6502183/>.
- [116] Harshal Arun Sonar and Jamie Paik. Soft Pneumatic Actuator Skin with Piezoelectric Sensors for Vibrotactile Feedback. *Frontiers in Robotics and AI*, 2:38, jan 2016. ISSN 2296-9144. doi: 10.3389/frobt.2015.00038. URL <http://journal.frontiersin.org/Article/10.3389/frobt.2015.00038/abstract>.
- [117] Merve Acer, Marco Salerno, Kossi Agbeviade, and Jamie Paik. Development and characterization of silicone embedded distributed piezoelectric sensors for contact detection. *Smart Materials and Structures*, 24(7):075030, jul 2015. ISSN 0964-1726. doi: 10.1088/0964-1726/24/7/075030. URL <http://stacks.iop.org/0964-1726/24/i=7/a=075030?key=crossref.56ec146600cdb501dd724a0052ffc05d>.
- [118] Anja Eva Maria Schmerbauch, Peter Eckert, Hartmut Witte, and Auke J. Ijspeert. Implementation and analysis of rich locomotion behavior on the bio-inspired, quadruped robot Serval, 2017. URL <http://opac.lbs-ilmenau.gbv.de/DB=1/FKT=>

- 1016/FRM=Anja%2BSchmerbauch/IMPLAND=Y/LNG=DU/LRSET=1/SET=1/SID=82447eff-1/SRT=YOP/TTL=1/SHW?FRST=1.
- [119] Auke Jan Ijspeert. Central pattern generators for locomotion control in animals and robots: A review. *Neural Networks*, 21(4):642–653, 2008. ISSN 08936080. doi: 10.1016/j.neunet.2008.03.014.
 - [120] Florin Dzeladini, Jesse van den Kieboom, and Auke Ijspeert. The contribution of a central pattern generator in a reflex-based neuromuscular model. *Frontiers in Human Neuroscience*, 8, jun 2014. ISSN 1662-5161. doi: 10.3389/fnhum.2014.00371. URL <http://journal.frontiersin.org/article/10.3389/fnhum.2014.00371/abstract>.
 - [121] Japan Biomimetic Intelligent Mechatronics Lab Titsumeikan University. No Title. URL <http://www.malab.se.ritsumei.ac.jp/en/robot/snake-like-robot/cpg-based-neural-controller-for-serpentine-locomotion>.
 - [122] Mrinal Kalakrishnan, Jonas Buchli, Peter Pastor, Michael Mistry, and Stefan Schaal. Learning, planning, and control for quadruped locomotion over challenging terrain. *International Journal of Robotics Research*, 30(2):236–258, 2011. ISSN 02783649. doi: 10.1177/0278364910388677.
 - [123] Barkan Ugurlu, Ioannis Havoutis, Claudio Semini, and Darwin G. Caldwell. Dynamic trot-walking with the hydraulic quadruped robot — HyQ: Analytical trajectory generation and active compliance control. In *2013 IEEE/RSJ International Conference on Intelligent Robots and Systems*, pages 6044–6051. IEEE, nov 2013. ISBN 978-1-4673-6358-7. doi: 10.1109/IROS.2013.6697234. URL <http://ieeexplore.ieee.org/document/6697234/>.
 - [124] P. Arena. The Central Pattern Generator: a paradigm for artificial locomotion. *Soft Computing*, 4(4):251–266, 2000. ISSN 1432-7643. doi: 10.1007/s0050000000051. URL <http://link.springer.com/10.1007/s0050000000051>.
 - [125] Masafumi Okada, Koji Tatani, and Yoshihiko Nakamura. Polynomial Design of the Nonlinear Dynamics for the Brain-Like Information Processing of Whole Body Motion. *ICra2*, 2(May):1410–1415, 2002. ISSN 10504729. doi: 10.1109/ROBOT.2002.1014741. URL <http://www.ynl.t.u-tokyo.ac.jp/Publications/papers02/icra02/okada1.pdf>.
 - [126] Alessandro Crespi and Auke Jan Ijspeert. AmphiBot II: An Amphibious Snake Robot that Crawls and Swims using a Central Pattern Generator. *Proceedings of the 9th International Conference on Climbing and Walking Robots (CLAWAR 2006)*, pages 19–27, 2006.
 - [127] Auke Jan Ijspeert, Alessandro Crespi, Dimitri Ryczko, and Jean Marie Cabelguen. From swimming to walking with a salamander robot driven by a spinal cord model. *Science*, 315(5817):1416–1420, 2007. ISSN 00368075. doi: 10.1126/science.1138353.

Bibliography

- [128] Hiroshi Kimura, Seiichi Akiyama, and Kazuaki Sakurama. Realization of dynamic walking and running of the quadruped using neural oscillator. *Autonomous Robots*, 7(3): 247–258, 1999. ISSN 09295593. doi: 10.1023/A:1008924521542.
- [129] M M Williamson. Neural Control of Rhythmic Arm Movements. *Neural networks*, 11(7-8): 1379–1394, 1998. ISSN 0893-6080. URL <http://www.sciencedirect.com/science/article/pii/S0893608098000483>.
- [130] Alessandro Crespi and Auke Jan Ijspeert. Online optimization of swimming and crawling in an amphibious snake robot. *IEEE Transactions on Robotics*, 24(1):75–87, 2008. ISSN 15523098. doi: 10.1109/TRO.2008.915426.
- [131] Monica A Daley and Andrew A Biewener. Running over rough terrain reveals limb control for intrinsic stability. *Proceedings of the National Academy of Sciences of the United States of America*, 103(42):15681–6, oct 2006. ISSN 0027-8424. doi: 10.1073/pnas.0601473103. URL <http://www.ncbi.nlm.nih.gov/pubmed/17032779><http://www.pubmedcentral.nih.gov/articlerender.fcgi?artid=PMC1622881>.
- [132] Monica A. Daley, James R. Usherwood, Gladys Felix, and Andrew A. Biewener. Running over rough terrain: guinea fowl maintain dynamic stability despite a large unexpected change in substrate height. *Journal of Experimental Biology*, 209(1), 2006.
- [133] J L Smith, P Carlson-Kuhta, and T V Trank. Forms of forward quadrupedal locomotion. III. A comparison of posture, hindlimb kinematics, and motor patterns for downslope and level walking. *Journal of neurophysiology*, 79(4):1702–1716, oct 1998. ISSN 0022-3077. doi: 10.1152/jn.1998.79.4.1687. URL <http://www.ncbi.nlm.nih.gov/pubmed/8899606>.
- [134] P Carlson-Kuhta, T V Trank, and J L Smith. Forms of quadrupedal locomotion. II. A comparison of posture, hindlimb kinematics, and motor patterns for upslope and level walking. *Journal of Neurophysiology*, 79(4):1687–1701, apr 1998. ISSN 0022-3077. doi: 10.1152/jn.1998.79.4.1687. URL <http://www.physiology.org/doi/10.1152/jn.1998.79.4.1687>.
- [135] J L Smith, P Carlson-Kuhta, and T V Trank. Forms of forward quadrupedal locomotion. III. A comparison of posture, hindlimb kinematics, and motor patterns for downslope and level walking. *Journal of neurophysiology*, 79(4):1702–1716, apr 1998. ISSN 0022-3077. doi: 10.1152/jn.1998.79.4.1687. URL <http://www.physiology.org/doi/10.1152/jn.1998.79.4.1702>.
- [136] Tomislav Horvat, Konstantinos Karakasiliotis, Kamilo Melo, Laura Fleury, Robin Thandackal, and Auke J. Ijspeert. Inverse kinematics and reflex based controller for body-limb coordination of a salamander-like robot walking on uneven terrain. In *IEEE International Conference on Intelligent Robots and Systems*, volume 2015-Decem, pages

- 195–201. IEEE, sep 2015. ISBN 9781479999941. doi: 10.1109/IROS.2015.7353374. URL <http://ieeexplore.ieee.org/document/7353374/>.
- [137] NaturalPoint. OptiTrack s250e, 2004. URL <http://www.naturalpoint.com/optitrack/products/s250e/>.
- [138] A Barre and S Armand. b-tk Biomechanical ToolKit.
- [139] MathWorks. MatLab, 2012.
- [140] D Brown. Tracker, video analysis and modeling tool, 2014. URL [https://www.cabrillo.edu/~sim\\$dbrown/tracker/](https://www.cabrillo.edu/~sim$dbrown/tracker/).
- [141] Kistler Holding AG. Kistler. Measure. Analyse. Innovate.
- [142] Peter Eckert, Alexander Spröwitz, Hartmut Witte, and Auke J. Ijspeert. Effect of spine movement on quadruped robot bounding locomotion, 2013. URL <http://opac.lbs-ilmenau.gbv.de/DB=1/SET=3/TTL=1/SHW?FRST=7>.
- [143] Vaughan Pratt. Direct least-squares fitting of algebraic surfaces, 1987. ISSN 00978930. URL <http://portal.acm.org/citation.cfm?doid=37402.37420>.
- [144] Peter Eckert, Behzad Bayat, Yanis Mazouz, and Auke J Ijspeert. Towards amphibious locomotion with Cheetah-Cub-AL. Technical report, 2017.
- [145] EUROBENCH – European Robotic framework for bipedal locomotion BENCHmarking. URL <http://eurobench2020.eu/>.
- [146] Massimo Vespignani. *Challenges in the Locomotion of Self-Reconfigurable Modular Robots*. PhD thesis, EPFL, 2015.



Ch. du Rossignol 1,
CH-1110 Morges
Mobile:+41 76 582 24 51
Mail:petereckert87@gmail.com
Nationality German, Permit B

Peter Eckert

PhD in Robotics - BioMechatronic Engineer - Mechanical Designer

Education

- 06/13 - 06/18 **PhD-Student/Assistant** [Biorobotics Laboratory, EPFL, Switzerland](#)
Main subjects: BioMechatronic design and development of quadrupedal robots, with focus on mechanics; Experimentation and validation; Development of a Benchmark for Agility.
Title of the Thesis: Towards Agility: Definition, Benchmark and Design Considerations for Small, Quadrupedal Robots".
Relators: Prof. Auke J. Ijspeert
- 10/12 - 04/13 **Master-thesis-student** [Biorobotics Laboratory, EPFL, Switzerland and TU Ilmenau, Germany](#)
Main subjects: BioMechatronic design and development of quadrupedal robots, with focus on mechanics; Experimentation and validation
Title of the Thesis: Effect of spine movement on quadruped robot bounding locomotion".
Relators: Dr. Alexander Spröwitz, Prof. Auke J. Ijspeert, Prof. Hartmut Witte
- 04/12 - 10/12 **Research Internship** [Biorobotics Laboratory, EPFL, Switzerland](#)
Main activities: Production of bio-inspired quadrupedal robots; Assistance for experimentation
Relators: Dr. Alexander Spröwitz, Prof. Auke J. Ijspeert
- 04/11 - 04/13 **Master-student (M.Sc.)** [TU Ilmenau, Germany](#)
Main direction: Mechatronics (M.Sc.) with specialization in BioMechatronics
Relators: Prof. Hartmut Witte
- 10/07 - 04/11 **Bachelor-student (B.Sc.)** [TU Ilmenau, Germany and TETRA GmbH, Germany](#)
Main direction: Mechatronics (B.Sc.)
Title of the Thesis: Entwurf eines UL-Roboterarms".
Relators: Christian Trommer, Dr. Andreas Karguth, Prof. Klaus Zimmermann

Publications

- P. Eckert and A. J. Ijspeert, Benchmarking Agility For Multi-legged Terrestrial Robots, IEEE Trans. Robot. - under review., 2018.
- K. Strübig, B. Bayat, P. Eckert, and A. J. Ijspeert, Design and Development of the Efficient Anguilliform Swimming Robot - MAR, IEEE Trans. Robot. - in prog., 2018.
- A. Andreoli, P. Eckert, B. Bayat, and A. J. Ijspeert, The Swimming Quadruped: an exploratory study of aquatic locomotion, Bioinspiration Biomimetics - in prog., 2018.
- S. W. Heim, M. Ajallooeian, P. Eckert, M. Vespignani, and A. J. Ijspeert, On designing an active tail for legged robots: simplifying control via decoupling of control objectives, Ind. Robot An Int. J., vol. 43, no. 3, pp. 338346, 2016.
- A. Sprowitz et al., Oncilla robot: a compliant, versatile, open-source, quadruped robot with pantograph legs, arXiv preprint arXiv:1803.06259, under review., 2018.
- P. Eckert, A. E. M. Schmerbauch, T. Horvat, K. Söhnle, H. Witte, and A. J. Ijspeert, Towards rich motion skills with the lightweight quadruped robot Serval - a design, control and experimental study, in SAB2018 - The 15th International Conference on the Simulation of Adaptive Behavior - under review, 2018.
- P. Eckert, A. Sprowitz, H. Witte, and A. J. Ijspeert, Comparing the effect of different spine and leg designs for a small bounding quadruped robot, in Proceedings - IEEE International Conference on Robotics and Automation, 2015, vol. 2015June, no. June, pp. 31283133.

S. Hauser, P. Eckert, A. Tuleu, and A. Ijspeert, Friction and damping of a compliant foot based on granular jamming for legged robots, in Proceedings of the IEEE RAS and EMBS International Conference on Biomedical Robotics and Biomechatronics, 2016, vol. 2016July, pp. 11601165.

S. Pouya, P. Eckert, A. Sproewitz, R. Moeckel, and A. Ijspeert, Motor control adaptation to changes in robot body dynamics for a complaint quadruped robot, vol. 8064 LNAI. 2013.

Other Info

- Woodworking enthusiast
- Father of a beautiful daughter and husband to a wonderful wife

March 13, 2018 Peter Eckert